OCTOBER 1981 LIDS-R-1156

SURVEILLANCE AND TARGET TRACKING

Edited By

Michael Athans
Wilbur B. Davenport, Jr.
Elizabeth R. Ducot
Robert R. Tenney

Proceedings of the Fourth MIT/ONR Workshop on
Distributed Information and Decision Systems
Motivated by Command-Control-Communication (C^3) Problems

Volume I

June 15 - June 26, 1981
San Diego, California

ONR Contract No. N00014-77-C-0532

PREFACE

This volume is one of a series of four reports containing contributions from the speakers at the fourth MIT/ONR Workshop on Distributed Information and Decision Systems Motivated by Command-Control-Communication (C^3) Problems. Held from June 15 through June 26, 1981 in San Diego, California, the Workshop was supported by the Office of Naval Research under contract ONR/N00014-77-C-0532 with MIT.

The purpose of this annual Workshop is to encourage informal interactions between university, government, and industry researchers on basic issues in future military command and control problems. It is felt that the inherent complexity of the C^3 system requires novel and imaginative thinking, theoretical advances and the development of new basic methodologies in order to arrive at realistic, reliable and cost-effective designs for future C^3 systems. Toward these objectives, the speakers, in presenting current and future needs and work in progress, addressed the following broad topics:

1) Surveillance and Target Tracking

2) Systems Architecture and Evaluation

3) Communication, Data Bases & Decision Support

4) C^3 Theory

In addition to the Workshop speakers and participants, we would like to thank Dr. Stuart Brodsky of the Office of Naval Research, and Ms. Barbara Peacock-Coady and Ms. Lisa Babine of the MIT Laboratory for Information and Decision Systems for their help in making the Workshop a success.

Cambridge, Massachusetts
October 1981

Michael Athans
Wilbur B. Davenport, Jr.
Elizabeth R. Ducot
Robert R. Tenney

SURVEILLANCE AND TARGET TRACKING

SURVEILLANCE AND TARGET TRACKING

FOREWORD

Almost three full days of this year's Workshop were devoted to surveillance and related issues. The discussion sessions on each day were lively and provocative. Two major themes characterized the remarks of the participants: 1) the design of surveillance systems and algorithms are critically dependent on the other parts of the C^3 system to which they must interface, and 2) there remains a great deal of work to be done before surveillance of a complex environment is well understood.

The objective of a surveillance system is to provide an accurate picture of the environment to the other parts of a C^3 systems. There are many users of the surveillance information; the only general statement that can be made is that different users will require information of different types, of different levels of aggregation, and with different priorities. There is no unique point at which the performance of a surveillance system can be measured; it must be evaluated in the context of the other C^3 elements and the overall command objectives.

On the technical side, there was general agreement that many open questions remain. Single sensor, single target, high signal-to-noise ratio problems are relatively well understood (from a theoretical point of view). Even the addition of either multiple sensors, multiple targets, or low signal-to-noise ratios one at a time produces problems which can usually be addressed with current theory. Taken in pairs or all together, however, particularly when limited, unreliable communications are present, brings one to a theoretical void.

In fact, in our opinion, it is not clear that general surveillance issues involving multiple sensors, multiple targets, and fusion centers can be formulated reasonably in a relevant context unless data communications constraints are explicitly included in the very problem formulation.

The surveillance papers included here are not in the order of presentation. *Atkinson's* paper first provides an overview of surveillance issues and nomenclature. The remaining papers are roughly sequenced along the physical to abstract dimension. *Psaraftis, Perakis, and Mikhahelvsky* present a normative model on the ocean environment suitable for use in a long range detection problems. The next four papers *Fortmann et. al., Bowman, Moore, and Kovacich* all address one of the currently popular topics in surveillance, multi-object tracking. *Pattipati et. al.,* then presents a problem formulation which will allow some current adhoc approaches to this problem to be placed in a more rigorous framework.

The subsequent papers move to a larger set of issues. *Tenney* surveys work at M.I.T. on surveillance, communication, and control; *Liu and Bongiovanni* look at a sensor placement problem. The next pair of papers discuss surveillance systems architectures; *Bugenhagen et. al.,* in an oceanic context, and *Kramer and Sandell* in an early air warning setting.

We conclude with two papers on the potential role of artificial intelligence techniques in surveillance systems; *Gross et. al.,* in a general sense and *Dillard* based on a specific production rule system.

DATA DEPENDENT ISSUES IN SURVEILLANCE PRODUCT INTEGRATION

David A. Atkinson
CTEC, Inc.
7777 Leesburg Pike
Falls Church, Virginia 22043

(CTEC Publication No. SAD-81-036 - June 8, 1981)

DATA DEPENDENT ISSUES IN SURVEILLANCE PRODUCT INTEGRATION

D.A. Atkinson
CTEC, Inc.

SUMMARY

This analysis is focused on the design problems encountered in the integration of ocean surveillance data that arise from the particular nature of the information delivered to and required from the system. The starting point is a definition of the ocean surveillance product, its uses, and the requirements specified for it. The general nature of the input data is covered in an overview of the characteristics of sensors and sources. Problems associated with the distribution of processing, in particular the target classification analysis, in a surveillance network are described. The important issue of multi-source integration (correlation) is covered by raising specific outstanding problems. Finally, the impact of these problems on surveillance system design approaches is discussed.

1. THE OCEAN SURVEILLANCE PRODUCT (OSP)

The six basic elements present in the OSP are listed in Viewgraph 2, together with a general characterization of the intelligence and operational uses of this product. These two general categories of use are clearly interdependent, and the seventh element listed as a part of the evaluated OSP indicates one form of this relationship. The basic elements and uses are those identified in the Navy's Ocean Surveillance Master Plan [1]. Different representations of the basic OSP information appear to be best suited to the needs of specific users. A tabulation of the track representations and classification levels that would support the needs of specific consumers of the OSP is presented in Viewgraph 3. Operational commanders with their attention focused on developments in the immediate future can make do with current position and velocity estimates, while intelligence analysts may require historical information. The lower level of geographic resolution for national users is dictated by the volume of information, although they may also require occasional high-resolution inputs. The classification levels indicated are presented to stimulate further debate, rather than as definitive specifications.

Quantitative performance requirements for location accuracy and timeliness may be specified by using the radius of uncertainty (ROU) defined in Viewgraph 4, and illustrated graphically in Viewgraph 5. A significant feature of this parameter is its dependence on the sum of the interval required for processing and transmitting OSP data and the interval between successive observations. The name adopted in the OSMP [1] is somewhat inappropriate: "radius of containment" describes this parameter more accurately. The measures of classification performance are rather obvious ones; however, they are quite difficult to determine in practice.

The area of data association (correlation) is one in which definitive measures of performance are very difficult to develop, as is illustrated in a number of Navy studies [2], [3], and [4] of this problem. The gate areas and probabilities of correct choice for specified decision rules, presented in Viewgraph 6, may be used to estimate performance. An interesting feature of these measures is the fact that signature descrimination capability (P_{SD} 1) lowers the effective target density by a simple factor. A formal proof of this intuitive result is presented in the Appendix of a report on an analytic correlation performance model [5].

2. SENSORS AND SOURCES

The large number of sensors that can contribute the basic data used to create the OSP precludes a detailed analysis of the characteristics of individual systems in this report. The overview presented here attempts to identify characteristics that significantly influence system design. Viewgraph 7 presents sensors grouped into three general categories: active; passive (monitoring) involuntary (signals); and passive (monitoring) voluntary (signals). The passive voluntary category includes the sensors vulnerable to the use of emissions control (EMCON) policies by hostile forces.

The basic classification data provided by sensors may be characterized as either image data or signature data (Viewgraph 8). The principles used to arrive at classification using such data are presented in Viewgraph 9. The comparison of images is essentially an interpretive process. In view of the very significant problems associated with automatic image recognition, the processing rate problem arising from the requirement for interactive analysis is likely to persist for some time. Signature comparison is normally made using tolerance intervals or a statistical distance functional defined in the abstract "emissions" parameter space.

The sensor position data we refer to here is the information provided by the primitive signal measurements as opposed to information that may be inferred from subsequent processing. Examples such as the fix, line of bearing (LOB), and the hyperbolic line of position arising from a time difference measurement are illustrated in Viewgraph 10. The primitive classes of position and velocity information are tabulated in Viewgraph 11, with an indication of the processing approach required to incorporate such observations into an updated state estimate. Time and Doppler shift differences differ from the others in the sense that a correlation of observed signals at two sites is required to extract the location information. In addition, curvilinear lines of position can yield ambiguous intersections. Statistical filters, such as the extended Kalman filter, can be used for updates when the interval between observations is comparable to or less than the typical interval between target maneuvers. The use of this approach in a system delivering time and Doppler difference data is described by Fortmann and Baron [6]. Some systems, in particular mosaic IR detectors, generate track segment observations as a part of their signal detection logic. These measurements may easily be converted into a complete (position + velocity) observation of the state vector. A major problem arises when the revisit interval becomes much longer than the interval between maneuvers. This is particularly severe for surface traffic in littoral areas where the constraint that "ships cannot walk" causes frequent maneuvers. In these situations the resulting state estimates may not support the operational user's requirements for position projection.

The characteristic classification and location information provided by a number of sensors that could contribute to the OSP is tabulated in Viewgraph 12. The sensitive nature of information on the accuracy of the data provided by such sources precludes a realistic discussion at this conference. Obviously, accuracy is a very important consideration in arriving at an evaluation of the potential contribution of a source to the OSP.

A number of factors associated with the operating principles and design of sensors have a significant impact on the timeliness of the data delivered by the sensor systems. Some of these factors are indicated in Viewgraph 13. Propagation delays are significant for acoustic systems detecting signals at long range. The time required for signal integration in order to suppress noise and achieve the desired frequency resolution must also be considered, since it can restrict coverage rate potential in large area surveillance systems. Processing to achieve a position fix and/or to classify the target detected also produce delays in delivery. Data transmission delays are a potential problem in multisite sensor systems that require network coordination and data exchange.

3. SURVEILLANCE NETWORKS

A surveillance system is an interconnected network leading from the basic sensing devices through various intermediate processing stages to delivery of an integrated product to the users. The processing stages are distributed in both space and time. The determination of the most effective configuration for an ocean surveillance network involves a vast number of issues, and our limits of time and competence require a focus on a specific example of a network configuration problem.

An abstract outline of data flow from source to user is presented in Viewgraph 14. The sensor/source segment encompasses reception of the basic signal, processing to detect (extract from the noise background) and integrate (convert to the desired form and resolution) this signal, and subsequent processing to refine the OSP elements delivered by the source. This stage is normally followed by processing at a regional or national center that serves to integrate the outputs of multiple sources (MSI), and to append prepositioned information on the target in certain cases. Preprocessing consists of data conversion and analysis employing only the data supplied by the source and prepositioned intelligence data (eg. a hull to emitter correlation (HULTEC) analysis). The user may be national command, a fleet or regional command, or a battle group or individual unit. The network configuration issue considered is the location of classification/signature processing in the network.

The diagram of the assumed source segment in Viewgraph 15 illustrates two of the options. The source network consists of detectors connected to initial processing facilities that extract the signature and location (assumed to be a LOB) data from the basic signal. One option is to place the classification processing at these initial processing facilities. Each of the initial facilities reports to a central source evaluation center. At this center, reports with matching signatures may be processed to obtain a position fix. In addition, the classification processing that matches these signatures with a signature fingerprint file could take place at the evaluation center. The third option is deferral of classification processing until the data are delivered to a regional MSI processor.

The distribution options and some of the factors that must influence the choice are presented in Viewgraph 16. The classification processing, as well as the association analysis that yields a position fix, clearly enhances the utility of the OSP delivered downstream. Processing centers represent potentially vulnerable elements of the system. Thus, early classification will provide the option of delivery of useful information in the event of failure at the source evaluation center or at a regional center. The full value of this option may be realized only if the user is equipped to process the location information (LOB) that can be delivered by an initial processor. Central classification can result in an increased level and likelihood of target identification because the information resulting from multi-source association is available. In addition, this option will ensure that users at various command levels are using a consistent situation picture. The data transmission loads require a detailed analysis in specific cases, because early classifiaction requires feedback of fingerprint updates while central clasification may involve transmission of more elaborate signatures.

The basic nature of signature processing has a significant impact on network design. Two basic uses of signature data are outlined in Viewgraph 17, which also discusses the associated data requirements. The differentiation between establishing a track designator and classification may be blurred by incorporating signature data for unidentified targets in the Fingerprint File. The most effective way to assess the confidence of a classification based on signature data is to compute the relative likelihood of alternative matches. This requires relatively complete files of observed signatures. This data should be regarded as relatively dynamic, with an update frequency determined by the time dependence of the emission parameters and alterations in deployment. The modeling of emission parameter time series for individual targets may be desirable in some cases.

Cases in which parametric separation is not sufficient to support unique classification will require a "dynamic signature" approach. The basic principle is presented in Viewgraph 18. If a combination of parametric and geographic separation is sufficient to permit a track designator (tracking) analysis, then the ability to maintain classification of a target follows directly from the ability to track it. Initial classificaion must be established, but this is the case for any signature-based analysis. Thus, initial classification is always based on multi-source correlation, but track maintenance is sufficient thereafter.

4. MULTI-SOURCE INTEGRATION (MSI)

The MSI problem and the closely associated multi-target tracking problem are technically sweet. This must account, in part, for the large number of potential solutions to these problems [3] which have been advanced in recent years. An analysis of advanced approaches to the multi-target tracking problem can be found in a review by Bar-Shalom [7]. More recent work is exemplified by the JPDA analysis of Bar-Shalom, Fortmann, and Schaeffe [8] and the highly regarded Bayesian multiple hypothesis system developed by Reid [9].

The basic principles that must be applied to the association of data from multiple sources are indicated in Viewgraph 19. Position comparison at simultaneous or nearly simultaneous view employs relatively simple algorithms, but it is likely to be successful only when the two sources produce very

accurate position measurements. Track matching also employs position data, as this is the data element common to nearly all OSP sources. Characteristic consistency tests are particularly useful where signature analysis has provided a partial classification (eg. identified a specific type of emitter). A Bayesian approach to the use of characteristic consistency in association analysis has been developed [10]. Operational characteristics can also be used in MSI, as they serve to pin point the time of anticipated events. The difficulty associated with adoption of an approach that relies on the typical operations of targets is its vulnerability to deception and exploitation in times of crisis.

An appreciation of the OSP processing at a regional processing center may be obtained from the hypothetical data flow illustrated in Viewgraph 20. The trade-off between time required for preprocessing, such as HULTEC analysis, and the resulting increase in efficiency of the selection of candidate tracks for association is an interesting issue in the design of the processing subsystem. Motion models, which may involve both position and signature projection, are employed in both the evaluation of candidates and the update of state vector and parameters which follows an association decision. These applications are different, and it is by no means evident that the same models should be used at both processing stages. The provision of review procedures to detect and recover from association errors is critically important in automatic decision systems.

A list of some interesting problems associated with MSI analysis is presented in Viewgraph 21. Problems associated with the impact of target maneuvers on position projections have long been recognized. The impact of volitional maneuvers is outlined in Viewgraph 22. The uncertainty of statistical distributions may lead to contradictory results when different decision rules are applied [11], and the identification of an optimal rule must be based on empirical analysis. The importance of maneuver detection and adjustment procedures for tracking filters applied to ocean surveillance is well known [12].

Ambiguity is always present when decisions must be based on uncertain information. In considering approaches to this problem, it is useful to distinguish between their contribution to an actual resolution of the ambiguity and their potential to clarify our picture of the ambiguous situation. The basic considerations are presented in Viewgraph 23, where the rapid growth in complexity and processing demands associated with complex decision algorithms are also noted. A second problem associated with representation is the determination of a form of representation of situation plot ambiguities that is useful to operational commanders

Classification chains occur in MSI when data containing different degrees of target identification is associated. Viewgraph 24 presents an interesting example where accurate positional data arising from a radar sensor may be associated with an ELINT report that also has high positional accuracy. Subsequent association with a series of low position accuracy HFDF reports using a combination of characteristic consistency (ie. emitter is compatible with target identified by HFDF) and track matching provides a complete target ID for the radar track. The opimal use of such classification

chains to upgrade the OSP is an interesting open problem. This example may also be used to illustrate the potential problems arising from data bias. If the reference frames employed by the three systems are inconsistent, statistical position comparison procedures will prove ineffective.

5. CONCLUSION

This analysis is , admittedly, rather long on problems and short on solutions. The time when the design of a surveillance system will be a straightforward engineering task still lies well ahead of us. The objective of this report will be realized if it functions as a primer to introduce you to the problems that can arise in the design of a real world ocean surveillance system. At this point, a few comments on design approaches seem appropriate.

- Multiple Data Paths: The provision of multiple data paths from source to user will enhance the survivability of the system. The problem with such a design arises from the temptation to use these paths simultaneously. The assumption that association of duplicate reports of an event will be trivial, because the data delivered will be identical, is naive.

- Simulation Testing: Simulation testing of tracking and decision algorithm performance may be very useful. It is clearly essential in the case of data sources still in the design phase. However, care should be exercised to conduct the tests in a ruthless manner. Significant errors and/or systematic bias should be incorporated in the simulated data. Robustness against such errors is essential in processing data from deployed sensors.

- Automation: High data rates may dictate a hands-off decision logic, but even in such cases an interactive interface is an important development tool. These systems can fail in ingenious ways.

- Sophisticated Decision Algorithms: The need for fancy analytical footwork to achieve some improvement in the processing of ambiguous data indicates a failure in overall system design. An effective ocean surveillance system should provide relatively unambiguous data.

REFERENCES

1. "Ocean Surveillance Master Plan," February 1980.

2. Kullback, J.H., and Owens, M.E.B., "Multisensor Correlation for Ocean Surveillance: Problems and Limitations," NRL Report 7258, May 1972.

3. Wiener, H.L., Willman, W.W., Goodman, I.R., and Kullback, J.H., "Naval Ocean-Surveillance Correlation Handbook, 1978," NRL Report 8340, Oct. 1979.

4. Wiener, H.L., Distler, A.S., and Kullback, J.H., "Operational and Implementation Problems of Multi-Target Correlator-Trackers," Proc. 1979 IEEE Conf. on Decision and Control, Dec. 1979

5. Atkinson, D.A., CTEC Report ITSS-CTEC-7, May 1981

6. Fortmann, T.E., and Baron, S., "Problems in Multi-Target Sonar Tracking," Proc. 1978 IEEE Conf. on Decision and Control, Jan. 1979.

7. Bar-Shalom, Y., "Tracking Methods in a Multitarget Environment," IEEE Trans. Auto. Control, AC-23, 618, August 1978.

8. Bar-Shalom, Y., Fortmann, T.E., and Schaeffe, M., "Joint Probabilistic Data Association for Multiple Targets in Clutter," Proc. 1980 Conf. on Information Sciences and Systems, March 1980.

9. Reid, D.B., "The Application of Multiple Target Tracking Theory to Ocean Surveillance," Proc. 1979 IEEEE Conf. on Decision and Control, Dec. 1979.

10. Atkinson, D.A., "A Bayesian Analysis of Surveillance Attribute Data," Proc. 1980 IEEE Conf. on Decision and Control, Dec. 1980

11. Atkinson, D.A., "A Comparison of Probability Gates and Weights in the Surveillance Association Problem," Proc. 3rd MIT/ONR Workshop on C^3 Problems, Vol 4, Dec. 1980.

12. Corman, D.E., "OTH/DC&T Engineering Analysis Vol. 8: Evaluation of Surface Ship Tracking Algorithms," JHU/APL, April 1979.

SURVEILLANCE INTEGRATION
BRIEFING OUTLINE

- DEFINE THE OCEAN SURVEILLANCE PRODUCT (OSP), ITS USES, AND QUANTITATIVE REQUIREMENTS
- CHARACTERIZATION OF SENSORS/SOURCES AND THE LOCATION AND CLASSIFICATION DATA THEY PROVIDE
- DISTRIBUTION OF PROCESSING IN SURVEILLANCE NETWORKS -- DATA REQUIREMENTS AND UTILITY
- MULTI-SOURCE INTEGRATION PRINCIPLES AND PROBLEMS
- SURVEILLANCE SYSTEM DEVELOPMENT PROBLEMS: A SELECTED LIST

DEFINITION OF THE OSP AND ITS USES

OSP ELEMENTS

1. TIME (EVENT OR RECEIPT OF SIGNAL)
2. STATE VECTOR (POSITION-VELOCITY COMPONENTS)
3. ACCURACY OF STATE VECTOR (CONTAINMENT ELLIPSOID)
4. CLASSIFICATION (UNIQUE ID, CLASS, TYPE, CATEGORY)
5. CONFIDENCE OF CLASSIFICATION (PROBABILITY THAT CLASSIFICATION IS CORRECT)
6. TRACK DESIGNATOR (UNIQUE ASSOCIATION INDICATOR)

OSP USES

OPERATIONAL

1. ALTER ALERT STATUS
2. DIRECT MOVEMENT OF FORCES
3. UTILIZATION OF WEAPONS AND SENSORS

INTELLIGENCE

1. STRATEGIC I&W
2. ORDER OF BATTLE
3. TACTICAL I&W
4. SCIENTIFIC INTELLIGENCE

EVALUATED OSP CONTAINS

7. INFORMATION SUPPORTING TACTICAL INDICATIONS AND WARNING (I&W) (RANGE AND CAPABILITIES OF WEAPONS AND SENSORS, ETC.)

USERS AND DATA REPRESENTATION

USER	APPLICATIONS	TRACK REPRESENTATION	MINIMUM USEFUL CLASSIFICATION
NATIONAL COMMAND	STRATEGIC I&W	T3	C2
AREA/FLEET COMMANDS	SITUATION MONITORING SENSOR TASKING AREA I&W	T2 OR T3	C1 OR C2
BATTLE GROUP UNIT	TACTICAL I&W TARGETING ORGANIC SENSOR TASKING	T1	C3

KEY

TRACK REPRESENTATIONS
- T1: STATE VECTOR + VARIANCE
- T2: TIME ORDERED POSITIONS
- T3: CURRENT CONTAINMENT AREA

CLASSIFICATION
- C1: COMPLETE ID
- C2: CLASS OR TYPE
- C3: CATEGORY
  (FRIEND-FOE; FISH-FOWL)

QUANTITATIVE PERFORMANCE REQUIREMENTS

LOCATION ACCURACY AND TIMELINESS VIA ROU (RADIUS OF UNCERTAINTY)

$$ROU_{MAX} = \left((S * T)^2 + A^2 \right)^{1/2}$$

A = MEASUREMENT ACCURACY

S = MAXIMUM TARGET SPEED

T = $T_U + T_R$ WITH

T_U = MEASUREMENT TO UPDATE INTERVAL

T_R = REVISIT INTERVAL

CLASSIFICATION PERFORMANCE MEASURES

F_C = FRACTION OF OBJECTS CLASSIFIED

P_C = PROBABILITY OF CORRECT CLASSIFICATION

T_C = INTERVAL FROM DETECTION TO CLASSIFICATION

(THESE PARAMETERS MAY BE SPECIFIED FOR VARIOUS TARGET TYPES)

ILLUSTRATION OF THE ROU CONCEPT

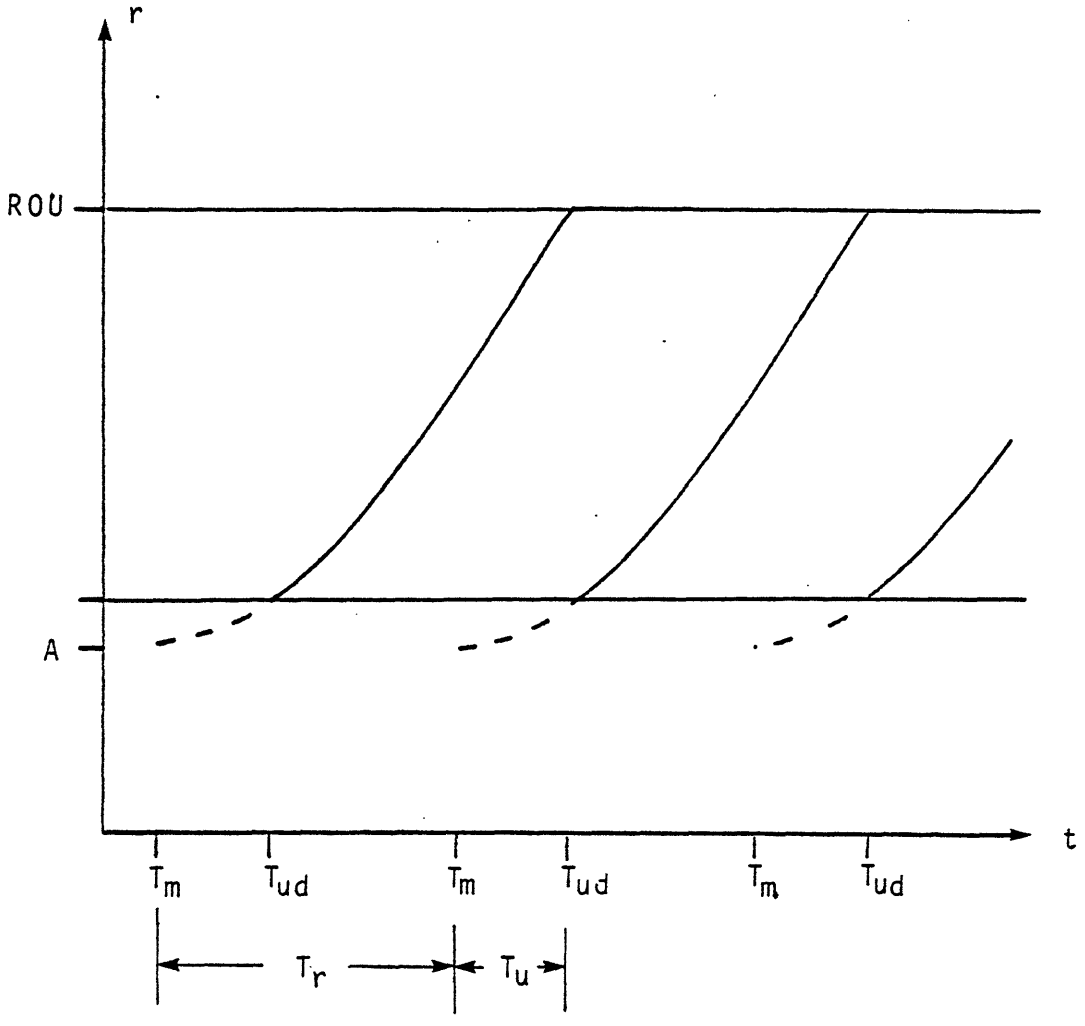

DATA ASSOCIATION PERFORMANCE ESTIMATES

CONTAINMENT AREAS:

PROJECTION $A_N = 2\pi Q \sigma_a^2 (-\ln\alpha)$

FEASIBILITY $A_M = \pi((S T_R)^2 + (3\sigma_a)^2)$

T_R = REVISIT INTERVAL S = TARGET SPEED

σ_a = MEASUREMENT ACCURACY

α = SIGNIFICANCE LEVEL Q = TRACKING EFFICIENCY PARAMETER ($1 < Q \leq 6$)

PROBABILITY OF CORRECT ASSOCIATION:

$Z = A \rho P_{SD}$

= TRAFFIC DENSITY

P_{SD} = SIGNATURE DISCRIMINATION (PROBABILITY THAT SIGNATURES OF DISTINCT TARGETS WILL BE ACCEPTED AS A MATCH)

RANDOM CHOICE INSIDE AREA

$P_{C1} = (1 - \exp(-z))/z$

CHOICE OF OBSERVATION NEAREST PROJECTED POSITION

$P_{C2} = (1 + 2Z_0)^{-1}$

WHERE $Z_0 = \pi Q \sigma_a^2 \rho P_{SD}$

GENERAL SENSOR TYPES

TYPE	EXAMPLES	SIGNAL DETECTED
ACTIVE	RADAR LASAR RADAR SONAR	E.M. (HF TO GHz) E.M. (IR - VISUAL) ACOUSTIC
PASSIVE INVOLUNTARY	OPTICAL IR DETECTORS HYDROPHONES	E.M. (IR - VISUAL) IR ACOUSTIC
PASSIVE VOLUNTARY	ELINT COMINT	E.M. (HF TO GHz) E.M. (PRIMARILY HF)

BASIC CLASSIFICATION DATA

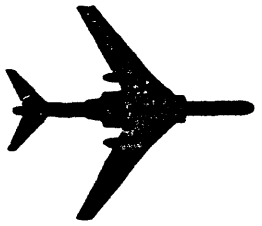

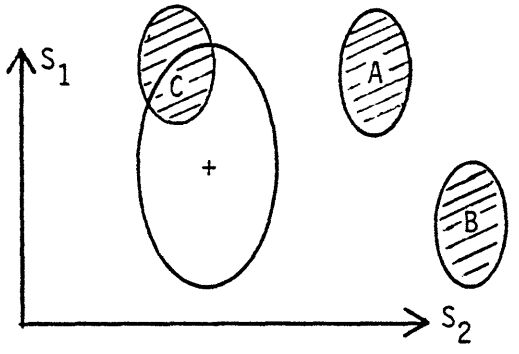

SIGNATURE DATA

CLASSIFICATION PRINCIPLES

BASIC DATA	ANALYSIS	PROBLEMS
IMAGE	COMPARISON WITH IMAGE FILE (NORMALLY MANUAL)	- ASPECT DEPENDENCE OF IMAGES - LOW PROCESSING RATE - HIGH DATA TRANSMISSION RATE
SIGNATURE	COMPARISON WITH FINGERPRINT FILE	- AMBIGUITY DUE TO OVERLAP IN - SIGNATURE SPACE - TIME DEPENDENCE OF SIGNATURE DATA

POSITION DATA EXAMPLES

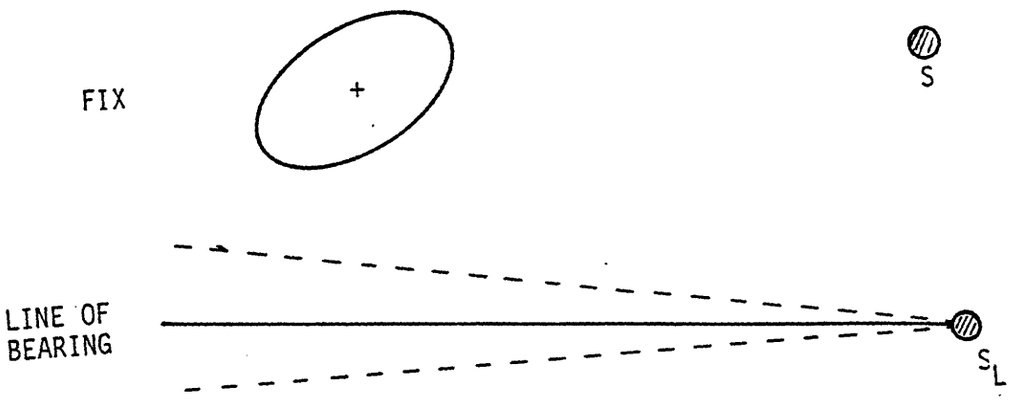

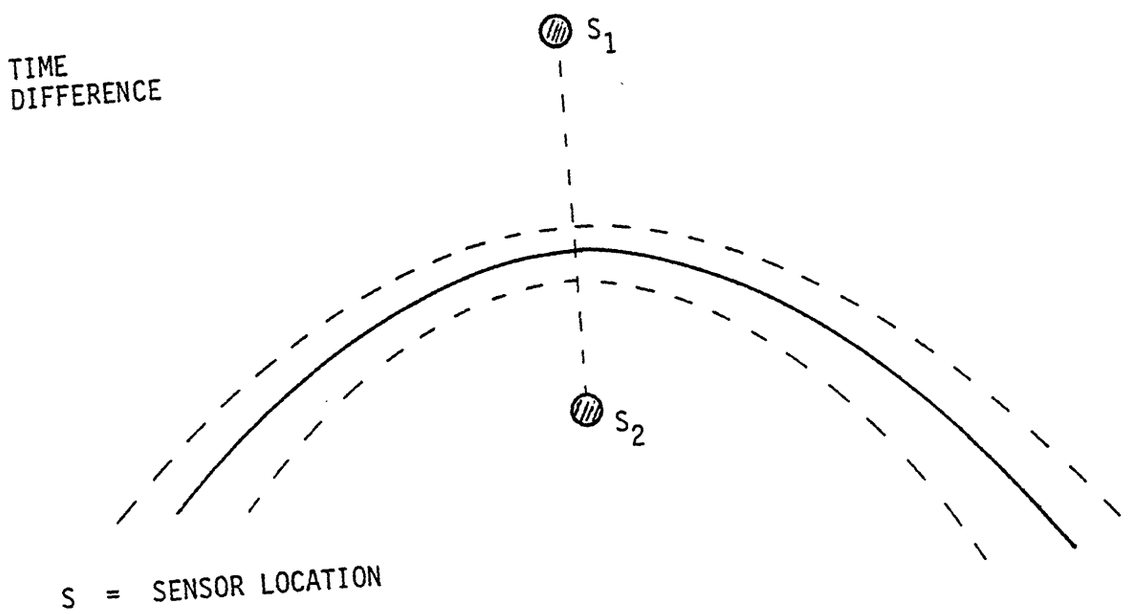

FORMS OF
POSITION AND VELOCITY INFORMATION

POSITION	PROCESSING CONSIDERATIONS
FIX + ELLIPSE	KALMAN FILTER UPDATES OF STATE VECTOR
LOB + ACCURACY	EXTENDED KALMAN FILTER REQURIED FOR UPDATES
HYPERBOLIC LOP (TIME DIFFERENCE + ACCURACY)	EXTENDED KALMAN FILTER REQUIRED FOR UPDATES REQUIRES MULTISITE ASSOCIATION
VELOCITY	PROCESSING
DOPPLER SHIFT + ACCURACY	RADIAL VELOCITY INCORPORATED IN FILTERS MEASUREMENT UPDATE
DOPPLER DIFFERENCE + ACCURACY	REQUIRES MULTISITE ASSOCIATION
TRACK SEGMENT	FROM SENSORS WHICH CREATE A TRACK AS PART OF THE SIGNAL DETECTION PROCESS

EXAMPLES OF SENSOR CHARACTERISTICS

SENSOR	TYPE	BASIC LOCATION DATA	CLASSIFICATION DATA
RADAR	A	FIX	SIGNATURE E.G., CROSS SECTION
HF RADAR	A	FIX + DOPPLER	CROSS SECTION
IMAGING RADAR (SAR OR ISAR)	A	FIX	IMAGE
PHOTO OR VISUAL	PI	FIX	IMAGE
ACOUSTIC ARRAYS	PI	LOB (ΔT,ΔD)	SIGNATURE (ACOUSTIC FREQUENCIES)
ELINT	PV	LOB (ΔT)	SIGNATURE (EMISSION PARAMETERS)
HFDF	PV	LOB	SIGNATURE OR MESSAGE CONTENT

KEY: A = ACTIVE
PI = PASSIVE INVOLUNTARY
PV = PASSIVE VOLUNTARY
LOB = LINE OF BEARING
ΔT = TIME DIFFERENCE
ΔD = DOPPLER DIFFERENCE

FACTORS INFLUENCING TIMELINESS

- SIGNAL PROPAGATION DELAYS: SIGNIFICANT FOR ACOUSTIC SYSTEMS ($C \simeq 2900K$)
- SIGNAL INTEGRATION TIMES: INTERVAL IS DETERMINED BY REQUIRED FREQUENCY RESOLUTION
- MULTISITE ASSOCIATION PROCESSING: FOR SOURCES WHOSE BASIC MEASUREMENT IS NOT A FIX
- CLASSIFICATION PROCESSING: IMAGE INTERPRETATION OR FINGERPRINT MATCHING
- TRANSMISSION DELAYS

SURVEILLANCE NETWORKS

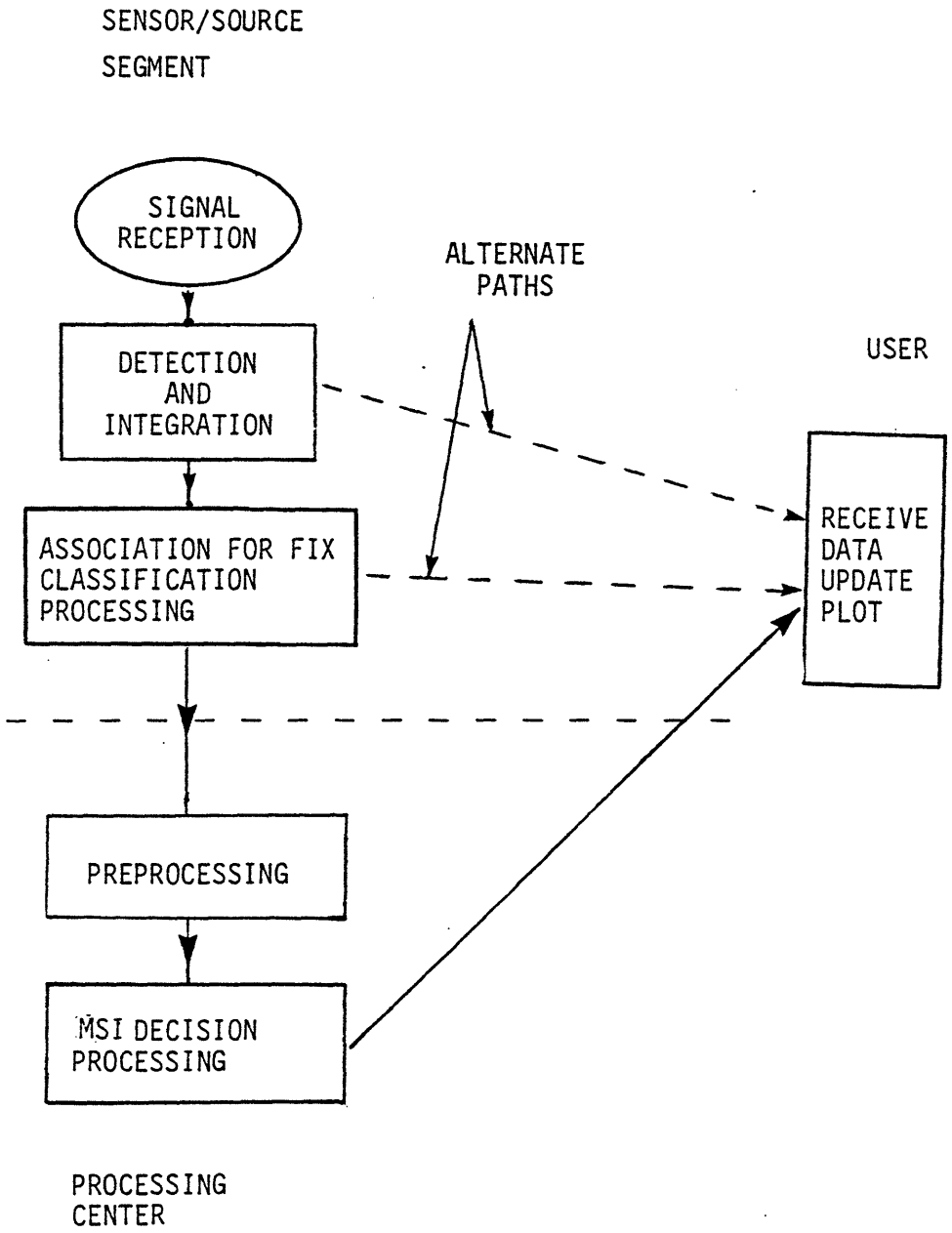

A SOURCE NETWORK

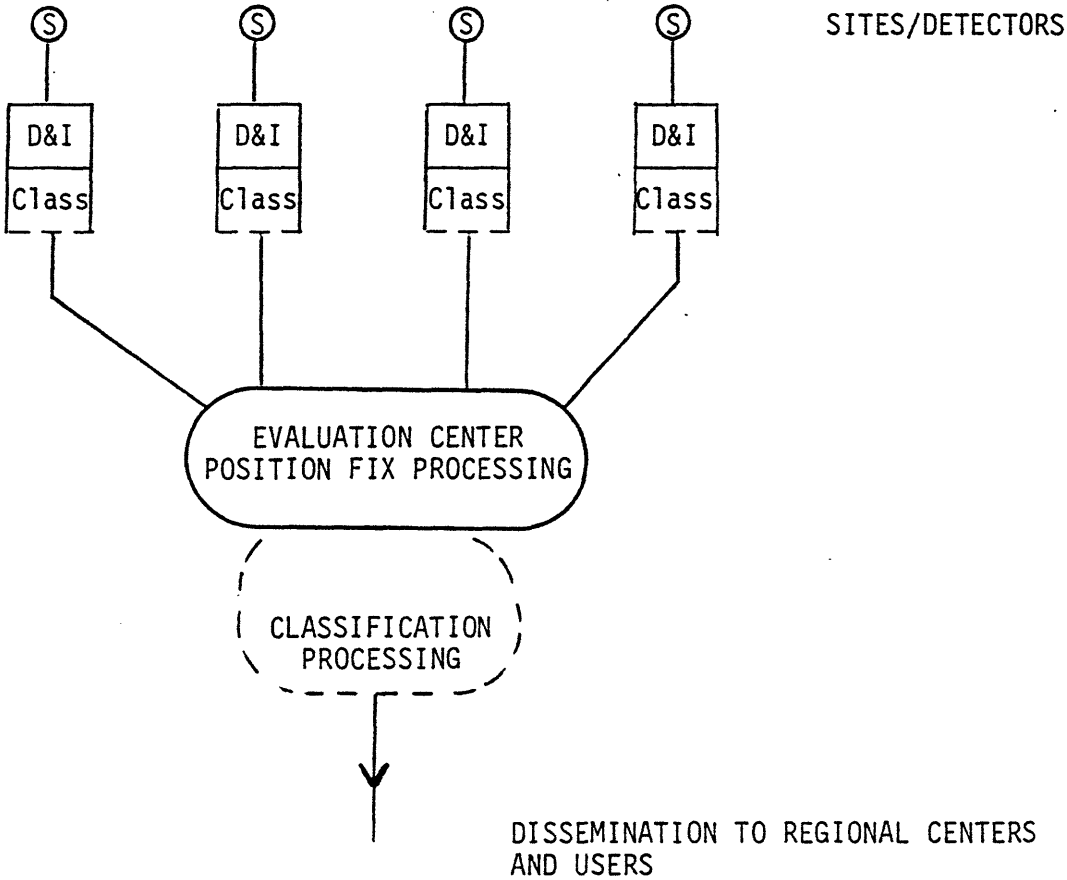

KEY: S = SENSOR

D&I = DETECTION AND INTEGRATION

CLASS = CLASSIFICATION PROCESSING

CLASSIFICATION PROCESSING OPTIONS

CLASSIFICATION PROCESSING CAN TAKE PLACE:

IMMEDIATELY AFTER SIGNAL INTEGRATION
AT A SOURCE CENTER IN CONJUNCTION WITH FIX DETERMINATION
AT A REGIONAL PROCESSING CENTER

CONSIDERATIONS:

EARLY CLASSIFICATION

- REDUCES DATA LOAD DOWNSTREAM FROM THE SOURCE
- CAN REDUCE VULNERABILITY IF THE USER CAN PROCESS THE BASIC POSITION DATA
- INCREASES THE FEEDBACK DATA LOAD BY MULTIPLYING FINGERPRINT DATA BASES

CENTRAL CLASSIFICATION

- CAN REQUIRE TRANSMISSION OF ADDITIONAL SIGNATURE DATA FROM THE SOURCE
- INCREASES THE LIKELIHOOD AND LEVEL OF CLASSIFICATION THROUGH MULTI-SOURCE DATA ASSOCIATION
- ENSURES A CONSISTENT REGIONAL PICTURE

SIGNATURE PROCESSING

TWO BASIC USES:

- COMPARISON OF REPORT AND TRACK SIGNATURES TO ESTABLISH A TRACK DESIGNATOR
- CLASSIFICATION OF TARGETS VIA A MATCH WITH FINGERPRINT FILE DATA

REQUIREMENTS:

- FEEDBACK FROM REGIONAL AND NATIONAL CENTERS TO MAINTAIN CURRENT FINGERPRINT FILES. (UPDATES INITIATED FOLLOWING EACH ASSOCIATION DECISION.)
- DETERMINATION OF CONFIDENCE OF CLASSIFICATION IS CRITICALLY DEPENDENT ON COMPLETENESS OF FINGERPRINT DATA.
- DATA ON GENERAL AREAS OF CONTAINMENT FOR TARGETS (POPULATION ANALYSIS) CAN BE USED TO ENHANCE THE ASSOCIATION ANALYSIS.
- TIME DEPENDENCE OF PARAMETERS, ARISING FROM CHANGES IN ASPECT OR ALTERED SOURCE CHARACTERISTICS, MUST BE MODELED.

DYNAMIC SIGNATURES

ABILITY TO TRACK (ASSOCIATE SUCCESSIVE TARGET OBSERVATIONS)

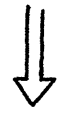

ABILITY TO MAINTAIN CLASSIFICATION FOLLOWING INITIAL ID

GENERALIZED SIGNATURE

= EMISSIONS SIGNATURE

+ GEOGRAPHIC CONTAINMENT

MSI PRINCIPLES

- POSITION COMPARISON AT SIMULTANEOUS VIEW
- TRACK MATCHING (A MORE COMPLEX POSITION COMPARISON)
- CHARACTERISTIC CONSISTENCY TESTS (E.G., ONLY CLASS A HAS RADARS OF TYPE B)
- OPERATIONAL CHARACTERISTICS (E.G., SHIPS NORMALLY COMMUNICATE WITH A TRAFFIC CONTROL NEAR THIS LOCATION)

DATA FLOW IN A REGIONAL
PROCESSING CENTER

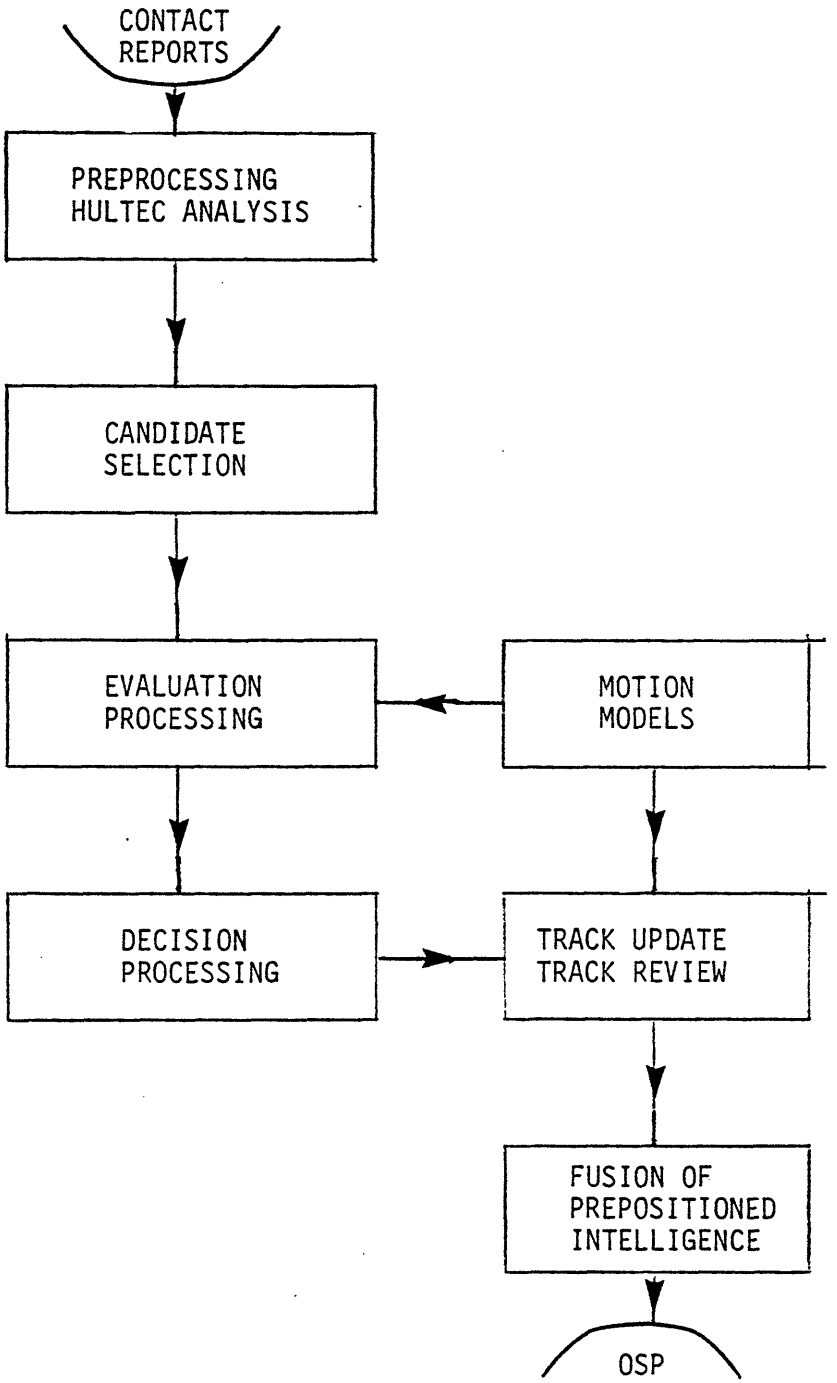

SELECTED MSI PROBLEMS

- MOTION MODELS: VOLITIONAL DYNAMICS
- AMBIGUITY: RESOLUTION AND REPRESENTATION
- CLASSIFICATION CHAINS
- ROBUSTNESS: ALGORITHMS VS. BIAS

VOLITIONAL DYNAMICS

ANALOG OF NEWTON'S FIRST LAW

"TARGETS MOVE AT CONSTANT SPEED ALONG STRAIGHT (RHUMB) LINES, EXCEPT WHEN THEIR COMMANDERS DECREE OTHERWISE."

MANEUVERS:

- INVALIDATE STATISTICAL DISTRIBUTION ASSUMPTIONS
- NECESSITATE EMPIRICAL TESTING OF MOTION MODELS

TIME SCALES:

T_M = TIME TO EXECUTE A TYPICAL MANEUVER

ΔT = MEAN INTERVAL BETWEEN MANEUVERS

FILTER CHOICE IS BASED ON RELATION BETWEEN REVISIT INVERVAL AND THESE TIMES.

AMBIGUITY

- RESOLUTION IS DESIRABLE, BUT THE IMPROVEMENTS WHICH CAN BE ACHIEVED WITHOUT NEW DATA ARE SEVERELY LIMITED

- REPRESENTATION IN A FORM USEFUL TO OPERATIONAL COMMANDS REMAINS AN OPEN PROBLEM

- MULTIPLE HYPOTHESIS SYSTEMS CAN CLARIFY THE REPRESENTATION OF AMBIGUITY, BUT FACTORIAL GROWTH OF STORAGE AND PROCESSING REQUIREMENTS IS A PROBLEM

A CLASSIFICATION CHAIN

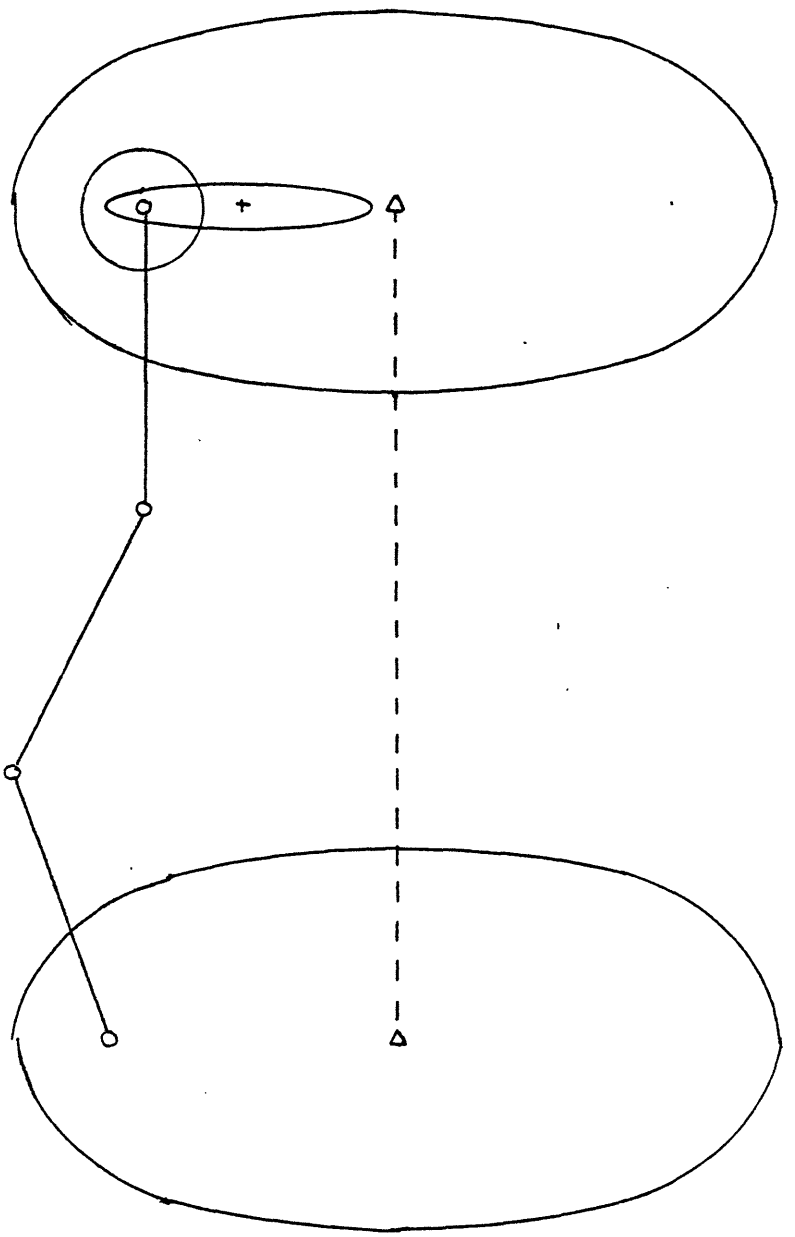

o - RADAR
\+ - ELINT
Δ - HFDF

} Associated by simultaneous view (partial classification)

} Associated by track matching + characteristic consistency (unique ID)

SELECTED DEVELOPMENT PROBLEMS

- MULTIPLE DATA PATHWAYS: THEY SHOULD EXIST BUT NOT NORMALLY BE USED.
- TRACKING UNDER ADVERSITY: SIMULATION TESTS SHOULD BE CONDUCTED IN A RUTHLESS MANNER.
- AUTOMATION: AN INTERACTIVE INTERFACE IS AN ESSENTIAL DEVELOPMENT TOOL, EVEN FOR "HANDS-OFF" SYSTEMS.
- SOPHISTICATED DECISION ALGORITHMS: THESE MAY REPRESENT A TACIT ADMISSION OF FAILURE IN OVERALL SYSTEM DESIGN.

MEMORY DETECTION MODELS FOR PHASE-RANDOM OCEAN ACOUSTIC FLUCTUATIONS

Harilaos N. Psaraftis

Anastassios N. Perakis

Massachusetts Institute of Technology
Cambridge, Mass. 02139

Peter N. Mikhalevsky

Naval Underwater Systems Center
New London, CT. 06320

(Work on this paper has been supported by the Office of Naval Research (Code 431) under contract N00014-79-C-0238)

MEMORY DETECTION MODELS FOR PHASE-RANDOM OCEAN ACOUSTIC FLUCTUATIONS

Harilaos N. Psaraftis[1] Anastassios N. Perakis[1] Peter N. Mikhalevsky[2]

1 Massachusetts Institute of Technology, Cambridge, Mass. 02139
2 Naval Underwater Systems Center, New London, CT. 06320

ABSTRACT

The basic problem of the ocean acoustic detection process is formulated analytically under the assumption of fully developed saturated phase random multipath acoustic fluctuations. Detection is defined as occuring whenever ρ, the root mean square pressure at the receiver, exceeds a specified threshold level ρ_0. A continuous time model is first developed for obtaining the probability density functions of the time between two successive detections and of the time ρ is above ρ_0 (holding time). This model is then compared with the extensively used (λ, σ) model and with data. The model is seen to exhibit similar long-term behavior but markedly different short-term characteristics as compared to the (λ, σ) model, a fact which is due to the memory of the process. A comparison of these models with data obtained from various field experiments demonstrates, in most cases, a significantly improved prediction capability over the (λ,σ) model.

Subsequently a two-state and a four-state discrete-time Markov models are derived and closed-form expressions for the probability mass functions of the corresponding interarrival and holding times are developed. The results obtained using the latter models are favorably compared with both the continuous-time model and the data, the greatest improvement lying in the much lower computational effort involved.

1. INTRODUCTION

Much of the work in the area of acoustic detection in the ocean has traditionally been based on the so-called (λ, σ) model characterized by the "relaxation time" $1/\lambda$ and the standard deviation σ of the "signal-to-noise ratio" [1]. Use of this model has relied heavily on parameter estimation from field experiments without application of the relevant physical and probabilistic structures of the process.

This situation has been improved recently by the efforts of several authors ([2] to [8]). Under the assumption of a fully developed saturated multipath phase-random field, probability distributions for several random variables such as ρ, the root mean square pressure at the receiver, $\dot{\rho} = d\rho/dt$, ϕ. the phase and $\dot{\phi} = d\phi/dt$, as well as many joint probability distributions have been derived. This new knowledge has enabled us to develop new continuous and discrete-time detection models, which are described in the following.

2. THE CONTINUOUS-TIME DETECTION MODEL

In this paper, detection at time t is defined as an upcrossing event for random variable ρ, through a specified threshold level ρ_0, as follows:

$$\rho(t) = \rho_0, \quad \dot{\rho}(t) \geq 0 \tag{1}$$

The unconditional probability of detection, denoted by $\lambda_1\, dt$, is by definition the probability that (1) is satisfied at some instant of time in the interval (t, t+dt) where t is random and dt is small.

It is straightforward to show [3, 8, 14] that if σ_1^2 is one half the long time average mean square pressure and ν is the root mean square single path phase rate (in rad/sec), then λ_1 (in sec^{-1}) is given by the following formula:

$$\lambda_1 = \frac{\rho_0 \nu}{\sigma_1 \sqrt{2\pi}} \exp(-\rho_0^2/2\sigma_1^2) \tag{2}$$

Eq. (2) holds under the assumptions of the phase random multipath model [4], in which ρ has a Rayleigh PDF, $\dot{\rho}$ a Gaussian PDF, and $\rho, \dot{\rho}$ are independent.

We call λ_1 the "unconditional detection rate" or the "per unit time unconditional probability of detection"; λ_1 is the average number of detections (or "arrivals") per unit time.

The conditional probability of detection, denoted by $\phi(t)dt$, is defined as the probability that a detection occurs at some instant of time in the interval (t, t+dt), given a detection occurred at time 0.

It is again straightforward to show [14] that if $f_{\rho_1\rho_2\dot{\rho}_1\dot{\rho}_2}(\rho_1,\rho_2,\dot{\rho}_1,\dot{\rho}_2)$ is the joint PDF of $\rho_1,\rho_2,\dot{\rho}_1,\dot{\rho}_2$, where subscripts 1 and 2 refer to times 0 and t respectively, then $\phi(t)$ (in sec^{-1}) is given by the following formula:

$$\phi(t) = \frac{1}{\lambda_1} \int_0^\infty \int_0^\infty \dot{\rho}_1 \dot{\rho}_2 f_{\rho_1\rho_2\dot{\rho}_1\dot{\rho}_2}(\rho_0,\rho_0,\dot{\rho}_1,\dot{\rho}_2) d\dot{\rho}_1 d\dot{\rho}_2 \tag{3}$$

We call $\phi(t)$ the "conditional detection rate", or the "per unit time conditional probability of detection". If the detection process had no memory, $\phi(t)$ would be equal to λ_1 for all t. Evaluation of (3) for the phase random process has however shown that this is not the case. Results showed that $\phi(t) \to 0$ as $t \to 0$ and $\phi(t) = \lambda_1$ for $t \geq t_0$. t_0 is the decorrelation time of the process and was observed to be in the neighborhood of $3/2\pi\nu$ to $4/2\pi\nu$. For t between 0 and t_0, the behavior of $\phi(t)$ was observed to be either monotonically increasing up to t_0, or to have a peak higher than λ_1 at some intermediate value of t. The existence of the peak was seen to depend on the selected value of σ_1, ν and ρ_0. A conditional probability similar to $\phi(t)$ is $\psi(t)$, defined as the probability that a downcrossing through ρ_0 occurs at some instant of time within (t, t+dt), given that an upcrossing occured at t=0. The formula giving $\psi(t)$ is similar to (3), the following:

$$\psi(t) = \frac{dt}{\lambda_1} \int_0^{\infty} \int_{-\infty}^{0} |\dot{\rho}_1 \dot{\rho}_2| f_{\rho_1 \rho_2 \dot{\rho}_1 \dot{\rho}_2}(\rho_0, \rho_0, \dot{\rho}_1, \dot{\rho}_2) d\dot{\rho}_1 d\dot{\rho}_2 \tag{4}$$

We now proceed to evaluate the PDF's of the interarrival and holding times:

We use the term "interarrival time" to denote the time between two successive detections. The exact evaluation of the PDF of the interarrival time seems to be very difficult. Rice [11], Longuet-Higgins [12] and McFadden [13] have presented several approaches to this problem in the general context of axis-crossing of random functions. We propose here the technique used successfully by Psaraftis [9], which states that a good way to approximate the above PDF is by the function:

$$F(t) = \begin{cases} \phi(t) \exp(-\int_0^t \phi(x)dx) & t>0 \\ 0 & t\leq 0 \end{cases} \tag{5}$$

We now define "holding time" to be the interval between any upcrossing through the threshold ρ_0 and the first downcrossing through ρ_0 that follows. By analogy, the PDF of the holding time can be approximated as follows:

$$H(t) = \begin{cases} \psi(t) \exp(-\int_0^t \psi(x)dx) & t>0 \\ 0 & t\leq 0 \end{cases} \tag{6}$$

where $\psi(t)$ is obtained by (4).

The determination of the interarrival and holding time PDF's exhibits a non-trivial complexity. The reason is that the joint PDF inside the integrals $f_{\rho_1,\rho_2,\dot{\rho}_1,\dot{\rho}_2}(\rho_1,\rho_2,\dot{\rho}_1,\dot{\rho}_2)$ is itself difficult to evaluate. In [4] & [11] it is shown that ρ_1 and ρ_2 are linked in a rather complex fashion, involving Bessel functions. Moreover, the correlation of ρ_1 with $\dot{\rho}_2$ and of ρ_2 with $\dot{\rho}_1$ is not a well-established function.

The exact evaluation of $\phi(t)$ and $\psi(t)$ involves the execution of a total of 3 nested numerical integrations. This was the reason why the computer implementation of the model originally presented significant computational difficulties. Subsequent refinements of this model were based on an approximation to the definition of detection using a modified but equivalent detection criterion that produced very accurate results with significantly reduced computational effort [14].

We now proceed to briefly describe the currently used (λ, σ) model and put it in a form compatible to our model:

The basic assumption of the (λ, σ) model is that "detection opportunities" are generated in time according to a Poisson process of parameter λ [1]. The reciprocal of λ is known as the "relaxation time" of the process and its value is usually taken arbitrarily from empirical considerations of the process, and without any explicit relationship to the detection threshold level. At any particular detection opportunity, a detection occurs if the level Λ in dB ($\Lambda = 10\log_{10} \rho^2$), which is assumed to be normally distributed, exceeds a specified threshold level Λ_o.

It is argued in [14] that a common basis of comparison between the (λ, σ) model and our continuous-time detection model should produce equal unconditional probabilities for both models. It turns out that in order to satisfy this requirement, the values of λ can be no longer be taken arbitrarily, but according to the formula:

$$\lambda = \frac{\nu \rho_0}{\sigma_1 \sqrt{2\pi}} \tag{7}$$

The above value of λ is called "equivalent λ". It is the value that λ should take in the (λ, σ) model so that this model has the same average number of detections per unit time with our new detection models. Hence, all comparisons of the (λ, σ) model with the continuous-time model implicitly assume that λ takes the above value. If this is the case, the (λ, σ) model has, in terms of our previously defined terminology, the following properties:

a) $\phi(t) = \psi(t) = \text{const} = \lambda_1$ (no memory)
b) PDF for interarrival time: Negative exponential given by: $f_t(t) = \lambda_1(\exp(-\lambda_1 t);\ t\geq 0$
c) PDF for holding time: 1/2-order Erlang (or Gamma) given by:

$$f_t(t) = \frac{\lambda_1}{\pi t} \exp(-\lambda_1 t); \quad t>0$$

We will now see how the continuous-time and the (λ, σ) models compare with the data that was made available to us.

From the analysis of the CASE experiment [7, 16] which was done at ranges varying from 200 to 400 km and frequencies of 15 and 33 Hz, we chose to present Record 21. Although a record of low signal-to-noise ratio, this was chosen for being one of the few records examined that satisfy the phase-randomness assumption, an assumption on which our detection models are based. In Figs. 1 (Interarrival Times) and 2 (Holding Times), a threshold of $\rho_0 = 1.75\sigma_1 = 7$ volts, $\sigma_1^2 = 15.95$ volts^2 and $\nu = .1734$ Hz were used. In both cases, the (λ, σ) model, unlike our model, fails to match the observed experimental histogram for small values of t ($t \to 0$). On the other hand, both models predict

equally well the behavior for times greater than the decorrelation time.

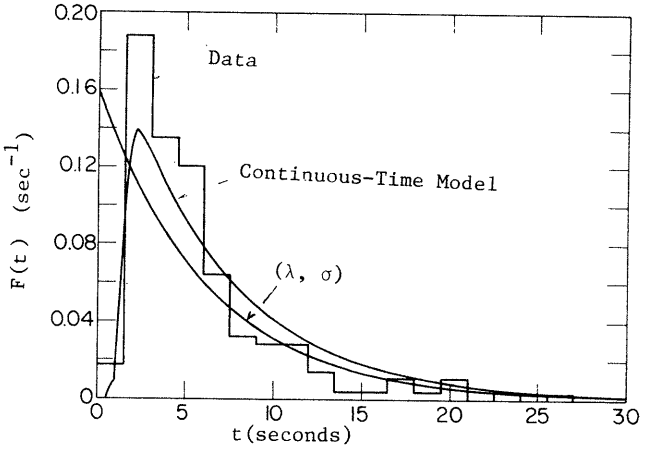

Fig. 1: Continuous Time Model. Interarrival Time

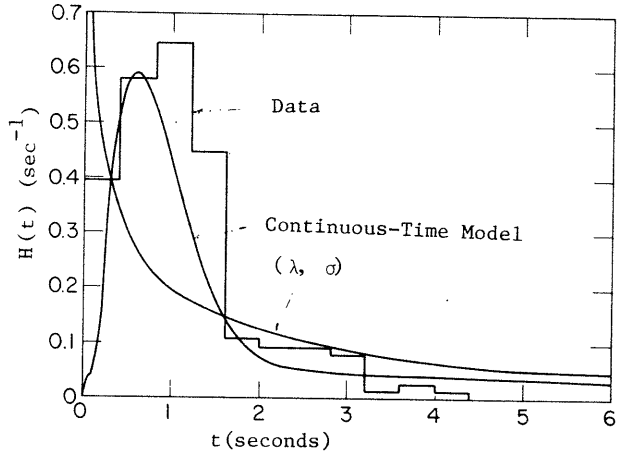

Fig. 2: Holding Time, Continuous Time Model

3. DISCRETE-TIME DETECTION MODELS

We now present equivalent discrete-time Markov models that are computationally less complex than the continuous time model and that can be more readily interfaced with sequential decision-making schemes such as target tracking algorithms. Two discrete-time models have been developed:

3.1. Two-State Markov Model

We define states U (for "up" and D (for "down") by the requirements $\rho \geq \rho_0$ and $\rho < \rho_0$ respectively, where ρ, ρ_0 are as defined for the continuous-time model. We assume that we observe the system at discrete points in time, 0,T,2T,..,nT,.., where T is a user-specified time increment. Then, for the Markov model of Figure 3, we have the following transition probabilities:

P_{UD} = prob($\rho < \rho_0$ at time T | $\rho \geq \rho_0$ at time 0) = a

P_{UU} = prob($\rho \geq \rho_0$ at time T | $\rho \geq \rho_0$ at time 0) = 1-a

P_{DU} = prob($\rho \geq \rho_0$ at time T | $\rho < \rho_0$ at time 0) = b

P_{DD} = prob($\rho < \rho_0$ at time T | $\rho < \rho_0$ at time 0) = 1-b

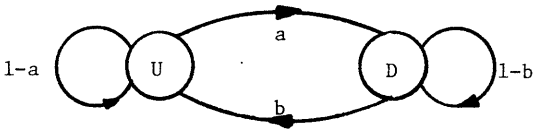

Fig. 3: Two-state Markov Model

If ρ_1, ρ_2 are the values of ρ at times 0 and T respectively, then we can evaluate a and b as follows:

$$a = \int_{\rho_0}^{\infty}\int_{0}^{\rho_0} f_{\rho_1\rho_2}(\rho_1,\rho_2)d\rho_1 d\rho_2 \Big/ \int_{\rho_0}^{\infty} f_\rho(\rho)d\rho$$

$$b = \int_{0}^{\rho_0}\int_{\rho_0}^{\infty} f_{\rho_1\rho_2}(\rho_1,\rho_2)d\rho_1 d\rho_2 \Big/ \int_{0}^{\rho_0} f_\rho(\rho)d\rho \qquad (9)$$

From [4] we know that

$$f_\rho(\rho) = \frac{\rho}{\sigma_1^2}\exp\left(\frac{-\rho^2}{2\sigma_1^2}\right), \text{ and that} \qquad (10)$$

$$f_{\rho_1\rho_2}(\rho_1,\rho_2) = \frac{\rho_1\rho_2}{\mu^2(1-\gamma^2)} I_0\left[\frac{\rho_1\rho_2}{\mu(1-\gamma^2)}\right]\exp\left[-\frac{(\rho_1^2+\rho_2^2)}{2\mu(1-\gamma^2)}\right] \qquad (11)$$

In (11) $\mu = \sigma_1^2$, $\gamma = \exp(-\nu^2T^2/2)$ and $I_0(x)$ is the modified Bessel function of order zero.

We now proceed to find expressions for the interarrival and holding time Probability Mass Functions (PMF's) using the two-state model. Suppose the following sequence of transitions:

Discrete time	0	1	2	3	..k,	k+1,	k+2	..n,	n+1
state	D	U	U	U	U	D	D	D	U

Then we define as

i) $P_H(k) \equiv$ prob(holding time = kT)

$\equiv$ prob (downcrossing between k and k+1 | upcrossing between 0 and 1)

Then $P_H(k) = b(1-a)^{k-1}a/b = (1-a)^{k-1}a$ (12)

and

ii) $P_I(n) \equiv$ prob(interarrival time = nT) =

$\equiv$ prob(upcrossing between n and n+1 | upcrossing between 0 and 1)

Then $P_I(n) = \sum_{k=1}^{n-1} b^2(1-a)^{k-1}a(1-b)^{n-k-1}/\omega$, or

$$P_I(n) = ab\sum_{k=1}^{n-1}(1-a)^{k-1}(1-b)^{n-k-1} \qquad (13)$$

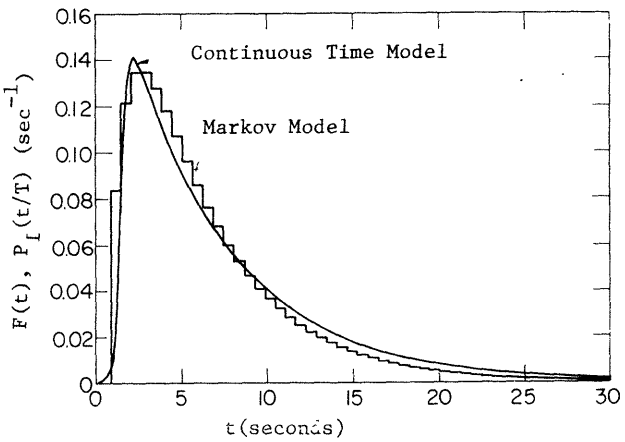

Fig. 4: Interarrival Time, 2-State Markov Model

Figure 4 presents a comparison of the interarrival time PMF of the two-state Markov model with the interarrival time PDF of the continuous-time model for Record 21 of the CASE data. (The data histogram for this record is shown in Fig. 1). The agreement of this very simple Markov Model with the data as well as with the continuous time predictions is quite satisfactory. The only parameter that has to be calibrated by the user is the time step T, which can be seen in Fig. 4 to be T = .6 sec. The results of a cursory sensitivity analysis showed that the form of the PMF predicted by the Markov model does not change appreciably over reasonable (less than one order of magnitude) changes in T. The holding time prediction of the two-state model sometimes compares with the data even better than that of the continuous-time model. Still, its form does not fully satisfy our intuition, since it has its most probable value in the first time increment (similarly to the (λ, σ) model having its mode at t=0). This somewhat counter-intuitive result, together with the apparent simplicity of the two-state model in its description of the dynamics of the underlying process, has motivated us to formulate a more refined Markov model, discussed below:

3.2. Four-State Markov Model

Introducing two additional states in the two-state model, we obtain the model of Figure 5, where we have:

State 1: $0 \leq \rho < \rho_0'$

State 2: $\rho_0' \leq \rho < \rho_0$

State 3: $\rho_0 \leq \rho < \rho_0''$

State 4: $\rho_0 \leq \rho < \infty$

Here ρ_0', ρ_0'' are artifical thresholds, chosen by the user. As before, the user also selects the time increment T. As it can be seen from Fig. 4 the system is a birth-death process.

For a given value or T, the transition probabilities of the four-state Markov model can be evaluated from the PDF's $f_\rho(\rho)$ and $f_{\rho_1,\rho_2,}(\rho_1,\rho_2)$ in a similar fashion as those for the two-state model. However, the derivation of expressions for

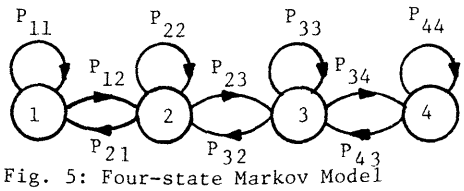

Fig. 5: Four-state Markov Model

the PMF's of the interarrival and holding times because now more involved, because "up" states are now states 3 and 4 and "down" states are states 1 and 2.

Defining $P_H(k)$ and $P_I(n)$ as in the two-state model, and also

$$P_N(n-k) \equiv \text{prob (non-holding time} = (n-k)T)$$
$$\equiv \text{prob (upcrossing between n and n+1} \mid \text{downcrossing between k and k+1)}$$

then it can be seen that

$$P_I(n) = \sum_{k=0}^{n} P_H(k)\, P_N(n-k) \qquad (14)$$

These PMF's can be evaluated by working in the z-transform domain, using modified flow graphs. It can be shown that the holding time PMF is given by the formula

$$P_H(n) = P_{32}[A^n - B^n - P_{44}(A^{n-1} - B^{n-1})]/(A-B) \qquad (15)$$

and that the non-holding time PMF by the formula

$$P_N(n) = P_{23}[C^n - D^n - P_{11}(C^{n-1} - D^{n-1})]/(C-D) \qquad (16)$$

where A,B,C and D are constants given in terms of the transition probabilities as follows:

$$A = 1/2[P_{33}+P_{44}+\sqrt{(P_{33}-P_{44})^2 + 4P_{43}P_{34}}]$$
$$B = 1/2[P_{33}+P_{44}-\sqrt{(P_{33}-P_{44})^2 + 4P_{43}P_{34}}]$$
$$C = 1/2[P_{11}+P_{22}+\sqrt{(P_{11}-P_{22})^2 + 4P_{12}P_{21}}]$$
$$D = 1/2[P_{11}+P_{22}-\sqrt{(P_{11}-P_{22})^2 + 4P_{12}P_{21}}]$$

Hence $P_I(n)$ can be evaluated by substituting (15) and (16) into (14).

Figure 6 is similar to Figure 4, with the difference that here the continuous-time model is compared with the four-state Markov model. (same CASE 21 Record as in Figs. 1 and 4). The results of the four-state model are only slightly superior to the ones of the two-state model. Here ρ_0' and ρ_0'', as well as T, have to be selected by the user. In Figure 6, T = .6 sec, $\rho_0' = 3.5$, $\rho_0'' = 14.$, with $\rho_0 = 7.$ volts, $\sigma_1^2 = 15.95$ volts^2 and $\nu = .1734$Hz same as in the two-state discrete-time and the continuous-state model comparisons. A brief sensitivity analysis has shown that better results are obtained for levels of ρ_0', ρ_0'' not close to ρ_0, (namely, $\rho_0' \leq \rho_0/2$ and $\rho_0'' \geq 2\rho_0$).

4. DISCUSSION AND CONCLUSIONS

The main conclusion from this study is that for phase-random ocean acoustic fluctuations, the

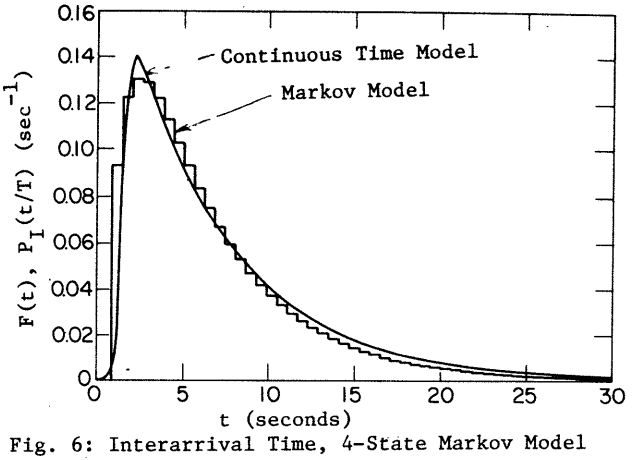

Fig. 6: Interarrival Time, 4-State Markov Model

detection process has memory. In that respect, a detection now will very strongly influence the probability of another detection at some time in the immediate future. Both continuous and discrete-time models as well as most of the data have shown that it is unlikely to have two detections separated by a short time interval. On the other hand, two detections separated by a sufficiently long time interval are uncorrelated. The de-correlation interval is a weak function of the selected threshold level ρ_0, yet it is always of the order of $.4/\nu$ to $.6/\nu$ (in seconds where ν is in Hz).

All models developed in this paper agree with the above. The properly used (λ, σ) model, exhibits a satisfactory behavior for large enough times, yet is unable, being memoryless, to correctly predict the detection probability immediately after a detection. Therefore, depending upon the magnitude of our time intervals with respect to the decorrelation time, the (λ, σ) behavior may (for long enough times) or may not (for short times) hold. Experimental histograms are much more in agreement with the PDF's (or PMF's) of our models than with the corresponding PDF's of the (λ, σ) model. The latter is always unable to predict the zero probability of a very short interarrival or holding time, exhibiting on the contrary its most likely values at zero time for both interarrival and holding time PDF's. Moreover, the (λ, σ) model makes poor predictions of the mode (which is always zero for both interarrival and holding time), whereas our continuous time model and the data examined suggest numbers in the ranges of $.4/\nu$ to $.3/\nu$ for the interarrival time and $.2/\nu$ to $.1/\nu$ for the holding time. If ν is small enough, therefore, the (λ, σ) predictions are quite inaccurate. Concerning the mean arrival and holding times, our model predictions are in better agreement with the observed values than the predictions of the (λ, σ) model.

Since the Markov models are efficient and accurate, they could be used in sequential decision-making schemes such as target tracking algorithms, they should be studied further, beginning with a more comprehensive sensitivity analysis for the calibration of arbitrarily chosen parameters (T, ρ_0', ρ_0'').

Finally, it should be noted that the detection models developed in this paper are not bound to assume a phase random model; their analysis framework can always accommodate any other model of acoustic propagation, provided that enough is known about the various PDF's of the relevant acoustic variables.

ACKNOWLEDGEMENTS

Work on this paper has been supported by the Office of Naval Research (Code 431) under contract N00014-79-C-0238. Results on the continuous-time model are a condensed version of Reference [14], a paper by the same authors submitted for publication in the Journal of the Acoustical Society of America.

REFERENCES

[1] Mc. Gabe, B.J. and Belkin, B., "A Comparison of Detection Models Used in ASW Operations Analysis," Daniel H. Wagner Associates, Paoli, PA, 1973.

[2] Dyer, Ira, J. Acoust. Soc. Am. 48, 337-345(1970).

[3] Dyer, Ira and Shepard, G.W., J. Acoust. Soc. Am., 61, 937-942 (1977).

[4] Hamblen, W.R. "Phase Random Multipath Model for Acoustic Signal Fluctuation in the Ocean and its Comparison with Data." Ph.D. Thesis, M.I.T. (1977).

[5] Mikhalevsky, P.N. and Dyer, Ira, J. Acoust. Soc. Am., 63, 732-738 (1978).

[6] Mikhalevsky, P.N. J. Acoust. Soc. Am. 66, 751-762 (1979).

[7] Mikhalevsky, P.N., "The Statistics of Finite Bandwidth, Modulated Acoustic Signals Propagated to Long Ranges in the Ocean, Including Multiple Source Effects," Ph.D. Thesis, M.I.T. 1979.

[8] Mikhalevsky, P.N., J. Acoust. Soc. Am. 67 (3), 812-815, (1980).

[9] Psaraftis, H.N., "Some New Aspects of Slamming Probability Theory", Journal of Ship Research, Vol. 22, No. 3, Sept. 1978.

[10] Perakis, A.N., "A New Probabilistic Detection Model for Phase Random Ocean Acoustic Fluctuations and its Comparison with Data," M.S. Thesis, M.I.T Dept. of Ocean Eng., January 1980.

[11] Rice, S.O., "Mathematical Analysis of Random Noise", Bell System Technical Journal, Vol. 23, 1944 and Vol. 24, 1945.

[12] M.S. Longuet-Higgins, "The Distribution of Intervals Between Zeros of a Stationary Random Function", Royal Phil. Soc., Transactions, Vol. 254, No. 1047, 1962.

[13] Mc Fadden, J.S., "The Axis-Crossing Intervals of Random Functions - II", IRE Transactions on Information Theory, II-4, 1958.

[14] Psaraftis, H.N., Perakis A.N., Mikhalevsky P.N., "New Models on the Ocean Acoustic Detection Process", paper to J.A.S.A. (1980).

[15] Porter, R. and Spindel,R. J. Acoust. Soc. Am. 61, 943-958, (1977).

[16] Anton, J.N., "A Fluctuation Data Base for the CASE Experiment," Technical Report 5204-2, Systems Control, Inc. April 1978.

DETECTION THRESHOLDS FOR MULTI-TARGET TRACKING IN CLUTTER

Thomas E. Fortmann
Bolt Beranek and Newman Inc.
10 Moulton Street
Cambridge, MA 02238

Yaakaov Bar-Shalom
Department of Electrical Engineering
and Computer Science
University of Connecticut
Storrs, Connecticut 06268

Molly Scheffe
Bolt Beranek and Newman Inc.
10 Moulton Street
Cambridge, MA 02238

1. INTRODUCTION

Garden-variety tracking problems involve processing measurements (e.g., range and azimuth observed by a sensor) from a target of interest and producing, at each time step, an estimate of the target's current position and velocity vectors. Uncertainties in the target motion and in the measured values, usually characterized as random noise, lead to corresponding uncertainties in the target state.

A common and versatile approach to such problems involves assuming that the state dynamics and the measurements are both corrupted by additive, white, possibly Gaussian noise; the solution is then the celebrated Kalman-Bucy filter [1, 2, 3, 4, 5], which is the conditional mean state estimator, best linear estimator, maximum a posteriori estimator, maximum likelihood estimator, or least-squares estimator,[1] depending upon one's point of view. The parameters that determine tracking performance in such a filter are the system matrices in the equations describing target state dynamics and measurements, which will be considered fixed for the purposes of this discussion, and the covariance matrices of the process and measurement noise, which specify the uncertainties in target motion and measured values, respectively.

In many tracking problems, particularly those arising in surveillance, there is additional uncertainty regarding the origin of the received data, which may (or may not) include

---

[1] In the least-squares case, the assumptions about noise are replaced by assumptions about error weightings.

measurements from the target(s) of interest, interfering targets, or random clutter (false alarms). This leads to the problem of data association or data correlation, which has been attacked on a number of fronts [6, 7, 8, 9, 10, 11, 12, 13, 14] and surveyed in [15, 16, 17]. In this situation, tracking performance depends not only upon the noise covariances, but upon the amount of uncertainty in measurement origin. In some of the approaches cited above [6, 7, 8, 9, 10], this dependence is explicit and is characterized in terms of the detection probability and clutter density (which is proportional to false alarm probability).

In typical applications, measurement data are provided to a tracker by upstream signal processing and detection algorithms, as indicated in Figure 1. The process noise covariances are normally selected on the basis of experience and intuition (i.e., they are guessed). The measurement noise covariances are either provided by the signal processing algorithm, as shown in the figure, or they are selected in the same manner as the process noise. In any case, the true noise levels are usually fixed by target dynamics and sensor configuration and cannot be adjusted on line.

Detection and false alarm probabilities, on the other hand, are highly interdependent and adjustable via a detection threshold: raising the threshold lowers both probabilities, and vice-versa. This relationship, which is also parameterized by signal-to-noise ratio (SNR), is usually characterized by means of a set of receiver operating characteristic (ROC) curves. The threshold is typically set by choosing a design point on the most applicable ROC curve, based on the perceived tradeoffs between false alarms and missed detections. However, to the best of our knowledge, these tradeoffs have never included any systematic or quantitative consideration of the effects downstream on data association and tracking performance.

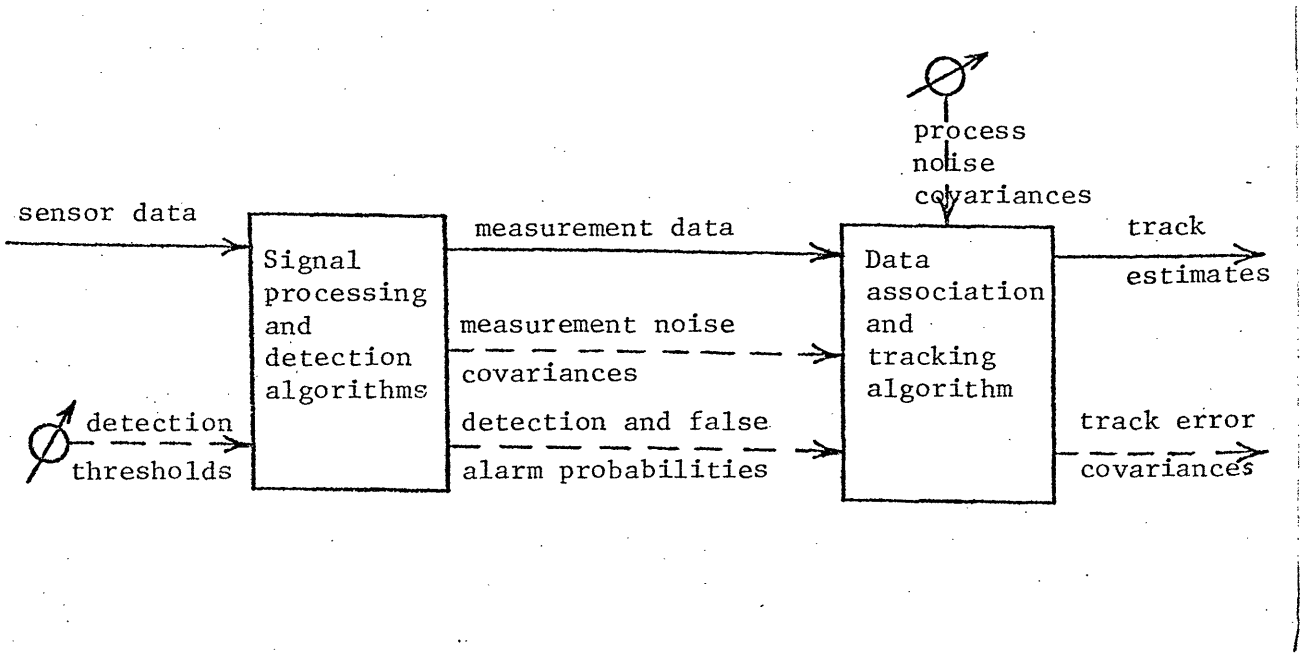

FIG. 1. TRACKING SYSTEM BLOCK DIAGRAM

In this paper we shall describe such a quantitative relationship. The dependence of a tracker's error covariance upon detection and false alarm probability is explicitly (but approximately) characterized by a scalar parameter q_2 in the covariance equation (modified Riccati equation). The scalar parameter depends upon the probabilities of detection and false alarm, and also upon the volume of the data association gate, which in turn depends on the state error covariance matrix $\underline{P}$. The modified Riccati equation can be iterated to convergence, yielding a steady-state $\overline{\underline{P}}$, and tracking performance can be characterized by a scalar metric such as the determinant or trace of $\overline{\underline{P}}$ (in surveillance applications, the root-mean-square position error is a convenient metric). This result is important for the following reasons:

1. Contour plots of the scalar tracking metric as a function of detection probability and false alarm probability form a set of "tracker operating characteristic" (TOC) curves, which can be superimposed on ROC curves for the detector or receiver of interest in order to determine graphically the operating point that "optimizes" tracker performance.

2. The stability of the tracking process depends critically on the detection and false alarm probabilities; a region of apparent instability of the modified Ricatti equation exists in the P_D-P_F plane of the TOC curves.

3. Allocation of tracking resources (both computation and communication) requires prediction of future state error covariances under various resource configurations, i.e., as a function of detection and false alarm probability and of process and measurement noise covariance.

4. The same derivations provide a solution to the related problem of determining the statistical properties of the modified likelihood function [18], used for decision making (e.g. maneuver detection) when measurement origins are uncertain.

A full version of this paper will be presented at and appear in the Proceedings of the 1981 IEEE Conference on Decision and Control.

REFERENCES

1. R. E. Kalman and R. S. Bucy, "New Results in Filtering and Prediction Theory," Trans. ASME: J. Basic Eng., Vol. 83, March 1961, pp. 95-108.

2. I. B. Rhodes, "A Tutorial Introduction to Estimation and Filtering," IEEE Trans. Auto. Control, Vol. AC-16, December 1971, pp. 688-706.

3. A. H. Jazwinski, Stochastic Processes and Filtering Theory, Academic Press, 1970.

4. P. S. Maybeck, Stochastic Models, Estimation, and Control -- Volume 1, Academic Press, 1979.

5. B. D. O. Anderson and J. B. Moore, Optimal Filtering, Prentice-Hall, 1979.

6. Y. Bar-Shalom and E. Tse, "Tracking in a Cluttered Environment with Probabilistic Data Association," Automatica, Vol. 11, September 1975, pp. 451-460.

7. T. E. Fortmann and S. Baron, "Problems in Multi-Target Sonar Tracking," Proc. 1978 IEEE Conf. on Decision and Control, San Diego, California, January 1979.

8. T. E. Fortmann, Y. Bar-Shalom, and M. Scheffe, "Multi-Target Tracking Using Joint Probabilistic Data Association," Proc. 1980 IEEE Conference on Decision and Control, Albuquerque, New Mexico, December 1980.

9. R. Singer, R. Sea, and K. Housewright, "Derivation and Evaluation of Improved Tracking Filters for use in Dense Multitarget Environments," IEEE Trans. Info. Theory, Vol. IT-20, July 1974, pp. 423-432.

10. D. B. Reid, "An Algorithm for Tracking Multiple Targets," IEEE Trans. Auto. Control, Vol. AC-24, December 1979, pp. 843-854.

11. E. Taenzer, "Tracking Multiple Targets Simultaneously with a Phased Array Radar," IEEE Trans. Aerospace and Electronic Systems, Vol. AES-16, September 1980, pp. 604-614.

12. C. L. Morefield, "Application of 0-1 Integer Programming to Multitarget Tracking Problems," IEEE Trans. Auto. Control, Vol. AC-22, June 1977, pp. 302-312.

13. D. L. Alspach, "A Gaussian Sum Approximation to the Multitarget Identification - Tracking Problem," Automatica, Vol. 11, May 1975, pp. 285-296.

14. R. W. Sittler, "An Optimal Data Association Problem in Surveillance Theory," IEEE Trans. Mil. Electron., Vol. MIL-8, April 1964, pp. 125-139.

15. Y. Bar-Shalom, "Tracking Methods in a Multi-Target Environment," IEEE Trans. Auto. Control, Vol. AC-23, August 1978, pp. 618-626.

16. H. L. Wiener, W. W. Willman, I. R. Goodman, and J. H. Kullback, "Naval Ocean-Surveillance Correlation Handbook, 1978," NRL Report 8340, Naval Research Lab, October 1979.

17. I. R. Goodman, H. L. Wiener, and W. W. Willman, "Naval Ocean-Surveillance Correlation Handbook, 1979," NRL Report 8402, Naval Research Laboratory, September 1980.

18. T. E. Fortmann and Y. Bar-Shalom, "Modification of the Likelihood Function to Account for Probabilistic Data Association," BBN Report 3964A (revised), Bolt Beranek and Newman Inc., November 1979, Contract N00039-78-C-0296.

MULTISENSOR MULTITARGET TRACKING FOR INTERNETTED FIGHTERS

Christopher L. Bowman
VERAC, Inc.
10975 Torreyana Road
Suite 300
San Diego, CA 92121

MULTISENSOR MULTITARGET TRACKING FOR INTERNETTED FIGHTERS

C. L. Bowman
VERAC, Incorporated
San Diego, CA 92121

ABSTRACT

The primary value of single platform multisensor integration (MSI) accrues from its synergistic use of multispectral target data, whereas multiplatform internetted surveillance integration, ISI, provides a common display for coordinated attack/defense. This paper introduces the general software architecture and proposes candidate algorithms to solve these sensor integration problems. The focus is on the track correlation problem and the utilization of distributed processing to reduce the computational burden.

1.0 INTRODUCTION

By distributing reliable specialized subsystems throughout our air force, and enhancing the coordinated battle planning capability which nets and exploits those subsystems, we can more cost effectively engage the enemy. The avionics approach to force multiplication advocated herein represents a potentially viable alternative to the current "autonomy and equality" force composition approach with its attendant problems of rising cost, shrinking force size, and reduced force effectiveness. A distributed avionics approach introduces system complexity which must be countered with reliable subsystems and flexible fire control software architectures. The force mix must be adaptable to a variety of situations to reduce single node vulnerability and enhance total force effectiveness. This will require increased subsystem and weapon dependence and a flexible software architecture which can be easily tailored to the mission plug-in modules. The result will be a reliance on stand-off weapons in the initial high-risk confrontations with later transitions to shorter range weapons only as required. Reliable and adaptable integrated surveillance, decision aids and asset control implementation software are necessary to display, assess, and manage this situation so that aircrews can focus on their most pressing problems.

The first step to better utilize sensor and weapon subsystems is automatic data integration, prioritized decision aids, and nonlethal subsystem mode control on the autonomous aircraft level. The functional flow for this integrated surveillance and fire control software is shown in Figure 1-1. The principal components of this software are the distributed sensor processors, multisensor integration (MSI), prioritization, asset management, and the crew displays and controls.

The second step is to net the fighters in order to improve the targeting of stand-off missiles in a dense environment. The overall internetted fighter system concept illustrated in Figure 1-2 is composed of internetted surveillance integration (ISI) and battle planning. ISI is the process of fusing sensor reports for various platforms together to provide a

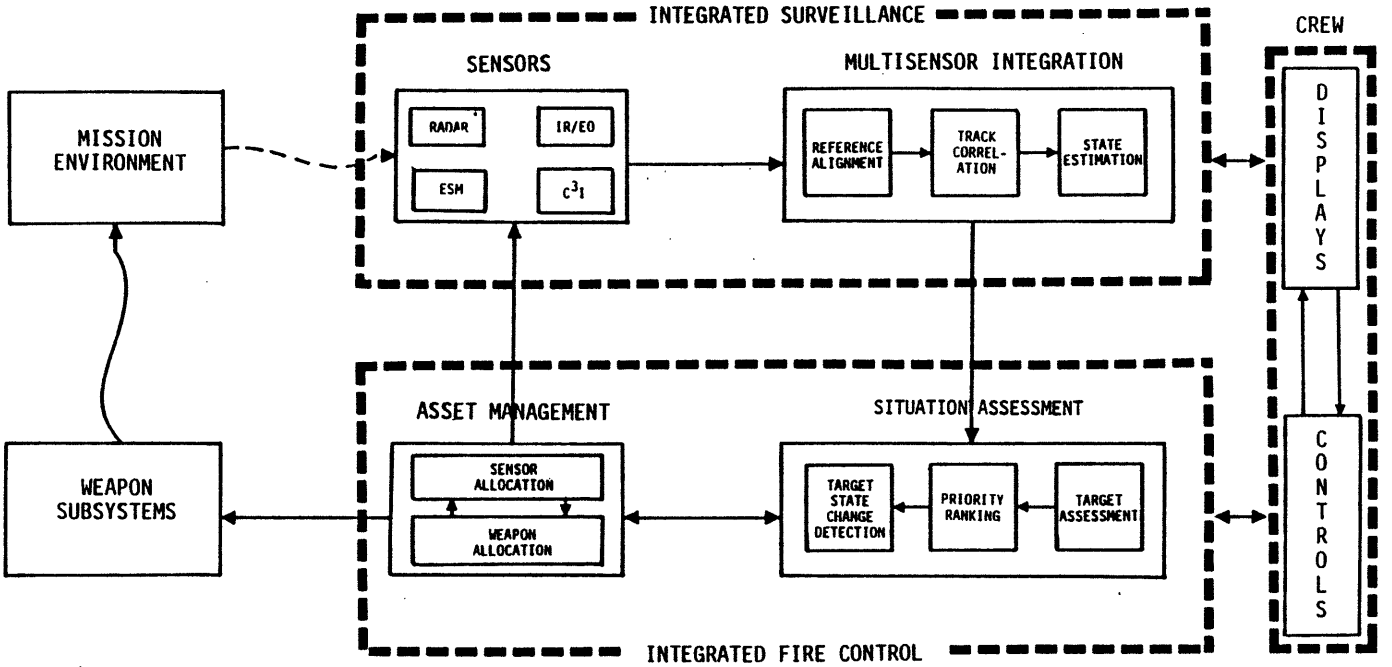

Figure 1-1. Single Aircraft Integrated Surveillance Fire Control

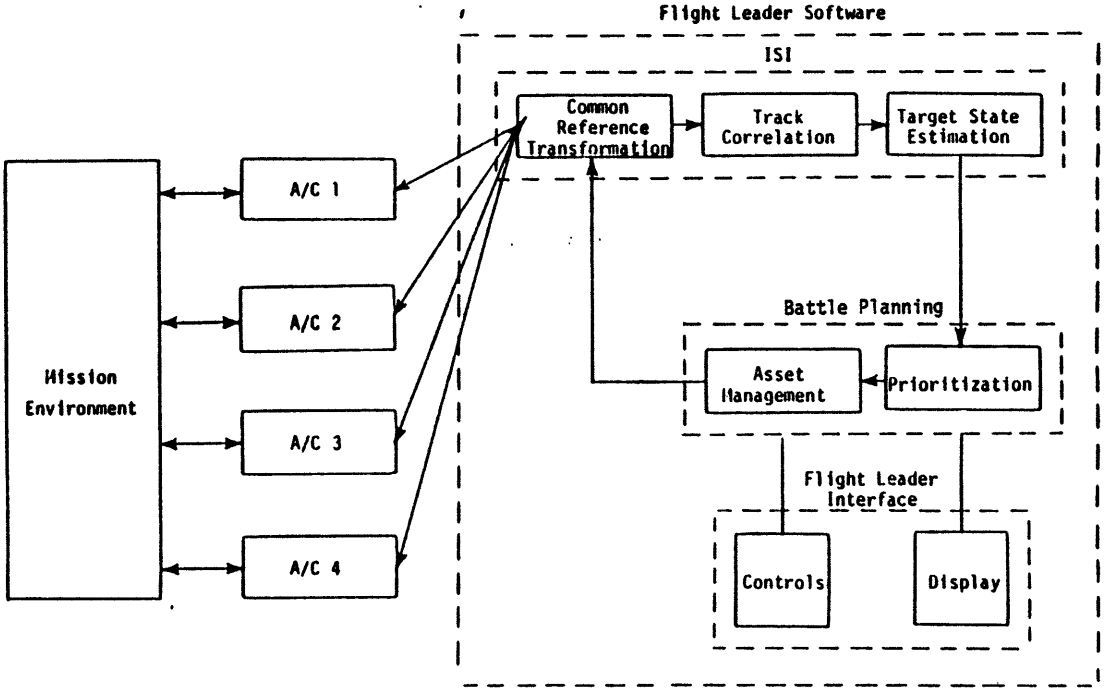

Figure 1-2. Internetted Fighter Concept

common description of the surveillance volume. The concept entails an automated fusion of all the sensors on each fighter in MSI and then a fusion of these MSI files on the flight leader platform. The MSI track file outputs from each fighter are communicated to the flight leader along with the link relative navigation data or GPS inertial data and any C^3I or JTIDS net track data. The baseline ISI performs the common reference processing, track correlation, and target state estimation.

This common ISI surveillance picture is used as the basis for target handover. The threat identification (FFN, Class or Type), prioritization, velocity vector and missile launch envelopes are available for display. Battle planning and asset management is performed by the flight leader. The flight leader software generates the internetted surveillance solution and common display file to aid in command and control of the flight. Each member of the flight must have this same software available so that they may assume the flight leader role when necessary. However, as a flight member they exercise alternate modules to validate these data integration files. As the engagement progresses the targets, that each flight member is engaging, are instantly displayed to the net to aid in their target selection. After target selection, each flight member begins to rely increasingly on his own MSI and decision software. Even so, the internetted processing will continue to be supported, to the extent possible, in order to maintain internetted situation displays and support reassessment and reengagement efforts.

2.0 MULTIPLE SENSOR INTEGRATION

Multiple sensor integration (MSI) is the first step in development of the internetted surveillance track file. The aircraft (MSI) problem, although complex, is summarized as follows: The objective of MSI is to automatically provide the best possible perception of the target set through synergistic use of multispectral sensors as depicted in Figure 2-1. MSI system criteria are of the maximum a posteriori form which incorporate target kinematics and identification data into a single objective functional.

The significant functional components of MSI are common reference processing, track correlation and target state estimation. The problem posed by track correlation can be segmented into hypothesis generation, evaluation, and selection. This problem is solved by utilizing the target kinematics and classification data as well as the a priori sensor and target information. The significant processing options selected for the implementation of the MSI functional components are shown in Figure 2-2. Although the best performance is obtained using the right-most column, the path shown has been selected to yield the best tradeoff of performance for reduced computational complexity/cost.

The resulting software development follows a two-step process defined as follows: Fusion Tree Selection, and Fusion Node Processing Description.

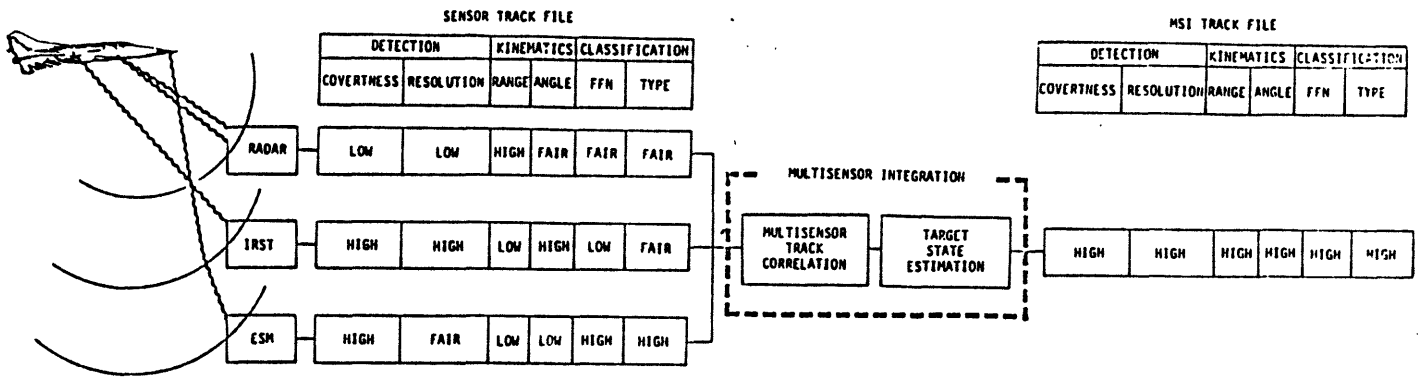

Figure 2-1. MSI Provides Synergistic Use of Multispectral Sensors

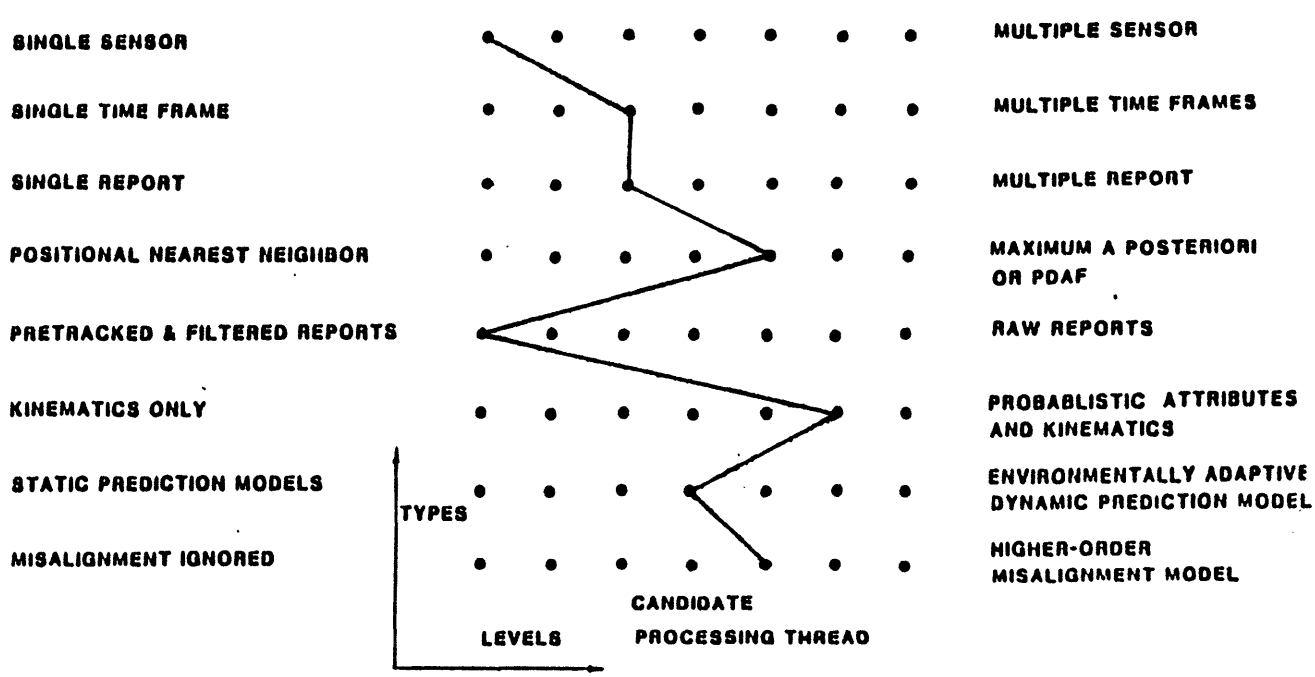

Figure 2-2. Multisensor Fusion Processor Options

2.1 Fusion Tree Selection

The goal of fusion tree selection is to segment the data processing into smaller batches to lessen computational and memory requirements while minimizing the loss of performance accuracy. Thus, the fusion tree is selected to take advantage of any natural segmentation of the problem. Altnough the fusion tree can be selected in real-time, it is selected here a priori to reduce the computational burden and complexity associated with real-time fusion tree selection. This and other computational reductions are driven by the requirement for a real-time onboard solution. A priori fusion tree selection for generic MSI includes the definition of the sensor data structures and the partitioning of this data for correlation.

The first step is to require each sensor to generate its own target track files, where each track file contains the best estimate of the target state at the current time given all past sensor observables. This provides the following benefits:

- reduces real-time data transfer requirements
- utilizes sensor specific track filters
- enhances system reliability due to decentralization and reduced computational complexity
- minimizes modifications of existing sensor systems
- reduces the MSI data filtering requirement.

The principal drawback of this assumption is that the sensor track files input into MSI are correlated across time and sensors for each target. However, since the multispectral sensors considered here have negligible raw observable correlation problems the effect of ignoring this correlation is reduced. The correlations in the target kinematic estimate errors have been treated in the literature [1,2]; however, here, to reduce computational complexity, this correlation is also ignored.

The sensor track files are assumed to contain both target kinematics and classification information. Both kinds of information can be useful for track correlation and neither should be left out. An example of this is the integration of radar tracks with limited identification information and a ESM sensor with type level ID and rough angular tracking data. Thus, the correlation is based simultaneously on the classification and angular track data.

To perform accurate real-time data integration of spatially separated sensors, the relative alignment of the sensors must be computed. The relative sensor misalignments separate naturally into the parallax error, base-to-base alignment, and the line-of-sight (LOS)-to-base alignment. The residual misalignment which remains after this common reference processing can be estimated by MSI to within the sensor track accuracy. These residual misalignments are modeled here as a bias plus a random noise in spherical coordinates. The choice of spherical coordinates is based on the restriction of passive sensors to predominately azimuth and elevation kinematics. In summary, the sensor data structures have been specified as follows:

- only filtered and tracked sensor track files are available
- target kinematics and classification data are utilized
- bias residual misalignments are modeled in spherical coordinates

The next step is to define the partition of the sensor track files for MSI processing. The partitioning is defined so as to limit the computational burden. Thus, it is implicitly assumed that the recursive correlation memory between partitions will be restricted.

The first partitioning to be defined is with respect to the time variable. This follows naturally from the user requirement to have track estimates (albeit report correlation results) periodically in real-time as the scenario unfolds. At each MSI file update time the most current track files from each sensor are correlated. Since the sensors provide tracks the high confidence correlation results from past MSI can be easily utilized to simplify the problem at each MSI update.

The second partitioning selected is to process the current sensor track files with the current MSI file on a sensor-by-sensor basis. For this partitioning, the order in which the sensors are processed in the fusion tree can significantly effect the number of candidate hypotheses that must be saved. The goal in ordering the sensors is to make the anticipated high confidence track correlation decisions first so that fewer candidate hypotheses need to be saved. Thus, the best sensor (i.e., accuracy and target detection) is selected to initialize the MSI track file each MSI update time frame. Here, this sensor is the radar. The remaining sensors are then correlated to the MSI track file one at a time. This sensor partitioned fusion tree is depicted in Figure 2-3.

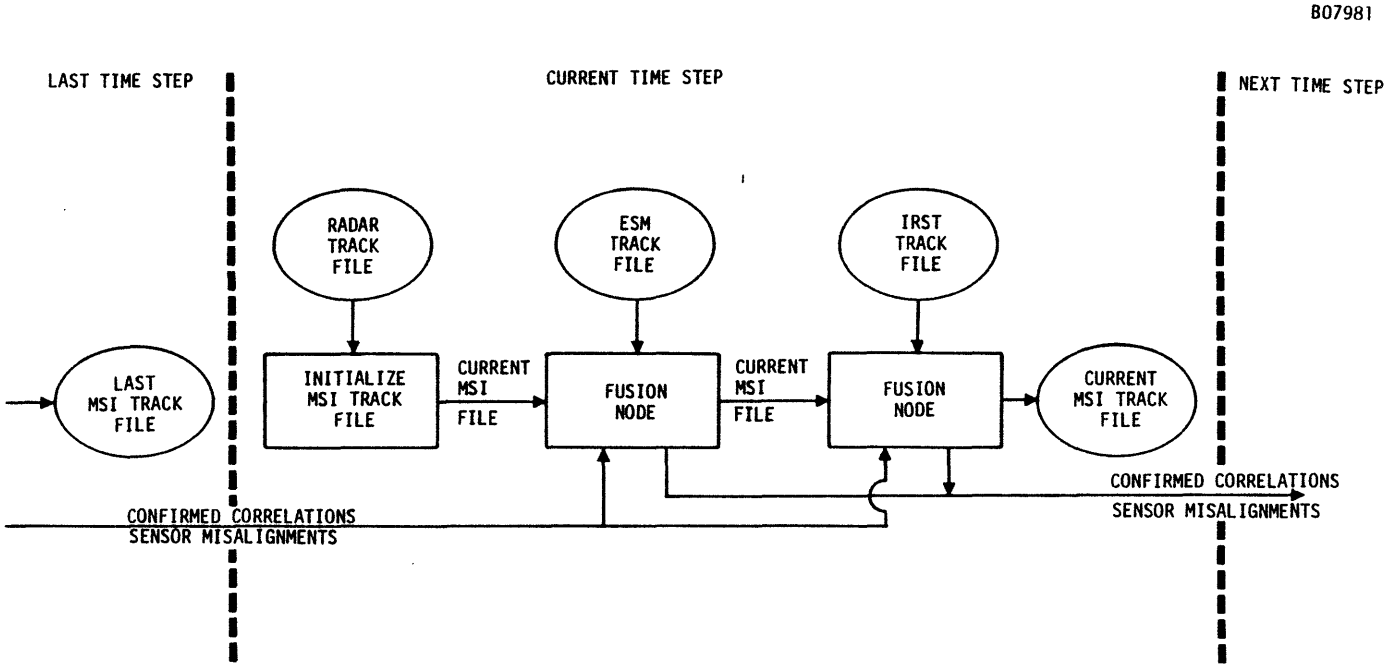

Figure 2-3. Sensor partitioned Track File Correlation Fusion Tree

2.2 Fusion Node Processing

For the fusion tree shown in Figure 2-3, each of the fusion nodes is similar. Namely, correlating a given sensor track file to the MSI track file. Thus, what is envisioned is a single fusion node processing architecture which can be applied at each fusion node. When the tracks within each sensor track file are correlated to the MSI track file as a whole, the full maximum a posterior solution requires a sum over all their targets of the correlation log-likelihoods, as shown in Reference [1]. However, to reduce the real-time computational burden the tracks can be scanned for the best single correlations. Here, such a fusion node is recommended. A candidate functional flow is given in Figure 2-4.

The first step is to define the sensor track file correlation objective criterion. The candidates, as discussed in Reference [3], are reviewed in Table 2-1. Of these, the second is selected since it has least computational burden and similar performance based on satisfying user requirements.

Table 2-1. Candidate Report Correlation Maximum A Posteriori Criteria

1. Joint multisensor correlation decision and target state estimation

$$\max_{H,\theta} P(H,\theta|\text{reports}) = \max_{H} \left[\max_{\theta} P(\theta|\text{reports},H)\right] P(H|\text{reports})$$

2. Multisensor correlation decision

$$\max_{H} P(H|\text{reports}) = \max_{H} \left[P(\text{reports}|H)\, P(H)\right]$$

3. Target state estimation

$$\max_{\theta} P(\theta|\text{reports}) = \max_{\theta} \left[\sum_{H} P(\text{reports}|H,\theta)\, P(H|\theta)\right] P(\theta)$$

As shown, this second criterion splits into the maximum likelihood, $P(R|H)$ term, and the prior $P(H)$ term. The first term provides a measure as to which MSI track to correlate to a sensor track while the second measures to what extent a correlation to any MSI track is expected. The fusion node processing is developed from the general report correlation architecture proceeding as follows:

- Hypothesis Generation
- Hypothesis Evaluation
- Hypothesis Selection

Hypothesis generation defines the feasible track correlations based on the current data and the prior correlation hypotheses. These feasible track correlations are then linked to form current correlation hypotheses. The feasibility track gating process is expected to provide a quick search of the data to indicate the track correlations which should be considered in more detail. Thus, it is not an exact statistical computation and it is

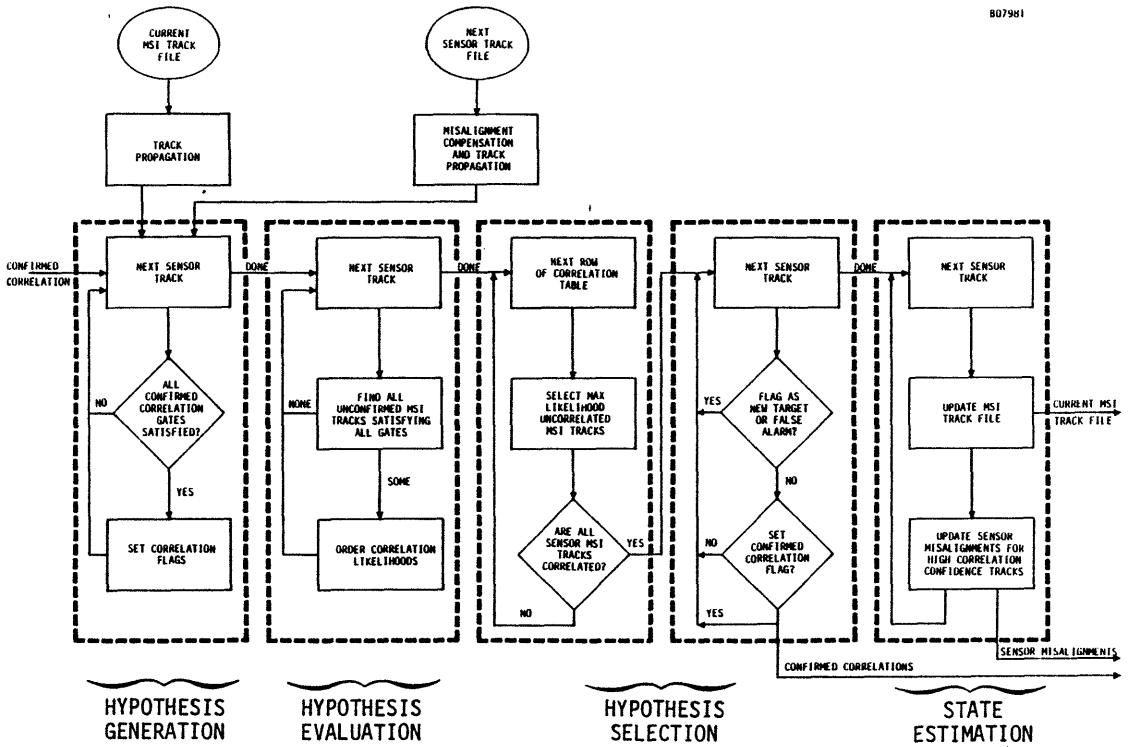

Figure 2-4. N-Pass MSI Fusion Node Functional Flow

anticipated to be performed in a series of gates. If there are not MSI tracks which pass all the gates, then the sensor track is labeled as a new target or a false alarm depending on the sensor and MSI probability of detection and false alarm statistics. In general, the nonlinearity of the report correlation problem caused by the unknown target count emphasizes the use of a hypothesis generation and evaluation feedback structure. However, since only a limited number of feasible hypotheses are expected here, this feedback is not proposed.

The hypothesis evaluation is based upon the following maximum a posterior track correlation criterion breakdown (see Reference 4):

$$P(H|Y(0),Y(1),Z(0),Z(1)) = P(Y(0)|Z(0),Z(1),Y(1),H) \quad (1)$$

$$\left[\sum_{k \in \text{classes}} P(Z(0)|H,\text{class } K)\, P(Z(1),Y(1)|H,\text{class } K)\, P(\text{class}K|H)\right] P(H)$$

where

$(Y(0),Z(0))$ and $Y(1),Z(1))$ are the kinematic and classification data from the sensor and MSI track files which are selected according to the assumption that for one of the two the target classification is made irrespective of its kinematic data, e.g., ESM

H is the correlation hypothesis that this data is from the same target

K is the index over a set of disjoint classes selected for each pairing such that for all K the following holds:

$$P(Z(0),Z(1),Y(1)|H,K) = P(Z(0)|H,K)\ P(Z(1),Y(1)|H,K) \quad (2)$$

This last equality clearly relies on the target class conditioning, since it is precisely the unconditioned correlation between Z(0) and (Z(1),Y(1)) that the target attribute track correlation criterion is based upon. The existence of such a set of disjoint target classes, K, is predicated upon the sensor target observables being noncommensurate. For example, Z(0) could represent a set of ESM observables like PRI and frequency and Z(1),Y(1) could represent a set of radar threat image observables along with the current radar kinematic track, Y(1). Typically this set of target classes will be the lowest common level of target classification that can be performed with the two sets of data. In order to avoid having to compute the terms in the summation above in the MSI software, the following step, utilizing Bayes Rule, is applied:

$$P(Z(0)|H,\text{class K}) = \frac{P(\text{class K}|Z(0),H)\ P(Z(0)|H)}{P(\text{class K}|H)} \quad (3)$$

and similarly for the (Z(1),Y(1)) term. The result is that the P(class K|Z(0),H) type terms can be computed at the sensor level. The P(class K|H) terms are the a priori probabilities of the targets being in class K which on application would be part of the mission data input to the fire control computer in either a look-up table or constant form.

At this point it should be emphasized that, although the Y(0) and Y(1) terms above are the track file kinematic estimates, the Z(0) and Z(1) terms are the raw attribute observables and not the track file target classification estimates. The reason for this is that, if track correlation were based on the track file classification data statistics rather than the raw data statistics, the performance accuracy can be noticeably degraded. A typical example of the degradation caused by using the track file target classification reports as the attribute data, is when a sensor may have a low probability of outputting a high confidence target classification estimate. In fact, this is an expected occurrence for the envisioned avionics sensors. Namely, the individual sensors are not expected to each completely solve the non-cooperative target identification problem most of the time. So, typically, for any given sensor there will be target classes for which it is not expected to correctly identify but for which it might be able to some of the time. By using these target classification report statistics, whenever the sensor is able to correctly identify this target class, such information would be discounted for track correlation due to its low probability of occurring. This reduces the contribution of a correct classification match in helping to solve the track correlation problem. Thus, the Z(i) refer to the raw data observables here.

The hypothesis evaluation criterion in equation (1) using (3) is computed as follows:

$$P(H|Y(0),Y(1),Z(0),Z(1)) \tag{4}$$

$$= \exp\left[-\frac{1}{2}(r^T V^{-1} r + \log|V|)\right] \left[\sum_{k \in \text{classes}} (P(\text{class } K|Z(0),H)\right.$$

$$\left. P(\text{class } K|Z(1),Y(1),H)|P(\text{class } K\ H))\right] P(H)$$

where

r is the residual, $[Y(0)-Y(1)]$, and V is the covariance of r.

H is the hypothesized MSI track correlation, MSI track initiation or false alarm declaration for the given sensor track, which is approximated as follows:

$$P(\text{Track Correlation Hypothesis}) = [1 - P_{FA}(\text{Sensor})]\ [1 - P_{FA}(\text{MSI})][P_D(\text{MSI})]$$

$$P(\text{MSI Track Initiation}) = [1 - P_{FA}(\text{Sensor})][1 - P_D(\text{MSI})]$$

$$P(\text{Sensor False Alarm}) = P_{FA}(\text{Sensor})$$

In addition, this term is also normalized with the expectations of the kinematics and classification terms.

The P(H) evaluation is typically the subject of much debate due to the inherent inaccuracies in the a priori sensor characteristics and scenario target kinematics and classification appearance expectations. It should be emphasized that this does not imply that this term should then not be computed. This term can still have a substantial effect to the extent it is known. Thus, the best estimate of these parameters should be made and, as always, to decrease their effect, the sensors are expected to be designed with as low a false alarm and as high a detection probability as possible. The estimate of these characteristics is expected to entail the use of look-up tables in real-time as a function of sensor mode, field-of-view, signal-to-noise ratio, etc.

Hypothesis selection determines the hypotheses to be retained for the next recursive step and the one to be used for the MSI update. The tradeoff, for retention, is the performance accuracy of retaining more hypotheses versus the reduced computational complexity associated with retaining fewer. Also, memory of past correlations must be maintained in order to keep ESM ID data associated with the radar tracks after the emitter file has been dropped.

3.0 INTERNETTED SURVEILLANCE INTEGRATION

This function generates a single surveillance picture for the flight from the internetted aircraft sensor information. The subfunctions are common reference processing, track correlation and target state estimation.

The focus here is on the multitarget 1-D, 2-D, and 3-D track correlation processing. The significant design options are the same as those given in Figure 2-2. The first step is the selection of the fusion tree which specifies the partition of the data for fusion node processing. This segmentation of the data is given in terms of which sensors, timeframes, and tracks are to be simultaneously correlated. The motivation for enhancing the fusion tree towards simultaneous consideration over multiple platform sensors, multiple timeframes, and multiple sensor track files, is summarized in Table 3-1.

Table 3-1. Enhanced ISI Fusion Tree Selection Motivations

- Multiple Platform Sensors
  - Improve number of 3-D tracks available for correlation
  - Remove two sensor angle-only track correlation ambiguities
- Multiple Time Frames
  - Provide memory of confirmed past ISI 3-D tracks
  - Buffer angle-only tracks for 3-D track initiation
- Multiple Sensor Track Files
  - Detect inter-platform misalignments
  - Improve correlations for weakly overlapping track files
  - Avoid correlated errors from MSI target ID files
  - Utilize like-sensor target attributes to solve angle-only correlations

As an example, the last option considered in Table 3-1 indicates the motivation for single sensor attribute data rather than the MSI file data. For the single aircraft case, it is desirable to take advantage of the non-commensurate nature of the onboard sensors by distributing the attribute-to-classification processing to each of the sensors. Then, the data bus load is lower and the MSI processing of the resulting classification trees is simpler. However, in the ISI problem the classification errors from each aircraft MSI file are significantly correlated, due to the commensurate nature of the target signatures upon which each is based. Thus, for correct target correlation, as well as target state estimation, the target attributes from each sensor on each netted aircraft are needed. In particular, the RF and PRI common ESM measurements can significantly reduce the angle-only correlation problem for dense environments. The drawback is that this increases the communication load and processing complexity. As a result, the extent of compensation for these correlations must be weighed against the improved accuracy which would result.

A candidate ISI functional design is given next which emphasizes a reduced communications and processing load. The options selected are as follows:

- Integrate only the platform MSI track files where the MSI files contain either 3-D or angle-only kinematic tracks, and target classification tree confidences. The platform relative navigation and alignment data is assumed available with each time tagged MSI file.

- The aircraft are correlated one at a time to the ISI track file except for the DOA data which is processed using pairs of aircraft.
- A single track file is used for the 3-D correlation and a three-time interval buffer is used for the 2-D correlations.
- The 3-D tracks are given correlation scores track-by-track and the 2-D tracks are given scores pair-by-pair.
- The standard, P(H|R), maximum a posteriori track correlation criterion is used as the correlation objective functional.

The ISI functional flow, as shown in Figure 3-1, is separated into reference processing, track correlation, and target kinematic and classification state estimation. The inputs are the internetted aircraft MSI files, along with their relative navigation and alignment.

The principal difference between ISI and MSI is the correlation of the angle-only tracks. For line-of-sight (i.e., azimuth and elevation) tracks the correlation residual requires the computation as shown in Figure 3-2. In addition, the usefulness of the angle rate information is degraded due to its projection into the unknown range rate of the alternative correlations. The most significant problem is that for alternative correlations which lie near the same plane determined by two platforms and a given target track, the solution becomes ambiguous. This commonly occurs when the netted aircraft are at co-altitude for all co-altitude target aircraft as depicted in Figure 3-3. These ambiguities also occur for all azimuth-only candidate track correlations. This problem is solved, albeit with additional

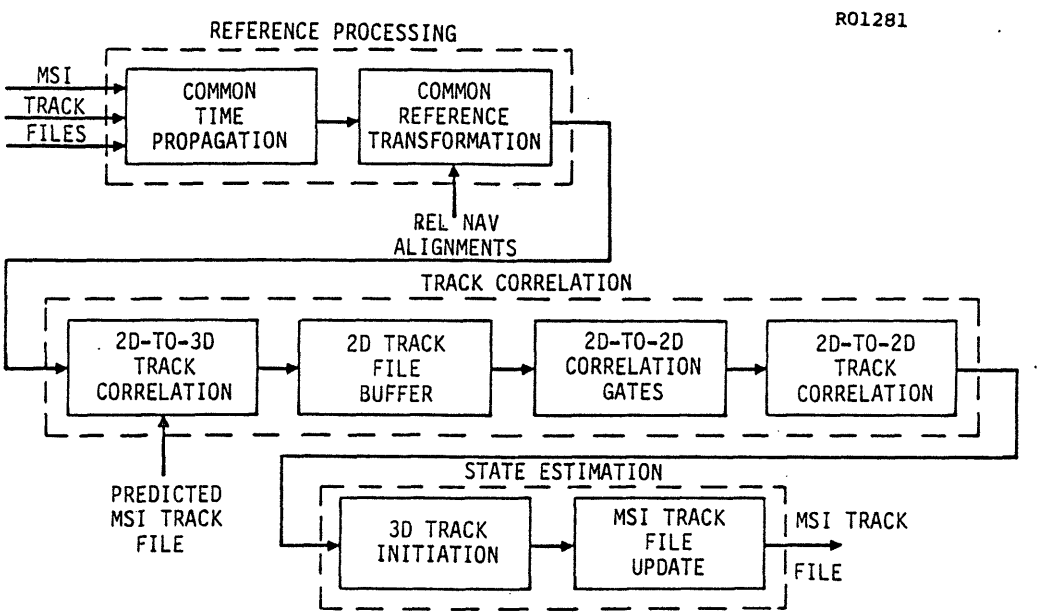

Figure 3-1. Internetted Surveillance Integration Functional Flow

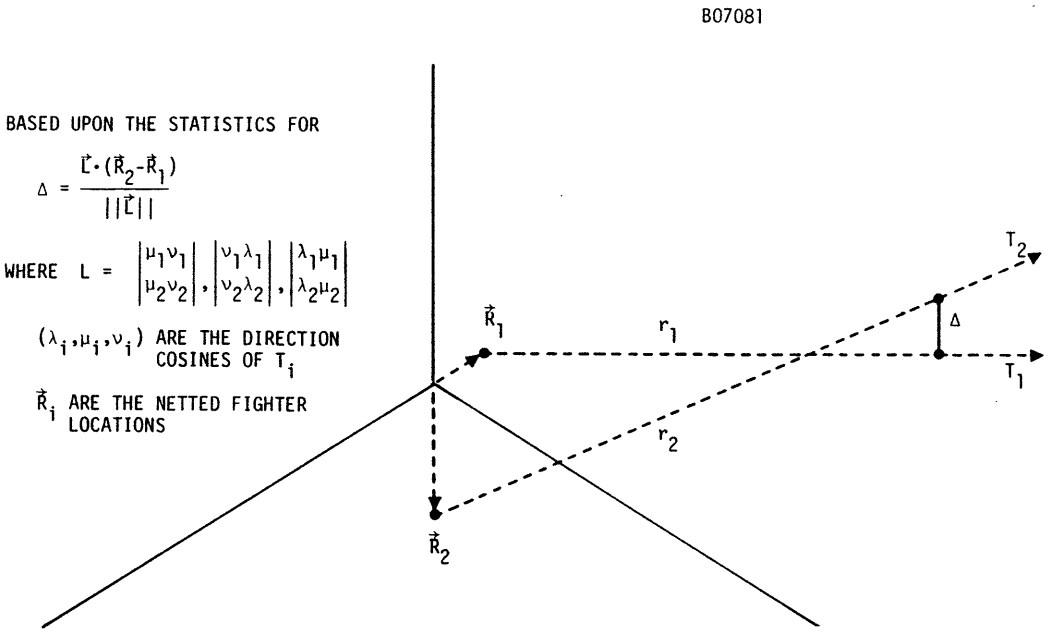

Figure 3-2. Line-of-sight Track Correlation Residuals

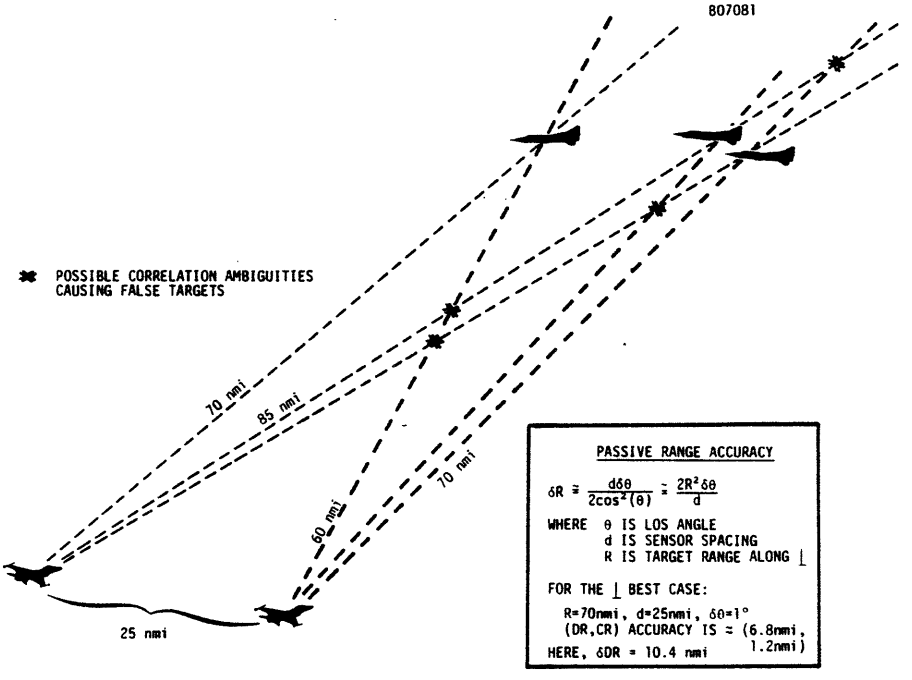

Figure 3-3. Passive Track Correlation Ambiguities

computational burden, by correlating three or more platform high probability of detection track files, simultaneously. In each case, the target classification data is utilized simultaneously with the kinematics as described above for MSI. Selection of the ISI fusion tree and fusion node processors which best trade the performance for the computational requirements remains to be accomplished.

4.0 SUMMARY

A Bayesian approach to integrated surveillance for both single and multiple platforms has been developed here. The motivation for this internetting of aircraft is summarized as follows:

• Cost	Hi/lo force mix performance multiplication via internetting
• Reliability	Reliable stand-alone subsystems are integrated and controlled
• Mission Adaptability	Flexible core architecture with preflight initialization software
• Chaos of Battle	Internetting to improve targeting of stand-off weapons and maintain local advantage
• Pilot Workload	Automated data fusion, decision aids and non-lethal subsystem controls
• Limited BVR-ID	Integration and memory of identification data from passive, active, and C^3I sources

The primary value of multisensor fusion accrues from its synergistic use of complementary multispectral sensor data. The report correlation problem is expected to be solved by sequentially processing a partitioned set of reports and utilizing both the kinematic and target classification data. The processing option selected is influenced by the computational requirements as well as the relative uncertainty in the data, especially with regard to the correlation hypothesis a priori information (e.g. individual sensor probability of detection and false alarm).

In conclusion, the algorithms proposed here utilize both target kinematics and target classification data in order to solve the track correlation problem. The problems attendent in utilizing distributed processing for MSI are shown to be of less concern than for ISI due to the multispectral independence of the single platform sensors. A preference of ISI correlations to 3-D targets before angle-only correlations is proposed with angle-only correlation ambiguities indicated.

REFERENCES

1. C. L. Bowman, "Maximum Likelihood Track Correlation for Multisensor Integration," 18th IEEE Conf. on Decision and Control, December 1979.

2. Y. Bar-Shalom, "On the Track-to-Track Correlation Problem," IEEE Trans. on Automatic Control, Vol. AC-26, April 1981.

3. C. L. Bowman, C. L. Morefield, "Multisensor Fusion of Target Attributes and Kinematics," 19th IEEE Conf. on Decision and Control, December 1980.

4. C. L. Bowman, C. L. Morefield, M. S. Murphy, "Multisensor Multitarget Recognition and Tracking," 13th Asilomar Conf. on Circuits, Systems and Computers, November 1979.

5. C. L. Bowman, J. M. Nash, "Synergistic Data Integration for Airborne Recognition and Tracking," 7th NCTR Conference, September 1980.

6. C. L. Morefield, "Application of 0-1 Integer Programming to Multitarget Tracking Problems," IEEE Trans. Automatic Control, Vol. AC-22, June 1977.

MARCY:
A MULTI-TARGET/MULTI-SENSOR TRACKING ALGORITHM

Michael H. Moore
SYSTEM DEVELOPMENT CORPORATION
4025 Hancock Street
San Diego, California 92110

1. INTRODUCTION

The problem of tracking in a multi-target/multi-sensor environment can be stated in terms of two principal sub-problems:

- o the data association/clustering problem, viz., partition the dataset into disjoint subsets or clusters with the datapoints in each cluster being associated with some one target (or with "noise data");
- o the data fusion/correlation problem, viz., estimate characteristics and quantities of interest about a target (e.g., positions, courses and speeds) from the data in the data cluster associated with it.

Thus, the data association/clustering problem arises from the multi-target aspect of the tracking environment (i.e., the possibility that there are zero, one, two, or more targets represented in the data), as illustrated in figure 1. This problem is difficult to solve because the number of ways to cluster the data is combinatorially large. And the data fusion/correlation problem arises from the multi-sensor aspect of the tracking environment, wherein one is faced with extracting all of the information about a target from datapoints that may differ in information content, statistical properties, etc., as illustrated in figure 2.

MARCY is an algorithm for solving both the data association/clustering problem and the data fusion/correlation problem. That is, MARCY is an algorithm for tracking in a multi-target/multi-sensor environment. MARCY, which is potentially a better tracking algorithm than such algorithms as OUTLAW HAWK and OUTLAW SHARK (these latter algorithms, which are now operational, also address the data association and fusion problems), currently lives at the Advanced Command/Control Architectural Testbed (ACCAT) at the Naval Ocean Systems Center (NOSC) in San Diego.

Our purpose here is to describe MARCY in some detail. We do this in three parts. First we give, in section 2, an overview of MARCY. In particular, we describe what it is like to run MARCY, and mention her two operating modes (batch mode and recursive mode). We list the algorithm's inputs and outputs, and we summarize the many versions of MARCY that are now in existence along with the tracking situations in which they have been used in practice. Secondly, we briefly describe, in section 3, how MARCY works. In particular, we indicate how MARCY is based on two principal subalgorithms: a Kalman filter of a novel kind for solving the data association/clustering problem in a "local" manner via data fusion/correlation; and an integer program for solving the data association/clustering problem in a "global" manner.

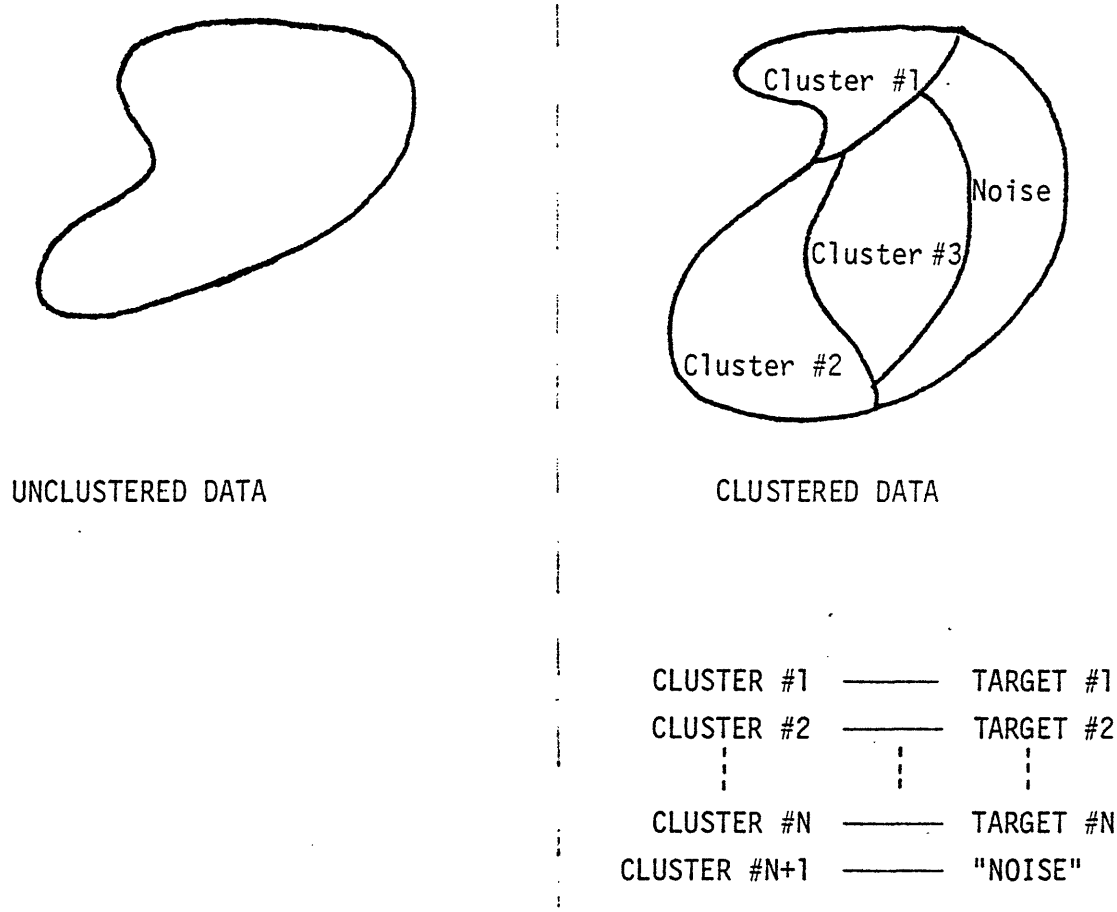

Figure 1. The Data Association/Clustering Problem

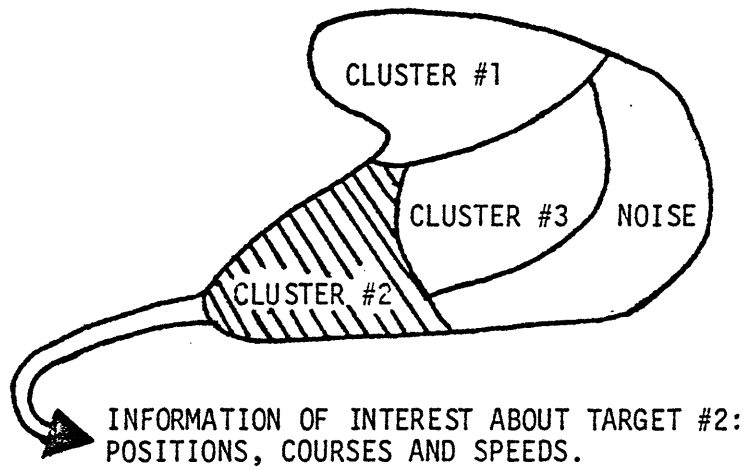

Figure 2. The Data Fusion/Correlation Problem

We also indicate how, in solving the overall data association/clustering problem, we avoid the combinatorial problem of explicitly considering all possible partitions of the dataset. Finally, in section 4 we give an example of a run with MARCY on a set of artificial data representing a hypothetical two-target/three-sensor ocean surveillance tracking scenario. This example illustrates, inter alia, the user/MARCY interface.

2. OVERVIEW OF MARCY

2.1 OPERATING MARCY

MARCY is, of course, computer-driven. MARCY is coded in some 6000 lines of FORTRAN source code. Graphic outputs are coded in PLOT10--a graphic package callable from FORTRAN that has been provided by the Tektronix Corporation for use on DEC PDP10 computers. The algorithm requires about 120K of core storage at loading time; much of this is, of course, paged out at running time. As mentioned above, the algorithm resides on a DEC PDP10 computer at the ACCAT facility at NOSC.

MARCY is interactive in character--that is, she prompts the user to guide her activities and responds to his control choices; as such, she is human-engineered to a degree (e.g., she is tolerant of "silly" errors on the part of the user).

Figure 3 is a high-level flowchart indicating how a user of MARCY operates the algorithm. As the figure shows, MARCY runs in either of two modes -- batch mode and recursive mode -- whose general appearances to the user are similar. In both modes, the user provides the algorithm with target-related data and with certain control parameters. The algorithm then performs "local data association/clustering" via data fusion/correlation to produce a candidate set of possibly overlapping data clusters or tracks. The user may manually modify these results at his option. The algorithm then goes on to perform "global data association/correlation" to produce a best possible subset of these tracks subject to the constraint that they do not overlap each other in datapoints (i.e., no two tracks have datapoints in common). At this point the user of MARCY may, as shown in figure 3, accept these results by outputting them to track files; alternatively, he may recycle back throught the track construction dialogue (presumably with different values for the control parameters) so as to try to obtain results that he likes better.

MARCY's two operating modes differ in the method of initialization of the Kalman filter that is at her heart, and in running speed. On the one hand, MARCY can, in batch mode, do multi-target/multi-sensor tracking well even when her filter is poorly initialized, but in doing so requires a long running time compared to what the running time would be in recursive mode. On the other hand, MARCY can, in recursive mode, do multi-target/multi-sensor tracking well only when her filter is well initialized, but in doing so requires a short running time compared to what the time would be in batch mode.

TABLE 1. MARCY's Principal Control Parameters

Parameters	Units	Remarks
Name of Peak Datafile	NA	File must be in user's directory
Latitude Coordinates	NA	North or South is positive
Longitude Coordinates	NA	East or West is positive
Sound Speed	Knots	
Minimum Track Length	NA	Must have $1 \leq$ min length $\leq$ max length ≤ 20
Maximum Track Length	NA	do
Number of Stations	NA	Between 2 and 15
Station Positions	degs	In chosen coordinates; negative values OK
Stations Courses	degs true	
Station Speeds	Knots	
Score Thresholds	NA	
R(1,1)	$secs^2$	
R(2,2)	$hertz^2$	
σ_1^2	$degs^2$	
σ_2^2	$(degs/hr^2)$	
DTMIN	hours	
DTMAX	hours	

Thus, MARCY's two running modes have complementary capabilities: the user runs MARCY in batch mode whenever necessary to initialize or re-initialize the estimated tracking scenario; and he runs her in recursive mode whenever possible to update track estimates handed off to her by batch mode.

2.2 MARCY's Inputs and Outputs

MARCY's inputs and outputs depend, of course, on the particular multi-target/multi-sensor tracking environment to which she is applied. We here describe the algorithm's inputs and outputs for the case of the ocean surveillance environment.

2.2.1 MARCY's Inputs In An Ocean Surveillance Tracking Environment

As figure 1 shows, MARCY's inputs are of two types:

- o values of control parameters;
- o target-related data.

MARCY obtains values for her control parameters either directly from the user (there is an extensive user/MARCY input dialogue for specifying parameter values) or from a previously created control parameter data file on disk. Table 1 shows the most important control parameters for which MARCY needs values.

After MARCY has a complete set of parameter values, the user may instruct her to print these values out for inspection. An example of such a printout is given in section 4. MARCY then offers the user an opportunity to change values of one or more parameters (without, of course, requiring that he respecify them all). The user may, at his option, save parameter values on a disk data file for his later use. MARCY reads target-related data from a previously prepared binary disk data file.

MARCY is, in principal, applicable in any multi-target/multi-sensor environment and thus can, in principal, accept any kind of target-related data. For each data type, MARCY must be supplied with the appropriate "measurement equation"--that is, the equation that relates that type of data to the target's position and motion.

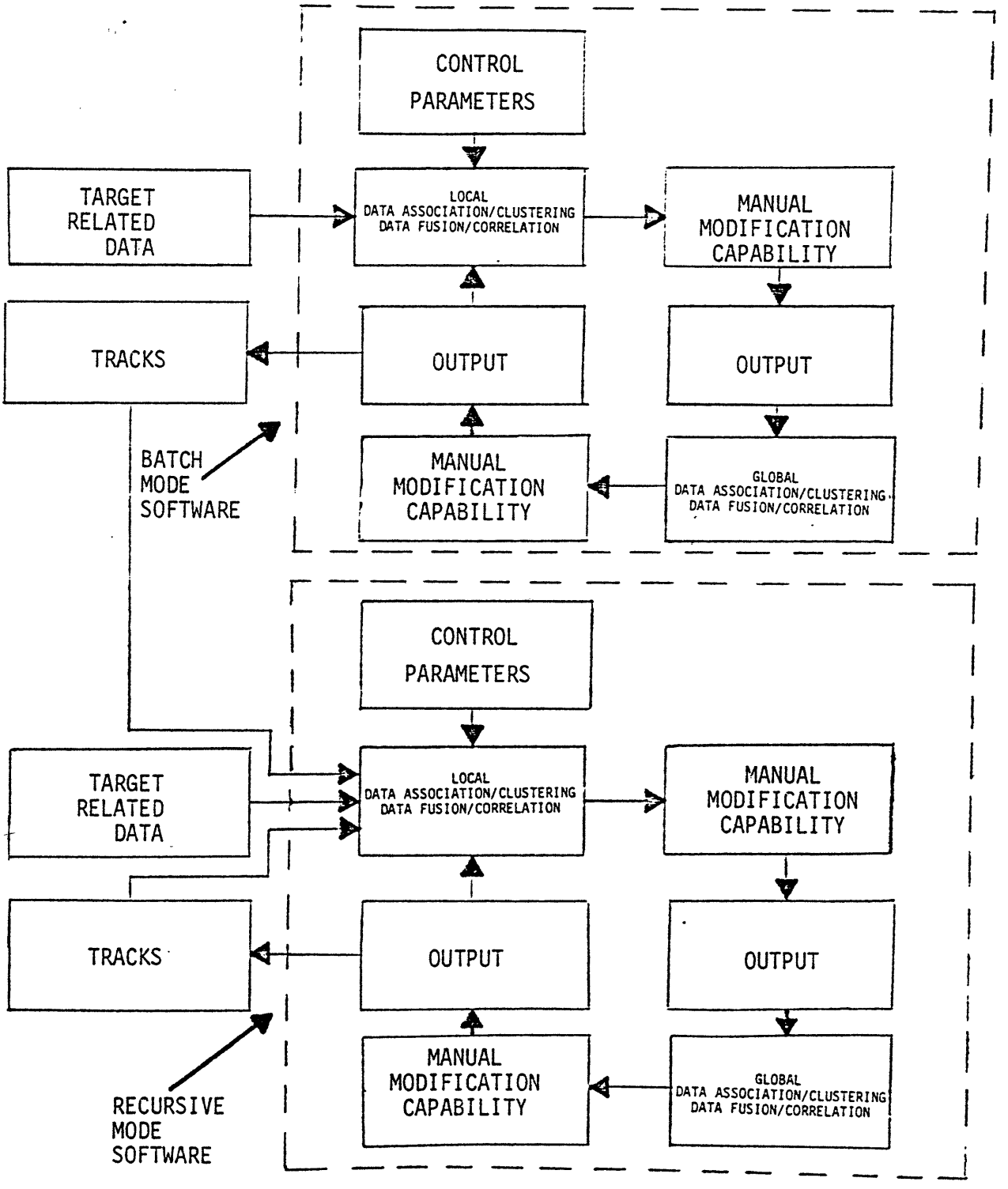

Figure 3. A High-Level View Of MARCY's Functions And The Flow Of Control

The current MARCY, however, has been developed with the ocean surveillance application foremost in mind. Thus, the current MARCY's data has most often been that of the ocean surveillance community, viz:

- o positional information
  - radar measurements;
  - pairwise coherence measurements;
  - active sonar reports;
  - pilot sightings;
- o bearing-only information
  - SOSUS lines, of bearing;
  - HF/DF lines of bearing;
  - passive sonar reports.

Indeed, much of the early work with MARCY has been with a single data type--that of pairwise coherence measurements. (Table 4, which appears in section 4 of this paper, shows an example of a dataset consisting of 48 pairwise coherence measurements, each line on the table being one such datapoint.)

2.2.2 MARCY's Outputs

As figure 3 shows, a user of MARCY has two major opportunities for output: one after MARCY's Kalman filter has solved the data association/clustering problem in a "local" manner, via data fusion/correlation; and the other after MARCY's integer program has solved the data association/clustering problem in a "global" manner. At either point, the user may request any of eleven types of information, of which seven are tabular in character and four are graphic in character, about all or a selected subset of the clusters or tracks found by the algorithm. Table 2 lists these types of output information. Examples of some of these types of output are given in section 4. After viewing any type of output the user may recycle through the output dialogue and make other output selections.

2.3 Versions of MARCY

The algorithm MARCY that we describe in this paper is applicable in a general multi-target/multi-sensor environment. As such, MARCY may be seen as the progenitor of a number of existing versions of the algorithm each one tailored for use in some one special practical situation.

Table 2. MARCY's Output Types

Type Number	Information Content
1	Water times, peak numbers
2	Water times, peak numbers, probability scores
3	Water times, peak numbers, probability scores, chi-square scores
4	Water times, peak numbers, probability scores, chi-square scores, measurement residuals
5	Water times, peak numbers, state vectors
6	Water times, peak numbers, state vectors, covariance matrices
7	Water times, peak numbers, position coordinates, courses and speeds
8	Plot of feasible tracks in geographic space
9	Plot of feasible tracks in measurement space
10	Plot of residuals versus time
11	Plot of covariance matrices versus time

Most of these special versions of MARCY have been created to support ocean surveillance experiments by the Advanced Research Project Agency (ARPA) of the Department of Defense. The ARPA experiments in which a version of MARCY has provided tracking support are:

Date	Experiment Name
Fall, 1978	Semi-Alerted Search Experiment (SASE)
Spring, 1980	Broad Area Search Experiment I (BASE-I)
Spring, 1981	Broad Area Search Experiment II (BASE-II)
Summer, 1981	Pathfinder

All of the versions of MARCY that have been created to support these experiments are equipped only with batch mode (i.e., none of them are equipped with recursive mode), and all operate on real data in real time.

3. HOW MARCY WORKS

MARCY works by solving the data association/clustering problem in two stages: a "local" stage and a "global" stage.

MARCY first solves the data association/clustering problem in a "local" manner, by which we mean that MARCY:

- considers (at least implicitly but not necessarily explicitly--see below) all possible partitions of the dataset into candidate clusters;
- scores, via data fusion/correlation (which is carried out by a Kalman filter applied to the data in each candidate data cluster), each data cluster for the degree of agreement between: a) what the data in the cluster would imply about the behaviour of a target under the assumption that the datapoints in the cluster are all due to that target; and b) a simple model of target motion, namely, one of constant course and speed.*
- rejects candidate data cluster whose scores are sufficiently poor--along with (implicitly) all other candidate data clusters that could be formed that contain such poorly scoring clusters as subsets.*#!*#

* A user of MARCY can arrange for the algorithm to accomodate maneuvering targets as well. He does so by supplying parameter values that specify a high uncertainity in the constant course and speed model (i.e., he specifies a large amount of "system noise").

#!# This idea, which as a moment's reflection will show is entirely rigorous, is what keeps MARCY computationally feasible. This idea is due to Charles L. Morefield of VERAC Corporation.

Figure 4 illustrates this process. The numbered circles in the figure represent individual datapoints (of any type). The columns of circles in the figure represent copies of the entire dataset. The figure shows MARCY building candidate clusters in a bottom-up fashion -- trying first all possible one-point data clusters, all possible two-point data clusters, all possible three point clusters, etc., rejecting (as indicated in the figure by solid vertical bars) all such candidate clusters that score poorly (along with, implicity, all other clusters containing the failing cluster as a subset). The surviving candidate clusters are then fed to the global data association/clustering process described below.

Note that it is possible, and indeed often happens, that, because data clusters are scored in a "local" manner (i.e., independently of each other), surviving data clusters can have datapoints in common. Such cases of surviving data clusters that overlap are bothersome because one then has instances of a datapoint being associated with more than one target! Thus, it is necessary to consider the surviving data clusters as a whole -- that is, in a global manner.

MARCY next addresses the data association/clustering problem in a "global" manner, by which we mean that MARCY:

- notes cases of local solutions to the data association/clustering problem and the data fusion/correlation problem in which surviving candidate data clusters have datapoints in common;

- selects, via a 0-1 integer program, the "best" subset of non-overlapping surviving data clusters.

Here, by "best" we mean that subset of non-overlapping data clusters the sum of whose local scores is better than the sum of scores of any other subset of non-overlapping surviving data clusters.*

Figure 5 illustrates this global data association/clustering process. The blobs on the left-hand side of the dotted line in the figure represent clusters of data that survive the local data association/clustering and data fusion/correlation process, and the numbers shown in those blobs represent their scores. Since there are cases of overlapping blobs, we must select a subset of them that do not overlap. We (more generally an integer program) find that the subset of blobs shown on the right-hand side of the figure is the "best"** such selection of non-overlapping blobs.

---

* This idea of a globally best subset of non-overlapping data clusters is also due to Charles L. Morefield (1).

** "Best" here means that the sum of the scores of the (non-overlapping) clusters is as large as possible.

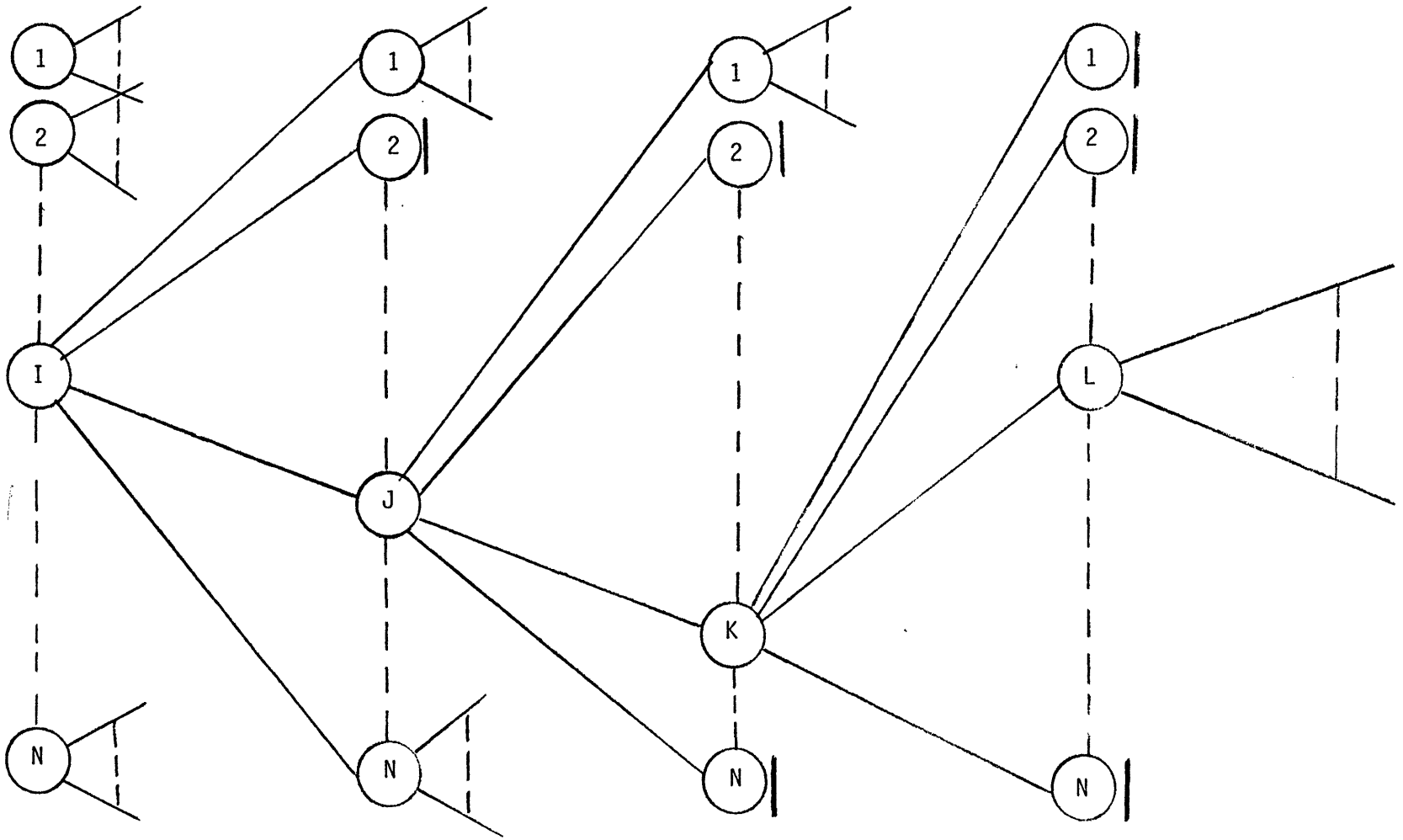

Figure 4. Local Data Association/Clustering Via Local Data Fusion/Correlation (Kalman Filtering)

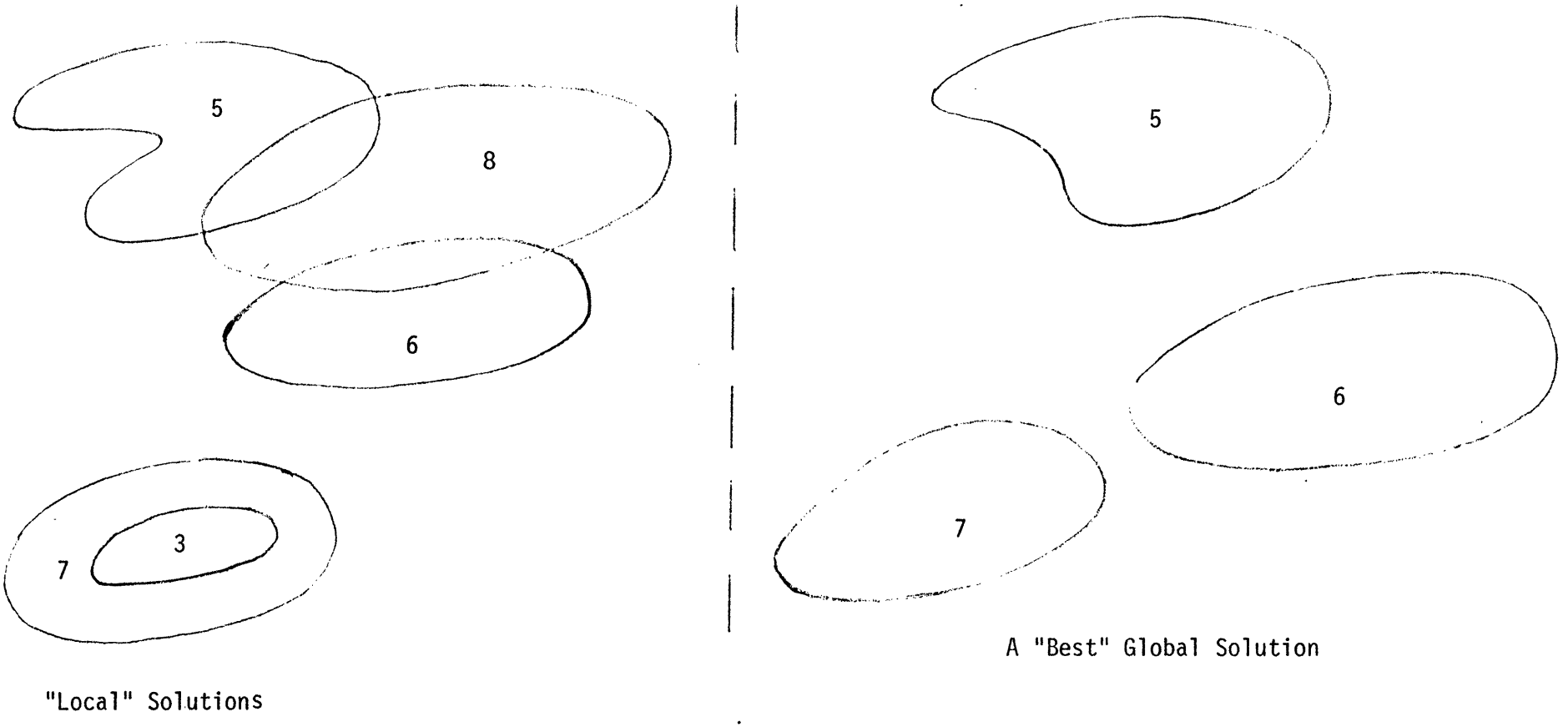

Figure 5. Global Data Association/Clustering Via 0-1 Integer Programming

4. AN EXAMPLE

Consider the hypothetical two-target/three-sensor ocean surveillance scenario shown in figure 6. Two targets move on constant courses at constant speeds: target #1 on course 170° at speed 20 knots, and target #2 on course 190° at speed 30 knots. These data, along with their initial positions at hour 0 as indicated, will result in the targets passing through one another at hour 10.*

The three sensors in the figure are SOSUS stations. They are fixed in space** and are arranged in a triangular configuration as shown. Table 3 describes this scenario in numerical terms. Table 3 also indicates the levels of "process noise" and "measurement noise" that will be injected into the scenario by a data generator in computing artificial target data based on the scenario in figure 6.

Table 4 shows a collection of 48 artificial pairwise coherence measurements that were computed from the data in table 3. Thus, the data in table 4 are synthetic data that represent the surveillance scenario shown in figure 6. This data comes to MARCY without any indication of the number or characteristics of the targets which produced them (the target numbers shown in the second column of table 4 are, of course, stripped away before the data is given to MARCY). MARCY's job is to unravel the data in table 4 so as to recover, as closely as possible, the scenario shown in figure 6.

Figure 7 shows the dialogue that a user of MARCY had with the algorithm in running MARCY on the data in table 4. Our description below of this dialogue is keyed to the figure by symbols of the form A , B , etc. The rectangles on the dialogue show entries made by the user.

At point A , the user is logging on to his account on the computer system. At point B , he sets the width of the terminal to 132 characters, thereby allowing for outputs with wide formats.

At point C , MARCY is invoked by hitting "MARCY". The algorithm is then loaded into core, and execution begins. MARCY first announces herself and then prints the running notes (these are overall reminders to the user) as shown.

At point D , MARCY determines whether or not the terminal in use is a Tektronix terminal. This information is necessary in order to be able to automatically clear the display, and for graphic output purposes.

---

* We chose this case so as to make it harder for MARCY to assign datapoints to targets than would otherwise be the case.

** MARCY can handle situations involving mobile SOSUS stations.

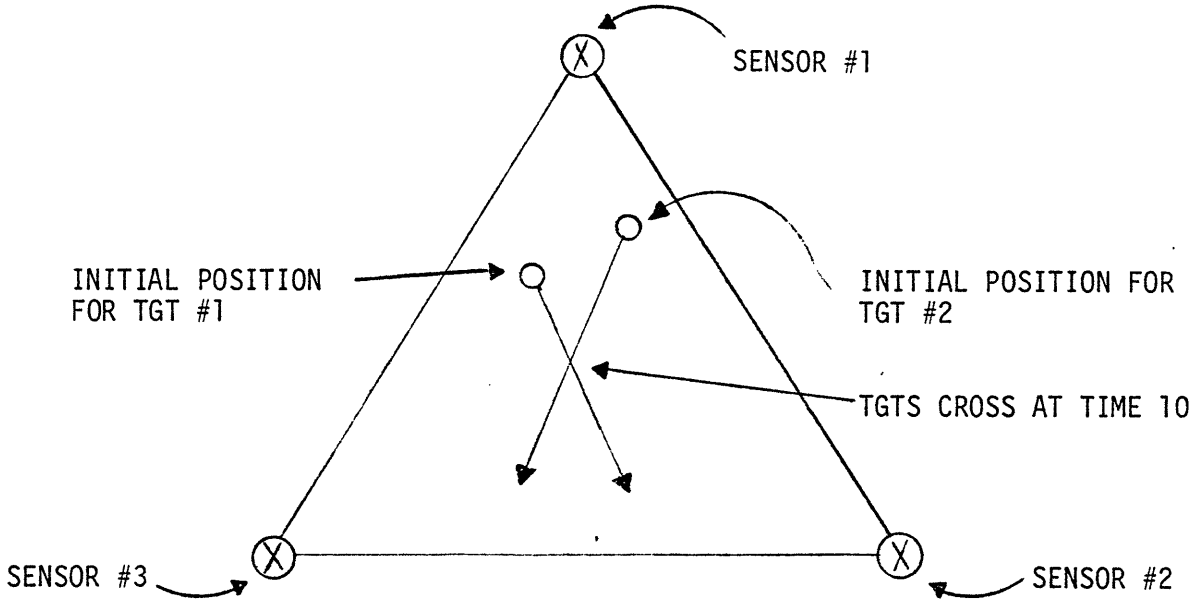

TGT #1: COURSE 170, SPEED 20 KTS

TGT #2: COURSE 190, SPEED 30 KTS

Figure 6. Hypothetical Ocean Surveillance Scenario.

DATA FOR CONSTRUCTION OF SYNTHETIC PEAKS

DATAFILE: PKSF6.DAT

STATION DATA

STATION NUMBER	NORTH LATITUDE	EAST LONGITUDE
1	30.0000	-130.0000
2	10.0000	-120.0000
3	10.0000	-140.0000

TARGET DATA

TARGET NUMBER	NORTH LATITUDE	EAST LONGITUDE	COURSE	SPEED	RADIATING FREQUENCY
1	23.2827	-130.6221	170.0	20.0	40.0
2	24.9240	-129.0618	190.0	30.0	60.0

PARAMETERS FOR ADDITIVE NOISE

	X----------PROCESS NOISE----------X				X-------MEASUREMENT NOISE--------X		
	LATITUDE	LONGITUDE	LATITUDE RATE	LONGITUDE RATE	TIME OF RECEIPT	FREQUENCY	BEARING
MEAN	0.00E+00	0.00E+00	0.00E+20	0.00E+00	0.00E+20	0.00E+00	0.00E+00
STD DEV	0.83E-02	0.83E-02	0.17E-01	0.17E-01	0.58E-02	0.10E-04	0.10E+00

WATER TIMES:	0.0000	1.0000	2.0000	3.0000	4.0000	5.0000	6.0000	7.0000	8.0000	9.0000
	10.0000	11.0000	12.0000	13.0000	14.0000	15.0000	16.0000	17.0000	18.0000	19.0000
	20.0000	21.0000	22.0000	23.0000						

Table 3. Data for Hypothetical Surveillance Scenario

DATAFILE: PKSFS.DAT

		X----------STATION INFORMATION----------X						X-------COHERENCE INFORMATION-------X			
		X--REFERENCE STATION---X			X----OTHER STATION-----X						
PEAK NUMBER	TARGET NUMBER	NUMBER	BEARING	BIN	NUMBER	BEARING	BIN	TOR	TIME DIFF	FREQ DIFF	COHERENCE
1	1	1	178	399	2	319	403	11.1947	318.0	0.3819	0.5020
2	2	3	60	604	2	296	602	21.2159	73.6	-0.1702	0.3517
3	1	1	181	398	2	321	402	6.1710	533.0	0.3954	0.5729
4	2	3	63	603	2	293	602	22.2105	109.8	-0.1463	0.0076
5	2	2	339	605	3	35	606	2.3474	31.0	0.1122	0.5060
6	2	1	181	595	2	316	604	11.2088	385.9	0.9499	0.1616
7	1	1	182	398	2	322	402	5.1769	513.7	0.3960	0.5037
8	2	2	331	605	3	33	606	0.3623	70.5	0.0704	0.6935
9	2	2	318	604	3	42	605	10.2229	30.6	0.1576	0.8693
10	1	2	317	403	3	50	401	18.2488	139.8	-0.1657	0.1477
11	1	1	183	398	2	323	403	3.1683	580.9	0.4323	0.9626
12	2	3	54	605	1	183	594	18.2281	206.0	-1.0243	0.2904
13	2	1	176	595	2	326	605	4.1470	659.9	0.9768	0.0164
14	1	1	184	398	3	34	402	1.1545	629.1	0.4414	0.3725
15	2	2	305	603	1	183	594	17.2578	23.9	-0.8957	0.3979
16	1	2	314	403	1	173	398	21.2396	63.1	-0.4733	0.3525
17	1	3	35	402	2	323	403	2.3386	10.5	0.0536	0.1512
18	1	1	176	398	2	318	403	14.2297	156.2	0.4100	0.8648
19	1	2	315	403	1	174	398	20.2466	20.6	-0.4844	0.3234
20	2	3	49	605	2	309	603	15.2566	30.3	-0.1925	0.6813
21	2	2	300	603	1	183	594	19.2554	151.6	-0.8191	0.4834
22	2	2	313	403	1	173	398	23.2194	158.2	-0.4962	0.8727
23	2	1	179	595	2	321	604	8.1814	444.9	0.8501	0.2855
24	2	1	178	595	2	323	604	7.1840	448.1	0.8669	0.6695
25	1	3	39	402	2	321	403	7.3107	9.3	0.0785	0.7322
26	1	2	313	403	2	55	401	22.2255	100.5	-0.1863	0.6668
27	2	3	45	606	2	313	604	13.2736	1.6	-0.1985	0.8045
28	2	2	326	604	3	37	606	5.3218	49.1	0.1495	0.9613
29	2	1	182	595	3	41	605	9.1895	398.1	1.0345	0.1448
30	2	3	60	603	2	293	602	23.1934	178.0	-0.1258	0.9401
31	1	1	176	399	2	318	403	15.2174	200.5	0.3593	0.2947
32	1	1	180	398	2	41	401	9.1934	305.2	0.2963	0.4613
33	2	2	330	605	3	34	606	1.3560	41.5	0.0834	0.6915
34	2	2	328	605	3	36	606	3.3483	35.4	0.1074	0.3139
35	1	3	33	402	2	324	403	0.3251	65.4	0.0537	0.7736
36	1	3	36	402	2	322	403	4.3256	13.6	0.0678	0.7017
37	1	2	319	403	3	43	401	12.2919	12.4	-0.1687	0.1612
38	2	3	58	604	2	298	603	20.2107	144.2	-0.1188	0.5455
39	2	3	47	606	2	311	604	14.2570	44.7	-0.1897	0.4610
40	1	2	319	403	3	42	401	10.2938	9.5	-0.1160	0.5961
41	2	1	181	594	2	316	604	12.2251	198.3	0.9788	0.6966
42	1	2	316	403	3	51	401	19.2474	160.2	-0.1282	0.5038
43	2	3	50	605	1	182	594	16.2564	43.0	-1.1061	0.2565
44	1	1	175	398	3	49	401	17.2362	221.7	0.2088	0.8619
45	1	1	180	398	2	329	403	8.1957	403.2	0.4386	0.6705
46	2	1	177	595	2	324	604	6.1743	500.2	0.9840	0.3675
47	1	1	175	398	3	48	401	16.2268	204.5	0.2823	0.4167
48	1	3	318	403	3	45	401	13.2890	51.7	-0.1702	0.3139

Table 4. Synthetic Pairwise Coherence Measurement Representing Hypothetical Surveillance Scenario

At point E , MARCY asks the user to specify the (spherical) coordinate system with which he desires to deal with the tracker. The user, as he is working in the North Pacific, naturally selects north latitude and west longitude as being positive. All coordinate inputs and outputs are then regarded by the user as being in this coordinate system.

At point F , MARCY asks the user for the speed of sound in knots.

At point G , MARCY asks for data concerning surveillance stations. The user, wishing to run the artificial data case with three immobile surveillance stations as illustrated in Figure 6, enters the station data as shown.

At point H , MARCY asks the user to supply the names of two scratch disk datafiles that will be used to store parameter values for batch and recursive modes. The user responds as shown.

The user has now finished entering the "universal parameters" (so called because they apply to both batch and recursive mode). MARCY prints these parameters out starting at point I , and asks the user to verify them. The user indicates that they are satisfactory. (If the user had made an error in entering one or more parameters or had he for any reason been dissatisfied with the values of the universal parameters, he could have indicated this fact to MARCY. MARCY would then have recycled through the relevant part of the input dialogue, thus giving the user the opportunity to change these values).

At point J , MARCY asks the user to indicate whether to run in batch mode or recursive mode (or to stop). The user chooses batch mode, as shown.

At point K , MARCY advises the user that it has begun the process of constructing tracks in batch mode.

At point L , MARCY asks the user whether he wishes to provide batch-mode parameters by restoring them from an old parameter datafile or by entering them manually. The user, not having already created a suitable parameter datafile, indicates that he will enter them manually.

At point M , MARCY asks the user to specify the first parameter -- the name of the target datafile. The user responds with "PKSF5" (i.e., the datafile whose contents are displayed in table 4) as shown.

At point N , MARCY asks the user to specify a lower bound and upper bound on the length of the tracks he is seeking.

At point O , MARCY begins a series of questions aimed at establishing what constraints, if any, the user wishes to place on tracks.

Basically, the user has an opportunity to constrain tracks by means of each type of data in the datafile: station numbers, bearings, frequency gins, times of receipt, time differences, frequency differences, and coherences. The user also has the opportunity to constrain a track's components by datapoint numbers. The first question concerns whether or not the user wishes to constrain a track's components by datapoint number. The user, not wishing to limit the tracker's attention to any particular datapoints in the datafile, answers "no". MARCY then goes on to ask the user whether he wishes to constrain tracks in other ways as shown. The user responds "no" to all of these questions except for the one involving the "times of receipt" (TOR) of datapoints where, as he wishes to limit the tracker's attention to the datapoints coming from the first five hours of the scenario shown in Figure 6, he does so as shown.

At point P , MARCY begins to ask for parameters that will be needed for local data association/clustering and data fusion/correlation (i.e., the Kalman filter). The first item is the measurement noise covariance matrix R. The user responds as shown. Note that MARCY advises the user of the units in which to respond.

At point Q , parameters $^{2}1$ and $^{2}2$, which are needed to determine the process noise covariance matrix Q, are asked for and received; again, desired units are provided.

At point R , the minimum water time and maximum water time between adjacent components of tracks are asked for and received.

Point S is concerned with the specification of initial state vectors and covariance matrices for MARCY's Kalman filter. The dialogue here is self explanatory (to those familiar with Kalman filtering).

At point T , MARCY asks for and receives the three types of thresholds by means of which local data association/clustering and data fusion/correlation is cut short. Here the availability of default options as shown make it easy for the user to specify standard values.

At point U , MARCY advises the user that values for all parameters have been received and asks the user whether or not he wants these parameters printed out for his inspection. The user, after indicating that he does, receives the printout as shown.

At point V , MARCY asks the user to indicate whether or not the batch-mode parameter values are satisfactory. Upon inspecting the printout of parameter values, the user decides that he would like to change the threshold for stagewise chi-square scores from 9 to 10. He indicates this fact to MARCY. MARCY responds to this by listing, beginning at point W , all the areas in which the user might wish to change parameter values. The user makes appropriate selections and, after MARCY recycles through the relevant part of the input dialogue, makes the desired change at point X .

At point Y , the user indicates to the tracker that he is now satisfied with the values of the batch-mode parameters. MARCY responds to this by saving these values in the batch-mode parameter datafile.

At point Z , MARCY asks the user whether or not he wants to look at the data in the specified peak datafile. The user responds "no" as shown. Had he responded "yes" instead, the user would find himself looking at table 4 (less the second column as mentioned previously).

MARCY's output in this case (i.e., for the target data shown in table 4 and the control parameter values shown in figure 7 above point Y) is shown in the remaining tables and figures: type 4 output is shown in table 5, type 7 output is shown in table 6 and type 8 output (a geographic graphical display) is shown in figure 8. As tables 5 and 6 show, MARCY produced six data clusters (each with 5 or 6 datapoints) in the local data association/clustering process. These six clusters divide into two sets of three clusters each. As figure 8 shows, each of these sets of clusters is traceable to one of the two targets in the hypothetical scenario of figure 6.

TRACK NUMBER	TRACK TRK	INDEX EXT	WATER TIME	PEAK NUMBER	PROB SCORE	X--CHI SQUARE SCORES--X STAGEWISE	CUMULATIVE	MEAS RESIDUALS DELTAT	DELTAF
1	1	0	-0.0010	8	-6.45	0.0152	0.0152	8.687	0.07035
			0.9953	33	-8.32	1.0792	1.0944	-24.269	0.01335
			1.9857	5	-10.52	1.3557	2.4501	-17.671	0.02875
			3.0112	34	-12.39	0.4222	2.8723	2.046	-0.02331
			4.0125	13	-19.32	0.0786	2.9509	-82.430	0.25292
2	2	0	-0.0010	8	-6.45	0.0152	0.0152	8.687	0.07035
			0.9953	33	-8.32	1.0792	1.0944	-24.269	0.01335
			1.9857	5	-10.52	1.3557	2.4501	-17.671	0.02875
			3.0112	34	-12.39	0.4222	2.8723	2.046	-0.02331
			4.0125	13	-19.32	0.0786	2.9509	-82.430	0.25292
			4.9977	28	-22.04	2.1881	5.1390	25.970	0.02848
3	3	0	1.0053	14	-7.31	0.0838	0.0838	-10.937	0.44141
			2.0106	17	-13.57	0.1864	0.2702	-46.682	0.15026
			3.0023	11	-17.16	3.0140	3.2843	23.054	-0.06198
			4.0092	36	-18.76	0.5059	3.7901	6.139	0.01519
			5.0020	7	-21.10	1.2052	4.9954	14.547	-0.03075
4	4	0	1.0048	33	-6.54	0.0719	0.0719	-21.027	0.08340
			1.9918	5	-8.71	0.7200	0.7919	-6.885	0.02879
			3.0082	34	-10.43	0.4120	1.2019	9.183	-0.01793
			4.0219	13	-17.38	0.0101	1.2120	-16.428	0.01642
			4.9974	28	-20.38	2.7201	3.9322	31.059	0.02088
5	5	0	-0.0084	35	-6.23	0.0100	0.0100	7.004	0.05368
			1.0139	14	-13.44	0.1248	0.1348	-64.489	0.47312
			2.0056	17	-15.71	1.6718	1.8066	-34.920	-0.00335
			3.0038	11	-19.09	2.7255	4.5321	4.985	-0.05936
			4.0109	36	-20.57	0.5344	5.0665	-5.700	0.01716
6	6	0	-0.0084	35	-6.23	0.0100	0.0100	7.004	0.05368
			1.0139	14	-13.44	0.1248	0.1348	-64.489	0.47312
			2.0056	17	-15.71	1.6719	1.8066	-34.920	-0.00335
			3.0038	11	-19.09	2.7255	4.5321	4.985	-0.05936
			4.0109	36	-20.57	0.5344	5.0665	-5.700	0.01716
			5.0020	7	-22.86	1.1264	6.1928	10.503	-0.03701

Table 5. Example of Type 4 Output

```
ARC-KA Tenex 1.34.34, ARC Exec 1.53.91
There are 9+5 Jobs and the Load av. 1s 2.85
Ⓐ @LOGIN MOORE
(Account)
Job 16 on TTY11 24-May-80  14119
Previous login: 24-May-80  12151
MOORE Over allocation by 1728 pages.
Ⓑ WIDTH 132
Ⓒ @MARCY

RUNNING NOTES:

     * SET TERMINAL WIDTH TO 132
     * RUN PROGRAM ON A TEKTRONIX TERMINAL IF GRAPHIC OUTPUT OPTIONS WILL BE SELECTED
     * ANSWER ALL YES OR NO QUESTIONS BY TYPING "YES" OR "NO"
     * PROGRAM DEVELOPED FOR ARPA BY MICHAEL H. MOORE

Is this a Tektronix Terminal
Ⓓ YES
```

Figure 7. Examples of user/MARCY dialogue.

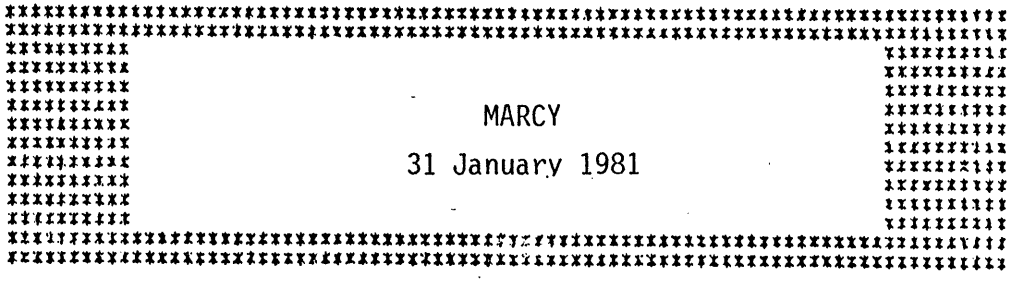

(E) ENTER TYPE OF COORDINATES DESIRED FOR INPUT AND OUTPUT

LATITUDE: NORTH=1, SOUTH=-1
LONGITUDE: EAST=1, WEST=-1

LATITUDE = [1]

LONGITUDE = [-1]

(F) ENTER SPEED OF SOUND

SOUND SPEED = [2803.564] (KNOTS)

(G) ENTER NUMBER OF SURVEILLANCE STATIONS (15 OR LESS)

NUMBER = [3]

ENTER FOR EACH SURVEILLANCE STATION:

* REFERENCE NUMBER
* INITIAL GEOGRAPHIC POSITION (DEGREES LATITUDE AND LONGITUDE)
* COURSE (DEGREES TRUE) AND SPEED (KNOTS)

STATION NUMBER	INITIAL POSITION LATITUDE	LONGITUDE	COURSE	SPEED
1	30	130	0	0
2	10	120	0	0
3	10	140	0	0

(H) ENTER NAMES OF PARAMETER DATAFILES (USE EXACTLY FIVE CHARACTERS)

BATCH-MODE PARAMETER DATAFILE = [BTMOD]

ITERATIVE-MODE PARAMETER DATAFILE = [ITMOD]

Figure 7. Examples of user/tracker dialogue (continued)

```
(I)  UNIVERSAL PARAMETERS

     COORDINATES IN USE FOR THIS RUN:   LATITUDE = NORTH
                                        LONGITUDE = WEST

     SOUND SPEED =  2883.564 (KNOTS)

     STATION PARAMETERS

     STATION        INITIAL POSITION
      NUMBER     LATITUDE   LONGITUDE     COURSE     SPEED

           1      30.0000    130.0000        0.0        0.0
           2      10.0000    120.0000        0.0        0.0
           3      10.0000    140.0000        0.0        0.0

     BATCH-MODE PARAMETER DATAFILE = BTMOD.DAT
     Recursive-Mode Parameter Datafile = ITMOD.DAT


     ARE THESE PARAMETERS SATISFACTORY
     YES
(J)  SELECT RUNNING MODE

          MODE 1:  BATCH MODE
          MODE 2:  Recursive-Mode
          MODE 3:  STOP

     MODE = 1


(K)  SEARCHING FOR TRACKS IN BATCH MODE ...
(L)  SELECT MODE OF SPECIFYING BATCH-MODE PARAMETERS

          MODE 1:  RESTORE PARAMETERS FROM OLD DATAFILE
          MODE 2:  ENTER PARAMETERS MANUALLY

     MODE = 2
     ENTER NAME OF PEAK DATAFILE (USE EXACTLY FIVE CHARACTERS)
(M)  DATAFILE = PKSF5
(N)  ENTER DESIRED BOUNDS ON LENGTH OF TRACKS
     MINIMUM LENGTH = 5
     MAXIMUM LENGTH = 6
```

Figure 7. Examples of user/tracker dialogue (continued)

```
(O) DO YOU WANT TO SPECIFY ANY ITEM NUMBER CONSTRAINTS ON COMPONENTS OF TRACKS
NO
DO YOU WANT TO SPECIFY ANY CONSTRAINTS ON STATIONS OF DATAPOINTS
NO
DO YOU WANT TO SPECIFY ANY CONSTRAINTS  ON BEARINGS OF DATAPOINTS
NO
DO YOU WANT TO SPECIFY ANY CONSTRAINTS ON FREQUENCY BINS OF DATAPOINTS
NO
DO YOU WANT TO SPECIFY ANY CONSTRAINTS ON TOR'S OF DATAPOINTS
YES
ENTER LOWER BOUND AND UPPER BOUND ON TOR

LOWER BOUND • 0     (HOURS)

UPPER BOUND • 6     (HOURS)

DO YOU WANT TO SPECIFY LOWER BOUNDS ON COHERENCES OF DATAPOINTS
NO
(P) ENTER PARAMETERS FOR KALMAN FILTER

ENTER DIAGONAL ELEMENTS OF R MATRIX (E FORMAT OK)

R(1,1) • 400      (SECS**2)
R(2,2) • 1E-10    (HZ**2)

(Q) ENTER PARAMETERS SIGMA1**2 AND SIGMA2**2 FOR Q MATRIX (E FORMAT OK)

SIGMA1**2 • 6.944E-05  (DEGS**2)
SIMGA2**2 • 2.778E-04 ((DEGS/HOUR)**2)

(R) ENTER PARAMTERS DTMIN AND DTMAX FOR TIME TEST

DTMIN • 0.1     (HOURS)
DTMAX • 1.1     (HOURS)
```

Figure 7. Examples of user/tracker dialogue (continued)

```
(S) SELECT MODE OF ESTIMATING INITIAL STATE VECTORS

        MODE 1:  COMPUTE ESTIMATES FOR SOME OR ALL STARTING PEAKS
        MODE 2:  PROVIDE ESTIMATES AS NEEDED FOR ALL STARTING PEAKS

MODE •[1]

SELECT TYPE OF COMPUTED ESTIMATES

        TYPE 1:  FOR ALL STARTING PEAKS
        TYPE 2:  FOR SELECTED STARTING PEAKS

TYPE •[1]

SELECT MODE OF ESTIMATING INITIAL COVARIANCE MATRICES

        MODE 1:  COMPUTE ESTIMATES (NOT IMPLEMENTED)
        MODE 2:  PROVIDE ESTIMATES MANUALLY IN ADVANCE.
        MODE 3:  PROVIDE ESTIMATES MANUALLY WHEN NEEDED

MODE •[2]

SELECT TYPE OF ADVANCE ESTIMATES

        TYPE 1:  FOR ALL STARTING PEAKS
        TYPE 2:  FOR SELECTED STARTING PEAKS

TYPE •[1]

SPECIFY CODES FOR STANDARD INITIAL VARIANCES

X-ONE SIGMA LEVEL-X

   POS          VEL
 COORD        COORD     CODE

 10 NM        10 KT        1
 30 NM        30 KT        2
 60 NM        60 KT        3

POSITION CODE •[3]

VELOCITY CODE •[3]
```

Figure 7. Examples of user/tracker dialogue (continued)

```
(T) ENTER THRESHHOLDS FOR SCORES

SELECT MODE OF SPECIFYING THRESHHOLDS FOR PROBABILITY SCORES

        MODE 1:  SELECT DEFAULT OPTION
        MODE 2:  ENTER THRESHHOLDS MANUALLY

MODE •[1]

SELECT DEFAULT OPTION

        OPTION 1:  HIGH THRESHHOLDS (-10 FOR ALL COMPONENTS)
        OPTION 2:  MED THRESHHOLDS (-50 FOR ALL COMPONENTS)
        OPTION 3:  LOW THRESHHOLDS (-100 FOR ALL COMPONENTS)
        OPTION 4:  VERY LOW THRESHHOLDS (-999 FOR ALL COMPONENTS)

OPTION •[4]

SELECT MODE OF SPECIFYING THRESHHOLDS FOR CUMULATIVE CHI-SQUARE SCORES

        MODE 1:  SELECT DEFAULT OPTION
        MODE 2:  ENTER THRESHHOLDS MANUALLY

MODE •[1]

SELECT DEFAULT OPTION

        OPTION 1:  VERY HIGH CONFIDENCE (0.99)
        OPTION 2:  HIGH CONFIDENCE (0.95)
        OPTION 3:  LOW CONFIDENCE (0.90)
        OPTION 4:  VERY LOW CONFIDENCE (0.50)

OPTION •[3]

ENTER THRESHHOLD FOR STAGEWISE CHI-SQUARE TEST AT EACH STAGE

THRESHHOLD •[9]

(U) DATA ENTRY IS COMPLETE

DO YOU WANT PARAMETERS TO BE PRINTED OUT
[YES]
```

Figure 7. Examples of user/tracker dialogue (continued)

```
PARAMETERS FOR BATCH-MODE TRACK CONSTRUCTION

PARAMETER DATAFILE • BTMOD.DAT

PEAK DATAFILE • PKSFS.DAT

MINIMUM TRACK LENGTH •  5
MAXIMUM TRACK LENGTH •  6

CONSTRAINTS ON TRACK COMPONENTS:  NONE

CONSTRAINTS ON STATIONS:  NONE

CONSTRAINTS ON BEARINGS:  NONE

CONSTRAINTS ON FREQUENCY BINS:  NONE

CONSTRAINTS ON TOR'S:  LOWER BOUND •  0.00 (HOURS)     UPPER BOUND •  6.00 (HOURS)

CONSTRAINTS ON COHERENCES:  NONE

 PARAMETERS FOR KALMAN FILTER

R • DIAG( 0.40E+03 (SECS**2),  0.10E-09 (HZ**2))

SIGMA1**2 •  0.69E-04 (DEGS**2)          DTMIN •    0.1000 (HOURS)
SIGMA2**2 •  0.23E-03 ((DEGS/HOUR)**2)   DTMAX •    1.1000 (HOURS)

XHAT(0/0) TO BE COMPUTED FOR ALL PEAKS

PHAT(0/0) PRE-SPECIFIED FOR ALL PEAKS: POSITION CODE • 3     VELOCITY CODE • 3

THRESHHOLDS FOR SCORES

TRACK                    CUMULATIVE     STAGEWISE
STAGE       PROB      CHI SQUARE     CHI SQUARE

    1     -999.0            4.6            9.0
    2     -999.0            7.8            9.0
    3     -999.0           10.6            9.0
    4     -999.0           13.4            9.0
    5     -999.0           16.0            9.0
    6     -999.0           18.5            9.0

CONFIDENCE LEVEL FOR CUMULATIVE CHI-SQUARE THRESHHOLDS •  3

(V) ARE THESE PARAMETERS SATISFACTORY
    (NO)
```

Figure 7. Examples of user/tracker dialogue (continued)

```
(W) INDICATE AREA WHERE CORRECTION IS NEEDED

        AREA 1:  PEAK DATAFILE
        AREA 2:  LENGTH OF TRACKS
        AREA 3:  COMPONENT CONSTRAINTS
        AREA 4:  STATION CONSTRAINTS
        AREA 5:  BEARING CONSTRAINTS
        AREA 6:  BIN CONSTRAINTS
        AREA 7:  TOR CONSTRAINTS
        AREA 8:  COHERENCE CONSTRAINTS
        AREA 9:  DATA FOR KALMAN FILTER

AREA =[9]

  INDICATE AREA WHERE CORRECTION IN PARAMETERS FOR KALMAN FILTER IS NEEDED

        AREA 1:  R MATRIX
        AREA 2:  PARAMETERS SIGMA1**2 AND SIGMA2**2
        AREA 3:  PARAMETERS DTMIN AND DTMAX
        AREA 4:  METHOD OF SPECIFYING THE XHAT(0/0) AND PHAT(0/0)
        AREA 5:  THRESHHOLDS FOR SCORES
AREA =[5]

ENTER THRESHHOLDS FOR SCORES

SELECT MODE OF SPECIFYING THRESHHOLDS FOR PROBABILITY SCORES

        MODE 1:  SELECT DEFAULT OPTION
        MODE 2:  ENTER THRESHHOLDS MANUALLY

MODE =[1]

SELECT DEFAULT OPTION

        OPTION 1:  HIGH THRESHHOLDS (-10 FOR ALL COMPONENTS)
        OPTION 2:  MED THRESHHOLDS (-50 FOR ALL COMPONENTS)
        OPTION 3:  LOW THRESHHOLDS (-100 FOR ALL COMPONENTS)
        OPTION 4:  VERY LOW THRESHHOLDS (-999 FOR ALL COMPONENTS)

OPTION =[4]

SELECT MODE OF SPECIFYING THRESHHOLDS FOR CUMULATIVE CHI-SQUARE SCORES

        MODE 1:  SELECT DEFAULT OPTION
        MODE 2:  ENTER THRESHHOLDS MANUALLY

MODE =[1]

SELECT DEFAULT OPTION

        OPTION 1:  VERY HIGH CONFIDENCE (0.99)
        OPTION 2:  HIGH CONFIDENCE (0.95)
        OPTION 3:  LOW CONFIDENCE (0.90)
        OPTION 4:  VERY LOW CONFIDENCE (0.50)

OPTION =[3]

ENTER THRESHHOLD FOR STAGEWISE CHI-SQUARE TEST AT EACH STAGE

(X) THRESHHOLD =[10]
```

Figure 7. Examples of user/tracker dialogue (continued)

```
DATA ENTRY IS COMPLETE

DO YOU WANT PARAMETERS TO BE PRINTED OUT
YES

PARAMETERS FOR BATCH-MODE TRACK CONSTRUCTION


PARAMETER DATAFILE = BTMOD.DAT

PEAK DATAFILE = PKSF5.DAT

MINIMUM TRACK LENGTH =  5
MAXIMUM TRACK LENGTH =  6

CONSTRAINTS ON TRACK COMPONENTS:  NONE

CONSTRAINTS ON STATIONS:  NONE

CONSTRAINTS ON BEARINGS:  NONE

CONSTRAINTS ON FREQUENCY BINS:  NONE

CONSTRAINTS ON TOR'S:  LOWER BOUND =  0.00 (HOURS)     UPPER BOUND =  6.00 (HOURS)

CONSTRAINTS ON COHERENCES:  NONE

PARAMETERS FOR KALMAN FILTER

R = DIAG( 0.40E+03 (SECS**2),  0.10E-09 (HZ**2))

SIGMA1**2 =  0.69E-04 (DEGS**2)          DTMIN =    0.1000 (HOURS)
SIGMA2**2 =  0.20E-03 ((DEGS/HOUR)**2)   DTMAX =    1.1000 (HOURS)

XHAT(0/0) TO BE COMPUTED FOR ALL PEAKS

PHAT(0/0) PRE-SPECIFIED FOR ALL PEAKS:  POSITION CODE =  3     VELOCITY CODE =  3

THRESHHOLDS FOR SCORES

TRACK                    CUMULATIVE     STAGEWISE
STAGE       PROB      CHI SQUARE     CHI SQUARE

    1     -999.0             4.6           10.0
    2     -999.0             7.8           10.0
    3     -999.0            10.6           10.0
    4     -999.0            13.4           10.0
    5     -999.0            16.0           10.0
    6     -999.0            18.5           10.0

CONFIDENCE LEVEL FOR CUMULATIVE CHI-SQUARE THRESHHOLDS =  3

(Y) ARE THESE PARAMETERS SATISFACTORY
YES

SAVING PARAMETERS ON PARAMETER DATAFILE BTMOD.DAT ...

PARAMETERS HAVE BEEN SAVED ON PARAMETER DATAFILE BTMOD.DAT

(Z) DO YOU WANT TO LOOK AT THE DATA IN THE PEAK DATAFILE
NO

HIT 'RETURN' WHEN READY TO CONSTRUCT TRACKS IN BATCH MODE
```

Figure 7. Examples of user/tracker dialogue (concluded)

TRACK NUMBER	TRACK TRK	INDEX EXT	WATER TIME	PEAK NUMBER	POSITION COORDINATES LATITUDE	LONGITUDE	COURSES AND SPEEDS COURSE	SPEED
1	1	0	-0.0010	8	25.0062	129.0801	272.7	3.00
			0.9953	33	24.9251	129.2984	274.0	3.54
			1.9857	5	23.5607	129.5018	188.2	40.63
			3.0112	34	23.8935	129.5519	193.2	21.53
			4.0125	13	22.9377	129.6473	190.0	28.30
2	2	0	-0.0010	8	25.0062	129.0801	272.7	3.00
			0.9953	33	24.9251	129.2984	274.0	3.54
			1.9857	5	23.5607	129.5018	188.2	40.63
			3.0112	34	23.8935	129.5519	193.2	21.53
			4.0125	13	22.9377	129.6473	190.0	28.30
			4.9977	28	22.4961	129.6945	192.3	28.72
3	3	0	1.0053	14	22.7757	130.5655	197.4	16.63
			2.0106	17	22.3383	130.1353	170.0	19.22
			3.0023	11	22.1394	130.1358	160.8	16.80
			4.0092	36	21.8653	130.0946	166.9	16.84
			5.0020	7	21.6533	130.0416	166.4	15.39
4	4	0	1.0240	33	24.4894	129.4529	272.7	3.47
			1.9918	5	23.7567	129.6880	188.2	38.14
			3.0262	34	23.4680	129.6188	190.0	27.76
			4.0019	13	22.9143	129.7228	189.8	28.32
			4.9974	28	22.4759	129.7267	192.1	28.75
5	5	0	-0.0204	35	23.2607	130.6576	88.8	3.17
			1.0139	14	23.7861	130.5068	168.9	19.35
			2.0096	17	23.4691	130.3289	169.9	19.19
			3.0038	11	23.1396	130.2869	169.8	16.86
			4.0109	36	21.8672	130.1782	166.7	16.87
6	6	0	-0.0204	35	23.2607	130.6576	89.8	3.17
			1.0139	14	23.7861	130.5068	168.9	19.35
			2.0096	17	23.4691	130.3289	169.9	19.19
			3.0038	11	23.1396	130.2869	169.8	16.86
			4.0109	36	21.8672	130.1782	166.7	16.87
			5.0020	7	21.6467	130.1169	166.2	15.41

Table 6. Example of Type 7 Output

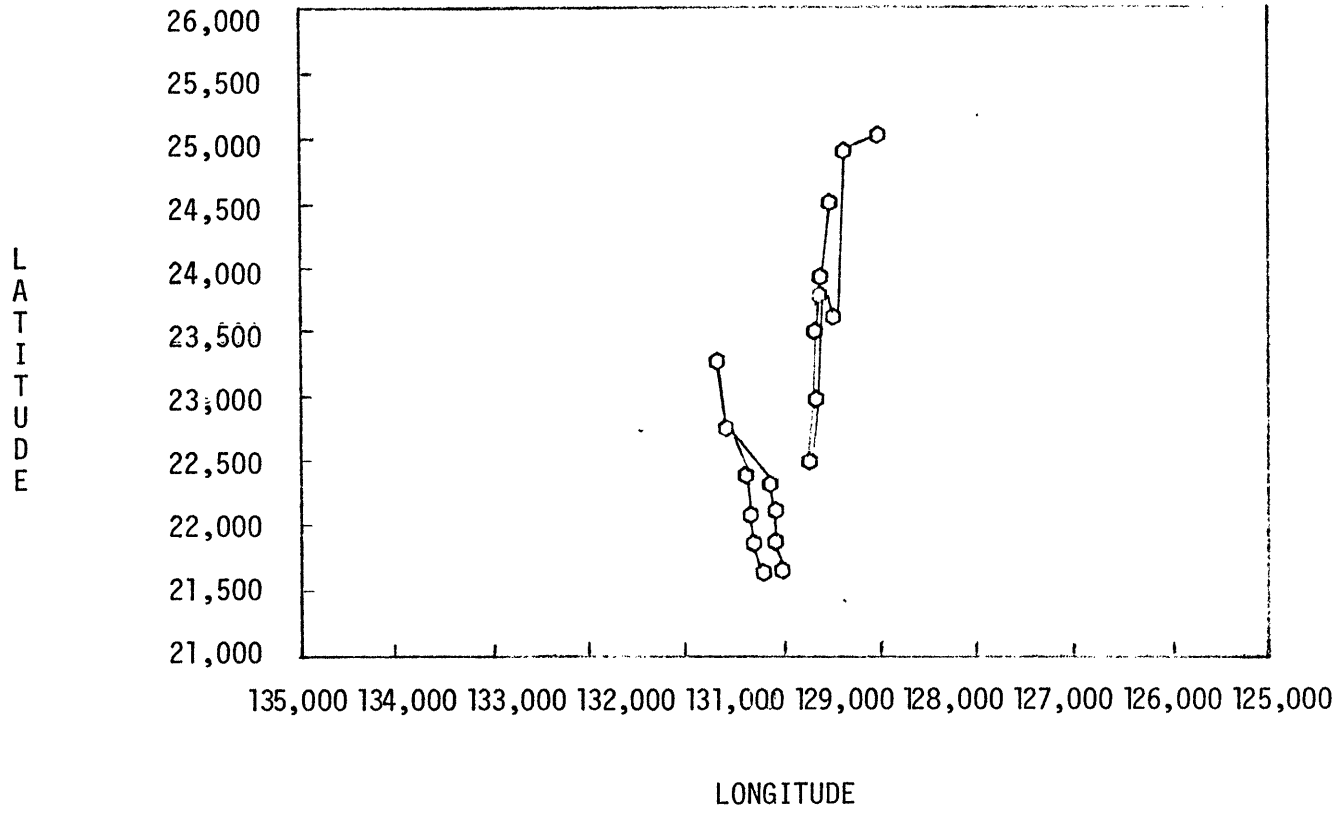

Figure 8. Example of Type 8 Output.

REFERENCES

1. Charles L. Morefield, "Application of 0-1 Integer Programming To Multi-Target Tracking Problems", IEEE Transactions on Automatic Control Volume AC-22 Number 3, June 1977, pp 302-312.

AN APOSTERIORI APPROACH TO THE MULTISENSOR CORRELATION OF DISSIMILAR SENSORS

Michael Kovacich
COMPTEK RESEARCH, INC.
Mare Island Department
P. O. Box 2194
Vallejo, CA 94592

AN APOSTERIORI APPROACH TO THE MUTLTISENSOR CORRELATION OF DISSIMILAR SENSORS

M. A. Kovacich
COMPTEK Research, Inc.
Mare Island Department
P.O. Box 2194
Vallejo, CA 94592

ABSTRACT

This paper discusses a novel aposteriori approach to the multisensor correlation of dissimilar sensors. In particular, the paper discusses the properties of a measure of track to track correlatibility that incorporates kinematical estimates, extracted features, platform identifications and, most importantly, the sequence of events exhibited by the tracks. It is shown that the measure of correlatibility is recursively calculable, exhibits robustness, incorporates the 'comparison' property (defined herein) and tends to one for the correct track pair.

I. BACKGROUND

The multisensor correlation function is depicted in the context of the surveillance function in Figure 1. The architecture displayed is typical of many military (especially Navy) surveillance systems. Multiple sensors are coupled to the tactical environment to generate streams of data. Each sensor system segments (clusters) the data stream into data substreams with each substream associated to a specific component (e.g. engine, emitter, hull) existing in the tactical environment. Each substream is further processed to yield kinematical estimates (generally not fully 3

dimensional) and identifiable features (attributes). Such a structure is denoted an intermediate track and the set of intermediate tracks for a sensor system form its intermediate track file.

The separate and, generally, dissimilar intermediate track files are then fused to form a single platform based global track file. The fusion process begins with multisensor correlation wherein it is determined which intermediate tracks refer to the same platform. The fusion process continues by combining the separate kinematical estimates to yield a more complete kinematical estimate and combining all available clues to generate a detailed platform identification.

As can be seen, the multisensor correlation function requires a framework that can measure track-to-track correlatibility based upon:

1) Kinematical estimates, extracted features and platform identification.

A more subtile requirement is that the multisensor correlation function be capable of measuring correlatibility based upon:

2) The sequence of characteristics (kinematical states, features, etc.) exhibited by the intermediate track.

The second requirement stems from the fact that in a noisy, hostile environment the information necessary to make good correlation decisions becomes available not at once but over time as the platforms exhibit their distinctive characteristics. The problem addressed in this paper is to exhibit a measure of correlatibility satisfying both of these requirements.

Many current multisensor correlation schemes do not adequately take into account the second requirement. For example, the usual measure of correlatibility that is derived from kinematical estimates is the chi-square statistic or the chi-square statistic plus the log-variance term. The problem with these measures of correlatibility are that they do not have a correlation 'memory', i.e. they measure the extent of current

kinematical agreement but do not reflect correlatibility based upon historical kinematical agreement. Therefore, these measures of correlatibility do not reflect all available information and must be considered definitely suboptimal. The correlation probability exhibited in this report is based directly upon a Bayesian framework and satisfies both of the above requirements for a measure of correlability. In particular, it accounts for all data and builds upon the sequence events exhibited by the tracks.

Some symbology is indicated in Figure 1:

$\vec{D}_A$ = the data stream generated by sensor A when coupled to the tactical environment. Same definition for $\vec{D}_B$ and $\vec{D}_C$.

$\vec{D}_{AJ}$ = the Jth data substream obtained after segmentation (cluttering, correlation) in the sensor system A.

$P[SP,F \mid \vec{D}_{AJ}]$ = the Jth intermediate track in sensor system A described as a conditional density over kinematical states and features.

$P[SP,ID \mid \vec{D}_{AJ}, \vec{D}_{BJ}, \vec{D}_{CL}]$ = a global track described as a conditional density over kinematical states and platform identifications conditioned upon the correlated data substreams indicated.

II. MOTIVATION FOR THE APOSTERIORI APPROACH

To further motivate the particular correlation probability to be chosen for detailed evaluation, consider Figure 2 wherein three general correlation approaches are indicated. The setting for this discussion consists of two intermediate track files with track J in one track file correlatible to tracks K and L in the other intermediate track file. H_{JK} and H_{JL} are the two correlation hypotheses: J and K represent the same

vehicle; J and L represent the same vehicle, respectively. The parameter appearing in the data substreams indicates that the data substream is current up till and including time, T_n.

The three approaches are

a) the strict aposteriori approach (top case)
b) the 'semi'-likelihood approach (middle case)
c) the strict likelihood approach (bottom case).

For each case a ratio is indicated that measures the relative strength of the two correlation hypotheses. The ratio would be compared to appropriate decision thresholds to yield correlation decisions.

It is well known that a decision rule based upon the strict likelihood approach is equivalent to one based upon the strict aposteriori approach for some set of apriori probabilities and some loss structure. Thus, at a theoretical level, decision rules based upon the top, and bottom approaches are equivalent. A significant problem occurs in a multisensor correlation context with the bottom approach. It lacks the 'comparison' property. The 'comparison' property is defined as the property whereby the ratio is meaningful no matter the quantity or units of the data items appearing in the data substreams. In the strict likelihood approach, the ratio is meaningful only if the number of data items in $\vec{D}_{BK}(n)$ and $\vec{D}_{BL}(n)$ are the same and that the respective data items have the same units. Otherwise, the likelihoods (densities in the continuum case) are not comparable.

To circumvent this problem, algorithms have been developed in which the comparison property is forced, for example, by discarding data items so that the numbers of data items are the same (Reference 1). This clearly compromises the approach at a very basic level. The strict aposteriori approach, on the other hand, obtains the comparison property since the probabilty that is calculated in not a probability or density of data items but rather of correlation hypotheses.

The middle approach in Figure 2, the 'semi'-likelihood approach, measures correlatibility by conditioning upon the previous data streams (up till T_{n-1}) and the correlation hypotheses, and calculates the probability (density in the continuum case) of obtaining the new data items at T_n. The 'semi'-likelihood approach suffers by not incorporating a correlation memory. Though the conditioning depends upon the previous data substreams, the probability or density is evaluated by considering the new data only. It does not build upon correlation probabilities calculated at earlier stages. On the other hand, the strict aposteriori correlation probability is based upon the full data streams and thus, at a theoretical level, incorporates all data into the measure of correlatibility.

Any other approach, other than those indicated, that measures correlatibility will lie along a continuum between the strict likelihood and the 'semi-'likelihood approaches. That is, any other approach will differ by more or less of the data substreams appearing in the conditioning or to the left of the conditioning bar. In all these cases, the approach will lack to a greater or lesser degree the comparison property or correlation memory. Based upon these observations, it was felt that, at a basic theoretical level, the strict aposteriori approach be followed.

III. PROPERTIES OF APOSTERIORI APPROACH

The aposteriori correlation probability between track J and K at time T_n is now discussed in more detail. See Figure 3. It is written recursively as a rational expression of the previous correlation probability and the correlation likelihood ratio. The correlation likelihood ratio measure the relative strength of obtaining the new data at T_n assuming the tracks are the same vehicle versus obtaining the new data assuming the tracks are not the same vehicle.

In Figure 4, the dependence of the correlation probability at T_n is expressed as a function of the correlation probability at T_{n-1} parameterized by the correlation likelihood ratio. Note that the

correlation probability increases if the correlation likelihood ratio exceeds one and decreases if it is less than one. Note also that the correlation probability is relatively insensitive to the correlation likelihood ratio when the previous correlation probability is near one. This property indicates that the correlation probability is fault tolerant or robust when it is near one, that is, sensor processing errors that cause the correlation likelihood ratio to be in error do not significantly effect the correlation probability as long as the correlation probability was near one.

The correlation probablity is now exhibited in more detail for a simple case of two radar ADT systems observing the same straight line vehicle. The ADT systems determine kinematical estimates using a 2 dimensional straight line Kalman filter. The new data items at T_n are the (x, y) coordinates of the radar detections of the two ADT systems.

$\vec{X}_J(n)$ = (x, y) coordinates of detection (centroid) of track J at T_n.

$\vec{X}_K(n)$ = (x, y) coordinates of detection (centroid) of track K at T_n.

The graph in Figure 6 characterizes the mean correlation probability as a function of the radar scan number when track J and track K, in fact, represent the same vehicle. Nominal radar accuracy measures were used. No sensor misalignment is assumed.

The intervals about each point represent the possible values of the correlation probability (with 90% condifence) <u>if</u> the correlation probability on the previous scan equals the average correlation probability of that scan.

The initial correlation probability is based upon the Gaussian density function that is coverted to a probability by multiplying by an area increment.

Note that the average correlation probability rises to one and that the variation in the correlation probability from scan to scan (the 90% confidence intervals) decreases. If track J and track K did not represent

the same vehicle, the correlation probability would not, in general, exhibit the same behavior. Also, it should be pointed out that the correlation probability rises more steeply to one in the three dimensional case and less steeply in the one dimensional case.

IV. SUMMARY

A summary of the properties observed so far concerning the aposteriori correlation probability are indicated in Figure 7. The correlation probability supports the multisensor correlation function since it is based on a general aposteriori framework. Its most novel features are that it explicitly measures the correlatibility of intermediate tracks based upon the sequence of events exhibited by the tracks; it is recursively calculable and tends to one for the correct pair of tracks; it becomes less sensitive to new data as it approaches one (fault tolerance); it obtains the 'comparison' property and, when considering the human operator, it is easily and directly interpreted.

Further studies are in progress to assess the operational utility of the correlation probability defined herein.

REFERENCES

1. Prove, R. W. Functional Description of Radar -ESM Track Correlation Algorithm. The John Hopkins University, Applied Physics Laboratory (1979). Confidential.

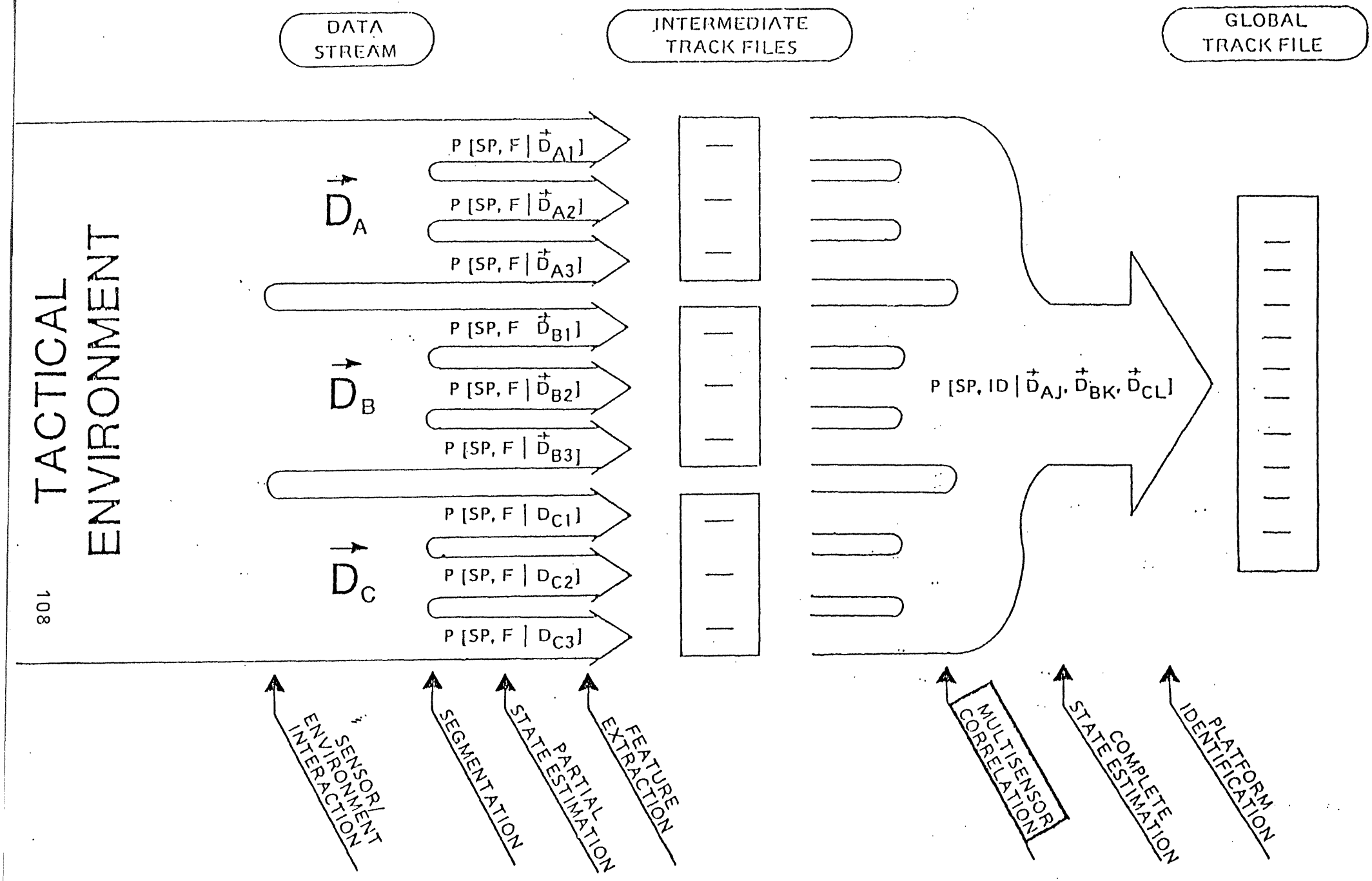

FIGURE 1 RELATIONSHIP OF MULTISENSOR CORRELATION TO THE SURVEILLANCE PROBLEM

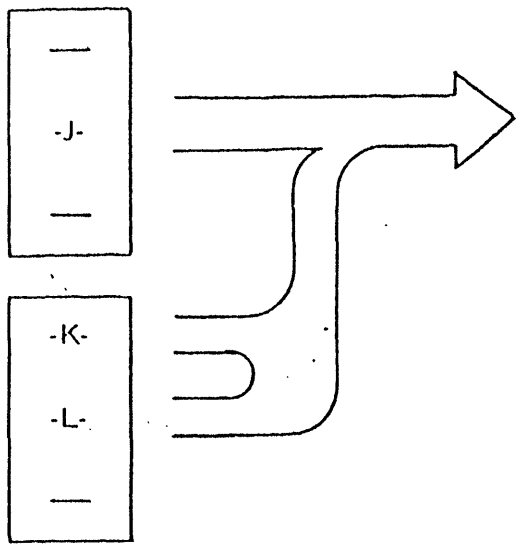

$$\frac{P\,[H_{JK} \mid \vec{D}_{AJ}(n), \vec{D}_{BK}(n)]}{P\,(H_{JL} \mid \vec{D}_{AJ}(n), \vec{D}_{BL}(n)]}$$

$$\frac{P\,[D_{AJ}(n), D_{BK}(n) \mid H_{JK}, \vec{D}_{AJ}(n-1), \vec{D}_{BK}(n-1)]}{P\,[D_{AJ}(n), D_{BL}(n) \mid H_{JL}, \vec{D}_{AJ}(n-1), \vec{D}_{BL}(n-1)]}$$

$$\frac{P\,[\vec{D}_{AJ}(n), \vec{D}_{BK}(n) \mid H_{JK}]}{P\,[\vec{D}_{AJ}(n), \vec{D}_{BL}(n) \mid H_{JL}]}$$

FIGURE 2 THREE CORRELATION APPROACHES CONTRASTED

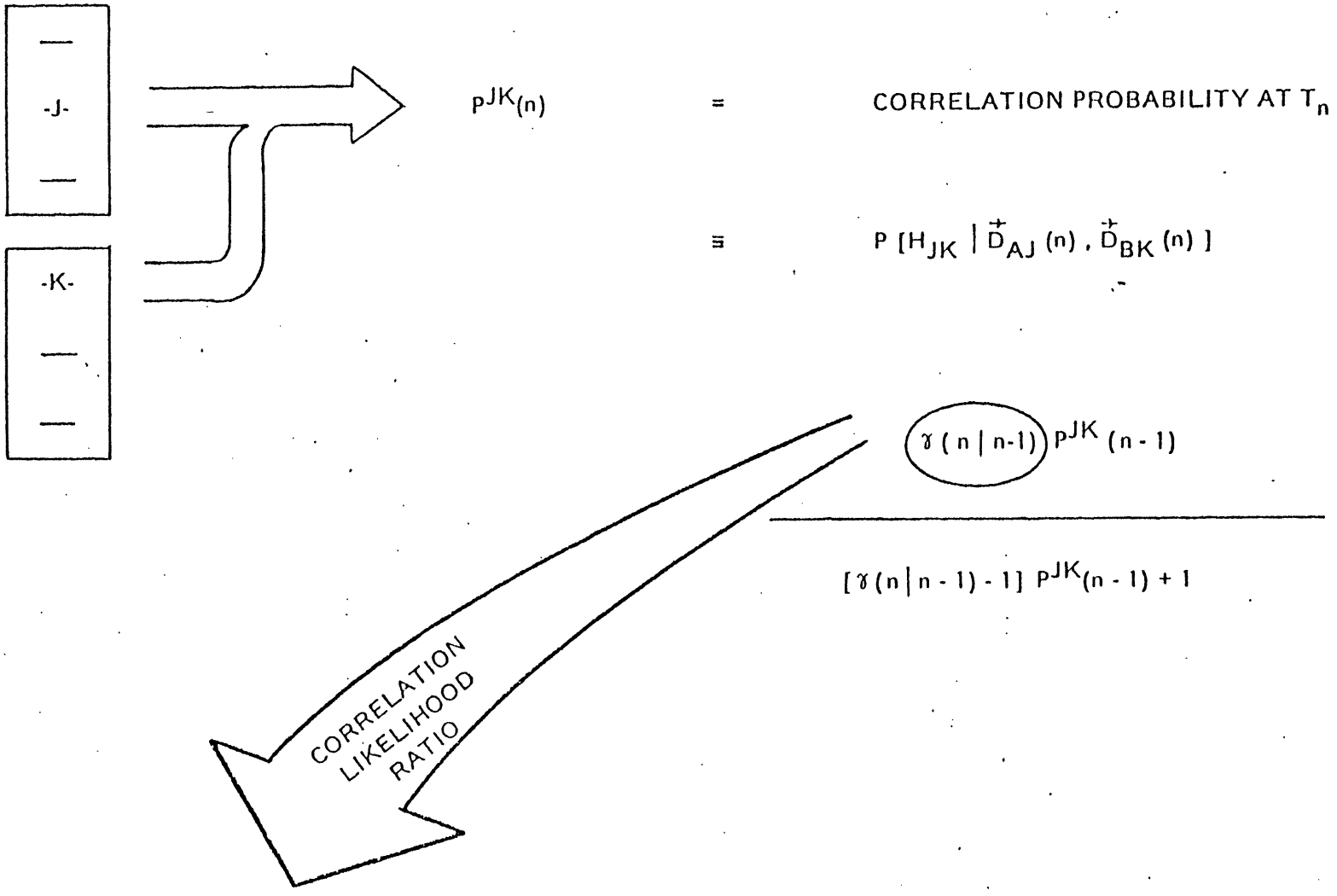

FIGURE 3 THE CORRELATION PROBABILITY UNDER INVESTIGATION

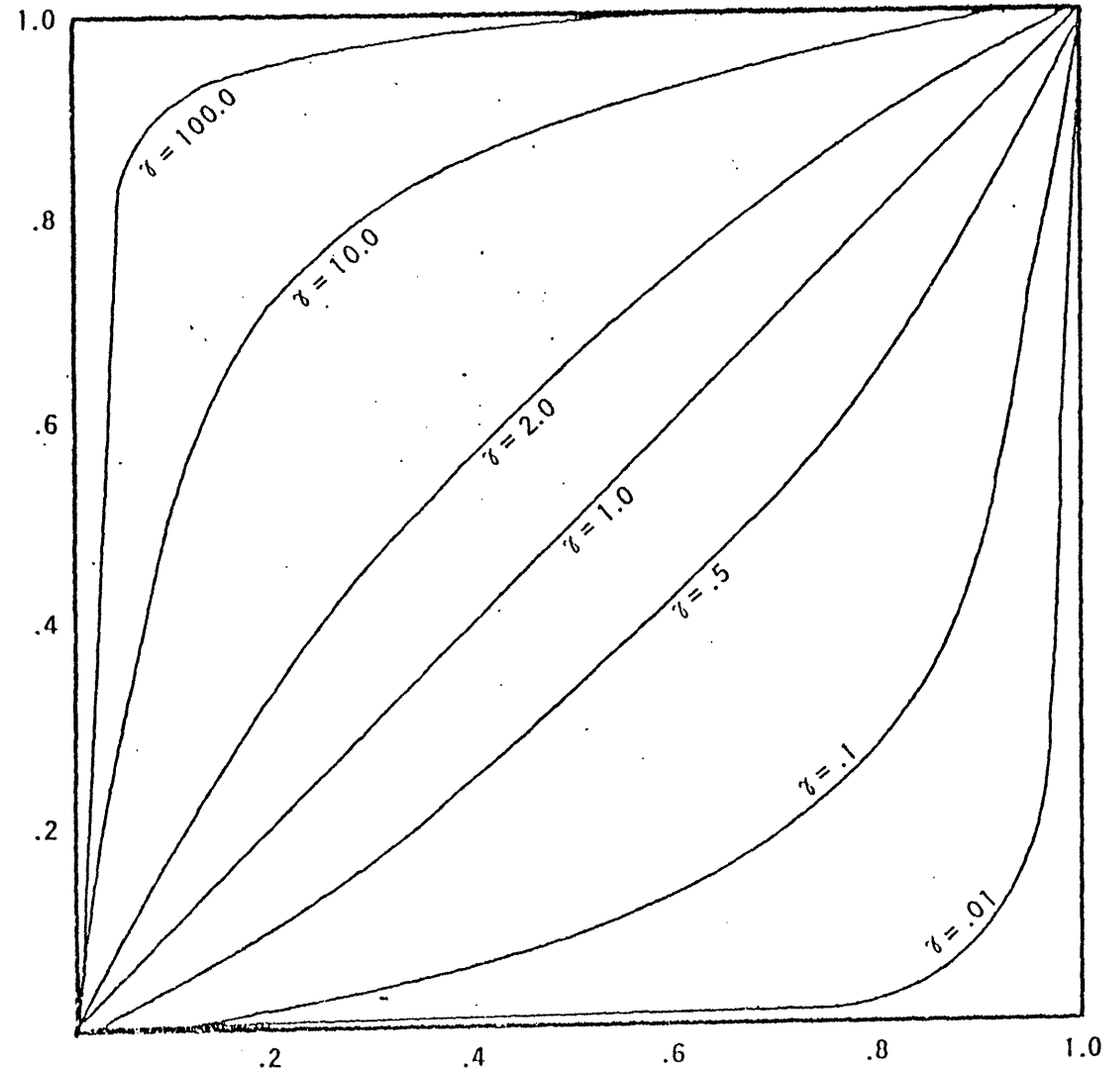

$$p^{JK}_{(n)} = \frac{\gamma\, p^{JK}_{(n-1)}}{[\gamma - 1]\; p^{JK}_{(n-1)} + 1}$$

FIGURE 4 THE DEPENDENCE ON THE CORRELATION LIKELIHOOD RATIO

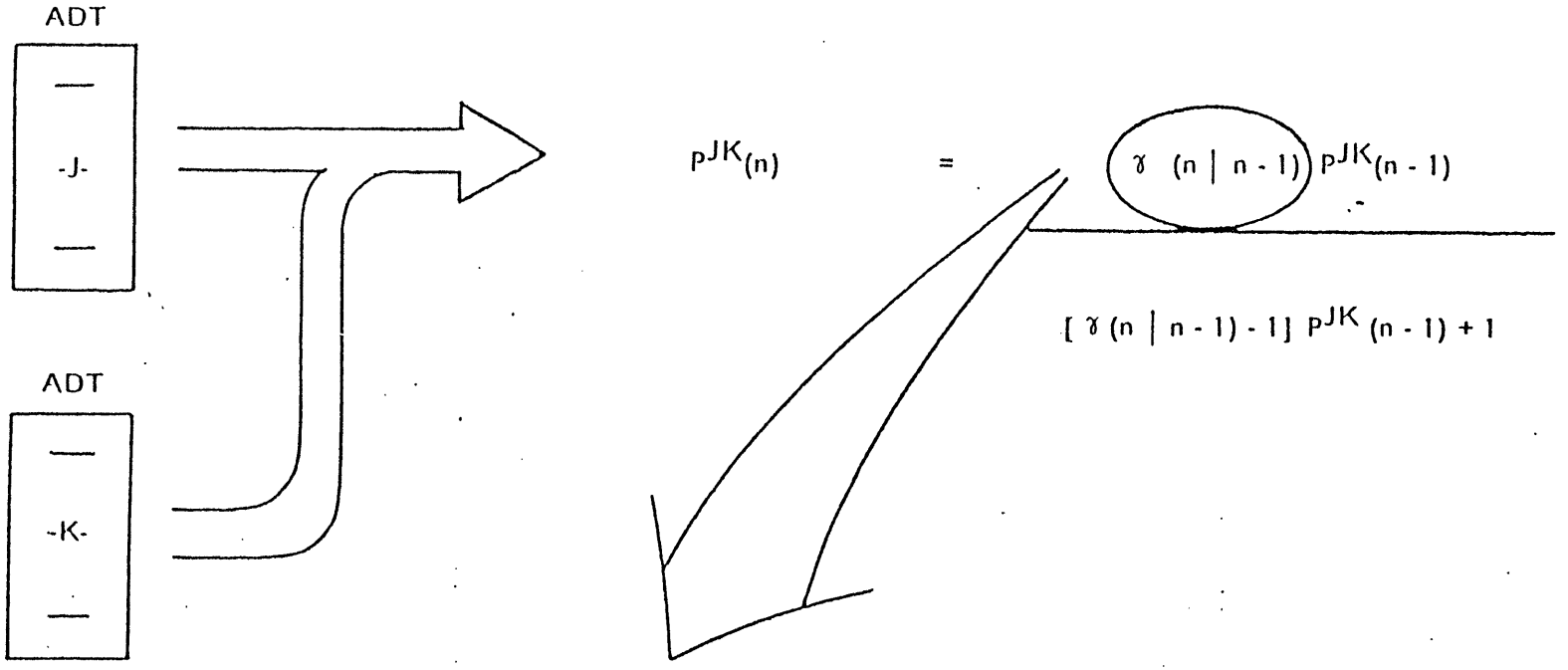

$$\gamma\ (n \mid n-1) = \frac{P\ [\vec{X}_J(n), \vec{X}_K(n) \mid H_{JK}\ \vec{D}_J(n-1), \vec{D}_K(n-1)]}{P\ [\vec{X}_J(n) \mid \vec{D}_J(n-1)]\ P\ [\vec{X}_K(n) \mid \vec{D}_K(n-1)]}$$

FIGURE 5 THE CORRELATION PROBABILITY FOR 2D STRAIGHT LINE TRACKS

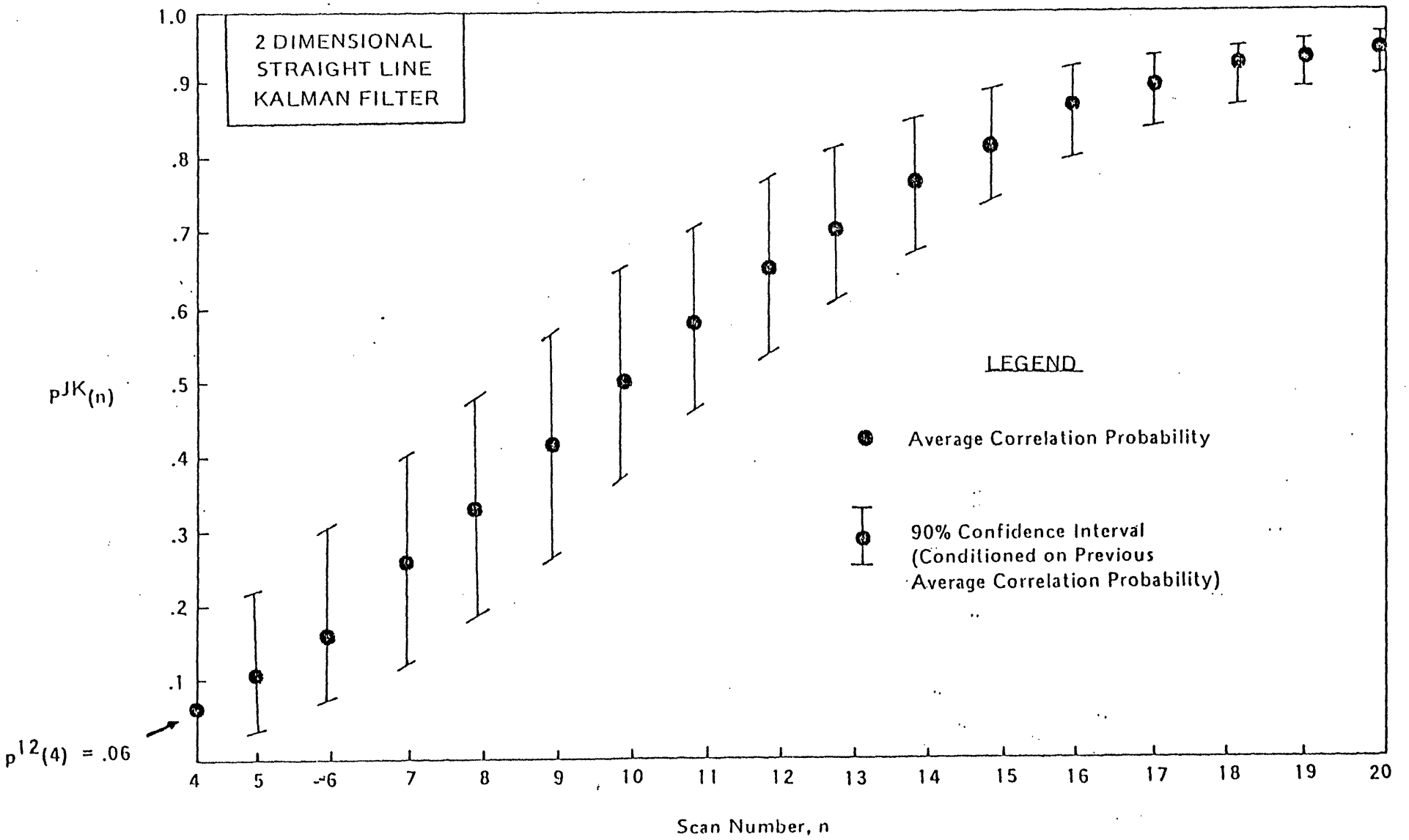

FIGURE 6 AVERAGE CORRELATION PROBABILITY AS A FUNCTION OF RADAR SCAN NUMBER FOR THE CASE TRACK J AND TRACK K IN FACT REPRESENT THE SAME VEHICLE

THE CORRELATION PROBABILITY:

- SUPPORTS MULTISENSOR CORRELATION OF DISSIMILAR SOURCES
- RECURSIVELY CALCULABLE
- PRESERVES MEMORY (TRACK HISTORY)
- TENDS TO 1 FOR CORRECT PAIR
- BUILT IN FAULT TOLERANCE
- 'COMPARISON' PROPERTY
- EASILY, DIRECTLY INTERRPRETED

FIGURE 7 SOME PROPERTIES SO FAR OBSERVED

A UNIFIED VIEW OF MULTI-OBJECT TRACKING

Krishna R. Pattipati
Nils R. Sandell, Jr.
Leslie C. Kramer

ALPHATECH, Inc.
3 New England Executive Park
Burlington, Mass. 01803

A UNIFIED VIEW OF MULTI-OBJECT TRACKING

by

Krishna R. Pattipati
Nils R. Sandell, Jr.
Leslie C. Kramer
ALPHATECH, Inc.
3 New England Executive Park
Burlington, Mass. 01803

1. INTRODUCTION

In many practical situations, dynamic systems are subjected to abrupt structural and parametric changes at random instants of time. A representative sample of such switching environments include:

- multi-object tracking problem in surveillance theory with realistic features such as uncertain observations due to false alarms caused by low signal to noise ratio or clutter; missing measurements due to detection probability less than one caused by noise or noise-like interference; non-uniform media; and changing target characteristics due to maneuvers [1]-[21];

- system failures caused by sudden external disturbances such as occurs in a power network subjected to transmission line trippings, generator shut-downs, malfunction of protective equipment, and the like [22]-[26];

- modeling uncertainties produced, for example, by the linear, finite-dimensional approximation of nonlinear, distributed and time-dependent dynamics of a chemical process or a power plant [27]-[29].

In this paper, we provide a general mathematical framework for classifying the existing state estimation and hypothesis testing problems [1]-[29] arising in systems subjected to random structural and parametric disturbances. The mathematical approach is based on an event-driven, linear stochastic system model comprising a hybrid (i.e., continuous and discrete) state space. It is shown that the problems of multi-target tracking in surveillance theory, Markov chain-driven systems, estimation under uncertain observations, maneuvering target tracking and system failure detection are special cases of this general formulation.

It is generally well known that implementation of the optimal (in the sense of minimum mean-square error) state estimate for these problems requires an exponentially growing number of hypotheses and, hence, memory and computational resources. Therefore, the main thrust of the previous research has been to devise techniques for reducing the number of hypotheses with little or no compromise on optimality. The general problem formulation of the present paper provides a common intellectual framework for comparing numerous existing (and proposed) hypothesis reduction techniques, and facilitates the development of a general purpose package for state estimation in switching environments. The computer algorithms permit a convenient comparison among various approaches in common numerical terms.

The paper is organized as follows. In Section 2, the estimation problem is formulated in the framework of an event-driven linear stochastic system model with hybrid state space. The optimal Bayesian estimate is derived in Section 3. The techniques for reducing the exponentially growing number of hypotheses are discussed in Section 4. Finally, the issues involved in the choice of a programming language for the implementation of the estimation algorithm are discussed in Section 5. It is concluded that the programming language PASCAL affords a flexible, general purpose implementation of the estimation algorithm.

2. PROBLEM FORMULATION

We consider a discrete-time, event driven system of Fig. 2-1 described by the state and measurement equations:

$$\underline{x}(k+1) = A\underline{x}(k) + \underline{w}(k) + \underline{e}(k) \tag{2-1}$$

$$\underline{z}(k) = C\underline{x}(k) + \underline{v}(k) + \underline{f}(k) \tag{2-2}$$

where the matrices A and C, and the deterministic bias vectors $\underline{e}(k)$ and $\underline{f}(k)$ are functions of a discrete-state stochastic process, $q(k) \in Q(k)$. The number of levels (i.e., number of discrete states or hypotheses), n_k in $Q(k)$ can be stage dependent. We call the set of hypotheses $Q(k)$, the <u>local set of hypotheses</u> at stage k. The noise sequences $\underline{w}(k)$ and $\underline{v}(k)$ are zero-mean, white-Gaussian noise sequences with covariances $W(k)$ and $V(k)$ dependent on the discrete-state process, $q(k)$. Clearly, the complete state description of the system at any stage k entails the mixed Markov process $\{\underline{x}(k), q(k)\}$.

It is required to find the minimum variance estimate of $\underline{x}(k)$ given the measurement set $\underline{z}^k \triangleq [\underline{z}(1), \underline{z}(2), \ldots, \underline{z}(k)]^*$ i.e., the conditional mean:

$$\hat{\underline{x}}(k|k) = E\{\underline{x}(k)|\underline{z}^k\} = \int_{\underline{x}(k)} \underline{x}(k)\, p(\underline{x}(k)|\underline{z}^k)\, d\underline{x}(k) \tag{2-3a}$$

and the conditional error covariance:

$$\Sigma(k|k) = E\{[\underline{x}(k)-\hat{\underline{x}}(k|k)][\underline{x}(k)-\hat{\underline{x}}(k|k)]'|\underline{z}^k\} \tag{2-3b}$$

The complexity of the event-driven system, and consequently of the estimation problem, is determined by the dynamics of $q(k)$, i.e., <u>number of levels n_k</u> of $q(k) \in Q(k)$ and the <u>nature of dependence</u> of $q(k)$ on the past measurement history, $\underline{z}^{k-1}$ and on the discrete-stochastic process history, $\underline{q}^{k-1} = [q(1), q(2), \ldots, q(k-1)]$. A partial list of problem formulations subsumed by Eqs. 2-1 and 2-2 is provided in the balance of this section.

2.1 MARKOV CHAIN-DRIVEN SYSTEMS

The process $q(k)$ takes on values 1, 2, ..., N and is described by the Chapman-Kolmogorov equation

$$\underline{\pi}(k+1) = \underline{\pi}(k)P \tag{2-4}$$

---

*The problem formulation may be generalized to include noisy observations on the discrete-state stochastic process, $q(k)$. In surveillance context, this generalization corresponds to data transfer from various field commanders to the data fusion process.

where $\underline{\pi}(k) = [\pi_1(k), \pi_2(k), \ldots, \pi_N(k)]$ is a row vector of discrete Markov state probabilities with $\pi_i(k) = P\{q(k)=i\}$ and $P = [P_{ij}]$ is a matrix of (possibly time varying) transition probabilities. That is, $P_{ij} = P\{q(k+1) = j | q(k) = i, \underline{q}^{k-1}, \underline{z}^k\} = p\{q(k+1) = j | q(k) = i\}$. The matrices A, C, and the bias vectors $\underline{e}$ and $\underline{f}$ are known for every $q(k) = 1, 2, \ldots, N$. It may be noted that when $q(k)$ is absorbing Markov chain (i.e., P=I), the formulation reduces to the well-known multiple model adaptive estimation (MMAE) algorithm, first derived by Magill [27].

2.2 STATE ESTIMATION UNDER UNCERTAIN OBSERVATIONS

The problem of state estimation when there is a nonzero probability that the state cannot be observed has been studied extensively in the literature [1]-[6]. In this case, the stochastic process $q(k)$ is a binary random variable and affects only the observation Eq. 2-2. Thus,

$$C = q(k)C \; ; \; q(k) = 0, \; 1 \tag{2-5}$$

and

$$V(k) = (1-q(k))V_0(k)+q(k)V_1(k) \tag{2-6}$$

The dynamics of $q(k)$ are represented by a two-state Markov chain described by an equation of the form (2-4), or as a binary independent random process. In the latter case, we have

$$P(q(k)=1 | \underline{q}^{k-1}, \underline{z}^{k-1}) = p(q(k)=1) = \delta \; ; \; p(q(k)=0) = 1-\delta \tag{2-7}$$

2.3 TRACKING IN A CLUTTERED ENVIRONMENT

The basic problem of tracking multiple targets is as follows: "given a set of returns (i.e., measurements) on the targets in each scan (stage) k, associate the measurements with the correct targets and determine an estimate of each target's state." Various solutions have been proposed for this problem, and [7]-[20] represent the state-of-the-art in multitarget tracking.

In a multitarget tracking problem, the $q(k)$ process affects only the measurement subsystem. In order to specify the $q(k)$ process for the tracking problem, we first consider a single target with cluttered measurements. If M_k is the number of measurements at stage k, and given that only one of them could have originated from the target of interest, then $q(k)$ assumes one of the following $n_k = M_k+1$ values:

$$q(k) = \begin{cases} 0 \text{ if none of the returns is correct} \\ i \text{ if the ith return is correct, } i=1,2,\ldots,M_k \end{cases} \tag{2-8}$$

The dynamics of $q(k)$ may be represented in various ways. For example, Barshalom and Tse [8] hypothesize a missed detection probability of α for the target, and then assume that no inference can be made on which of the M_k returns is correct from past data; so that

$$p(q(k)=0 | \underline{q}^{k-1}, \underline{z}^{k-1}) = \alpha; \text{ and } p(q(k)=i | \underline{q}^{k-1}, \underline{z}^{k-1}) = \frac{1-\alpha}{M_k} \tag{2-9}$$

Clearly, other representations are possible. Note in particular that the problem of state estimation under uncertain observations is mathematically equivalent to single target tracking in clutter with $M_k=1$. (Compare Eqs. 2-7 and 2-9). In a multitarget tracking problem with M_k returns, the process

$q(k) \in Q(k)$ represents a particular assignment of M_k returns among all the possible targets. These are N_f false targets, N_n new targets, and N_d of the previously hypothesized N_t targets (confirmed and tentative) such that $N_f + N_n + N_d = M_k$. With the assumption that each target can be associated with at most one measurement for each hypothesis (assignment) per scan, $Q(k)$ is the set of <u>all possible</u> assignments of M_k measurements among all the possible targets. The number of possible assignments (i.e., levels) n_k are:

$$N_k = \sum_{N_d=0}^{\min(M_k,N_t)} \sum_{N_n=0}^{M_k-N_d} n_{dn} \tag{2-10}$$

where

$$n_{dn} = \binom{M_k}{N_d}\binom{M_k-N_d}{N_n} \frac{N_t!}{N_t-N_d!} = M_k! \left(\frac{N_t!}{N_d!N_t-N_d!}\right)\left(\frac{1}{N_n!M_k-N_d-N_n!}\right) \tag{2-11}$$

The above specifications of n_k, where new targets can be initiated, corresponds to Reid's algorithm [15]. He specifies the $q(k)$ process as follows:

$$p(q(k)|\underline{q}^{k-1},\underline{z}^{k-1}) = P\left\{\begin{array}{l}\text{a particular assignment containing } N_d \text{ of } N_t \\ \text{previously hypothesized targets, } N_f \text{ false targets,} \\ N_n \text{ new targets such that } N_d+N_f+N_n=M_k \end{array} \middle| \underline{q}^{k-1},\underline{z}^{k-1}\right\}$$

$$= P\left\{\begin{array}{l}\text{an assignment containing } N_d, N_f, \text{ and } N_n \\ \text{assignments containing } N_d, N_n, N_f \end{array} \middle| \text{all}\right\}$$

$$\cdot P\{N_d,N_f,N_n|\underline{q}^{k-1},\underline{z}^{k-1}\}$$

$$= P_{dn} \cdot P\{N_d|\underline{q}^{k-1},\underline{z}^{k-1}\} \cdot P\{N_f|\underline{q}^{k-1},\underline{z}^{k-1}\} \cdot P\{N_n|\underline{q}^{k-1},\underline{z}^{k-1}\} \tag{2-12}$$

Reid assumes that all the assignments containing the <u>same</u> N_d, N_f, and N_n are equiprobable, i.e., $P_{dn} = 1/n_{dn}$. Also, the number of targets detected at stage k, N_d is assumed to have a binomial distribution:

$$P\{N_d|\underline{q}^{k-1},\underline{z}^{k-1}\} = \binom{N_t}{N_d} \cdot P_D^{N_d} \cdot (1-P_D)^{N_t-N_d} \tag{2-13}$$

where P_D is the probability of detection. Finally, both the number of new targets and false targets are assumed to follow Poisson distributions given by:

$$P\{N_n|\underline{q}^{k-1},\underline{z}^{k-1}\} = \frac{(\beta_n y)^{N_n} \cdot \exp[-\beta_n y]}{N_n!} \tag{2-14}$$

$$P\{N_f|\underline{q}^{k-1},\underline{z}^{k-1}\} = \frac{(\beta_f y)^{N_f} \cdot \exp[-\beta_f y]}{N_f!} \tag{2-15}$$

Thus, Eq. 2-12 simplifies to:

$$P\{q(k) \mid \underline{q}^{k-1}, \underline{z}^{k-1}\} = \frac{(\beta_n Y)^{N_n} \cdot (\beta_f Y)^{N_f}}{M_k!} P_D^{N_d} (1-P_D)^{N_t - N_d} \cdot \exp\{-(\beta_f+\beta_n)Y\} \tag{2-16}$$

When no new targets are allowed, Eq. 2-10 simplifies to:

$$n_k' = \sum_{N_d=0}^{\min(M_k, N_t)} \binom{M_k}{N_d} \cdot \frac{N_t!}{N_t - N_d!} \tag{2-17}$$

and corresponds to Bar-Shalom's [9] version of the multitarget tracking problem. For example, when $M_k = N_t = 3$, we have $n_k = 86$ and $n_k' = 34$. Thus, the number of possible assignments at each stage k are, in theory, considerably larger in Reid's version of the multitarget tracking problem [15] than in Bar-Shalom's [9]. When clutter density is high, the difference $(n_k - n_k')$ could be quite large ($\approx M_k \, 2^{M_k - 1}$ assuming $M_k >> 2$ and $N_t = 1$). This suggests that the initiation of new target tracks via an operator-interactive process may be preferable to an automated track initiation!

2.4 MANEUVERING TARGET TRACKING

The usual analysis of a tracking situation consists of describing the target dynamics by the state-space equations of the form 2-1 and 2-2 and designing a Kalman filter to provide the conditional mean estimate $\hat{\underline{x}}(k|k)$. This type of analysis works well until the target suddenly changes course or speed. One method of modeling a maneuver, suggested by Moose [21], is to let the bias vector $\underline{e}(k)$ in Eq. 2-1 assume N distinct (known) values, $\underline{e}_1$, $\underline{e}_2$, ..., $\underline{e}_N$. The transitions between any $\underline{e}_i$ and $\underline{e}_j$ are modeled by a Markov process.*

$$q(k) = i \Longleftrightarrow \underline{e}(k) = \underline{e}_i; \; i=1,2,\ldots,N \tag{2-18}$$

The dynamics of q(k) are described by Eq. 2-4.

2.5 SYSTEM FAILURE DETECTION

Recently failure detection and identification (FDI) has been the subject of considerable interest [22]-[26]. An important subclass of FDI problems is the detection and estimation of soft failures, viz., the bias errors and changes in the noise levels. The failure events are modeled as additive disturbances. The failure detection case can be modeled by

$$\underline{x}(k+1) = A\underline{x}(k) + \underline{w}(k) + q(k)\underline{e} \tag{2-19a}$$

$$\underline{z}(k) = C\underline{x}(k) + \underline{v}(k) + q(k)\underline{f} \tag{2-19b}$$

where q(k) = 1 for failure and q(k) = 0 otherwise. The bias vectors $\underline{e}$ and $\underline{f}$ are, in general, unknown and have to be estimated online. However, we will not address this question here, as there is a large literature on this subject [24], [35].

---

*It should be noted that Moose assumes a semi-Markov process for the transitions, but actually uses a Markov process model in the final implementation.

This concludes the list of special cases of our problem formulation. We now turn to the derivation of optimal (Bayesian) state estimate.

3. OPTIMAL BAYESIAN ESTIMATE

The sequence of measurements $\underline{z}^k = [\underline{z}(1),\underline{z}(2),\ldots,\underline{z}(k)]$ is a function of the particular sequence of the random process $\underline{q}^k = [\underline{q}(1),\underline{q}(2),\ldots,\underline{q}(k)]$. Therefore, if we define

$$Q^k = Q(1) \times Q(2) \times \ldots \times Q(k) = \{\underline{q}^k\} \tag{3-1}$$

as the global set of hypotheses at stage k, the cardinality of Q^k is

$$N_c(k) = |Q^k| = \prod_{i=1}^{k} n_i \tag{3-2}$$

The conditional mean, $\hat{\underline{x}}(k\,k)$ is given by

$$\hat{\underline{x}}(k|k) = \sum_{\underline{q}^k \varepsilon Q^k} \hat{\underline{x}}(k|k,\underline{q}^k) P(\underline{q}^k|\underline{z}^k) \tag{3-3}$$

In Eq. 3-3, $\hat{\underline{x}}(k|k;\underline{q}^k)$ is the conditional mean of $\underline{x}(k)$ given $\underline{z}^k$ and a particular sequence of the stochastic process, $\underline{q}^k$ and $P(\underline{q}^k|\underline{z}^k)$ in the posterior probability of the sequence $\underline{q}^k$ given $\underline{z}^k$. Clearly, $\hat{\underline{x}}(k|k)$ is the convex combination of the conditional estimates $\hat{\underline{x}}(k|k;\underline{q}^k)$.

The conditional error covariance, $\Sigma(k|k)$ is given by

$$\Sigma(k|k) = \sum_{\underline{q}^k \varepsilon \underline{Q}^k} P(\underline{q}^k|\underline{z}^k)\{\Sigma(k|k;\underline{q}^k) + [\hat{\underline{x}}(k|k;\underline{q}^k) - \hat{\underline{x}}(k|k)]\cdot[\hat{\underline{x}}(k|k;\underline{q}^k) - \hat{\underline{x}}(k|k)]'\} \tag{3-4}$$

where $\Sigma(k|k;\underline{q}^k)$ is the a posteriori estimation error covariance matrix for a given $\underline{q}^k$.

There are two important features of Eq. 3-4 that are worth noting. First, the conditional error covariance, $\Sigma(k|k)$ is a function of measurement data, due to the presence of terms $P(\underline{q}^k|\underline{z}^k)$, $\hat{\underline{x}}(k|k;\underline{q}^k)$ and $\hat{\underline{x}}(k|k)$. Second, $\Sigma(k|k)$ is not just a convex combination of the covariances of individual terms, $\Sigma(k|k;\underline{q}^k)$: it includes additional terms of the (positive semidefinite) dyadic form $[\hat{\underline{x}}(k|k;\underline{q}^k) - \hat{\underline{x}}(k|k)]\cdot[\hat{\underline{x}}(k|k;\underline{q}^k) - \hat{\underline{x}}(k|k)]'$. This shows that the covariance increases by the presence of terms whose estimates are significantly different from $\hat{\underline{x}}(k|k)$, weighted by $P(\underline{q}^k|\underline{z}^k)$. The structure of the optimal Bayesian estimation algorithm is shown in Fig. 3-1.

The conditional mean and covariance are evaluated as follows. Since the density $p(\underline{x}(k)|\underline{z}^k,\underline{q}^k)$ is Gaussian, the density $p(\underline{x}(k+1|\underline{z}^k;\underline{q}^k)$ is also Gaussian The corresponding means $\hat{\underline{x}}(k|k;\underline{q}^k)$ and $\hat{\underline{x}}(k+1|k;\underline{q}^k)$ are given by a Kalman filter of the form

$$\hat{\underline{x}}(k+1|k;\underline{q}^k) = A\hat{\underline{x}}(k|k;\underline{q}^k) + \underline{e}(k) \tag{3-5}$$

$$\hat{\underline{x}}(k+1|k+1;\underline{q}^{k+1}) = \hat{\underline{x}}(k+1|1;\underline{q}^k) + K\underline{r}(k+1;\underline{q}^{k+1}) \tag{3-6}$$

where $\underline{r}(k+1;\underline{q}^{k+1})$ is the innovation process:

$$\underline{r}(k+1;\underline{q}^{k+1}) = \underline{z}(k+1) - C\hat{\underline{x}}(k+1|k;\underline{q}^k) - \underline{f}(k+1) \tag{3-7}$$

Here, K is the Kalman gain calculated from the following equations:

$$\Sigma(k+1|k;\underline{q}^k) = A\Sigma(k|k;\underline{q}^k)A' + W(k) \tag{3-8}$$

$$S(k+1;\underline{q}^{k+1}) = C\Sigma(k+1|k;\underline{q}^k)C' + V(k+1) \tag{3-9}$$

$$K = \Sigma(k+1|k;\underline{q}^k)C'S^{-1}(k+1;\underline{q}^{k+1}) \tag{3-10}$$

$$\Sigma(k+1|k+1;\underline{q}^{k+1}) = (I-KC)\Sigma(k+1|k;\underline{q}^k) \tag{3-11}$$

It should be noted that A, $\underline{e}(k)$ and W(k) are functions of q(k), and C, $\underline{f}$ and V(k+1) are functions of q(k+1) in Eqs. 3-5 through 3-11. Here, $\Sigma(k+1)|\overline{k;\underline{q}^k)}$ is the a priori estimation error covariance matrix for a given $\underline{q}^k$. The innovation process $r(k+1;\underline{q}^{k+1})$ is zero mean, with covariance $S(k+1;\underline{q}^{k+1})$ and is normally distributed.

The only remaining item in Eqs. 3-3 and 3-4 is the a posteriori probability $P(\underline{q}^k|\underline{z}^k)$. Using Bayes' rule, this probability is given by

$$p(\underline{q}^k|\underline{z}^k) = a_K^{-1}p(\underline{z}^k|\underline{q}^k)p(\underline{q}^k) \tag{3-12}$$

where $a_k = p(\underline{z}^k)$ is a normalizing constant, $p(\underline{z}^k|\underline{q}^k)$ is the likelihood function, and $P(\underline{q}^k)$ is the a priori probability of the sequence $\underline{q}^k$. The likelihood function $p(\underline{z}^k|\underline{q}^k)$ may be evaluated recursively from

$$p(\underline{z}^k|\underline{q}^k) = p(\underline{z}(k)|\underline{z}^{k-1},\underline{q}^k)\cdot p(\underline{q}(k)|\underline{q}^{k-1},z^{k-1})\cdot p(\underline{z}^{k-1}|\underline{q}^{k-1})\,[p(q(k)|\underline{q}^{k-1})]^{-1} \tag{3-13}$$

Since in most applications q(k) is independent of $\underline{z}^{k-1}$, the likelihood function simplifies to

$$p(\underline{z}^k|\underline{q}^k) = p(\underline{z}(k)|\underline{q}^k,\underline{z}^{k-1})\ p(\underline{z}^{k-1}|\underline{q}^{k-1}) \tag{3-14}$$

Using the normality of innovation process, the negative log-likelihood function may be computed recursively from

$$\lambda(q^k) = -\log_e p(\underline{z}^k|\underline{q}^k) = \lambda(\underline{q}^{k-1}) + \frac{1}{2}\left[\underline{r}'(k;\underline{q}^k)S^{-1}(k;\underline{q}^k)\underline{r}(k;\underline{q}^k) + \dim(\underline{z}(k))\log_e(2\pi) + \log_e\left|S(k;\underline{q}^k)\right|\right] \tag{3-15}$$

with $\lambda(q^0) = 0$. Since $\underline{r}$ is Gaussian and white, $\lambda(q^k)$ will have a chi-square distribution with $\Sigma_{i=1}^{k}$ dim z(i) degrees of freedom. The hypotheses for which λ exceeds a certain threshold may be dropped [13], [16].

A more direct recursive formula for $P(\underline{q}^k|\underline{z}^k)$ can be derived as

$$P(\underline{q}^k|\underline{z}^k) = C_k^{-1}\ p(z(k)|\underline{q}^k,\underline{z}^{k-1})\ P(q(k)|\underline{q}^{k-1},\underline{z}^{k-1})\ P(\underline{q}^{k-1}|\underline{z}^{k-1}) \tag{3-16}$$

where $C_k = p(\underline{z}(k)|\underline{z}^{k-1})$ is a normalizing constant. Again, the hypotheses for which $P(\underline{q}^k|\underline{z}^k)$ is less than a certain threshold may be deleted [14], [15]. As mentioned earlier, the complexity of the estimation algorithm is determined by the quantity $P(q(k)|\underline{q}^{k-1},\underline{z}^{k-1})$ in Eq. 3-16.

Equations 3-3 through 3-16 constitute the recursive relations for the optimal Bayesian estimate. There are two important characteristics of this estimate that are worth noting. First, the optimal (condition mean) estimate

is a nonlinear function of the measurements due to the terms $P(\underline{q}^k|\underline{z}^k)$. Second, the computation of $\hat{\underline{x}}(k|k)$ requires an ever-growing number of filters with an associated growing memory and computational requirement. Thus, at stage k, we need $N_c(k)$ (cardinality of Q^k) elemental estimates, $\hat{x}(k|k;\underline{q}^k)$; $N_c(k)$ covariance matrices, $\Sigma(k|k;\underline{q}^k)$; and $N_c(k)$ posterior probabilities, $P(\underline{q}^k|\underline{z}^k)$. This is clearly impractical and hence, techniques must be devised to reduce the number of hypotheses. These are discussed in the next section.

4. HYPOTHESIS REDUCTION TECHNIQUES

The basic idea of hypothesis reduction techniques is to transform the global set of hypotheses Q^k into a smaller global set $\hat{Q}^k$ such that the memory and computational requirements are minimized, while maintaining the "near" optimality of the estimation algorithm. The various available techniques may be categorized into the following five groups: (1) use of a simplified dynamic model of the q(k) process; (2) hypothesis deletion; (3) hypothesis merging; (4) decoupling of hypotheses (cluster formation); and (5) use of system constraints to advantage.

A practical estimation algorithm may employ one or more of the above reduction techniques. Also, note that the hypothesis reduction techniques have close analogy to the methods of aggregating Markov chains [30], [31]. This analogy is pursued elsewhere [32].

4.1 SIMPLIFIED MODELS OF THE q(k) PROCESS

When q(k) is described by an N state Markov chain with N absorbing states (i.e., the transition probability matrix P=I), the global set of hypotheses Q^k is independent of k with a cardinality of N. The optimal Bayesian estimate can be implemented by a bank of N Kalman filters, each corresponding to one of the N absorbing states. The resulting estimation algorithm is the well-known multiple model adaptive estimation (MMAE) algorithm [27]-[29].

A more realistic description of the q(k) process, however, is via a weakly coupled Markov chain. In this case, the transition probability matrix, $P=I+\varepsilon B$, where ε is small. That is, P is diagonally dominant. Note than in this case, even for small ε, the optimal Bayesian estimate $\hat{\underline{x}}(k|k)$ is the weighted sum of N^k elemental estimates $\hat{\underline{x}}(k|k;\underline{q}^k)$ as in Fig. 3-1. However, intuition suggests that as long as $\sigma/\varepsilon >> \max(T_{Ri})$, where $\sigma = (t_k - t_{k-1})$ is the time step and T_{Ri} is the "response time" of the ith Kalman filter in the multiple model, then the MMAE algorithm should be "nearly" optimal. That is, the posterior probability of hypotheses with nonidentical elements is negligible and the number of hypotheses that are almost identical, and that have nearly identical estimates and covariances is large. The former set of hypotheses can be deleted, while the latter can be merged (as shown in the following) so as to reduce the computational load of the estimation algorithm. Thus, the weakly coupled Markov chain formulation provides an analytic framework to study hypothesis reduction techniques and is a subject for future research.

4.2 HYPOTHESIS DELETION

The basic idea of hypothesis deletion is to simply prune unlikely hypotheses in view of the measurements or via a heuristic technique. A straightforward heuristic pruning procedure is to simply limit the number of hypotheses to be included in the estimation algorithm. This is the approach employed

by Singer, et al. [7] in developing an N-scan (stage) filtering algorithm for a single target tracking. At each stage k, this algorithm keeps hypotheses corresponding to the last N scans, viz., $\sum_{i=k-N+1}^{k} n_i$ hypotheses, where $n_i = M_i + 1$, and M_i is the number of returns at stage i. A remarkable conclusion of their simulation was that with only N=1, near optimal performance was achieved. However, this conclusion is not, in general, valid in the multi-target tracking problem. For example, Keverian and Sandell [16] found that it was essential to have N>1 in tracking targets with crossing tracks.

Pruning on the basis of measurements may be accomplished using the likelihood function $p(\underline{z}^k|\underline{q}^k)$ (or equivalently, the negative log-likelihood function $\lambda(\underline{q}^k)$), or the a posteriori probability $p(\underline{q}^k|\underline{z}^k)$. The former approach was employed by Smith and Beuchler [13], Fraser and Meier [20], Sittler [11] and Keverian and Sandell [16]. The method of Keverian and Sandell [16] computes the likelihood function after each branching and keeps only the M most likely hypotheses at each stage. This prevents hypotheses with probability less than the current minimum of the M hypotheses from being extended. The choice of the parameter M is critical and determines the complexity versus optimality tradeoff of the estimation algorithm. The pruning technique based on posterior probabilities was employed by Reid [15]. He eliminates all hypotheses with a probability less than a threshold, α. Morefield [14] uses an optimization-based integer programming formulation to delete unlikely hypotheses; this is a batch processing approach. An illustration of a typical pruning technique is shown in Fig. 4-1.

If $\hat{Q}^k$ is the set of hypotheses remaining at stage k, then the corresponding prior and posterior probabilities must be normalized to have sum equal to 1. Thus,

$$\hat{P}(\underline{q}^k) = P(\underline{q}^k) \cdot \Big[\sum_{\underline{q}^{k'} \in \hat{Q}^k} P(\underline{q}^{k'}) \Big]^{-1} \qquad (4\text{-}1)$$

and a similar expression for the posterior probabilities. $\hat{Q}^k$ forms the basis for enumerating the subsequent set of hypotheses $Q^{k+1} = \hat{Q}^k \times Q(k+1)$ at stage k+1.

4.3 HYPOTHESIS MERGING

Hypothesis merging is the process of combining hypotheses in a "suitable" manner. The hypothesis merging techniques may be categorized into single-stage (also known as zero-scan or nonback-scan) and multistage (or multiple scan) algorithms. The multistage algorithms can be subdivided into fixed-scan (or fixed-depth) algorithms [15] and variable-scan (or variable-depth) algorithms [16]. A single-stage algorithm allows only one hypothesis to remain after each stage. Prime examples of the single-stage algorithms are the probabilistic data association filter (PDAF) of Bar-Shalom and Tse [8], the approximate Bayesian estimation algorithm of Sawaragi, et al. [2], and the algorithm of Athans, Whiting and Gruber [3]. The algorithms of Reid [15] and Keverian and Sandell [16] are representative of multistage algorithms. We briefly summarize these two types of hypothesis merging below.

4.3.1 Single-Stage Algorithms

The single-stage algorithms of [2], [3], and [8] make the fundamental assumption that the conditional density $p(\underline{x}(k)|\underline{z}^{k-1})$ is Gaussian with mean

$\underline{x}(k|k-1)$ and covariance $\Sigma(k|k-1)$. In our formulation, this assumption has the following consequences: (1) only one hypothesis $\underline{q}^{k-1}$ is retained at stage $k-1$, so that $|\underline{Q}^{k-1}| = 1$. Thus, $P(\underline{q}^{k-1}|\underline{z}^{k-1}) = 1$; (2) $P(\underline{q}^{k}|\underline{z}^{k}) = P(q(k)\ \underline{z}^{k})$, so that the set of hypotheses at stage k, $\underline{Q}^{k} = \underline{Q}^{k-1} \times \underline{Q}(k) = \underline{Q}(k)$ has n_k elements; and (3) the conditional densities $p(\underline{z}(k)\ \underline{z}^{k-1},\underline{q}^{k})$ in Eq. 3-21 are simply $p(\underline{z}(k)|\underline{z}^{k-1},q(k))$ and have known form.

In the probabilistic data association filter (PDAF), $q(k)$ takes on values $0,1,2,\ldots,M_k$ as in Eq. 2-8. Therefore, the posterior probability Eq. 3-16 simplifies to

$$P(q(k)=i|\underline{z}^{k}) = \beta_{k,i} = b_k^{-1} \cdot p(\underline{z}(k)|\underline{z}^{k-1},q(k)=i)P(q(k)=i|\underline{z}^{k-1}) \qquad (4\text{-}2)$$

where $b_k = P(\underline{z}(k)|\underline{z}^{k-1})$ is a normalization constant. Using the model of $P(q(k)=i|\underline{z}^{k-1})$ in Eq. 2-9, and the assumption that $P(\underline{x}(k)|\underline{z}^{k-1})$ is Gaussian, β_{ki}s are easily computed.

Since the $q(k)$ process affects only the measurement subsystem and since $p(\underline{x}(k)|\underline{z}^{k-1})$ is assumed to be Gaussian, a single Kalman-like algorithm (with a data dependent covariance matrix satisfying a Riccati equation) is adequate to implement the PDAF algorithm. The derivation is straightforward and may be found in Refs. [8], [32]. The structure of hypothesis merging is displayed in Fig. 4-2. The algorithms of [2], [3] have precisely the same form as in Fig. 4-2, but somewhat simpler due to inherently simpler assumptions on their structure.

4.3.2 Multistage Algorithms

The basic idea of a multistage algorithm is to combine only those hypotheses that have "similar" state estimates and covariances. Two hypotheses $\underline{q}^{k'}$ and $\underline{q}^{k''}$ of the same length are said to be similar, if their corresponding state estimates $\hat{\underline{x}}(k|k;\underline{q}^{k'})$, $\hat{\underline{x}}(k|k;\underline{q}^{k''})$ and their covariances $\Sigma(k|k;\underline{q}^{k'})$, $\Sigma(k|k;\underline{q}^{k''})$ satisfy the following criteria:

$$\left|\hat{\underline{x}}_i(k|k;\underline{q}^{k'}) - \hat{\underline{x}}_i(k|k;\underline{q}^{k''})\right| \leq \varepsilon_i\left[\sqrt{\Sigma_{ii}(k|k;\underline{q}^{k'})} + \sqrt{\Sigma_{ii}(k|k;\underline{q}^{k''})}\right];\ i=1,2,\ldots,\dim(x)$$

and (4-3a)*

$$\frac{\left|\Sigma_{ii}(k|k;\underline{q}^{k'}) - \Sigma_{ii}(k|k;\underline{q}^{k''})\right|}{\Sigma_{ii}(k|k;\underline{q}^{k'})} \leq \varepsilon_2 \qquad (4\text{-}3b)$$

This situation may occur, for example, when two hypotheses are nearly identical except for a few stages back and there is a limit on the total number of stages to be considered in the algorithm. When these earlier stages are dropped, Eq. 4-3 is satisfied. Then, $\underline{q}^{k'}$ and $\underline{q}^{k''}$ may be combined into $\underline{q}^{k}$ such that the hypothesis $\underline{q}^{k}$ has the following properties:

$$\underline{q}^{k} = \underline{q}^{k'} \quad \text{or} \quad \underline{q}^{k''} \qquad (4\text{-}4)$$

$$P(\underline{q}^{k}) = P(\underline{q}^{k'}) + P(\underline{q}^{k''}) \qquad (4\text{-}5)$$

---

* Note that this assumes independence of $\underline{q}^{k'}$ and $\underline{q}^{k''}$, which is generally not valid. Recently, Bar-Shalom [36] has provided a formulation that relaxes this assumption at the cost of solving an additional matrix linear equation for each pair of sequences.

$$P(\underline{q}^k|\underline{z}^k) = P(\underline{q}^{k'}|\underline{z}^k) + P(\underline{q}^{k''}|\underline{z}^k) \tag{4-6}$$

$$\hat{\underline{x}}(k|k;\underline{q}^k) = \frac{P(\underline{q}^{k'}|\underline{z}^k)\hat{\underline{x}}(k|k,\underline{q}^{k'}) + P(\underline{q}^{k''}|\underline{z}^k)\hat{\underline{x}}(k|k;\underline{q}^{k''})}{P(\underline{q}^k|\underline{z}^k)} \tag{4-7a}$$

$$\Sigma(k|k;\underline{q}^k) = \frac{1}{P(\underline{q}^k|\underline{z}^k)}\Big[P(\underline{q}^{k'}|\underline{z}^k)\Sigma(k|k;\underline{q}^{k'}) + P(\underline{q}^{k''}|\underline{z}^k)\Sigma(k|k;\underline{q}^{k''}) \tag{4-7b}*$$

$$+ \frac{P(\underline{q}^{k'}|\underline{z}^k)P(\underline{q}^{k''}|\underline{z}^k)}{P(\underline{q}^k|\underline{z}^k)} \{\hat{\underline{x}}(k|k;\underline{q}^{k'}) - \hat{\underline{x}}(k|k;\underline{q}^{k''})\}\{\hat{\underline{x}}(k|k;\underline{q}^{k'}) - \hat{\underline{x}}(k|k;\underline{q}^{k''})\}'\Big]$$

Equations 4-7a and 4-7b assume that the sum of two nearly identical Gaussian densities is Gaussian and that the mean and covariance of the resulting distribution should be the same as the mean and covariance of the sum. Thus, hypothesis merging eliminates the redundant enumeration of the hypothesis tree as shown in Fig. 4-3.

4.4 DECOUPLING OF HYPOTHESES (CLUSTER FORMATION)

The basic idea of this technique is to decompose the set $Q(k)$ of n_k levels at stage k into ℓ_k <u>independent</u> sets $Q_1(k), Q_2(k), \ldots, Q_{\ell_k}(k)$ with smaller number of levels $n_{1k}, n_{2k}, \ldots, n_{\ell_k k}$, respecitvely. There are at least two ways to decompose $Q(k)$ into $Q_i(k)$, viz., additive and product forms. In additive form, the levels $n_{1k}, n_{2k}, \ldots, n_{\ell_k k}$ are such that $n_k = \sum_{i=1}^{\ell_k} n_{ik}$ and is appropriate when $q(k)$ process is represented by ℓ_k decoupled Markov chains. The multiple model adaptive estimation algorithm falls into this category with $\ell_k=N$, the number of states in the Markov chain and $n_{ik}=1$ for $i=1,2,\ldots,N$. In product form, however, a level in $Q(k)$ represents <u>a particular</u> way of combining the various levels of $Q_1(k), Q_2(k), \ldots, Q_{\ell_k}(k)$, taking one level from each. The product form is appropriate in a multitarget tracking problem, where the entire set of targets and measurements can be divided into independent clusters via gating (validation region) criterion [8], [9], [15], and [16] based on residuals or the actual observations.

In order to illustrate the effect of the decomposition on computational requirements, assume for the present, that $\ell_k=\ell$, $n_k=n$, and $n_{ik}=n_i$, $i=1,2,\ldots,\ell$ at each stage k. The decomposition of $Q(k)$ into ℓ independent sets $Q_1(k)$, $Q_2(k), \ldots, Q_\ell(k)$ implies that the set of hypotheses Q^k of cardinality $N_c(k)=n^k$ can be decomposed into ℓ <u>independent</u> sets of hypotheses Q_i^k, $i=i,2,\ldots,\ell$ each with smaller cardinality $N_{ci}(k)=n_i^k$. Thus, the total set of hypotheses is reduced to $\hat{Q}^k$ with cardinality $\hat{N}_c(k)$ given by

$$\begin{aligned} \hat{N}_c(k) &= \sum_{i=1}^{\ell} N_{ci}(k) \qquad \text{(Additive Decomposition)} \\ \hat{N}_c(k) &= \prod_{i=1}^{\ell} N_{ci}(k) \qquad \text{(Product Decomposition)} \end{aligned} \tag{4-8}$$

*In actual implementation, the order of computation should be $\Sigma, \hat{\underline{x}}, P(\underline{q}^k|\underline{z}^k)$ or $P(\underline{q}^k)$ for maximum efficiency.

Typically, $\hat{N}_c(k) << N_c(k)$. Thus, instead of solving one large problem with n levels at each stage k, we can solve simpler problems, each with n_i levels, independently. Since the computational requirements grow exponentially with the number of levels, this decomposition can result in tremendous savings in computer storage and computation time. In addition, the probabilities of hypotheses $\underline{q}^k \in \underline{Q}^k$ are related to those in $\underline{q}_i^k \in \hat{Q}_i^k$ as follows.

In the case of additive decomposition,

$$P(\underline{q}^k | \underline{z}^k) = P(\underline{q}_i^k | \underline{z}^k) \quad \text{if} \quad \underline{q}^k \in Q_i^k \quad ; \quad i=1,2,\ldots,\ell \tag{4-9}$$

For the product decomposition, we have

$$P(\underline{q}^k | \underline{z}^k) = \prod_{i=1}^{\ell} P(\underline{q}_i^{\ell} | \underline{z}^k) \quad ; \quad \underline{q}^k \in \hat{Q}^k \tag{4-10}$$

The general case, where ℓ_k and n_{ik} are stage dependent, is a straightforward extension of the above ideas. In this case, we have nonstationary coupling among the sets of hypotheses. Suppose, at stage k-1, we have m_{k-1} global, independent sets of hypotheses Q_1^{k-1}, Q_2^{k-1}, ..., Q_{mk-1}^{k-1}. The local set at stage k, Q(k) is decomposed into ℓ_k independent sets $Q_1(k)$, $Q_2(k)$, ..., $Q_{\ell_k}(k)$. Then, the global independent sets at stage k, viz., Q_1^k, Q_2^k, ..., Q_{mk}^k for the case of product decomposition are formed as follows: (1) If none of the $Q_i(k)$, $i=1,2,\ldots,\ell_k$ is associated with a Q^{k-1}. Then $Q_j^k = Q_j^{k-1}$. The association is determined via a gating criterion mentioned earlier; (2) If any $Q_i(k)$ is associated with (or coupled to) only one Q_j^{k-1}, then $Q_j^k = Q_j^{k-1} \times Q_i(k)$ where X indicates a cartesian product (this also includes the case when several $Q_i(k)$ are assocaited with the same Q_j^{k-1}); (3) If a $Q_i(k)$ is associated with more than one global set Q_j^{k-1}, then the global sets Q_j^{k-1} are combined into super global set, Q_s^{k-1}. If the sets Q_j^{k-1} associated with $Q_i(k)$ are denoted by a set A_i, then Q_s^{k-1} is the cartesian product:

$$Q_s^{k-1} = \prod_{j \in A_i} Q_j^{k-1} \tag{4-11}$$

The number of hypotheses in Q_s^{k-1} is the product of the hypotheses in Q_j^{k-1}, $j \in A_i$. The posterior probabilities of $\underline{q}^{k-1} \in Q_s^{k-1}$ is given by

$$P(\underline{q}^{k-1} | \underline{z}^{k-1}) = \prod_{j \in A_i} P(\underline{q}_j^{k-1} | \underline{z}^{k-1}) \quad ; \tag{4-12}$$

and (4) If none of the Q_j^{k-1}, $j=1,2,\ldots,m_{k-1}$ is coupled to a $Q_i(k)$, then a new set of hypotheses $Q_I^k = Q_i(k)$ is formed. Thus, the number of global independent sets of hypotheses m_k at stage k is given by

$$m_k = m_{k-1} - \sum_{i=1}^{\ell_k} (\text{no. of elements in } A_i - 1) + \text{new sets of hypotheses} \tag{4-13}$$

Figure 4-4 illustrates the process of forming supersets and creating new sets for $\ell_k=3$ and $m_{k-1}=4$. The case of additive decomposition is straightforward.

4.5 USE OF SYSTEM CONSTRAINTS TO ADVANTAGE

Almost all the algorithms in multitarget tracking use the assumption that a target can give rise to atmost one measurement at each stage. This gives

rise to a tremendous reduction in the number of hypotheses. For example, in the problem of tracking a single target in clutter with M_k returns, the number of hypotheses are reduced from 2^{Mk} to (M_k+1) by this assumption.

5. PROGRAMMING LANGUAGE SELECTION AND THE ESTIMATION ALGORITHM

The computer implementation of the state estimation and hypothesis reduction algorithm requires the construction and evaluation of hypothesis trees, as well as the propagation of state estimates and their covariances. Thus, the implementation requires recursion (i.e., tree structure manipulation) and iteration (i.e., numerical computations). The FORTRAN language, despite its controversy [33], is well suited to iterative computations, but is "clumsy" at manipulating recursive tree structures. The artificial intelligence language, LISP, on the other hand, is a natural and powerful medium to construct and evaluate hypothesis trees. However, it is extremely slow and awkward at scientific computations (e.g., matrix multiplication). A happy compromise appears to be the language PASCAL (similar to ALGOL 68) that has flexible recursive and iterative features. Table 5-1 provides a (subjective) comparison of FORTRAN, LISP, and PASCAL on the basis of several practical issues.

The programming language PASCAL offers several advantages [34]: (1) It enables one to develop flexible programs using a small number of basic constructions (e.g., IF-THEN-ELSE, FOR, PROCEDURES, etc.); (2) One can construct both algorithms and data structures hierarchically. PASCAL provides more general data dypes, and extensive data structures (e.g., TYPE, SET, RECORD, etc.) that clarifies computations on data; (3) PASCAL programs are relatively easy to debug, compile, and verify. They run efficiently on most computers; (4) Well-written PASCAL programs are easy to read and write; (5) Recursive structure of PASCAL permits structured programming in an efficient manner; and (6) In most installations, FORTRAN libraries can be accessed via PASCAL.

The major drawback of PASCAL is that it exists primarily in an academic atmosphere and is not tried by the real world. However, this should not be a deterrant in writing programs in PASCAL, since the (so-called) potential languages of the future (e.g., ADA) borrow concepts from PASCAL. Undoubtedly, programming in PASCAL affords a general and flexible implementation of the estimation algorithm.

A flow diagram of the estimation algorithm is shown in Fig. 5-1. It consists of six major modules with the following functions:

- MAIN PROGRAM selects the option specified by the user and acts as a major logic control for the hypothesis testing module.
- MEASUREMENT MODULE reads the observation data from a tape.
- APRIORI INFORMATION MODULE initializes the clusters using previous knowledge of the system characteristics and includes specific information about various options in order to reduce the computational effort involved in the hypothesis testing module.
- HYPOTHESIS TESTING MODULE forms new data-association hypotheses for the set of measurements in each scan using system related constraints (e.g., almost one measurement per target), updates clusters, and reduces hypotheses by merging similar hypotheses and eliminating unlikely ones. This module is the heart of the computer package.
- ESTIMATION MODULE implements prediction-correction equations of the Kalman filter and bias estimation algorithms useful in failure detection problems.
- OUTPUT MODULE prints and plots various results as required.

6. SUMMARY AND CONCLUSIONS

In this paper, we have shown that a broad class of practical estimation problems arising in surveillance theory and in switching systems can be encompassed within a unifying conceptual framework. The analytic formulation was based on an event-driven linear stochastic model with a large, hybrid (discrete and continuous) state space. The general formulation of the present paper permitted the understanding of diverse "special case" algorithms in the literature on common intellectual grounds. This generality also allows the development of a general purpose computer package for convenient comparison of various existing and proposed algorithms for these problems in common numerical terms.

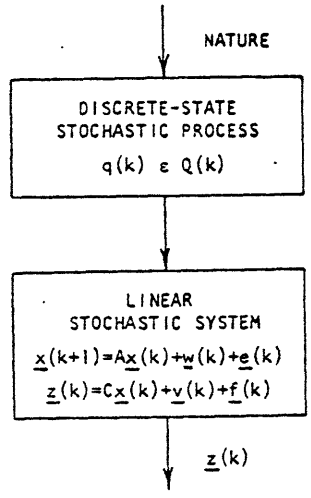

Figure 2-1. Event-Driven Stochastic System.

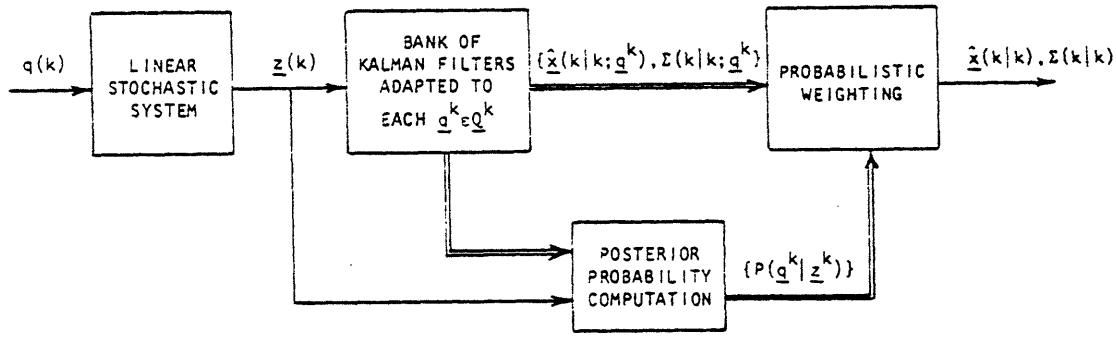

Figure 3-1. Optimal Bayesian Estimation Algorithm.

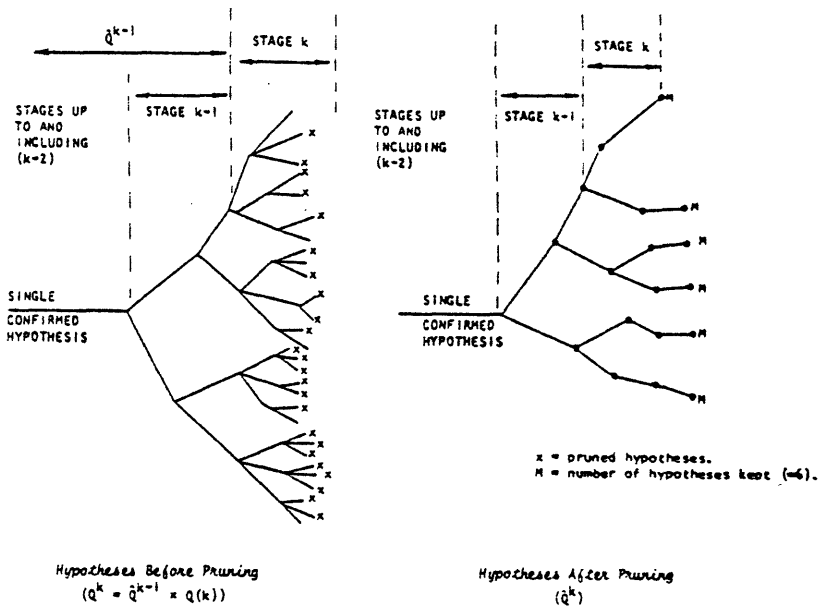

Figure 4-1. Hypothesis Deletion Technique.

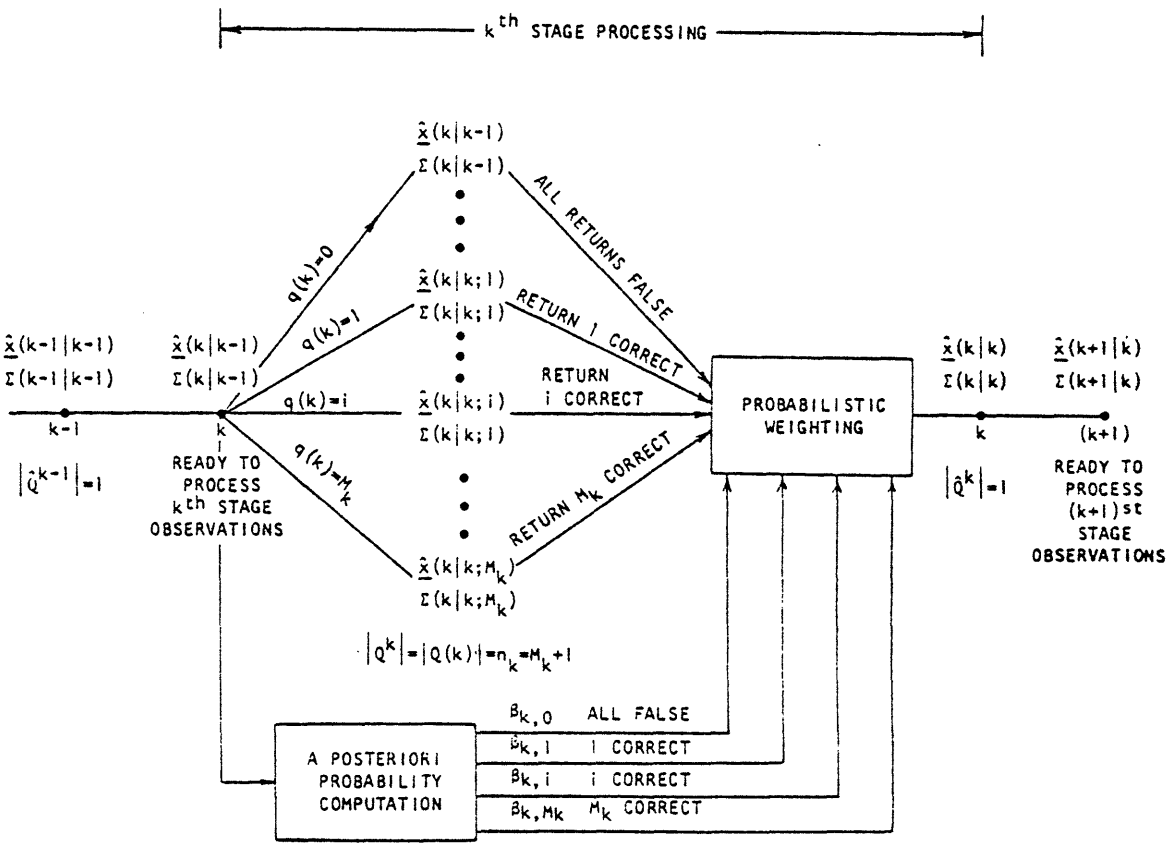

NOTE: PDAF CAN BE IMPLEMENTED BY A SINGLE KALMAN-LIKE FILTER

Figure 4-2. Hypothesis Merging in the Probabilistic Data Association Filter (PDAF).

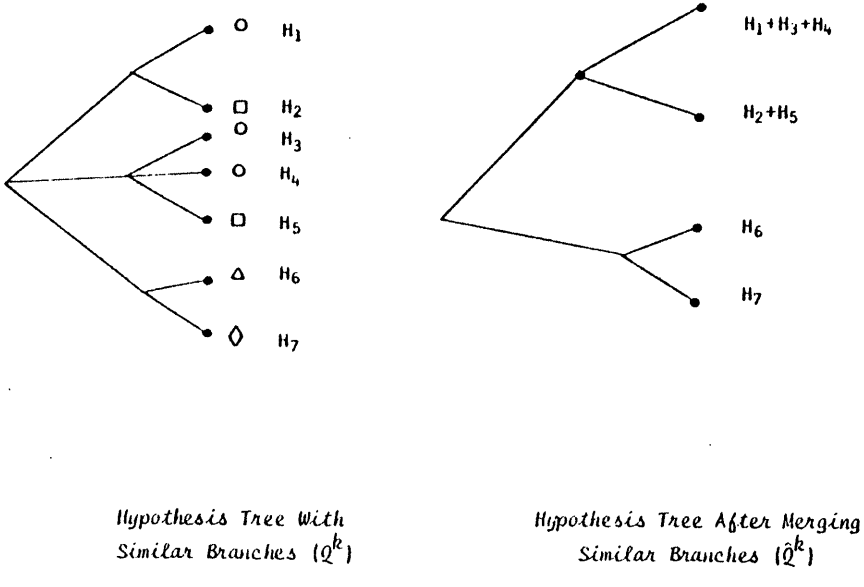

Figure 4-3. Hypothesis Merging in Multistage Algorithms.

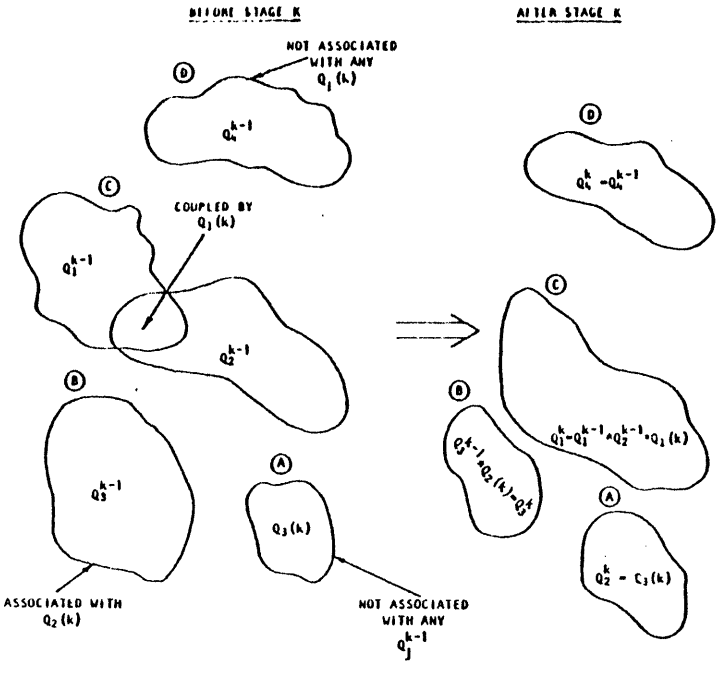

Figure 4-4. Cluster Formation.

TABLE 5-1. AN APPRAISAL OF FORTRAN, LISP, AND PASCAL PROGRAMMING LANGUAGES

Feature \ Language	FORTRAN	LISP	PASCAL
1. Program development (write, debug, maintain, etc.)	Fair to Poor	Fair	Very Good
2. Readability	Fair to Poor	Fair to Poor	Good
3. Readily available compiler	Very Good	Poor	Fair
4. Numerical computation	Good	Poor	Good
5. Recursion	Poor	Good	Good
6. Data structures	Poor	Fair	Good
7. Use of packages	Very Good	Poor	Fair
8. Portability	Very Good	Poor	Fair
9. Ease of learning	Very Good	Fair	Good
10. Efficiency	Good	Poor	Good

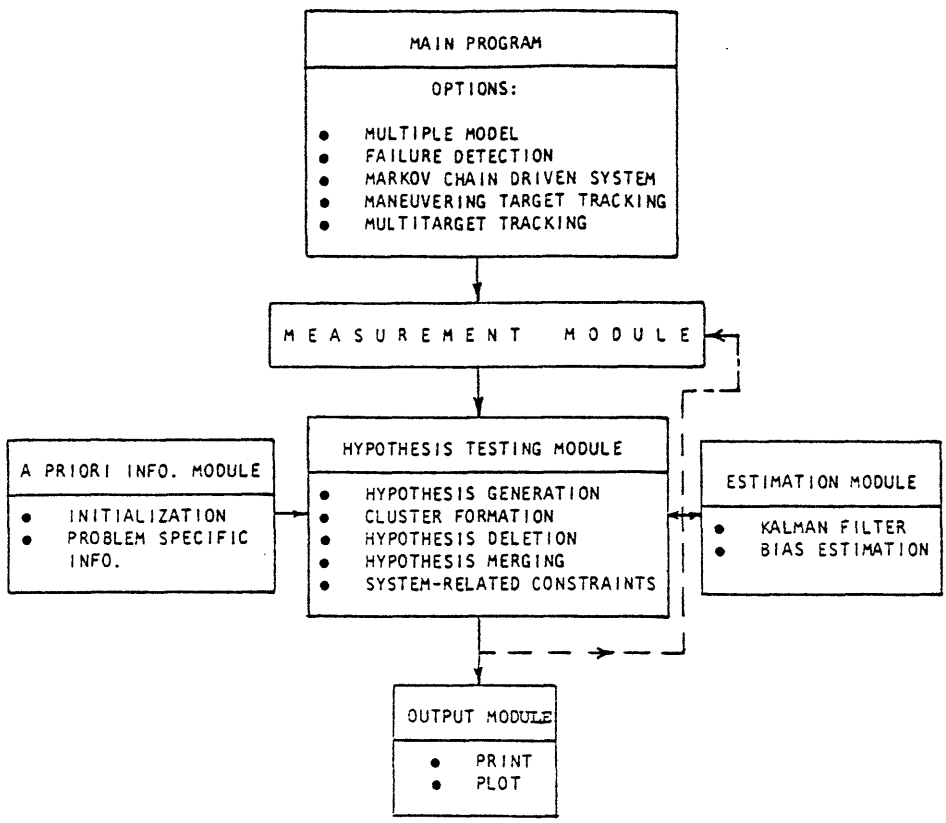

Figure 5-1. Flow Diagram of the Estimation Algorithm.

REFERENCES

1. Nahi, N.E., "Optimal Recursive Estimation with Uncertain Observations," IEEE Trans. on Inform. Theory, Volume IT-15, July 1969, pp. 457-462.

2. Sawaragi, Y., T. Katayama, and S. Fujishige, "Sequential State Estimation with Interrupted Observation," Information and Control, Volume 21, 1972, pp. 56-71.

3. Athans, M., R.H. Whiting, and M. Gruber, "A Suboptimal Estimation Algorithm with Probabilistic Editing for False Measurements with Applications to Target Tracking with Wake Phenomena," IEEE Trans. on Automatic Control, Volume AC-22, June 1977, pp. 372-384.

4. Jaffer, A.G. and S.C. Gupta, "Optimal Sequential Estimation of Discrete Processes with Markov Interrupted Observations," IEEE Trans. on Automatic Control, Volume AC-16, October 1971, pp. 471-475.

5. Jackson, R.N. and D.N.P. Murthy, "Optimal Linear Estimation with Uncertain Observations," IEEE Trans. on Automatic Control, Volume AC-21, May 1976, pp. 376-378.

6. Hadidi, M.T. and S.C. Schwartz, "Linear Recursive State Estimators Under Uncertain Observations," IEEE Trans. on Automatic Control, Volume AC-24, December 1979, pp. 944-948.

7. Singer, R.A., R.G. Sea, and K.B. Housewright, "Derivation and Evaluation of Improved Tracking Filters for use in Dense Multitarget Environments," IEEE Trans. on Inform. Theory, Volume IT-20, July 1974, pp. 423-432.

8. Bar-Shalom, Y. and E. Tse, "Tracking in a Cluttered Environment with Probabilistic Data Association," Automatica, Volume 11, 1975, pp. 451-460.

9. Bar-Shalom, Y., "Extension of the Probabilistic Data Association Filter in Multitarget Tracking," in Proc. of the 5th Symposium on Nonlinear Estimation, September 1974, pp. 16-21.

10. Alspach, D.L., "A Guassian Sum Approach to the Multitarget Identification-Tracking Problem," Automatica, Volume 11, 1975, pp. 285-296.

11. Sittler, R.W., "An Optimal Data Association Problem in Surveillance Theory," IEEE Trans. on Military Electronics, Volume MIL-8, April 1964, pp. 125-139.

12. Stein, J.J. and S.S. Blackman, "Generalized Correlation in Multi-target Tracking Data," IEEE Trans. on Aerospace and Electronic Systems, Volume AES-11, November 1975, pp. 1207-1217.

13. Smith, P. and G. Buechler, "A Branching Algorithm for Discriminating and Tracking Multiple Objects," IEEE Trans. on Automatic Control, Volume AC-20, February 1975, pp. 101-104.

14. Morefield, C.L., "Application of 0-1 Integer Programming to Multitarget Tracking Problems," IEEE Trans. on Automatic Control, Volume AC-22, June 1977, pp. 302-311.

15. Reid, D.B., "An Algorithm for Tracking Multiple Targets," IEEE Trans. on Automatic Control, Volume AC-24, Number 6, December 1979, pp. 843-854.

16. Keverian, K.M. and N.R. Sandell, Jr., "Multiobject Tracking by Adaptive Hypothesis Testing," LIDS-R-959, M.I.T., December 1979.

17. Bar-Shalom, Y., "Tracking Methods in a Multitarget Environment," IEEE Trans. on Automatic Control, Volume AC-23, August 1978, pp. 618-626.

18. Fortmann, T.E., Y. Bar-Shalom, and M. Scheffe, "Multitarget Tracking Using Joint Probabilistic Data Association," 1980 IEEE Conf. on Decision and Control, Albuquerque, New Mexico, December 1980.

19. Sandell, N.R., Jr., G.S. Lauer, and L.C. Kramer, "Research Issues in Surveillance C^3," IEEE Conf. on Decision and Control, Albuquerque, New Mexico, December 1980.

20. Fraser, L. and L. Meier, "Mathematical Models and Optimum Computation for Computer-Aided Active Sonar Systems," SRI Final Report (First Year), Prepared for U.S. Navy Electronic Lab., San Diego, California, Contract Number N123-(953)54486A, March 1967.

21. Moose, R.L., "An Adaptive State Estimation Solution to the Maneuvering Target Problem," IEEE Trans. on Automatic Control, Volume AC-20, June 1975, pp. 359-362.

22. Newbold, P.M. and Y.C. Ho, "Detection of Changes in the Characteristics of a Gaussian-Markov Process," IEEE Trans. on Aerospace and Electronic Systems, Volume AES-4, Number 5, September 1968, pp. 707-718.

23. Buxbaum, P.J. and R.A. Haddad, "Recursive Optimal Estimation for a Class of Non-Gaussian Processes," Proc. of Symposium on Computer Processing in Communications, Polytech. Inst. of Brooklyn, April 1969, pp. 375-399.

24. Willsky, A.S. and H.L. Jones, "A Generalized Likelihood Approach to the Detection and Estimation of Jumps in Linear Systems," IEEE Trans. on Automatic Control, Volume AC-21, February 1976, pp. 108-112.

25. Liu, J., "Detection, Isolation, and Identification Techniques for Noisy Degradation in Linear-Discrete-Time Systems," IEEE Conf. on Decision and Control, New Orleans, Louisiana, December 1977, pp. 1132-1139.

26. Tulpule, Bhal R. and C.H. Knapp, "Robust Dtection and Estimation of Soft Failures in Linear Systems," IEEE Conf. on Decision and Control, Albuquerque, New Mexico, December 1980.

27. Magill, D.T., "Optimal Adaptive Estimation of Sampled Processes," IEEE Trans. on Automatic Control, Volume AC-10, October 1965, pp. 434-439.

28. Lainiotis, D.G., "Optimal Adaptive Estimation: Structure and Parameter Adaptation," IEEE Trans. on Automatic Control, Volume AC-15, Number 2 April 1970, pp. 160-170.

29. Athans, M. and C.B. Chang, "Adaptive Estimation and Parameter Idenfification Using Multiple Model Estimation Algorithms," Technical Note 1976-28, Lincoln Laboratory, M.I.T., Cambridge, Massachusetts, June 1976.

30. Kemeny, J.G. and J.L. Snell, Finite Markov Chains, New York: Springer-Verlag, 1976.

31. Courtois, P.S., Decomposability: Queueing and Computer System Applications, New York: Academic, 1977.

32. Pattipati, K.R., Sandell, N.R., Jr., "A Unified View of State Estimation in Switching Environments," Tech. memo. 111, ALPHATECH, Inc., Burlington, Mass., May 1981.

33. Dijkstra, E., "The Humble Programmer," Comm. of the ACM, Volume 15, Number 10, October 1972.

34. Grogono, P., Programming in PASCAL, New York: Addison Wesley, 1980.

35. Ignagni, M.B., "An Alternate Derivation and Extension of Friedland's Two-Stage Kalman Estimator," IEEE Trans. on Automatic Control, Vol. AC-26 No. 3, June 1981, pp. 746-750.

36. Bar-Shalom, Y., "On the Track-to-Track Correlation Problem," IEEE Trans. on Automatic Control, Vol. Ac-26, No. 2, April 1981, pp. 571-572.

OVERVIEW OF SURVEILLANCE RESEARCH AT M.I.T.

Robert R. Tenney
Massachusetts Insttitute of Technology
Laboratory for Information and Decision Systems
Room 35-211
Cambridge, MA 02139

(Acknowledgement is gratefully given to the Office of Naval Research for Supporting this work under contract N00014-77-C-0532) August, 1981 LIDS-P-1126.

ABSTRACT

Surveillance systems provide a setting for many nonclassical optimal estimation problems. These include detection and target tracking (with maneuvers, clutter, and/or several targets and sensors) as well as problems which deal with the higher level issues of a C^3 systems. The latter include mixed detection and communication problems (motivated by geographically distributed sensors) and sensor scheduuling/resource allocation problems.

I. Introduction

Research in command and control systems finds a number of important illustrative examples in the area of surveillance. The problem of detecting, locating, and identifying a large number of moving, maneuvering objects, using many dispersed sensors, is extremely rich. This paper describes the work accomplished in the past years at MIT on a subset of these problems, as well as an indication of the direction of our future work.

A. The Problem

The rich structure of surveillance problems defies pidgeonholing them into established disciplines, yet three broad classes of problem can be considered. The first, estimation, deals with the processing of data obtained through sensors, and reducing it to information relevant to the objects in the surveillance volume. The second class, communication, deals with the transfer of information between sensors and processors in the face of restrictions on communication facilities (either in terms of bandwidth or delay). The third class, control, includes both scheduling sensors (those that must be pointed in a specified direction, or otherwise commanded) and allocating weapons to targets (i.e., fire control). This paper will discuss these three classes independently, yet their interrelationship should not be overlooked.

The unifying framework behind all surveillance research is provided by the structure of the problem. While surveillance is essentially a problem of real time data reduction, it has certain characteristics which greatly influence the research directions to be taken. Principle factors are:

1. Multiple targets of different types
2. Multiple sensors of different types
3. Limited communication, with constraints on connectivity, bandwidth, and delay, and
4. Low signal-to-noise ratios.

Not all surveillance problems are characterized by all four attributes, but we feel that the nature of the tactical naval engagement, in

an era of sophisticated electronic warfare, necessitates consideration of all of them.

Our view is that every surveillance problem in practice is different, yet all share these common attributes. Thus we approach surveillance as a generic problem, addressing the fundamental technical problems independently of any specific sensor system.

The role of surveillance in the overall C^3 process is also important to us. Surveillance problems are "mini-C^3" problems - they reflect most of the issues of the overall C^3 problem but have a much more available analytical structure. Thus one part of our research strategy is to use surveillance as the starting point for work which addresses successively larger parts of the general command and control problem. Specifically, the first steps in this succession are to include communication, data bases, and weapon allocation into the surveillance research.

The goals of our work, then, are twofold: first, design of specific algorithms for surveillance problems (e.g., multiobject tracking in clutter), and second, understanding of the architectural issues. Such issues include a) the flow of information in a surveillance net, b) management of surveillance assets, c) the organization of a surveillance system, and d) evaluation of a systems performance using quantitative measures.

B. The Model

The unifying model of the objects and environment around a surveillance system has two parts. The targets are modelled as independent, hybrid stochastic systems. The sensors are hybrid observations processes which introduce errors and noise.

Target models are driven by a Markov chain representing the "mode of operation" of each target. Modes include the birth or death of a target as it enters or leaves the region of interest, maneuvers, long-term fading and reappearance of its signal, identification, etc. Each discrete state i indexes a linear, Gaussian, time-varying dynamical model

$$x(t+1) = A_i(t)x(t) + B_i(t)w_i(t) \qquad w_i(t) \sim N(0, Q_i(t)) \qquad (1)$$

with states representing positions, velocities, etc. (The LG assumption never holds in practice; it provides a framework which can be used as a basis for approximations such as the extended Kalman filter.)

The sensors are modelled as binary channels coupled with a linear process. With certain probabilities of detection, which for a first approximation depend only on the discrete part of the target state, an output is produced

$$y(t) = Cx(t) + v(t) \qquad v \sim N(0,R(t)) \qquad (2)$$

for each target. Other outputs arise as a result of a clutter process; the number of clutter points is given by a Bernoulli process and each point takes values given by a Gaussian distribution on the measurement space. The "observation" of each sensor is thus a set of points at each time.

C. Issues

As mentioned above, the issues addressed in our work, using this model or variants thereof, fall into three broad categories. The major topics of research, and the people associated with them, are:

1. Estimation:

   Targat tracking (Castanon, Levy)
   Data association (Hughes, Liao)
   Hybrid estimation (Roth, Bruneau)

2. Communication:

   Distributed detection (Ekchian, Ozbek)
   Track management (Salman)
   Organization (Ekchian)

3. Control:

   Search and scheduling (Ekchian)
   Weapons allocation (Ekchian)

II. Estimation

The work most closely associated with classical estimation theory falls into three subclasses. The first deals with the general problem of decentralized estimation of the state of a linear system. The second is data association - assigning elements of a sensor's observation set to targets of interest. The third addresses the estimation process for hybrid systems in general, seeking the most likely discrete state trajectory and the continuous state estimate conditioned thereon.

A. Linear Systems

The work on decentralized estimation for linear systems was motivated by a situation where several sensors each acquired observations of a linear process. Each could produce a local estimate based on these observations; the interesting question centers on the role of a fusion center which received (prefiltered) data from each sensor and seeks to reconstruct the best global estimate. The reconstruction can be done perfectly unless other restrictions are made (such as linear prefiltering, sampled data communications, reduced order local estimates, etc.), and suboptimal schemes have been found for numerous cases.

B. Data association

Much attention has been devoted to the problem of multiobject tracking, but usually in a high signal-to-noise ratio or single sensor setting. A natural extension to this involves distributing the tracking computation through a network of sensors. This begins to introduce communication issues (or the single sensor algorithms would apply), and opens the door to broader C^3 problems.

An algorithm has been devised and implemented to perform data association in a realistic setting (many missed detections, false alarms, non-Gaussian noise, highly nonlinear observations). The basic structure is one of growing trees of hypotheses with heuristic pruning for computational feasibility. The algorithm has been evaluated in extensive Monte Carlo simulations.

Two startling conclusions resulted from this work beyond the feasibility demonstration. They concerned the sensitivity of the algorithm's performance to parameters describing the environment: false alarm rates, detection probabilities, etc. Contrary to prior speculation, this sensitivity was quite low in the range of reasonable values. However, the data association is quite sensitive to the covariance matrix used to describe the noise driving the target dynamics. These results are consistent with the interpretation that the data association is dominated by target kinematics and not by prior probabilities.

C. Hybrid estimation.

The problem of estimating the state of a hybrid process such as our target model combines discrete state and linear-Gaussian estimation. Each of these subproblems can be solved quite elegantly by itself: the former by the Viterbi algorithm and the latter by a Kalman filter. The marriage of these two algorithms is our goal.

The Viterbi algorithm is essentially a tree growing/pruning algorithm, but the breadth of the tree is limited to the size of the discrete state space. It seeks the most likely trajectory through these states. By appending the linear dynamics to the discrete states, bounding argument supply optimal pruning rules which eliminate candidate trajectories as they can never be most likely (i.e., no matter what observations appear in the future, a more likely candidate exists). Results in this direction are preliminary, but those obtained so far require only statistics that can be generated by a Kalman filter.

III. Communication

Communication enters the surveillance picture when data is obtained through several sensors among which only finite communication channels exist. Traditional approaches to communications issues address such problems as coding, routing, and flow control as though the communications assets are a utility, available to users on an equal basis. We prefer the view that the communications resources are embedded in a specific (surveillance) problem: that their function is to support a decision process with specific goals, rather than maximize the number of bits or packets passed through a link.

The integration of the target tracking and communication functions can take place at two levels: the conceptual and the analytic. The former focusses on the question: what should be communicated in order to support a distributed surveillance algorithm?, while the latter investigates specific, well posed problems to derive optimal communications policies, with the objective of generalizing from the simple results to more general conclusions.

A. Multisensor management.

The conceptual approach matches well with the distributed multi-object tracking algorithm mentioned above. There is a clear relationship between a target's motion through a field of sensors, and the shifting center of the processing required to track it. This immediately suggests a target-oriented approach to data association; the hypotheses concerning a target and the measurements assigned to it constitute a data base in each sensor or node. In the absence of communication, such data bases are disjoint; communication introduces the possibility of information exchange such as target handoff from sensor to sensor. While providing the greater continuity of coverage required of a surveillance network, this introduces the added complexity of overlapping data bases and the control required to manage them. Viewing each data base as a set of hypotheses which are suggested, confirmed, or denied by interactions between nodes, gives a glimmer of an approach to dealing with the command and control aspects of surveillance. However, the problem is only at

the formulation stage now.

B. Detection

The analytic approach to introducing communication into estimation problems has evolved from some early work done on distributed detection. The underlying problem formulation has:

1. A number of discrete hypotheses which can occur with known prior statistics;
2. A number of sensors receiving noisy observations of those hypotheses,
3. Some restricted (e.g., binary) communication variables from sensor to sensor, and
4. An objective function penalizing various (output) decisions for each hypothesis.

For a number of problems, optimal decision rules have been obtained. Usually these are of a structure similar to centralized detection rules, e.g., likelihood ratio tests. These structures can be parameterized by a finite number of parameters, and the parameters found by standard optimization techniques.

From a theoretical point of view, these results are interesting as these problems exhibit a highly nonclassical information structure. Reduction from a functional optimization (for decision rules) to a parametric optimization (for thresholds) yields a great simplication in these often intractable problems.

More importantly, light is being shed on some organizational aspects of surveillance system. For instance, given two sensors of different quality which can be connected by a unidirectional, limited communication channel, which should be upstream of the other? Examples show that the two possible arrangements can yield different levels of performance when optimal decision rules are employed. Is one always better? There is a strong conjecture that the upstream (transmitting) sensor should be the one of lower quality; the receiver should have the best observational data. If this is indeed true, it opens the door to other statements which can be made concerning organization and interconnection of surveillance assets.

IV. Control

The interface of traditional surveillance functions, such as detection, localization, and identification, to the other functions of a command and control system, such as resource allocation and fire control, is only starting to be probed. We have identified two problems which are related to the preceeding discussions and also allow an optimal solution to be found.

A. Search

Many sensors must be directed in their operation, either to physically or electronically point in a specific direction, or to selectively process the received signal (e.g., selecting frequency bands, beam forming, etc.) The control of these sensors must be compatible with the subsequent information flow in order to achieve the goals of the system as well as possible.

Our search and scheduling research centers on the following generic problem. A number of bins exist; an object may or may not be present in each. Each of several sensors may examine one bin at a time; the sensors have detection and false alarm probabilities which vary from bin to bin and sensor to sensor. The problem is to determine which bin should be examined by each sensor at each point in time. Naturally this depends on the objective function which defines optimality; a particularly convenient one, from an analytical point of view, penalizes the a posteriori distribution for each bin at each sensor with functionals of the form

$$p_0^{1-\alpha} p_1^{\alpha} \tag{3}$$

where (p_0, p_1) are the no target/target probabilities and $0 \leq \alpha \leq 1$. Optimal selection strategies have been found for this problem.

B. Research allocation.

As a start on integrating the weapons aspects of C^3 into surveillance, we considered a simple SAM problem. A number of sites are equipped with radar, missiles, and communications, each of limited range. Enemy aircraft appear in any pattern on one side of the fortified area; their objective

is to cross to the other side. For surprisingly restricted capabilities of the local sites, we found an allocation strategy which quaranteed the maximum number of kills with only three bits of communication per target, sent, at worst, to a single site two hops distant! We are seeking to generalize this result to other, more general problems.

V. Conclusion

Surveillance is a part of C^3. To the extent that they determine the objectives of a surveillance system, the other functions of C^3 are part of surveillance. Surveillance produces a variety of well posed, tractible analysis problems which allow constructive and significant extensions to current theory. A small number of these problems have been solved; most are yet to be examined. Because of their generic nature and wealth of structure, we will continue to address surveillance problems actively and with clear intent to extend to as much of the overall C^3 problem as possible.

A DIFFERENTIAL GAME APPROACH TO DETERMINE PASSIVE TRACKING MANEUVERS

Pan-Tai Liu

Mathematics Department
University of Rhode Island
Kinston, Rhode Island 02881

Paul L. Bongiovanni

Code 3521
Naval Underwater Systems Center
Newport, Rhode Island 02840

(Presented at the fourth MIT/ONR Workshop on Command and Control)

A DIFFERENTIAL GAME APPROACH TO DETERMINE PASSIVE TRACKING MANEUVERS

ABSTRACT

This paper describes our efforts to formulate the submarine passive tracking problem as a two-person, zero-sum differential game. By choosing an appropriate performance criterion which reflects the objectives of both participants, namely the pursuer (ownship or tracking vehicle) and the evader (target), we wish to determine the optimal tracking maneuvers. The selected performance criterion, which is of the Bolza type, consists of two terms: (1) an integral term which represents the total acoustic information available to the tracking vehicle and (2) a quadratic in the relative distance at the terminal time. Both terms are dependent upon the speed of each participant which become the controls in this particular formulation of the problem. Hence we convert the submarine passive tracking situation into a two-person, zero-sum differential game where the state vector is the components of the relative horizontal position between the two vehicles. For this game, the pursuer wishes to maximize the performance criterion, while the evader wishes to minimize it. In a differential game one seeks the saddle-point solution. However in this problem, due to the nature of the performance criterion, one cannot be found. Since we are only interested in finding the optimal tracking maneuvers, we have chosen to find the max-min solution. The result is that the pursuer selects his speed to maximize the optimal return to the evader. We show the necessary conditions that determine the max-min solution. Finally we illustrate this technique with a numerical example and also include a discussion of the numerical results.

1. Background

The concept of differential game theory was first introduced by Isaacs [1] in 1965. Since that time many papers have been published which address this topic. However there has been a paucity of papers which deal with the surveillance-evasion problem as a differential game. Several authors have cast the tracking problem into a differential game format by using Isaacs homicidal chauffeur game as a model for the dynamics. In the first paper, Dobbie [2] cast the surveillance-evasion problem into a differential game format, assuming perfect information for the pursuer and evader. The rules of the game are simple: the pursuer wishes to keep the relative position of the evader within his detection region, while the evader wants to escape from the detection region. The game terminates when the evader's position is outside the pursuer's detection region. The basic assumptions associated

with this model are that the pursuer has a speed advantage over the evader, but is restricted in his maneuvering. He solves the problem for circular as well as arbitrary detection regions. The same tracking problem was extended by Lewin and Breakwell [3] to the game where the objective of the evader is to strive to escape (provided that he can) in minimum time from the pursuer's detection circle, while the pursuer wishes to maximize this time. In this paper the authors discuss various results that they have obtained purely by graphical construction. However, since they failed to provide any specific conclusions, it is hard for one to evaluate the utility of their very interesting results.

2. Introduction

In a previous paper (4), we have considered the problem of determining optimal vehicle speeds for passive tracking maneuvers. The problem was treated from the point-of-view of a pursuit-evasion differential game in which the tracking vehicle played the role of the pursuer, while the target, in an attempt to escape, played the role of evader. In our formulation of the problem, the game is characterized by those items listed in Viewgraph 1. A special feature of the approach is that the integral term in the performance criterion embodies the acoustic effects which uniquely characterize the information. Furthermore, no saddle-point solution exists, so instead we seek the max-min solution.

A typical submarine tracking scenario for passive target tracking is illustrated in Viewgraph 2. The true relative position is denoted by the vector (z_1, z_2). However, in our problem we assume that the pursuer knows only the nominal (approximate) relative position (x_1, x_2).

3. Mathematical Formulation

Consider the encounter of two submarines. Each has detected and classified the other. The evader is assumed to have perfect information while the pursuer or tracking vehicle knows only the approximate state vector (x_1, x_2).

The dynamic equations which describe the behavior of the state vector are presented in Viewgraph 3. Included is a list of the controls for ownship (pursuer) and the target. We assume that ownship selects θ_0, θ_1, t_1 and t_f a priori. Meanwhile the evader selects an evasion strategy which consists of running away from the pursuer on a course opposite to the bearing line between the two vehicles.

In passive target tracking, information concerning the target is typically available as a sonar bearing corrupted with noise. The relationship between the state vector and the bearing measurement is nonlinear. Viewgraph 4 illustrates the steps performed to linearize the measurement about the approximate state vector (x_1, x_2). The acoustical noise n is assumed to be white Gaussian noise with zero mean and variance σ_n^2. The variance can be shown (see Ref. (4)) to be a function of the speed of each vehicle and the relative distance between them. The equation for the variance is specified in Viewgraph 4.

Viewgraph 5 presents the necessary steps to convert the raw measurements into a scalar measure which embodies the information in these measurements. The matrix H has been specified previously in Viewgraph 4, and although not specifically stated

$$Q = \sigma_n^2$$

The objectives of ownship and the target are specified in Viewgraph 5. From these objectives we have formulated a two-person zero-sum differential game with the following performance criterion

$$J(\underline{u},v) = \int_{t_0}^{t_f} \frac{e^{\alpha \| \underline{u} \| - \beta v}}{\| \underline{x} \|^4} \, dt - \frac{\gamma}{2} \| \underline{x}(t_f) \|^2$$

where the first term on the right is the total amount of information received in the interval (t_0, t_f), and the second term is the final relative distance. The parameter γ is a positive constant that allows the weighting of the importance between these two terms.

4. Max-Min Solution for Ownship

To fulfill both objectives specified in Viewgraph 5, ownship has to choose fixed speeds v_0 and v_1 for the two phases of the tracking engagement so as to maximize $J(\underline{u}, v)$ against the worst possible $\underline{u}$. Mathematically, as stated in Viewgraph 7, this is equivalent to maximizing

$$F(v_0, v_1) = \min_{\underline{u}} J(\underline{u}, v)$$

Therefore by choosing v_0^* and v_1^*, ownship can be sure of a performance no worse than $F(v_0^*, v_1^*)$.

To determine v_0^* and v_1^* against the worst possible ν^* (since $\underline{u} = \nu x_1, \nu x_2$), ν is the target control variable) we invoke a set of necessary conditions listed in Viewgraph 8. The transversality conditions and the differential equations for the Lagrange multipliers are also specified on this viewgraph.

5. Numerical Example

To illustrate the procedure for determining v* by utilizing the necessary conditions specified in Viewgraph 8, let us consider the example where the pursuer chooses a constant v* throughout the entire course of action. In addition, the pursuer chooses θ_0 and θ_1, making this example a two phase tracking problem. Viewgraph 9 illustrates the tracking trajectory for ownship and a typical evasion maneuver for the target.

The example is characterized by two six minute tracking legs, so that the terminal time for the game is 12.0 minutes. We make the assumption that the evader's strategy is to run away from the pursuer on a course opposite to the bearing line. Some typical numbers are chosen for the constants α, β and γ as shown in Viewgraph 9. The constant γ is of such a small magnitude because of the $||\underline{x}||^4$ quantity in the denominator of the information term of the performance criterion.

The method of steepest descent was used to solve the numerical optimization problem and find v*. Several performance criterion curves are shown in Viewgraph 10 for different $[\theta_0, \theta_1]$ selections. Also shown in this figure is the necessary condition for v represented by h(v) ,

$$h(v) = \int_{t_0}^{t_f} \frac{\partial H}{\partial v} (\underline{x}^*, \underline{u}^*, v^*, \underline{p}^*) dt$$

The results show that when the necessary condition (h(v)=0.0) is satisfied the performance criterion is a maximum. The label J[15-60] denotes the performance criterion curve when θ_0=15.0 degrees and θ_1=60.0 degrees.

For comparison in Viewgraph 11 we have plotted the performance criterion curves for θ_0=15.0 degrees and θ_1=60.0, θ_1=90.0 degrees. We note in the case where θ_1=90.0 degrees that a larger tracking speed maximizes J but there is no gain in performance, in fact the maximum is somewhat lower. Therefore, by having a large course change between the first and second leg,

which is good from the standpoint of improving tracking algorithm performance, there is no gain in the performance criterion we have selected, i.e., one that also includes the terminal relative distance. The vehicle trajectories for these two cases are illustrated in Viewgraphs 12 and 13. A large tracking speed in the θ_1=90.0 degrees case is countered by an equally large evasion speed so that the terminal relative distance is nearly the same in both cases.

To emphasize the importance of the choice of θ_0, we have plotted the vehicle trajectories for the two situations when θ_0=0.0 degrees, θ_0=30.0 degrees and θ_1=60.0 degrees in Viewgraphs 14 and 15. As previously pointed out, tracking algorithm performance is enhanced by a large course change between the two legs. However experience has also shown that running toward the target on the first leg is detrimental to tracking algorithm performance. Thus a typical tracking trajectory would be θ_0=0.0 degrees and θ_1=60.0 degrees when the target is at an initial bearing of 45.0 degrees. Note in Viewgraph 14 that the evader can take advantage of this strategy to increase the relative distance from 4.0 Kyds at t_0=0.0 to 8.0 Kyds at the terminal time. The pursuer's strategy from our viewpoint can be significantly improved if he chooses a course on the first leg more closely equal to the initial bearing to the target. As shown in Viewgraph 15, he can even close the relative distance between himself and the evader from 4.0 Kyds at t_0=0.0 to 3.4 Kyds at the terminal time. The optimal course change for the tracking vehicle is a compromise between acquiring sufficient information for the tracking algorithm and optimizing the criterion we have considered. This problem needs further investigation.

REFERENCES

1. Isaacs, R., Differential Games, John Wiley and Sons, Inc., New York, 1965.

2. Dobbie, J.M. "Solution of some surveillance-evasion problems by methods of differential games," Proceedings of the 4th Inter. Conf. on Oper. Res. (Eds. Hertz and Melese) Wiley-Interscience, 1966, pp. 170-184.

3. Lewin, J. and Breakwell, J.V., "The surveillance-evasion game of degree," J. of Opt. Theory and Appl., Vol. 16, Nos. 3, 4, August 1975, pp. 339-353.

4. Liu, P.T. and Bongiovanni, P.L., "Optimal vehicle tracking maneuvers: a differential game theoretic approach," IEEE Trans. on Auto. Control (submitted January 1981).

A DIFFERENTIAL GAME APPROACH TO DETERMINE PASSIVE TRACKING MANEUVERS

CHARACTERIZED BY:

1. DYNAMIC MODEL FOR THE GAME

2. UNIQUE CHARACTERISTICS OF THE INFORMATION (ACOUSTIC EFFECTS)

3. PERFORMANCE CRITERION WHICH REFLECTS THE OBJECTIVES OF THE TWO PARTICIPANTS

4. ESTIMATION AND CONTROL OF A STOCHASTIC SYSTEM IS CONVERTED TO A DETERMINISTIC PROBLEM

5. NO SADDLE-POINT SOLUTION EXISTS,INSTEAD WE FIND THE MAX-MIN SOLUTION

SUBMARINE TRACKING CONFIGURATION FOR PASSIVE TARGET TRACKING

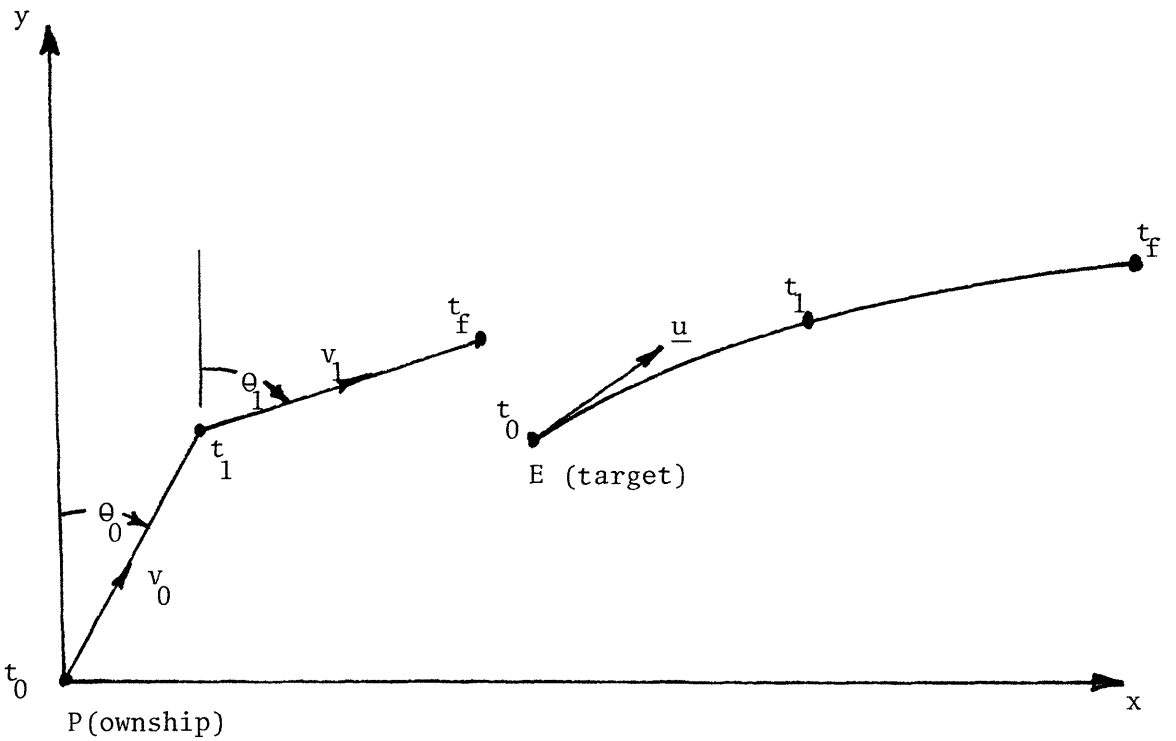

(x_p, y_p) : POSITION OF PURSUER (OWNSHIP)

(x_E, y_E) : POSITION OF EVADER (TARGET)

$(x_E - x_p, y_E - y_p) = (z_1, z_2)$: TRUE RELATIVE POSITION

- ASSUME PURSUER KNOWS THE NOMINAL (APPROXIMATE) RELATIVE POSITION - (x_1, x_2)

MATHEMATICAL MODEL

- STATE EQUATIONS

$$\dot{x}_1 = \nu x_1 - v \text{ SIN } C_p$$

$$\dot{x}_2 = \nu x_2 - v \text{ COS } C_p$$

- OWNSHIP PARAMETERS

v: SPEED

C_p: COURSE

TWO PHASES (legs)

$$\left.\begin{array}{l} v = v_o \\ C_p = \theta_o \end{array}\right\} \quad t_o < t < t_1$$

$$\left.\begin{array}{l} v = v_1 \\ C_p = \theta_1 \end{array}\right\} \quad t_1 < t < t_f$$

- TARGET PARAMETERS

(u_1, u_2) : VELOCITY

$(u_1, u_2) = (\nu x_1, \nu x_2)$, EVADER IS ASSUMED TO RUN AWAY FROM THE PURSUER ON A COURSE OPPOSITE TO THE BEARING LINE.

PASSIVE SONAR BEARING MEASUREMENTS

BEARING MEASUREMENT:

$$y = \tan^{-1}(z_1/z_2) + n$$

LINEARIZED MEASUREMENT ABOUT (x_1, x_2):

$$y = H(\underline{x})\ (\underline{z} - \underline{x}) + n$$

WHERE

$$H = \left[\frac{x_2}{x_1^2 + x_2^2} \qquad \frac{-x_1}{x_1^2 + x_2^2} \right]$$

n: ACOUSTICAL NOISE, ASSUMED TO BE WHITE GAUSSIAN WITH ZERO MEAN AND VARIANCE σ_n^2

σ_n^2: FUNCTION OF THE SPEED OF BOTH VEHICLES AND THE RELATIVE DISTANCE.

EQUATION FOR σ_n^2:

$$\sigma_n^2 = k\| \underline{x}\|^2\ e^{-\alpha\|\underline{u}\|} + \beta v$$

WHERE k, α, AND β ARE POSITIVE CONSTANTS.

INFORMATION IN IMPERFECT BEARING MEASUREMENTS

IN LINEAR RECURSIVE ESTIMATION WITH MEASUREMENT:

$$y = H\underline{z} + n$$

THE TRACE OF THE INFORMATION MATRIX

$$I_t = H^T Q^{-1} H$$

DETERMINES TO A LARGE EXTENT THE ERROR COVARIANCE, WHERE

$$E(n(t)n(\tau)) = Q\delta(t-\tau)$$

IN OUR PROBLEM

$$Q^{-1} = \frac{e^{\alpha\|\underline{u}\| - \beta v}}{k\|\underline{x}\|^2}$$

AND

$$tr\,[I_t] = \frac{e^{\alpha\|\underline{u}\| - \beta v}}{k\|\underline{x}\|^4}$$

OWNSHIP OBJECTIVES

1. OBTAIN MAXIMUM INFORMATION TO ACCURATELY ESTIMATE RELATIVE POSITION OF TARGET.

2. MINIMIZE THE FINAL RELATIVE DISTANCE TO TARGET.

TRACKING STRATEGY OF OWNSHIP:

$$v_o, v_1$$

AND ASSUME THAT θ_o AND θ_1 ARE PREDETERMINED - TYPICALLY A 60^o LEAD-LAG TRAJECTORY IS SELECTED.

A PERFORMANCE CRITERION CONSIDERING BOTH OBJECTIVES ABOVE CAN BE EXPRESSED AS:

$$J(\underline{u},v) = \int_{t_o}^{t_f} \frac{e^{\alpha \|\underline{u}\| - \beta v}}{\|\underline{x}\|^4} dt - \frac{\gamma}{2} \|\underline{x}(t_f)\|^2$$

γ IS A POSITIVE CONSTANT.

MAX-MIN APPROACH FOR OWNSHIP

DETERMINE v_o AND v_1 SO AS TO MAXIMIZE

$$F(v_o,v_1) = \min_{\underline{u}} J(\underline{u},v)$$

$$= J(\underline{u}^*(v_o,v_1),v)$$

WHERE $v = \{v_o,v_1\}$

OR TO ENSURE THAT

$$\min_{\underline{u}} J(\underline{u},v^*) \geq \min_{\underline{u}} J(\underline{u},v)$$

BY CHOOSING v_o^* AND v_1^*, OWNSHIP CAN BE SURE OF A PERFORMANCE NO WORSE THAT $F(v_o^*,v_1^*)$.

CONDITIONS FOR OPTIMALITY

NECESSARY CONDITIONS FOR v_o^*, v_1^* AND ν

DEFINE

$$H = \frac{e^{\alpha \|\underline{u}\| - \beta v}}{\|\underline{x}\|^4} + p_1(\nu x_1 - v \sin C_p) + p_2(\nu x_2 - v \cos C_p)$$

$$\dot{p}_1 = \frac{x_1 e^{\alpha \|\underline{u}\| - \beta v}}{\|\underline{x}\|^6} (4 - .14 \|\underline{u}\|) - \nu p_1$$

$$\dot{p}_2 = \frac{x_2 e^{\alpha \|\underline{u}\| - \beta v}}{\|\underline{x}\|^6} (4 - .14 \|\underline{u}\|) - \nu p_2$$

$$p_i(t_f) = -\gamma x_i(t_f) \qquad i = 1,2$$

THEN:

$$\frac{\partial H}{\partial \nu}(\underline{x}^*, \underline{u}^*, v, \underline{p}^*) = 0 \qquad \text{FOR ALL } t.$$

$$\int_{t_o}^{t_1} \frac{\partial H}{\partial v}(\underline{x}^*, \underline{u}^*, v^*, \underline{p}^*)\, dt = \int_{t_1}^{t_f} \frac{\partial H}{\partial v}(\underline{x}^*, \underline{u}^*, v^*, \underline{p}^*)\, dt = 0$$

NUMERICAL EXAMPLE

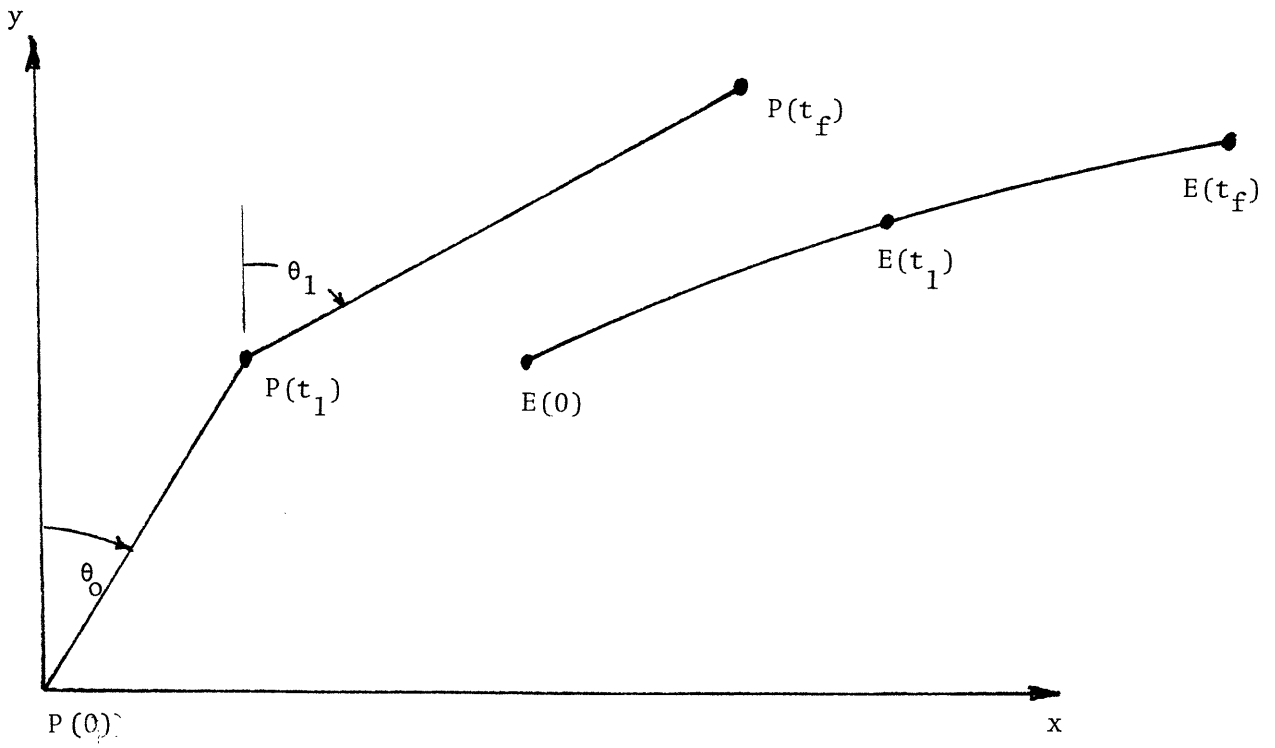

TRACKING TRAJECTORY FOR OWNSHIP AND TYPICAL EVASION MANEUVER FOR THE TARGET

TWO PHASE TRACKING PROBLEM

- TWO SIX MINUTE LEGS
- EVADER RUNS AWAY FROM PURSUER ON A COURSE OPPOSITE TO THE BEARING LINE.
- $\alpha = .14$, $\beta = .10$ AND $\gamma = .0002$.

PERFORMANCE CRITERION AND THE NECESSARY CONDITION AS A FUNCTION OF TRACKING SPEED

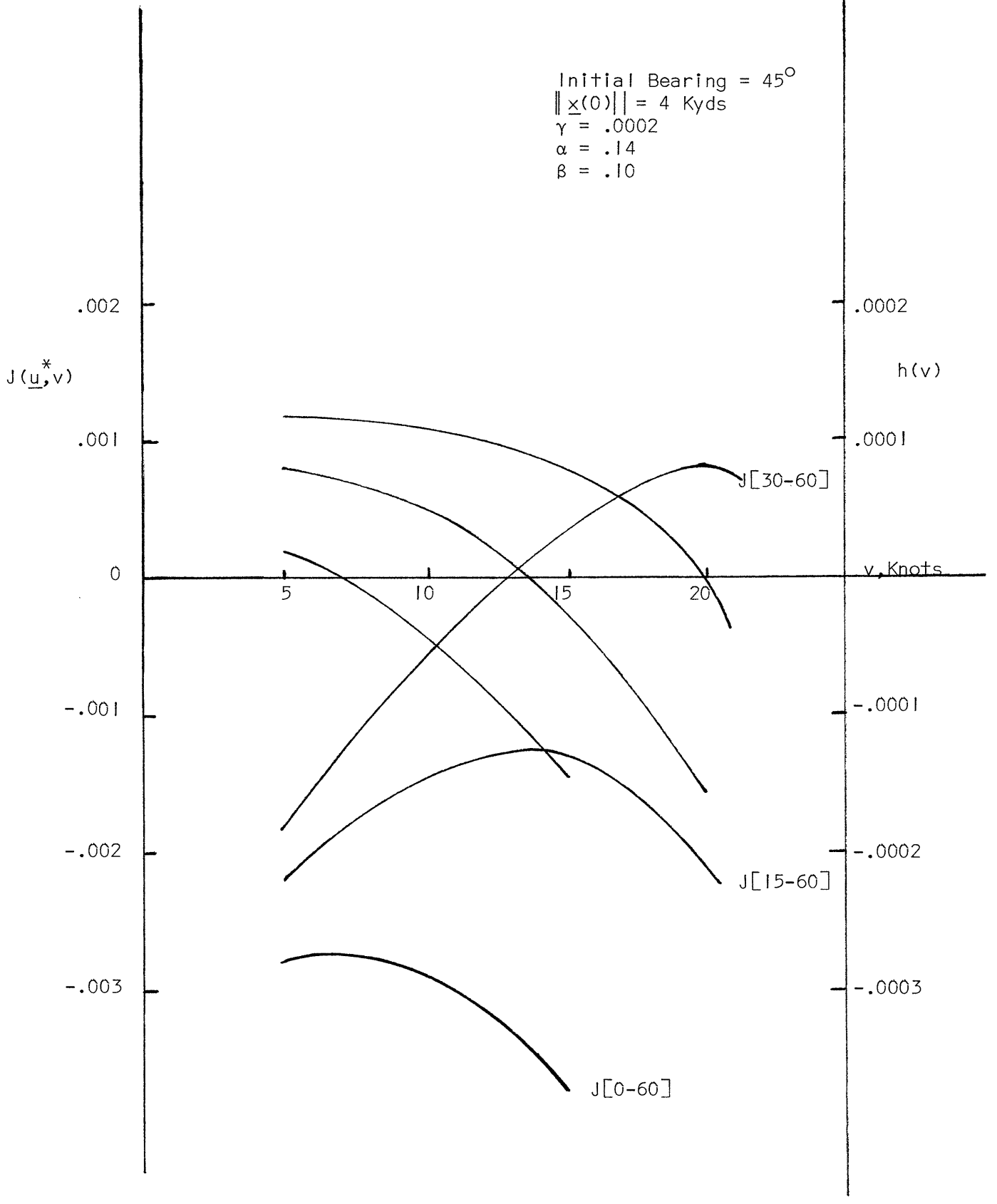

PERFORMANCE CRITERION AS A FUNCTION OF TRACKING SPEED FOR TWO DIFFERENT STRATEGIES
(TWO SIX MINUTE LEGS)

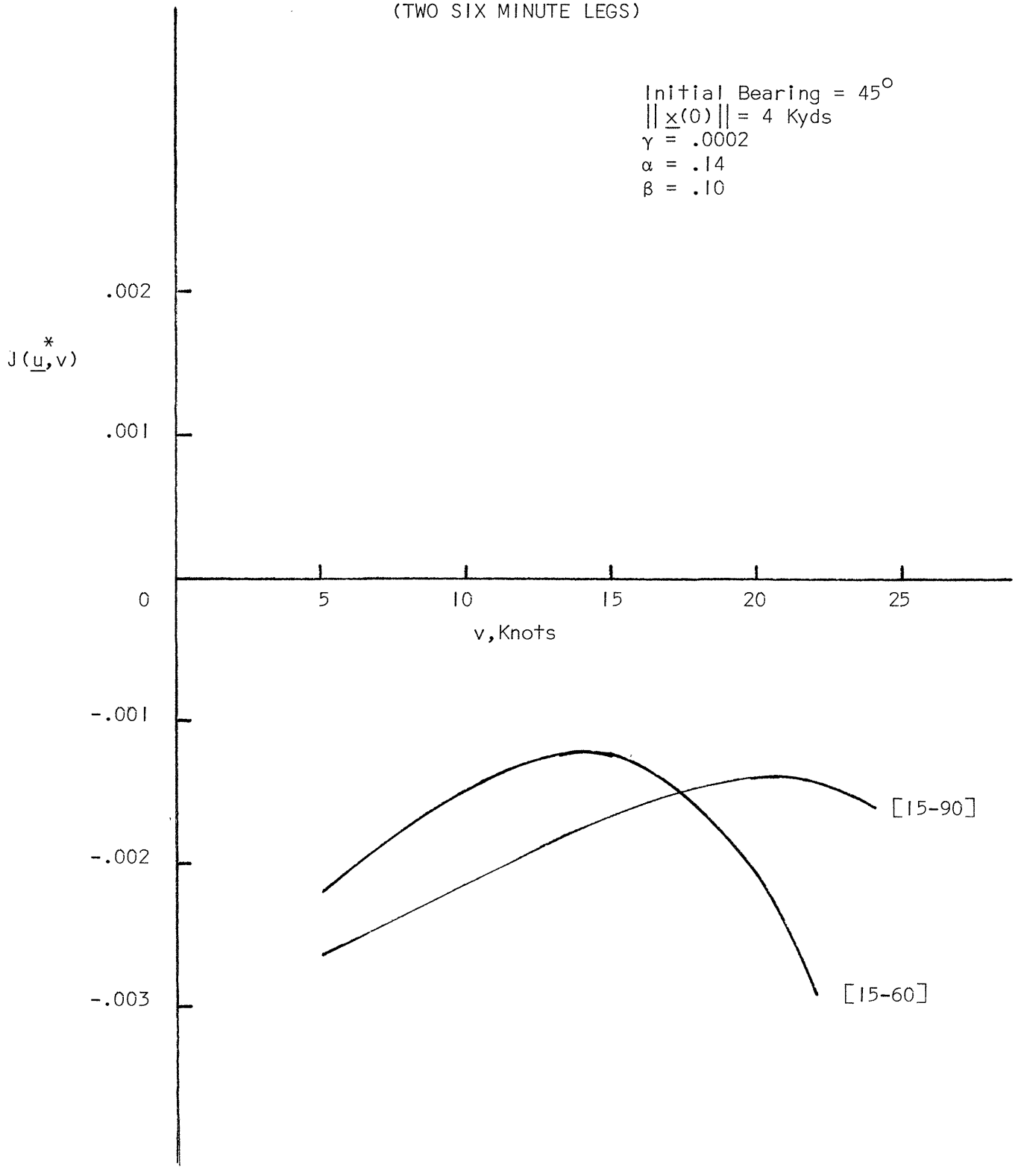

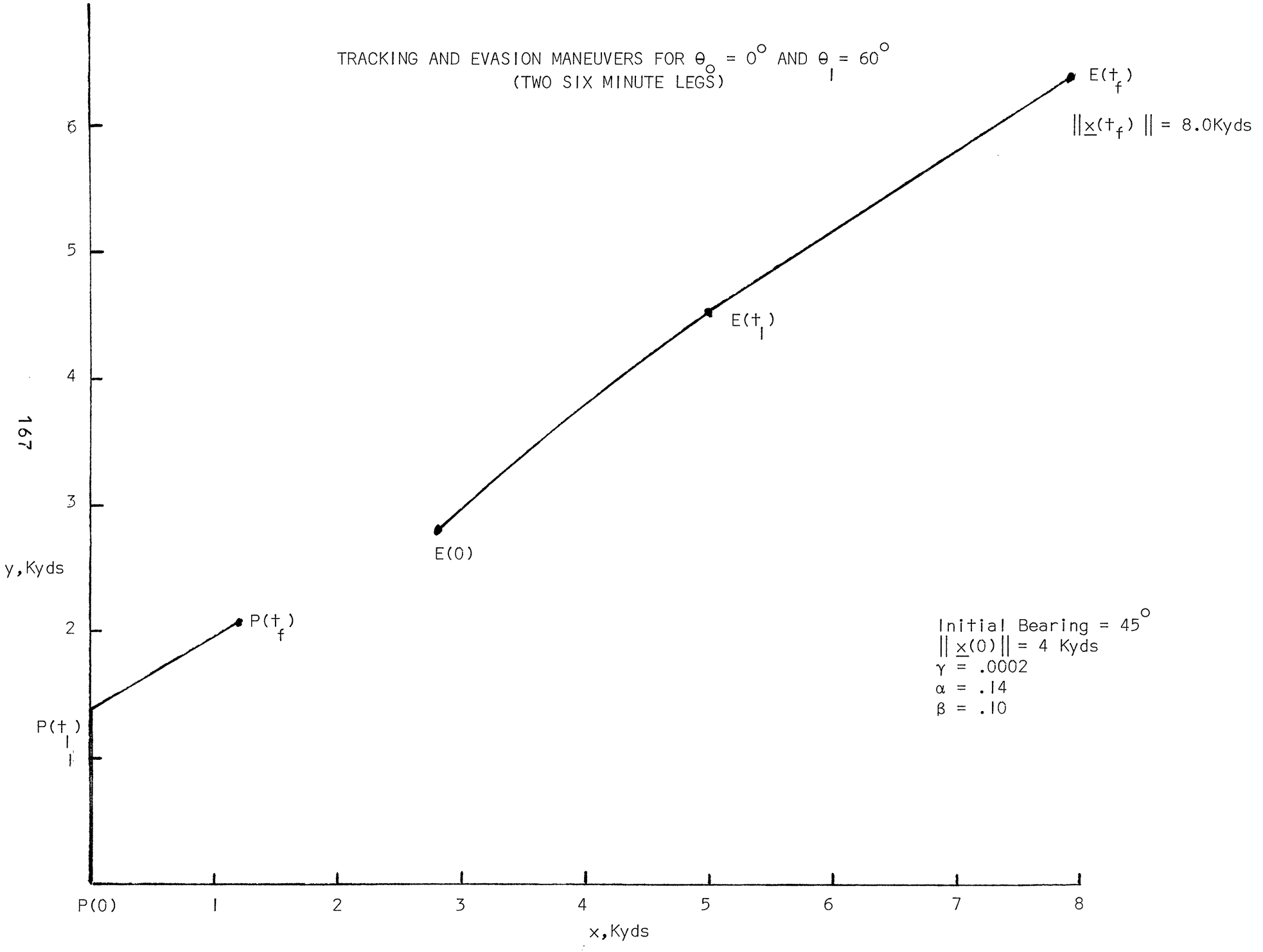
TRACKING AND EVASION MANEUVERS FOR $\theta_o = 0^o$ AND $\theta_1 = 60^o$
(TWO SIX MINUTE LEGS)
$E(t_f)$
$\|\underline{x}(t_f)\| = 8.0$Kyds
$E(t_1)$
$E(0)$
$P(t_f)$
$P(t_1)$
$P(0)$
Initial Bearing = 45^o
$\|\underline{x}(0)\| = 4$ Kyds
$\gamma = .0002$
$\alpha = .14$
$\beta = .10$
y,Kyds
x,Kyds
0
1
2
3
4
5
6
7
8

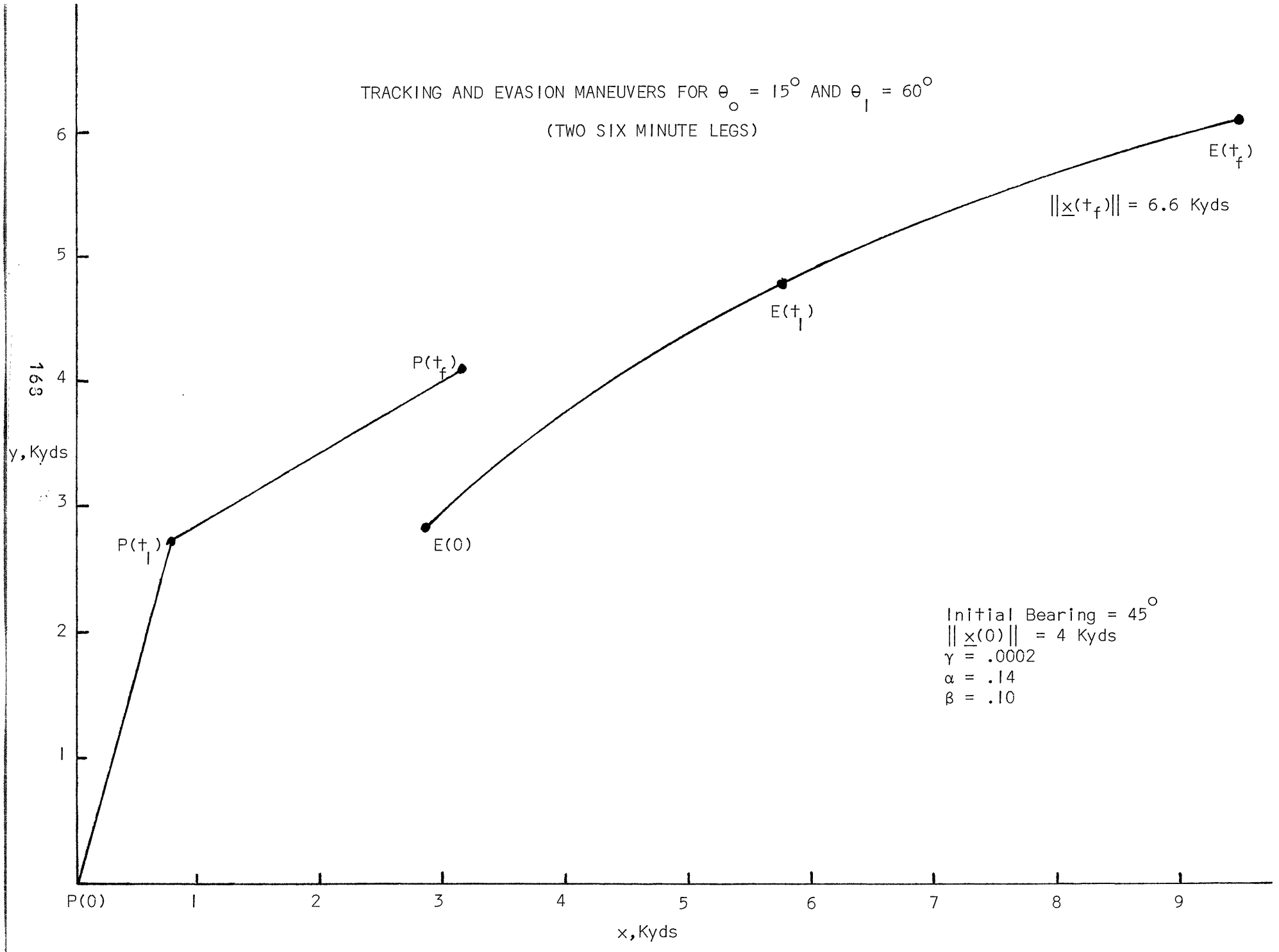
TRACKING AND EVASION MANEUVERS FOR θ_o = 15° AND θ_1 = 60°
(TWO SIX MINUTE LEGS)
$E(t_f)$
$\|\underline{x}(t_f)\|$ = 6.6 Kyds
$E(t_1)$
$P(t_f)$
$P(t_1)$
E(0)
P(0)
Initial Bearing = 45°
$\|\underline{x}(0)\|$ = 4 Kyds
γ = .0002
α = .14
β = .10
y, Kyds
x, Kyds
1
2
3
4
5
6
7
8
9

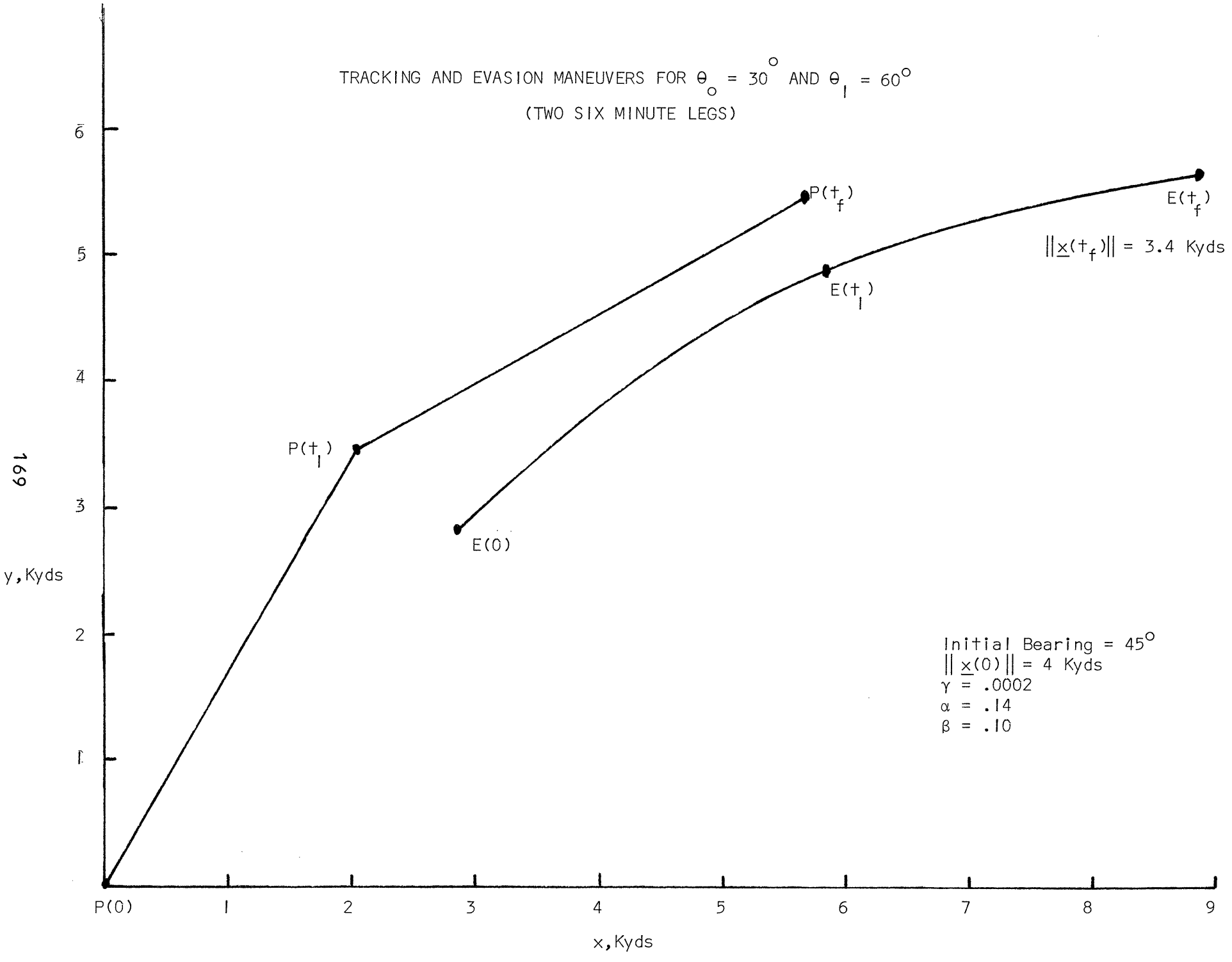
TRACKING AND EVASION MANEUVERS FOR $\theta_o = 30^\circ$ AND $\theta_1 = 60^\circ$
(TWO SIX MINUTE LEGS)
$P(t_f)$
$E(t_f)$
$\|\underline{x}(t_f)\| = 3.4$ Kyds
$E(t_1)$
$P(t_1)$
$E(0)$
Initial Bearing = 45°
$\|\underline{x}(0)\| = 4$ Kyds
$\gamma = .0002$
$\alpha = .14$
$\beta = .10$
y, Kyds
x, Kyds
P(0)
1
2
3
4
5
6
7
8
9

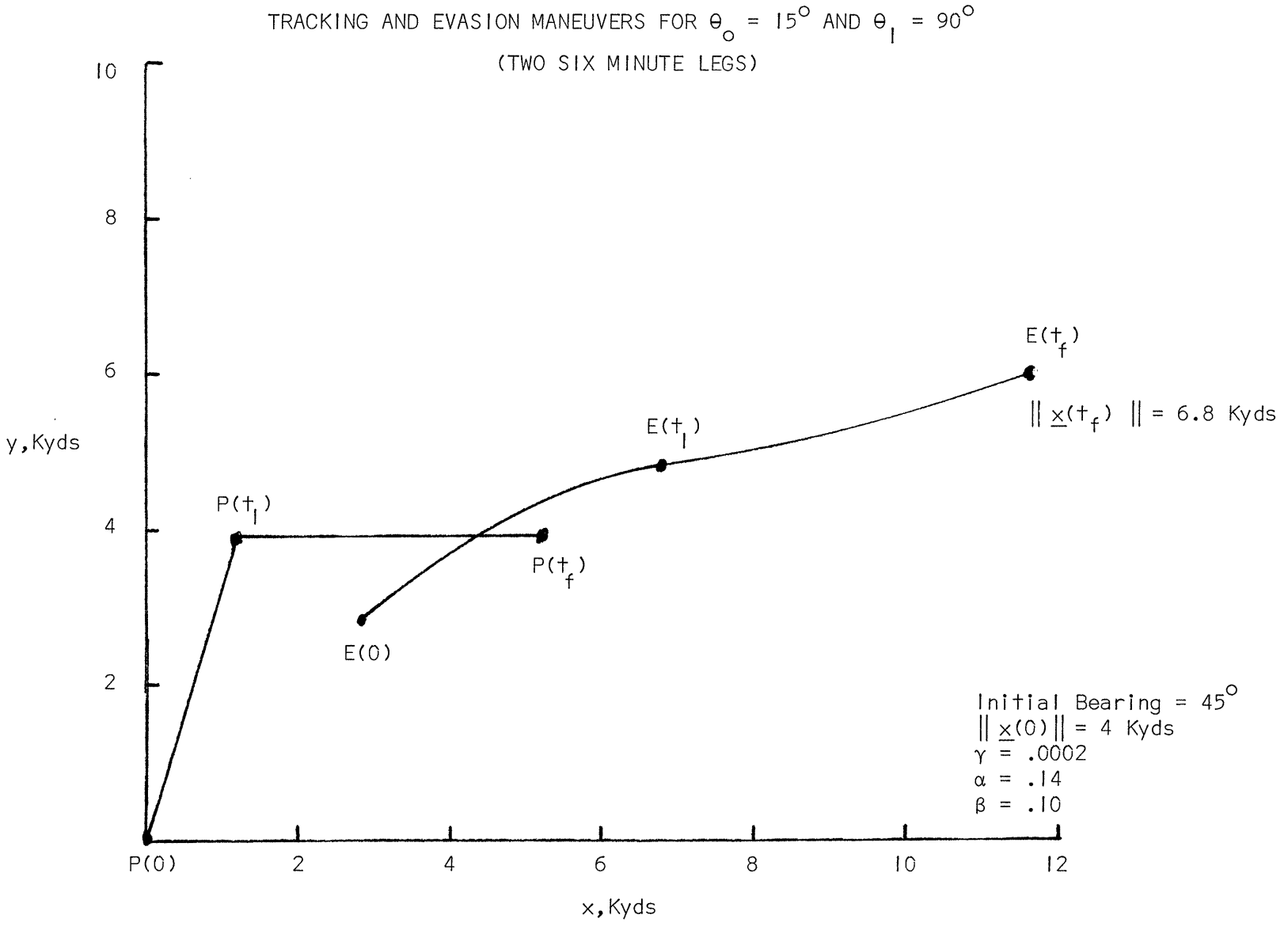
TRACKING AND EVASION MANEUVERS FOR θ_o = 15° AND θ_1 = 90°
(TWO SIX MINUTE LEGS)
10
8
6
4
2
y,Kyds
$E(t_f)$
$\| \underline{x}(t_f) \|$ = 6.8 Kyds
$E(t_1)$
$P(t_1)$
$P(t_f)$
E(0)
P(0)
2
4
6
8
10
12
x,Kyds
Initial Bearing = 45°
$\| \underline{x}(0) \|$ = 4 Kyds
γ = .0002
α = .14
β = .10

DESCRIPTION OF AND RESULTS FROM A SURFACE OCEAN SURVEILLANCE SIMULATION

Thomas G. Bugenhagen
Bruce Bundsen
Lane B. Carpenter

Applied Physics Laboratory
The Johns Hopkins University
Laurel, Maryland 20810

(This work was supported by the Naval Electronics Systems Command under Task G3AO of Contract N00024-81-C-5301 with the Department of the Navy).

Description of and Results from a Surface Ocean Surveillance Simulation

T. G. Bugenhagen, B. Bundsen, and L. B. Carpenter
The Applied Physics Laboratory, Johns Hopkins University

Laurel, Md. 20810

ABSTRACT

As a part of the Over-the-Horizon/Detection, Classification and Targeting (OTH/DC&T) Engineering Analysis Program performed by The Johns Hopkins University Applied Physics Laboratory (JHU/APL) in support of the Naval Electronic Systems Command (NAVELEXSYSCOM) (PME 108-2), it was necessary to establish ocean surveillance system requirements in a realistic environment. The area tracking and correlation (ATAC) model was developed and used to perform analyses for defining these surveillance requirements in a setting where high interest ships interact with merchant ships traveling in shipping lanes.

This work was supported by The Naval Electronics Systems Command under Task C3A0 of Contract N00024-81-C-5301 with the Department of the Navy.

1. INTRODUCTION

Adequate surveillance of an ocean area may require tracking large numbers of targets over a broad area using a variety of sensors. Often, the density of background ships in the area is high enough to cause interference with the tracking of high interest targets. The high interest targets themselves may execute maneuvers at unknown times, further complicating the situation. As a part of the OTH/DC&T analysis effort, it was necessary to determine the requirements of ocean surveillance system parameters for this setting. In some previous analyses, the merchant ship traffic was assumed to be uniformly distributed throughout the area. This is quite different from the actual situation where the merchant ships travel in shipping lanes. To define the ocean surveillance requirements in a realistic environment, the area tracking and correlation (ATAC) model was developed. It is a simulation of the ocean surveillance situation including:

a. Generation of merchant and high interest ship positions as they move across an arbitrarily defined ocean area in defined shipping lanes;
b. Development of simulated sensor reports from a variety of sensors;
c. Initialization of tracks;
d. Correlation of the reports to previously established tracks;
e. Continuation and projection of the tracks to any chosen time; and
f. Measurement of the accuracy of the correlations by comparing with the actual (ground truth) tracks stored in the computer.

In the present version of the ATAC model, three different sensors were modeled and used in the analysis: two active radar sensors and a passive sensor that is assumed to give reports only on the high interest ships. The passive sensor is assumed to also give a unique identity of the ships on which it reports. Of the two active radar sensors, one is assumed to give only position reports, while the other gives position and velocity measurements on the ships. A later version of the ATAC model also includes sensors that give line-of-bearing measurement reports.

2. THE AREA TRACKING AND CORRELATION MODEL

Figure 2-1 illustrates the functional flow when the ATAC model is used in a Monte Carlo loop with simulation of ship traffic and sensor reports. Each block of the diagram will be explained, in turn, in both Sections 2 and 3.

The three basic steps to the model are: (1) developing sensor reports, (2) assigning sensor reports, and (3) scoring. The first step is subdivided into three parts: scenario, process noise, and measurement noise.

In the scenario, the ocean area is defined (by four corners in latitude and longitude), the structure of the shipping lanes is established, and the density of the merchant shipping is set. In the process noise subdivision, the ship heading errors and velocity errors are defined, after which specific simulated ships and their motion can be generated. Measurement noise takes into account the sensor parameters to generate sensor reports, which are perturbed from the ground truth (actual) positions according to the position error associated with the sensor.

In the correlation phase, which makes up all of step 2, the sensor reports are associated (correlated) with existing ship tracks in a track file by using Kalman filtering and probabilistic decision making. The time step loop in this part of the block diagram is meant to show that as sensor reports are periodically generated and received (based on the sensor update interval), the correlator associates the reports to tracks. At each time step, certain measures of effectiveness are calculated and then averaged at the end of the time period for which the model was run.

After running the ATAC model with one choice of the process noise and sensor parameters, a new set of values is chosen. The process is repeated as shown by the Monte Carlo loop. The measures of effectiveness are collected for each such iteration and used to give the grand averages used in the analysis.

ATAC is currently programmed in the PL-1 programming language and run on an IBM 3033 computer. It uses about 1.5 megabytes of storage and about 10 seconds of comptuer processing time for one iteration involving roughly 20 ship contact reports every hour over an area of 40,000 nmi^2 in a given 10-hour time period.

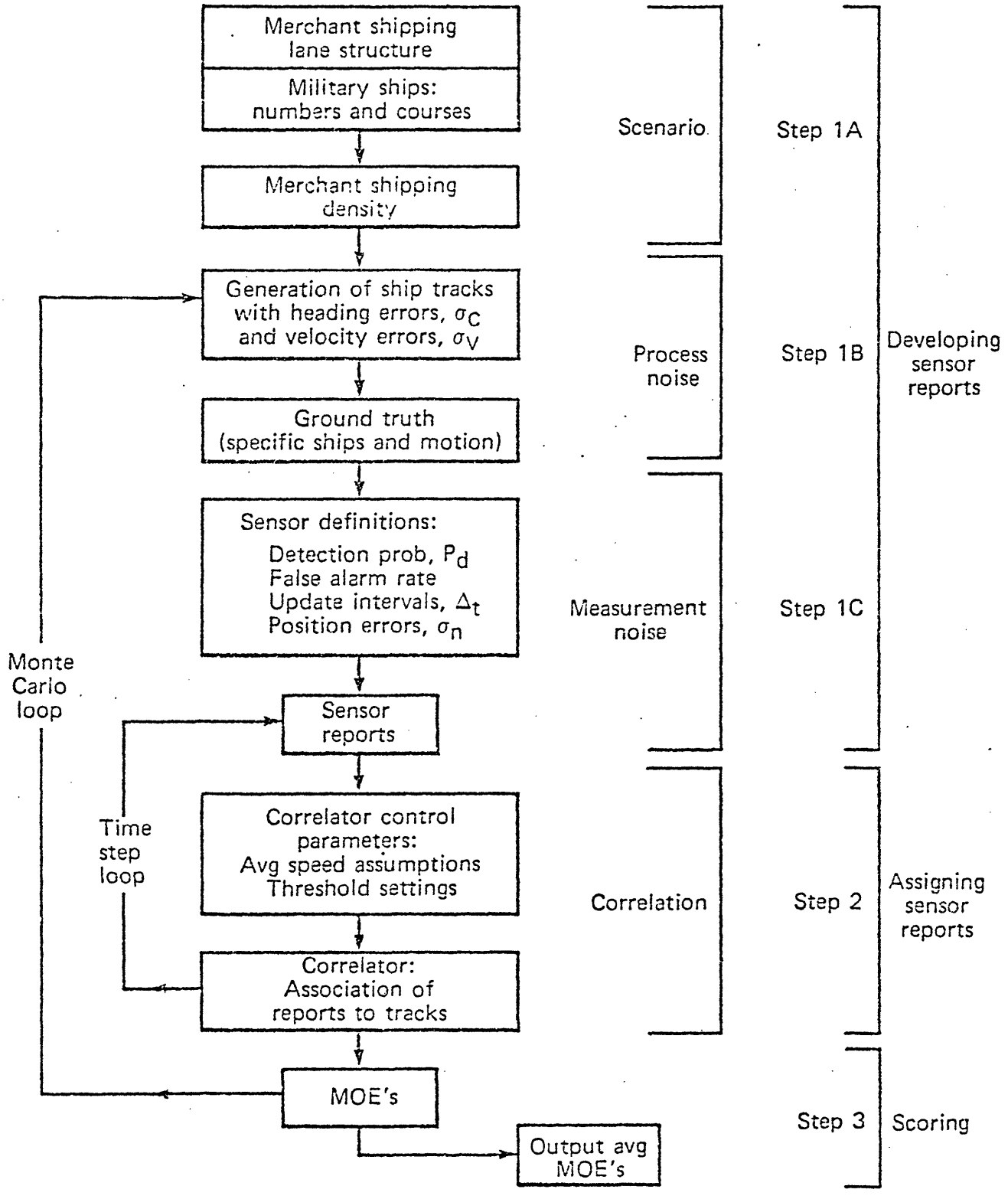

Fig. 2-1 Area Tracking and Correlation Model Monte Carlo Functional Flow Diagram

2.1 BACKGROUND SHIP TRAFFIC

Background ship traffic in a region of interest (ROI) is generated along shipping lanes defined as a sequence of geographic coordinates (turn points). Each lane has a width established by assuming a normal distribution about a mean path with a standard deviation that can be input. Within each shipping lane, individual ships of a given type are generated from a departure rate, which is either input or calculated on the basis of ship density considerations. Ship tracks consist of a time history of geographic coordinates between which motion is maintained with constant course and speed. The time spacing of the points is small enough so that intermediate positions may be determined by interpolation.

2.2 HIGH INTEREST SHIP TRACKS

The procedure used to generate the tracks of high interest ships is different from that used for background ships. A master file contains data for a number of sample paths, each representing a ship maneuvering randomly to avoid detection while attempting to maintain a particular average speed and course. The state equations from which these tracks are generated are written in a latitude-longitude system, and the ship follows a rhumb line between observations. Input parameters are:

a. Initial ship latitude and longitude;
b. Maximum ship speed permitted;
c. Mean ship velocity desired;
d. Mean target course (angle);
e. Standard deviation of maneuver speed, and beta, a parameter describing the relationship between a random change in course and a change in speed.

2.3 GENERATION OF SENSOR REPORTS

After the ship paths and movement along the paths have been established, sensor reports (using data from this simulated ship traffic) are generated. Simulated ground truth position data on ships, within some geographical region of interest, is perturbed according to assumed sensor error distributions. An input detection probability permits missed detections, and the capability of generating false targets is provided.

2.4 CORRELATION OF SENSOR REPORTS

The correlator attempts to make the associations from the sequence of sensor reports that have been developed. As the sensor reports are periodically generated and received (based on the sensor update interval), the correlator associates the reports to tracks. Once the associations have been made, a ship tracker (based on a Kalman filter) is used to develop the individual tracks.

This procedure works well as long as none of the ships are maneuvering. When a ship maneuvers, a contact report's distance measure, obtained from the tracker, may be large. This may cause the report to be thrown out because it either failed a threshold test or was not assigned in the best hypotheses. To overcome this problem and to efficiently assign contact reports from maneuvering and non-maneuvering targets, the correlator has been designed to process four different types of ship motion in stages, with one type of motion processed in each stage. The four stages and the corresponding motion processed are listed in Table 2-1. The correlator processes through all four stages each time a set of contact reports is received.

Table 2-1

Correlator Stages for Processing Ship Motion Models

Stages	Ship Motion Processed
1	Slow, Straight
2	Fast, Straight
3	Slow, Maneuvering
4	Fast, Maneuvering

When all the possible associations between contacts and tracks have been made in one stage, the contacts and tracks are removed as candidates for successive stages. Since most of the merchant ship traffic will be following a constant heading (rhumb-line sailing) at moderate speeds, they will usually be processed in the first or second stages. When they are removed, the remaining contacts and tracks can be associated in a more efficient manner.

2.5 TECHNICAL DESCRIPTION OF THE CORRELATION OF SENSOR REPORTS

The correlator developed for use in the ATAC simulation is a technique for assigning reported contacts on the ocean surface to existing ship tracks or to previously reported points (to initiate a track). In general, the sensors are assumed to be giving information on many contacts at approximately the same time with the results being correlated with the current track file. In this sense, ATAC does report-to-track correlation.

2.5.1 FEASIBILITY TABLE

The construction of hypotheses begins with the construction of the feasibility table. The table is simply a listing of the current track file versus the new set of contacts and an indication of which of the contacts are feasible to be associated with each of the tracks. Feasibility is defined in terms of possible ship speeds and sensor errors. A maximum ship speed, v_{max}, is used to determine the distance a ship could travel in the time, Δt, since the tracks were last updated. If d_{ij} is the distance from the last position of track i to contact j, then the association is, by definition, feasible if

$$d_{ij} \leq \left[(v_{max}\Delta t) + 3\sqrt{\sigma_{ni}^2 + \sigma_{nj}^2} \right]$$

where σ_{ni} is the sensor error associated with the last position of the i^{th} track and σ_{nj} is the sensor error associated with the j^{th} contact.

After determining which contacts are feasible for a given track, the figure of merit is calculated for each of these contacts. The figure of merit used is $\log f_i(Z_j)$ where the function f_i is given by the distribution of the expected position of the i^{th} track after time, Δt, since the last update and Z_j is the j^{th} contact.

2.5.2 UNIQUE ASSIGNMENTS

There is one exception to this rule of calculating the figure of merit. If there is only one feasible contact for a track and if that contact is not feasible for any other track, then that contact is arbitrarily assigned to the track. This procedure is called "Unique Assignment" in the program.

The figure of merit is not calculated. For all remaining locations where a contact is feasible, the figure of merit is calculated. The resulting table of values is called the distance table in the program.

2.5.3 THRESHOLD TESTS

The values for the feasible contacts are then subjected to a threshold test to further reduce the number of ambiguities for each track. Specifically, if

$$\log f_i (Z_j) \leq T_h ,$$

where T_h is the arbitrarily chosen threshold, then the contact Z_j is retained as one of the possible contacts for track T_i.

2.5.4 UNIQUE MINIMUMS

Before going into the hypothesis generation routine, one further attempt at reducing the number of ambiguities is made. The attempt is to try to find contacts that give "unique minimum" values of the figure of merit for some of the tracks. The rows of the distance table represent the tracks currently being carried and the columns represent the new set of contacts to be assigned. For each row, the contact is found that yields the smallest figure of merit. These are called "row minimums." Likewise, for each column, the track is located for which the figure of merit is smallest. These are called "column minimums." When a row minimum is also a column minimum, then an assignment of that contact to the corresponding track will be made if neither of the following two conditions is violated:

a. There must be no other row minimums for that column (contact), and
b. There must be no other column minimums for that row (track).

2.5.5 THRESHOLD LOWERING AND ITERATION ON HYPMAX

The number of hypotheses that could be generated when initiating tracks with the first two sets of reports is a function of shipping density and the circular area within which a ship could have moved in the time interval,

ΔT, between the reports. If the ships in the area were uniformly distributed throughout the area, the number of contacts from the second set of reports that could be associated with each contact from the first set is

$$N \approx \rho\pi \left(v_s \Delta T + 3 \sqrt{\sigma_{n1}^2 + \sigma_{n2}^2} \right)^2$$

where

ρ = shipping density,

v_s = upper bound on ship speed,

ΔT = time between reports, and

σ_{n1}, σ_{n2} = sensor accuracy of 1st and 2nd reports.

This number by itself can become large. However, the number of hypotheses that can be generated can become very large. As a result, when the update interval or the location errors increase, the correlator processing time increases dramatically. This is shown in Figure 2-2, in which the actual processing time for one replication is plotted versus the update interval. A similar curve for the sensor accuracy would reach the upper limit when $\sigma_n \approx 4$ nmi.

To keep the processing time and costs within bounds and still obtain results when $\Delta T > 2.0$ hrs or $\sigma_n > 4$ nmi, it is necessary to reduce the thresholds that limit the size of the uncertainty areas and, therefore, the number of hypotheses that can be generated. An estimate of the number of hypotheses that could be generated is made. If this number is less than an upper bound (called HYPMAX), hypothesis generation begins. If the estimate is greater than HYPMAX, the threshold, T_h, is reduced by a set amount, and any entry in the feasibility table larger than the new threshold value is removed. A new estimate of the number of hypotheses is made and compared with HYPMAX again. This process is repeated until the estimate is below HYPMAX. The result is called the ambiguity table. Thus, for each track that has not been assigned a unique contact, the ambiguity table lists those contacts that are both feasible and have a figure of merit less than the final threshold value resulting from the iterative reduction process.

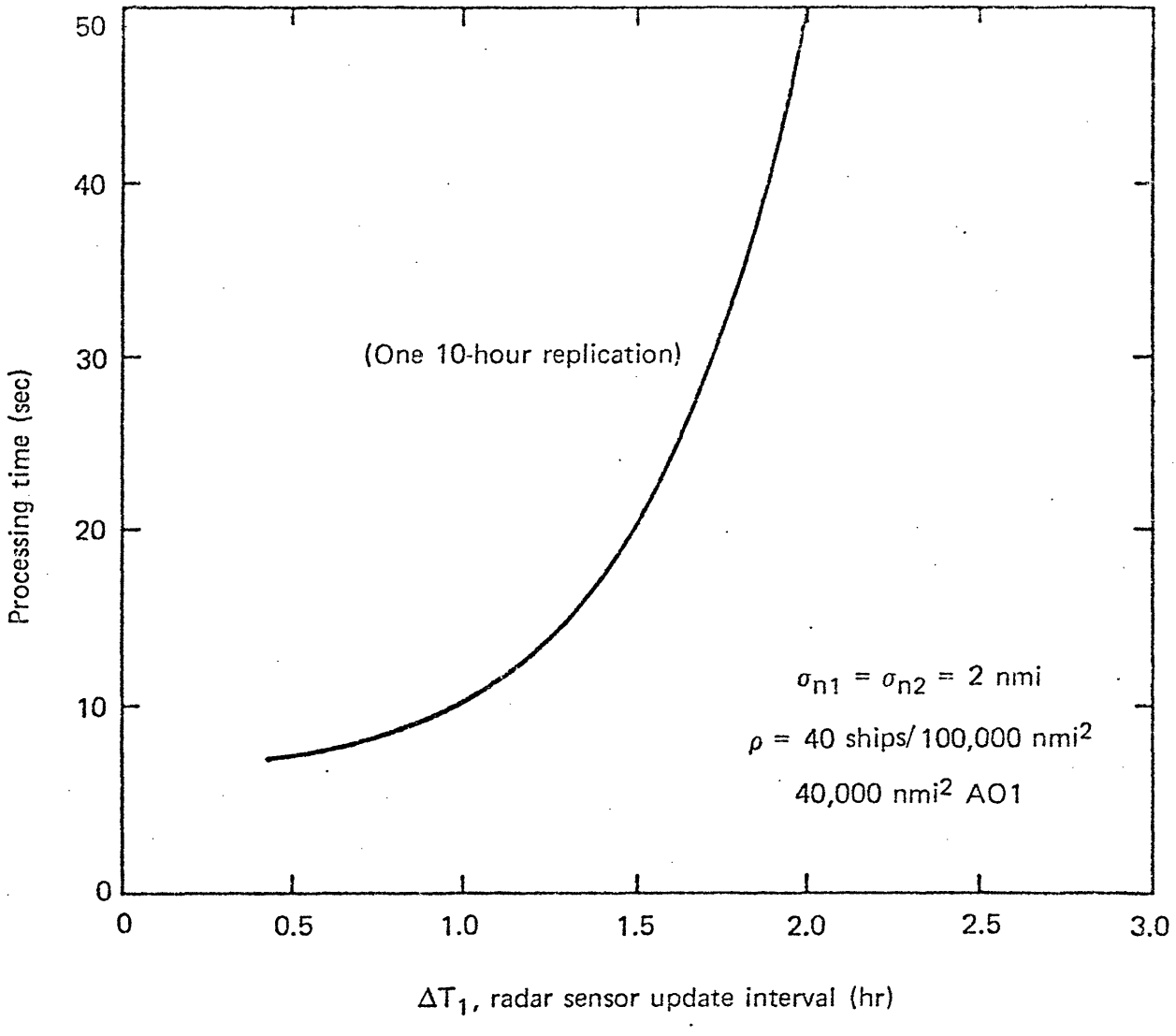

Fig. 2-2 Computer Processing Time vs Radar Sensor Update Interval

2.5.6 GENERATION OF HYPOTHESES

To generate the hypotheses, the ambiguity table is used. A pointer is set at the first unused contact for each track (row) starting with the last track in the table. The resulting assignments constitute the first hypothesis. If there are unused contacts remaining, they are saved as possible beginnings of new tracks. If there are insufficient contacts, then one or more of the tracks must have received a detection miss. The technique for generating the hypotheses in these cases is discussed in paragraph 2.5.8.

Successive hypotheses are generated by incrementing the position of the pointer for the first track to the next unused contacts. When the last contact is used for the first track, the position of the pointer for the second track is incremented once and the process repeated for the first track.

After all contacts have been used for the second track, the process is repeated for the third track and so on for the remaining tracks. The overall process can be compared to an odometer with each track representing one wheel of the odometer. As the last digit (contact) is used on one wheel (track) of the odometer, the next wheel is incremented one or more digits. Methods are included to keep from generating illegal or inconsistent hypotheses (i.e., ones in which a contact is used more than once).

2.5.7 TRACKER

A basic part of the correlator is the tracker that is described in Reference (b). The tracker is used to give a figure of merit for relating a contact report to a track. The state equations of the tracker are outlined below.

If (L_{K-1}, M_{K-1}) are the latitude and longitude in radians of a ship contact at the time of the $(K-1)^{th}$ observation, then the coordinates of the ship, at the time of the K-th observation t_K hours later, will be given approximately by

$$L_K = L_{K-1} + \frac{V_{NK}}{R_e} t_K + w_L,$$

$$M_K = M_{K-1} + \frac{V_{EK}}{R_e \cos L_{K-1}} t_K + w_M,$$

where R_e is the radius of a spherical earth, V_{NK} is the average velocity of the ship North, V_{EK} is the average velocity East, and w_L and w_M are noise terms. In

addition, it is assumed that the rate of change of the latitude and longitude (here called λ_K and μ_K) are

$$\lambda_K = \frac{V_{NK}}{R_e} + w_\lambda, \text{ and}$$

$$\mu_K = \frac{V_{EK}}{R_e \cos L_{K-1}} + w_\mu,$$

where w_λ and w_μ are velocity noise terms that allow for random minor deviations in velocity and for maneuvers. If we define

$$X_K = \begin{pmatrix} L_K \\ M_K \\ \lambda_K \\ \mu_K \end{pmatrix}, \quad \phi_K = \begin{pmatrix} 1 & 0 & t_K & 0 \\ 0 & 1 & 0 & t_K \\ 0 & 0 & 1 & 0 \\ 0 & 0 & 0 & 1 \end{pmatrix}, \quad W_{K-1} = \begin{pmatrix} w_L \\ w_M \\ w_\lambda \\ w_\mu \end{pmatrix}$$

$$\lambda_{K-1} = \frac{V_{NK}}{R_e} \text{ and } \mu_{K-1} = \frac{V_{EK}}{R_e \cos L_{K-1}},$$

then these may be written as

$$X_K = \phi_K X_{K-1} + W_{K-1}.$$

It is assumed that the noise terms are white and Gaussian with zero mean and covariance matrix Q_K.

2.5.8 EVALUATION OF HYPOTHESES

If X is the state vector of a track and $\hat{X}_K$ (+) is the updated estimate at time K, then the projected estimate of the state at time K + 1 is

$$\hat{X}_{K+1}(-) = \phi_K \hat{X}_K(+)$$

where ϕ_K is the transition matrix. When the targets are not maneuvering or maneuvering only slightly, the measurement errors can be approximated as Gaussian so that the probability density, $f(\hat{X}_K)$, is effectively Gaussian. This allows the Kalman filter projection routines in the tracker to be used, which then can give figures of merit for associating reports to track. Techniques showing how to handle large maneuvers are discussed in paragraphs 2.4 and 2.5.9.

The uncertainty in the estimated position given by the projection routines of the Kalman tracker is represented by the covariance matrix P(-). The distribution of $\hat{X}_K$ is given by

$$f(\hat{X}_K) = \frac{1}{(2\pi)^2 \left|P(-)\right|^{1/2}} \exp\left[-\frac{1}{2}(\hat{X}_K - M_K)^T P(-)^{-1} (\hat{X}_K - M_K)\right]$$

where $M_K = E(\hat{X}_K)$.

If there are n tracks being kept and m contact reports, Z_{Ki}, received at time K, with $m \leq n$, then

$$f_1(Z_{K1}) \cdot f_2(Z_{K2}) \cdots f_m(Z_{Km})$$

is the likelihood function for the hypothesis that, for all i, the report Z_{Ki} should be associated with the track whose projected uncertainty is given by f_i. The likelihood of this particular assignment or hypothesis is

$$L_j = \log \prod_{i=1}^{m} f_i (Z_{Ki})$$

and the assignment that produces the maximum L_j is called the maximum likelihood assignment or hypothesis.

If we define

$$\tilde{Z}_{Ki} = Z_{Ki} - \hat{X}_{Ki}(-)$$

then

$$L_j = -n \ln 2\pi - \frac{1}{2} \sum_{i=1}^{n} \left[\ln \left| P_{Ki}(-) \right| + \tilde{Z}_{Ki}^{T} P(-)^{-1} \tilde{Z}_{Ki} \right] .$$

When reports are missing (i.e., when there are less reports than tracks), then each hypothesis has one (or more) fewer terms in it. However, no one hypothesis is favored more than another since each will contain the same number of "zeroes."

The last equation is used to evaluate each hypothesis with a certain number of the best ones retained. When only the single best hypothesis is kept, it will give the preferred tracks at that time.

2.5.9 INITIATION

In the ATAC model, track initiation is accomplished with the aid of the Riceian distribution [References (g) and (h)]. This distribution is the result when an object, whose initial position has a circular normal distribution, moves with a constant speed v in an unknown direction for a time t. All directions are assumed to be equally likely. Thus, if the distribution of the initial position is given by

$$f(r) = \frac{1}{2\pi^2} \exp \left[- r^2/2\sigma^2 \right]$$

then the distribution of the final position after a time t is given by

$$f(r,t) = \frac{1}{2\pi\sigma^2} \exp \left[- (r^2 + u^2t^2)/2\sigma^2 \right] I_o \left(\frac{rut}{\sigma^2} \right)$$

where I_o is the ordinary Bessel function of zeroth order. For a given time interval t, the distribution of target positions has spread outward into an annular region.

It is not only at the beginning of the simulation that tracks must be initialized. Even after tracks have been established, there are new ships entering the area and, therefore, tracks to be initialized. In either case, the log of f(r,t) is used for each hypothesis that assigns a second report to a point saved from a previous set of sensor reports. The distance between two such reports is r in the last equation. Speeds of 12 and 24 knots were assumed for two type ships, slow and fast, as described in paragraph 2.4. The value of σ assumed is

$$\sigma^2 = \sigma_1^2 + \sigma_v t^2 + \sigma_2^2$$

where

σ_1^2 = variance of the first position measurement,

σ_2^2 = variance of the second position measurement,

σ_v^2 = variance of the speed estimate, and

t = time between the measurements.

Besides its use for track initiation, the Riceian distribution is also used for maneuvering targets in the ATAC model. If a particular track is not updated in one of the first two motion models (non-maneuvering) described in paragraph 2.4, then the Riceian distribution is applied again from the last point of the track to see if possible contacts exist outside the normal projected uncertainty ellipse that could be associated with the track. If there are no such contacts, then the track is given a miss for this reporting time. If there is at least one such contact, then the one that minimizes the likelihood equation from the previous section is chosen to update the track. In effect, the track is reinitialized from the last point. As before, two speeds (12 and 24 knots) are assumed for the two maneuvering motion models.

2.6 MEASURES OF EFFECTIVENESS AND SCORING

The technique used to establish requirements for the ocean surveillance parameters in Reference (a) is similar to that used in other requirements analysis. First, a nominal case value is chosen for each of the parameters in the problem. Then, a sensitivity analysis is done by varying the value of each parameter, one at a time, over a specified range and calculating certain measure of effectiveness (MOEs).

2.6.1 TRACK PURITY

This MOE is intended to measure how pure a track is in the sense of the track having the same ID number for each contact report. It is the number of previous time steps that a ships' identity number agrees with the current identity divided by the number of time steps up to and including the current one.

2.6.2 MEAN RADIAL PREDICTION ERROR

At each time step, the tracks are projected 1 hour ahead. The predicted position is then compared with the ground truth position at the future time and the error between them calculated.

3. RESULTS OF THE PARAMETER SENSITIVITY ANALYSIS

The results of the ATAC Parameter Sensitivity Analysis are presented in the following graphs of the MOE as a function of the parameter under consideration. The MOE being considered can be plotted against only one of the parameters at a time; therefore, it is necessary to select a set of nominal values for the parameters. The selected nominal values are listed in Table 3-1.

In Figure 3-1, the track purity index decreases rapidly. When the active sensor is aided by the passive sensor the situation is much improved. When the radar sensor update interval is increased to larger values the result is few reporting times in the overall period. Consequently, there are proportionately more passive sensor reports which provide identification of the high interest ships. Since the passive sensor reports are correlated with few errors, there is less chance for error overall and the purity index remains high.

The prediction error 1 hour in the future from the sensor reporting times is plotted in Figure 3-2. In general, the errors for the background ships increase as the update interval increases while that for the high interest ships fluctuates around a constant value. Some of the fluctuations are due to the coincidence of the radar sensor observation times and the high interest ship maneuver times. When the passive sensor is added, the result is that the error for the high interest ships is not very dependent on the update interval.

In Figures 3-3 and 3-4 the radar sensor accuracy is varied. The main characteristic of these curves is the improved track purity for the high interest ships when the passive sensor is used.

Table 3-1. ATAC Parameters

ΔT_1	Radar Sensor Update Interval	1 hr
σ_{n1}	Radar Sensor Ship Location Error	2 nmi
P_{d1}	Radar Sensor Detection Probability	0.95
ΔT_2	Passive Sensor Update Interval**	2 hrs
σ_{n2}	Passive Sensor Ship Location Error	3 nmi
P_{d2}	Passive Sensor Detection Probability	0.95
ρ	Background Shipping Density (No. of Ships per 100,000 nmi^2)	50
P_{FA1}	Radar Sensor False Alarm Rate	0.2 For Each Report Time*
P_{FA2}	Passive Sensor False Alarm Rate	0.2 For Each Report Time*
σ_c	Background Shipping Navigation Error	2 degrees
σ_v	Background Shipping Speed Error	1 KT

*Each batch of reports at every time step is assigned a 0.2 mean probability of including a false alarm. Thus, one false report can be expected for every five time steps.

**The passive sensor is assumed to detect only the high interest ships and give their identity.

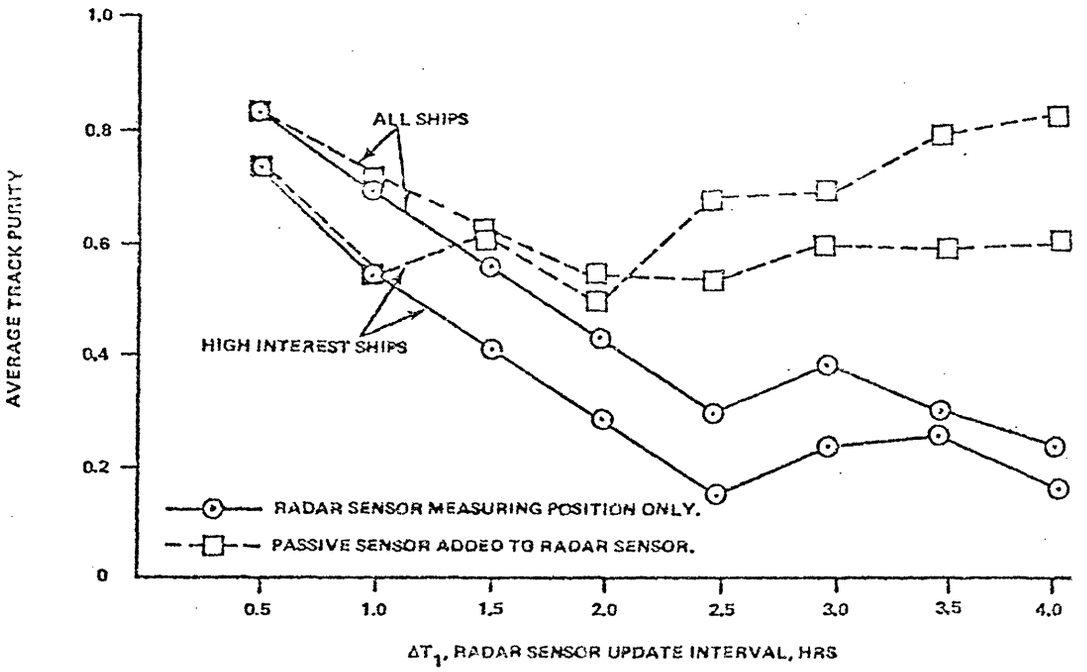

Figure 3-1 Track Purity vs Radar Sensor Update Interval

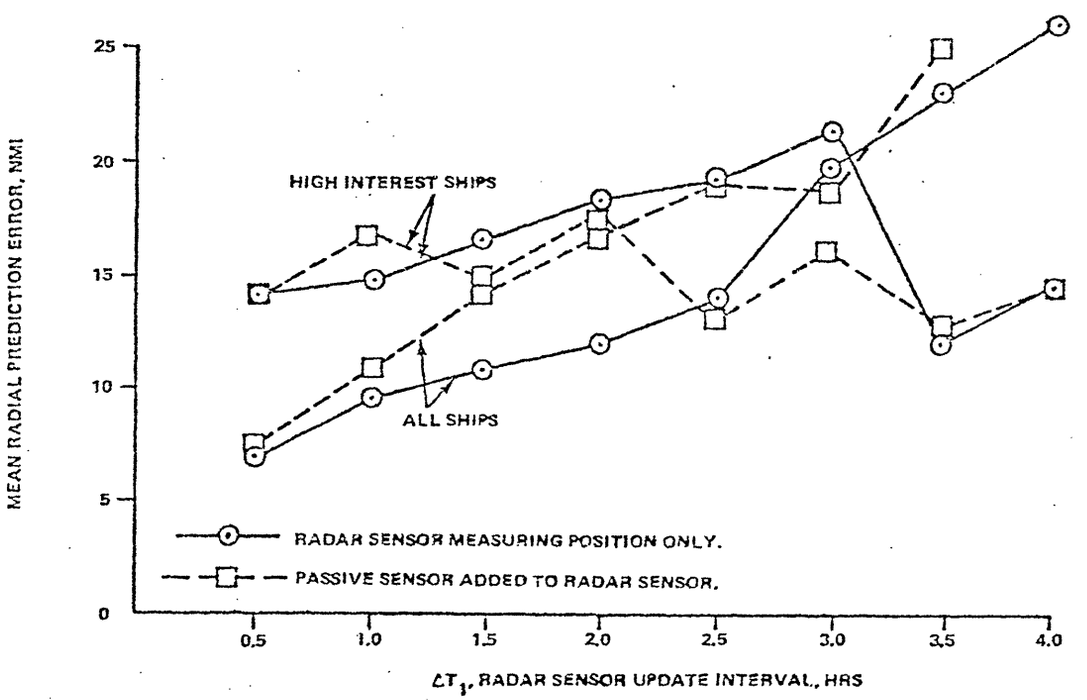

Figure 3-2 Prediction Error vs Radar Sensor Update Interval

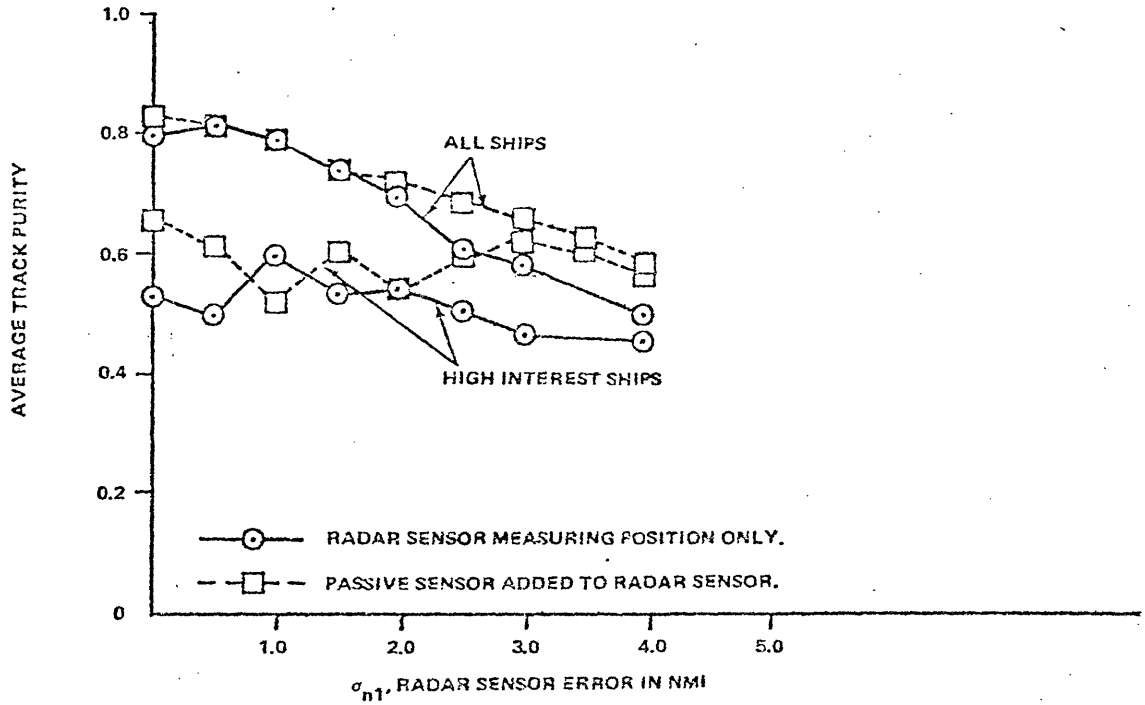

Figure 3-3 Track Purity vs Radar Sensor Accuracy

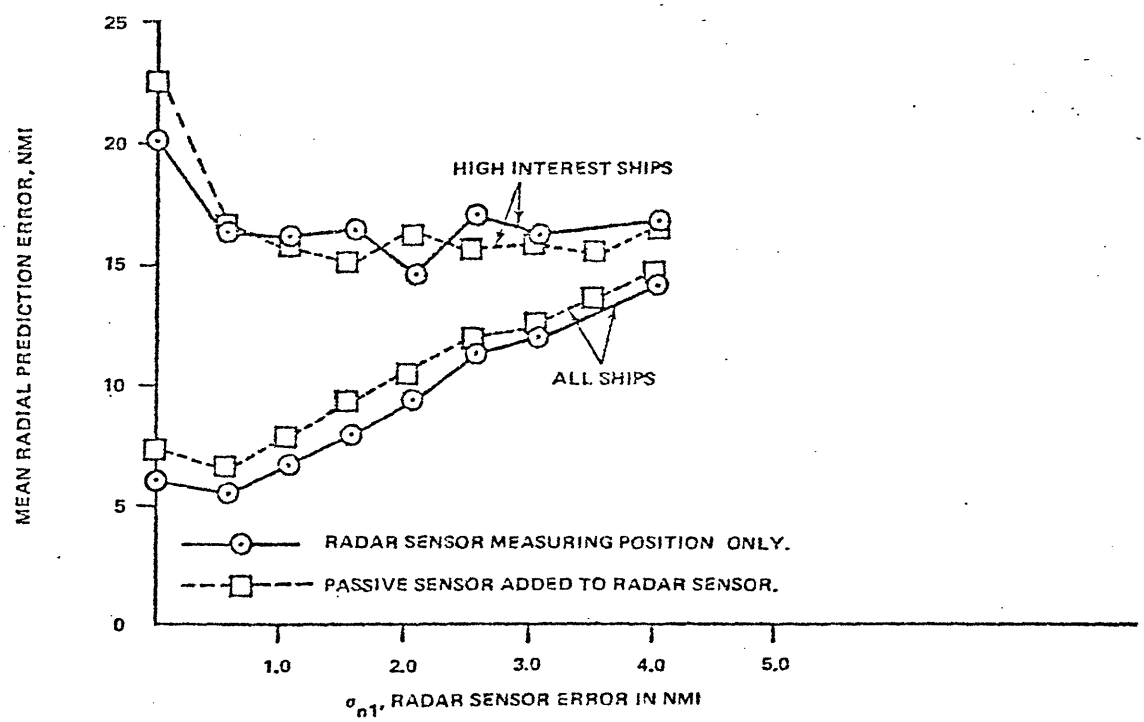

Figure 3-4 Prediction Error vs Radar Sensor Accuracy

4. CONCLUSIONS

The correlation approach used here was adequate to handle the size problem analyzed in determining ocean surveillance requirements. However, it was necessary to incorporate some threshold reduction techniques to keep the number of hypotheses from getting too large. This is done by limiting the size of the uncertainty areas. The costs incurred are more errors in correlation.

The ATAC model could be extended to include a weapon targeting model that simulates the launching of OTH weapons. It could then be used as a tool for defining and developing improvements to the information collection, processing, and distribution portions of the U.S. Navy's OTH-T capability. Previously generated requirements could also be compared with Fleet exercise data in the model.

Section 5

REFERENCES

(a) The Johns Hopkins University Applied Physics Laboratory Secret report FS-80-076, dated March 1980, "OTH/DC&T Engineering Analysis, Volume 9, System Requirements (U)."

(b) The Johns Hopkins University Applied Physics Laboratory Unclassified Report FS-79-032, dated March 1979, "OTH/DC&T Engineering Analysis, Volume 5, A Kalman Filter Rhumb-Line Ship-Tracking Algorithm," by T. G. Bugenhagen and L. B. Carpenter.

(c) The Johns Hopkins University Applied Physics Laboratory Confidential report FS-79-276, dated December 1979, "OTH/DC&T Engineering Analysis, Volume 8, Evaluation of Surface Ship Tracking Algorithms (U)," by D. E. Corman.

(d) The Johns Hopkins University Applied Physics Laboratory Unclassified report CIA 1597, dated August 1980, "Computer Programs for Area Tracking and Correlation Model."

(e) Culbertson, J. S., Unpublished notes, Preliminary Draft of Background Ship Motion Model, dated 5 July 1978.

(f) The Johns Hopkins University Applied Physics Laboratory Secret report FS-77-118, dated September 1977, "Clipper Bow for Targeting Anti-Ship Cruise Missiles (U)," by T. G. Bugenhagen, B. Bundsen, D. V. Kalbaugh, J. H. Walker, and M. B. Williams.

(g) Rice, S. O., "Mathematical Analysis of Random Noise," Bell System Technical Journal, 1945-46, Volume 23, pp. 282-332 and Volume 24, pp. 46-156.

(h) Office of the Chief of Naval Operations, Washington, D.C., B. O. Koopman, OEG Report No. 56, 1946, "Search and Screening."

AN OTH SURVEILLANCE CONCEPT

Leslie C. Kramer
Nils R. Sandell, Jr.
ALPHATECH, INC.
3 New England Executive Park
Burlington, Mass. 01803

(This work was supported by the Office of Naval Research and the Naval Ocean System Center under contract number N0001l4-80-C-0309).

Presented at the Fourth MIT/ONR Workshop on Command and Control,
San Diego, CA. June 1981.

AN OTH SURVEILLANCE CONCEPT*

by

Dr. Leslie C. Kramer
Dr. Nils R. Sandell, Jr.
ALPHATECH, INC.
3 New England Executive Park
Burlington, MA 01803

1. INTRODUCTION

In this paper, we describe a brief study into techniques for detecting and providing warning of low-altitude airborne threats approaching United States Marine Corps units in the field. Such threats are difficult to detect since they can be masked by terrain features until quite close if sensors located within or above U.S.-controlled territory are used. If sensor altitude is increased to look over terrain features, the sensor's vulnerability is increased and its deployment typically becomes quite expensive. The alternative approach, viz., deploying sensors forward into enemy-controlled territory, is promising but difficult from the viewpoints of delivery, sensor vulnerability, and information retrieval.

The purpose of the research reported here was to examine these issues in light of modern technology and its probable advancement through the late 1980s and early 1990s. Three objectives for this work were defined:

1. To identify promising sensors and sensor systems which could provide USMC forces with adequate warning of impending attack by low-flying aircraft.

2. To characterize the capabilities and the relative advantages and disadvantages of alternative concepts.

3. To interpret the results of this work in terms of its implications for future research directions.

We will show in this paper how the ground rules and scenario defined prior to beginning this work, coupled with the characteristics of the classes of sensors physically feasible, clearly lead to a preferred approach to solving the problem.

*This work was supported by the Office of Naval Research and the Naval Ocean System Center under contract number N00014-80-C-0309.

2. SYSTEM MISSION AND SCENARIO

The mission of the over-the-horizon (OTH) surveillance concept sought was to detect, to localize, to count, and to identify the threat in a timely manner. More specifically, the surveillance system should:

1. Provide 5 to 10 minutes warning of approaching threats of all types: fixed- and rotary-wing, subsonic and supersonic speeds.

2. Count threat aircraft at a coarse level, i.e., differentiate between a few (1 or 2) and many (10 to 20 or more).

3. Locate the approach sector to about 10° relative to a reference point (e.g., an antiaircraft battery).

4. Identify the threat as to aircraft type, if possible.

Specific threat aircraft were not identified, in fact, results were developed parametrically versus target speed, which was the only number of importance given the level of detail of this analysis. For the sake of evaluating particular cases when desired, the following speeds were adopted as typical and nonspecific:

- Helicopters: 130 kt = 70 m/s
- Subsonic Airplanes: 500 kt = 260 m/s = M 0.8
- Supersonic Airplanes: 975 kt = 500 m/s = M 1.5

Appropriate bands about these speeds were then considered when needed.

Friendly and hostile forces were visualized as residing on opposide sides of the forward edge of the battle area (FEBA). The friendly territory was defined to be 20 km wide and 20 km deep. The hostile territory was defined to also be 20 km deep but somewhat wider (30 km) to provide some latitude for the threat approach azimuth. We found that restricting attention to an area this size made it impossible to satisfy the warning time requirement in all situations, so again a parametric approach was adopted as we illustrate below.

3. METHODOLOGY

The purposes of this research were to quickly identify promising OTH detection concepts suitable for USMC applications and to recommend appropriate further effort. These purposes would not be served by detailed consideration of the multitude of physically realizable sensors. Rather, the approach adopted was to consider generic sensor characteristics (such as range, target handling capability, data rate, etc.) in order to determine what characteristics were required to meet the surveillance objectives defined for this study. With these characteristics identified, particular physical sensors or classes

of sensors could then be considered to determine how to best meet the mission objectives. This is not to say that existing or projected physical sensors were ignored as requirements were developed. In this regard, we are particularly indebted to individuals at ERADCOM and MERADCOM who provided valuable information regarding present surveillance concepts.

The various means shown in Table 1 for detecting aircraft were considered, and the sensors associated with these means of detection were considered from the viewpoint of the characteristics listed in Table 2. The operational environment faced by the USMC was a very important consideration at all times. The USMC mission environment cannot be overemphasized as a factor determining the types of equipment suitable for Corps use. An equally important factor is the USMC system environment; any novel system proposed must operate compatibly with other USMC assets, either existing or projected.

In the remainder of this paper, we will present selected technical results developed in the course of this investigation, and we will describe the surveillance concept recommended for further consideration. Additional detail may be found in reference [1].

4. DETECTION AND WARNING TIME

In order to minimize the delay between the time when the threat enters the surveillance system coverage and actual provision of warning to a decision-maker capable of responding, one must understand the source of the delays. Figure 1 illustrates the situation. The warning time is determined by the time it takes the threat to fly from where it is when you find out about it to where you are (line segment B in the figure). The time lost, so to speak, is the time that elapses from the instant the target emits an observable within surveillance range to the time when you are notified (line segment A). The components of this delay (i.e., the lost time) are observable propagation time and the time needed for signal processing, data processing, data intrepretation, and data dissemination. We are interested in determining when various constituents of this delay are dominant.

For electromagnetic observables, the propagation time is essentially zero; the observable travels at 3×10^8 m/s. For seismic and acoustic observables, the speed is much slower: 1,000 to 2,000 m/s for seismic (under certain conditions, seismic signals can propagate as slowly as 200 m/s) or 300 to 350 m/s for acoustic. If one considers a typical maximum range for acousto-seismic sensors, say 10 km, then the observable propagation time could be as long as 5 to 30 seconds. While appreciable, this is a relatively small part of the minimum warning time requirement.

How long should the data handling take? Electronic signal and data processing should (with advanced technology) only require a small fraction of the 5- to 10-minute warning desired. We conclude that only one situation arises in which the warning differs significantly from the threat travel time from entry point into the surveillance coverage to the defended location: the situation in which human data handling is carried out in a system employing

TABLE 1. WAYS TO DETECT AIRCRAFT

Electromagnetic

- Radar (any wavelength)
- Self-emitted thermal (IR, mmW?)
- EM emissions intercept
  - Communications
  - Engine/Equipment Noise
- Reflected visible (sun, moon, stars)
- Intercepted Background ("holes")
- Magnetic

Mechanical

- Acoustic
- Seismic

TABLE 2. SENSOR CHARACTERISTICS

Functional

- Range
- Signal Propagation Time
- Target Handling Capability
- Resolution (various "dimensions")
- Accuracy
- Communications Requirements
- Processing Requirements
- Vulnerabilities (jamming, noise, decoys, blind zones, attack ("ARM"))
- Signal Path Propagation Character

Physical/Operational

- Size, Weight, Power Requirements
- Lifetime (shelf, use)
- Deployability (range, spped, accuracy)
- Mobility
- Ruggedness
- Cost (expendable?)
- Compatibility with Other Systems

long-range acoustic sensors. Thus, we prefer completely automatic data handling and deployment of acoustic sensors (if used) close to the anticipated threat.

The threat time-of-flight (TOF) is simply related to its speed as shown in Figure 2. The solid lines indicate the threat speed (plotted along the ordinate) which results in a 5-, 10-, or 20-minute transit time for a given range (plotted along the abscissa). Below each solid line is a dotted line indicating the corresponding speed if a 100-second delay is introduced into the acquisition cycle. Higher speeds mean shorter warning, of course. One sees at once that for 5 to 10 minutes of warning, high-speed threats must be detected well before they enter the 20- to 40-km deep region of interest described in Section 2. Only helicopters can be detected in time within this region. The implication is that either forward sensor deployment, long sensor range (as much as 100 to 200 km in some cases), or both is necessary to adequately warn of high-speed threats.

5. RESOLUTION AND ACCURACY

Spatial resolution refers to the sensor system's ability to determine that two objects located close together are in fact distinct. Accuracy refers to the system's ability to locate a single object along various measurement "directions" with small error. We quote the word "directions" here because we mean to consider measurements such as angle or range rate as well as up, down, left, or right.

Resolution and accuracy are typically related since if an object can be described as occupying a given resolution cell, that is, a box in measurement space of size such that objects outside it can be distinguished from the one inside, the object's position is known to the cell size at worst. In many practical situations, the error will actually be a small fraction of the resolution cell size. For example, radar accuracy in range, angle, or doppler (i.e., range rate) is frequently described by an equation of the form

$$\sigma = K \frac{\Delta}{\sqrt{SNR}} \qquad (1)$$

where σ is the error (the standard deviation of the random process representing the measurement), Δ is the resolution, K is a factor near unity, and SNR represents the signal-to-noise ratio [2]. Thus, for SNR equal to 10 to 100 (10 to 20 decibels), which represents typical "fair" to "good" measurements, the error σ will be on the order of 1/3 to 1/10 of the resolution Δ. Much finer range, angle, or doppler "splitting" is physically feasible at even higher values of SNR.

We wish to consider whether resolution or accuracy is the driving design consideration for the systems and mission under study. We will show that in general, a sensor with adequate resolution to allow coarse threat counting

will automatically have adequate accuracy to define the threat's position and heading as required. This conclusion follows from an assumption that the surveillance system would be adequately able to count the threat if it could resolve aircraft separated by 100 m or so. This would also permit the system to adequately judge the size of a formation in the event that many aircraft were flying together with less than 100 m separating adjacent ones. We will consider below the implications of this assumption.

The requirement that the threat be located to within a 10° sector can be interpreted several ways. In the previous section, we showed that the threat must be detected several tens of kilometers from its target if adequate warning is to be provided; a 10° sector will be many kilometers wide at these detection ranges. Thus, if the sensor system has spatial resolution on the order of hundreds of meters, it will certainly be capable of localizing the threat to within a 10° sector.

An alternative interpretation of the 10° requirement, based on threat velocity, is that the system be able to determine the threat's heading to 10°. A simplified means of analyzing this question is indicated in Figure 3. The analysis is based upon assuming that the system computes velocity from finite differences of position. A realistic system would use a more sophisticated approach, thus the results we derive below are conservative: they upper bound the likely course direction estimation error.

Suppose position measurements are made of the threat at two locations separated by a distance d as shown in Figure 3. Then the (straight-line) course of the threat must pass through the two error volumes centered at the position measurements as the figure indicates. The angular error in the course direction can be related to the position measurement error in the cross-range direction as shown in the graph, which is a plot of the equation

$$y = 2 \cdot \frac{d}{2} \cdot \tan\left(\frac{\theta}{2}\right) \simeq \frac{1}{2}\, d\theta \qquad (2)$$

where y is the cross-range error and $\theta/2$ is the cone half-angle. The approximation $\tan(\theta/2) \simeq \theta/2$ is good to 1 percent for θ less than 20°. One can see that if the threat is observed over a range band of 1 to 5 km (i.e., d = 1 to 5 km) a cross-range error of about 90 to 450 m is adequate. If cross-range resolution is on the order of 100 m to permit threat counting as suggested earlier, the cross-range error will typically be on the order of 10 m (one-tenth the resolution) as we indicated earlier. Thus we again conclude that resolution adequate for counting the threat will automatically result in accuracy adequate for determining its angular sector.

Having concluded that requiring 100-m spatial resolution will result in both adequate resolution and adequate accuracy, we consider the implications of requiring resolution on this order. We will focus on determining the angle resolution provided by typical sensors of different types in order to identify those approches which appear to match the needs of an OTH surveillance system. Attention will be restricted to angle resolution because range resolution of

the order required is generally easy to obtain from a technical viewpoint if sensors are used which provide range resolution at all (i.e., active radar). Note, however, that we have not concluded that range resolution is essential.

The angle resolution Δ associated with a physical sensor having aperture dimension s and operating at a wavelength λ is generally given by an equation of the form

$$\Delta = K \frac{\lambda}{s} \tag{3}$$

where the angle Δ is measured in radians, λ and s are measured in common units, and K is a factor near unity which depends on several considerations, for example, the aperture shape. By solving this equation for s as a function of λ and Δ, taking K = 1, and combining with the equation

$$y \cong R\Delta \tag{4}$$

to obtain the cross-range resolution in meters (y) in terms of the angular resolution in radians (Δ) at range R expressed in meters, one can develop Figure 4. Here curves of constant cross-range resolution are shown in the plane described by range-to-target along the abscissa and aperture size along the ordinate. Several ordinate scales are shown, corresponding to several typical sensor wavelengths: IR (10 microns), millimeter wave radar (λ = 3mm, corresponding to 100 GHz frequency), microwave radar (λ = 10 cm, corresponding to 3 GHz or S-Band), and an acoustic sensor operating at 100 Hz. If typical operating ranges for various sensors are selected as well as typical aperture sizes, one sees that the cross-range resolution requirement of about 100 m is met for alternative sensors as shown in the figure.

6. SENSOR TYPES AND CHARACTERISTICS

In this section we discuss general characteristics of several sensor classes as applied to the OTH surveillance mission. In many cases, we make assertions about sensors which we do not support by detailed calculations or references yet which may be controversial if taken out of context (e.g., "long-range radars tend to be expensive"). We believe that within the context of the discussion our assertions are reasonable, and that taken overall our ultimate recommendations given below are justified.

RADAR

Radar sensors generally provide excellent quality data at a relatively high "generalized cost." By this we mean that radars can provide functional characteristics of the type listed at the top of Table 2 at a level that far exceeds the requirements of the mission defined in Section 2, but that several disadvantages accrue relative to some of their physical and operational characteristics as listed at the bottom of the table.

Radars can be built using modern technology that have long range and fine resolution. Accuracy can be quite high. Many targets can be processed simultaneously. Signal processing technology is well understood and reasonably easy to implement. The physics of radar signal propagation are well understood and system performance can be predicted with some confidence. These characteristics imply that radars are excellent sensors for some applications. We argue, however, that they are not very well matched to the low-altitude aircraft detection mission. Several factors lead to this assertion.

First, radars are vulnerable to countermeasures because they are active: they broadcast in order to receive. This makes radars vulnerable to anti-radiation missiles which home on their emissions. Also, adaptive jammers can be built which listen to radar emissions and adjust their interference output for maximal effect. By use of sophisticated signals and the associated signal processing technology, these vulnerabilities can be minimized. Such measures increase the cost of the radar, however.

Second, the apparent long range available with radar sensors is illusory for this mission due to the effect of terrain masking. Low altitude air threats will be hidden from view by hills if the radar is at low altitude over friendly territory. If it is at high altitude or deployed forward over enemy territory, vulnerability to attack is increased and deployment cost is increased as well.

The third and final factor to consider is that radars tend to be expensive in general terms. If only a few are deployed to fulfill a mission, they must have long range (and thus large power-aperature product) for broad coverage. Also, an ability to handle many targets is needed. If many short-range sensors are deployed to fulfill a mission, the number required will result in a large total cost even if unit cost is modest.

PASSIVE OPTICS

The obvious advantages of passive optical sensors are that they can be quite small and light physically and that they can provide very high quality data (in the sense of fine spatial resolution). Their small size and weight make them well suited to applications requiring high mobility, however they require careful design if they are to be rugged and reliable. Their primary disadvantage is relatively short range in bad weather or when faced with optical countermeasures such as smoke. Also, search is difficult due to their typically narrow field of view.

We examined optical sensors (both active and passive) at some length during this study, primarily from the viewpoint of sensitivity calculations. The goal was to determine the current state-of-the-art; the details are collected in [1]. While we are able to make first-order judgments regarding the range reasonably expected under various circumstances, we could not develop definitive results without a more detailed threat signature characterization than that available to us. Our results are therefore largely parametric, as shown in Figure 5. Here we plot the noise-equivalent temperature difference (NETD) at various ranges for a typical passive IR sensor with various values of atmospheric attenuation. The NETD indicates the temperature

difference between object and scenic background which results in a signal just at the noise level; for a signal-to-noise ratio of x, the object-minus-background temperature difference must be x times NETD. The sensor parameters are given in [1]. They are not meant to represent any particular current sensor; they are, however, typical. We assume a sensor operating in the 8 to 14 micron waveband with a 300°K background. The figure shows that an operating range of up to 5 km or so is reasonable to expect for these sensors.

ACOUSTO-SEISMIC SENSORS

Acousto-seismic sensors were discussed extensively with individuals at Lincoln Laboratory, ERADCOM, and MERADCOM. We found that the potential disadvantages of acousto-seismic surveillance are limited range, a poorly understood signal environment, and an immature system technology. The consensus we observed was that the technology of acousto-seismic (i.e., mechanical-wave or MW) sensors and sensor systems is in its early stages of development but that this technology is very promising. The real thrust of the research in the MW arena is the analysis of system questions rather than transducer questions. Very sensitive microphones and seismic transducers are already available; the real issue is how to process the resulting signals and data in order to associate the measurements with particular physical emitters in a multitarget environment and to extract the information about them which is desired.

The range expected of MW sensors is not yet clear. Several individuals interviewed quoted maximum ranges of 10 km or so for both acoustic and seismic detection of single aircraft under quiet, well-understood measurement conditions. Under realistic battle conditions, one would expect the operating range of MW sensors to be shorter. On the other hand, their cost may be low enough and their size and weight may be low enough that large numbers could be delivered to cover the required surveillance zone, even with maximum range of 5 km or so. A more serious question surrounds the utilization of MW sensors in a complicated, noisy battle environment. This environment requires very sophisticated signal and data processing and interpretation. Compounding this problem is the fact that the signal propagation physics for MW sensors is not well understood (compared, for example, with electromagnetic signals) so that the "known" signal being sought in the noise is not very well known at all.

In contrast to the disadvantages faced today by MW surveillance systems, there is a potentially huge payoff in mission utility if the problems are successfully resolved. The components can be small and inexpensive. They can be put where needed by several means. Their capabilities (e.g., in terms of spatial resolution) are well matched to the requirements for this mission, and their physical characteristics (e.g., size, weight, ruggedness) are well matched to the needs of a highly mobile USMC force. For these reasons, we recommend a more extensive investigation to define a system using MW sensors as the primary threat detection mechanism and to identify and catalog the issues associated with it.

7. CONCLUSIONS AND RECOMMENDATIONS

As a result of our studies, we recommend that an OTH surveillance approach encompassing two classes of sensors be considered: numerous hearing-like sensors ("ears") for fulfilling functions requiring only coarse spatial resolution coupled with a much small number of vision-like sensors ("eyes") which would carry out tasks requiring high resolution. Our immediate recommendation is that this concept, which we describe more fully below, be defined in sufficient detail that the USMC can make a well-informed judgment as to whether or not to develop some or all of it.

The concept we propose is described as follows: We envision the ears to be acousto-seismic sensors deployed beyond the FEBA. These would be delivered by artillery, by remotely piloted vehicles (RPVs), or by manned aircraft.* In the last case, sensor delivery would be a new task assigned to existing air assets; no new aircraft can be dedicated to this task, and in fact, a delivery mechanism which does not interfere with existing tasks would be required. The information collected by these sensors would be relayed back to the USMC C^3 system via smart repeaters: repeaters with a certain amount of internal data processing capability. These would reside on both sides of the FEBA as required.

The eyes would be RPV-borne infrared (IR) sensors. (Millimeter-wave radar sensors are a possible alternative.) For most situations, these sensors would have to be on station when required; the time-to-station is typically excessive if one contemplates launching these vehicles on demand. Often, a logical location for prestationing such sensors is obvious, e.g., near an enemy airfield or along an important approach route.

In operation, the system we propose would behave much as a human does: the ears cue the eyes. One hears a noise, which results in a head turn to identify the cause in the event that further data is needed.

An important aspect of the two-sensor-class system we envision is a nonheirarchic, distributed information processing and dissemination mechanism. Such a mechanism is shown pictorially in Figure 6. The architecture depicted allows data fusion (i.e., the combination and interpretation of data from several sensors or transducers) at several levels, with the concomitant feature that information can be identified and routed to relevant users as soon as it is derived from data, thereby circumventing further delays in the system.

We believe that this system structure offers several advantages. It is clear, for example, that the USMC contains a heirarchy of decisionmakers whose information needs vary over a wide span. The individual in charge of a single antiaircraft battery is concerned with a much smaller part of the threat than the officer responsible for the entire task force. A surveillance system which can simultaneously fill the needs of decisionmakers at each end of this spectrum obviously offers distinct advantages. Benefits accrue in terms of reduced reaction time, for example, if warning information can be provided to the force capable of responding to it without passing through

*In an advanced scenario, battlefield robots could be used for sensor emplacement.

intermediate stages of handling while simultaneously presenting higher level echelons of command with suitably condensed or abstracted reports of the threat and the reaction to it. The architecture we suggest can accomplish this. Developing in detail the means to accomplish it, both from a hardware and a software viewpoint, is a present focus of C^3 research.

A major advantage of the concept we propose is that it is a natural extension of the already existing Remote Battlefield Sensor System (REMBASS) which is being readied for deployment by the U.S. Army and the USMC in the early 1980s [3]. The approach to aircraft detection we propose would add new elements to the mission for which REMBASS is designed, however we believe that many aspects of the research and development which have gone into REMBASS and its predecessor systems bear on the OTH aircraft detection problem.

The surveillance concept description just presented is obviously quite sketchy. We believe the concept is sound. Nevertheless, many issues come to mind immediately. We recommend that these issues be addressed in subsequent work. Among these issues are questions related to utility, operations, phenomenology, and architecture.

By utilitarian issues, we mean to ask: does the system tell you what you want to know, when and where you want to know it. To resolve this, further work needs to be done to define the threat and to determine precisely what information is needed by different USMC decisionmakers.

By operational issues, we mean to ask: what sort of components make sense from a USMC operational viewpoint, particularly with regard to sensor delivery, to system mobility, and to interface with the existing and planned USMC C^3 network.

By phenomenological issues, we mean to ask: What do the targets of interest look like and sound like to the sensors we propose. Some data was examined in the course of this research. It appears that, for example, acousto-seismic data has very high potential for providing target identification, however a great deal of processing is required to extract the information. Defining this information extraction process is a major focus of several research projects. Many system issues (as compared to one-target, one-sensor issues) such as data association among targets and measurement correlation among transducers remain to be resolved.

By architectural issues, we mean to ask: how should the information processing be distributed. What sorts of "computers" are required at what physical and functional locations within the system? Is packet radio the proper technology for information retrieval?

The issues described above are relevant to USMC surveillance system research and development in general as well as to any future consideration of the particular surveillance concept we suggest. Whether or not our concept is pursued further, these questions should continue to be addressed in fundamental terms. We stress in particular the importance of further research into acousto-seismic approaches to surveillance. This technology is poorly understood at present from the system viewpoint, as we have said, yet it offers great potential for fulfilling a critical need for our military forces.

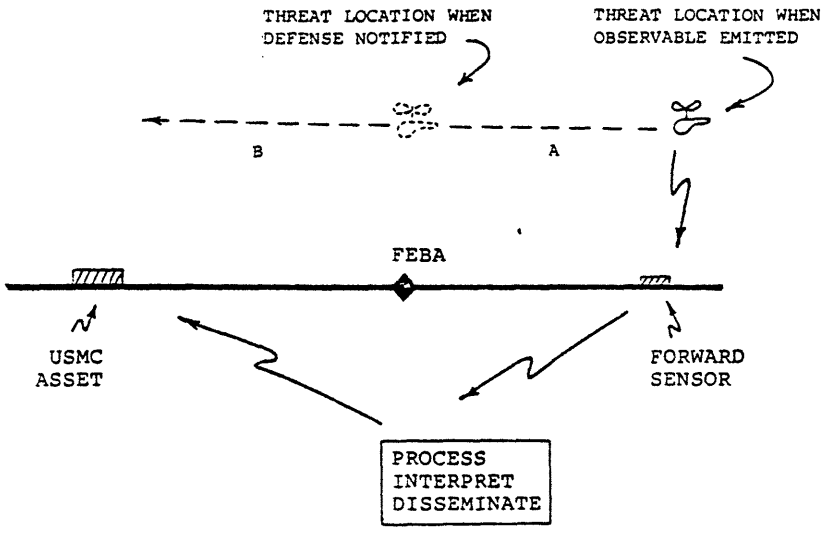

Figure 1. Determinants of Warning Time.

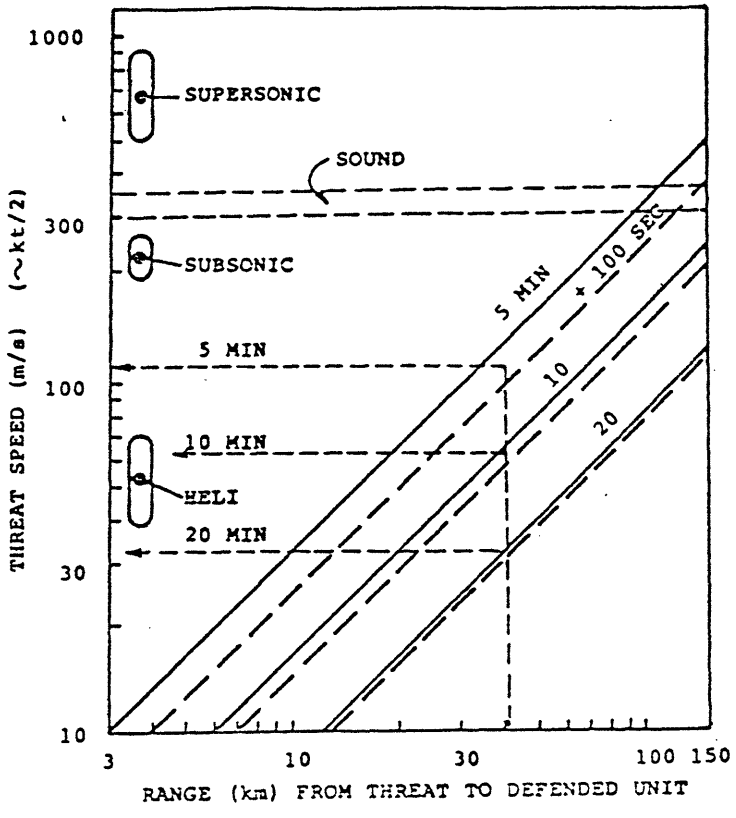

Figure 2. Maximum Warning Time Equals Threat Flight Time.

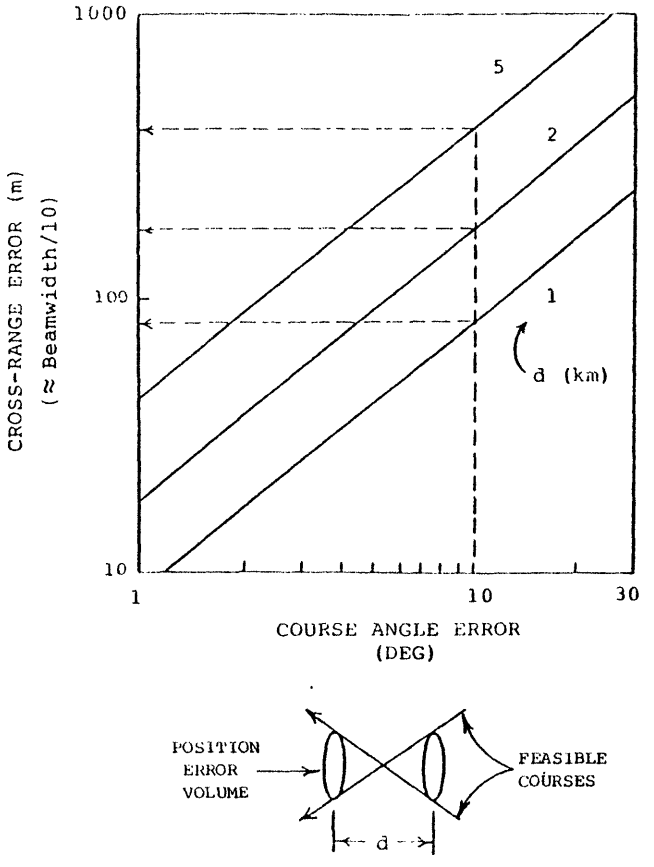

Figure 3. Cross-Range Error Allowable for Course Determination.

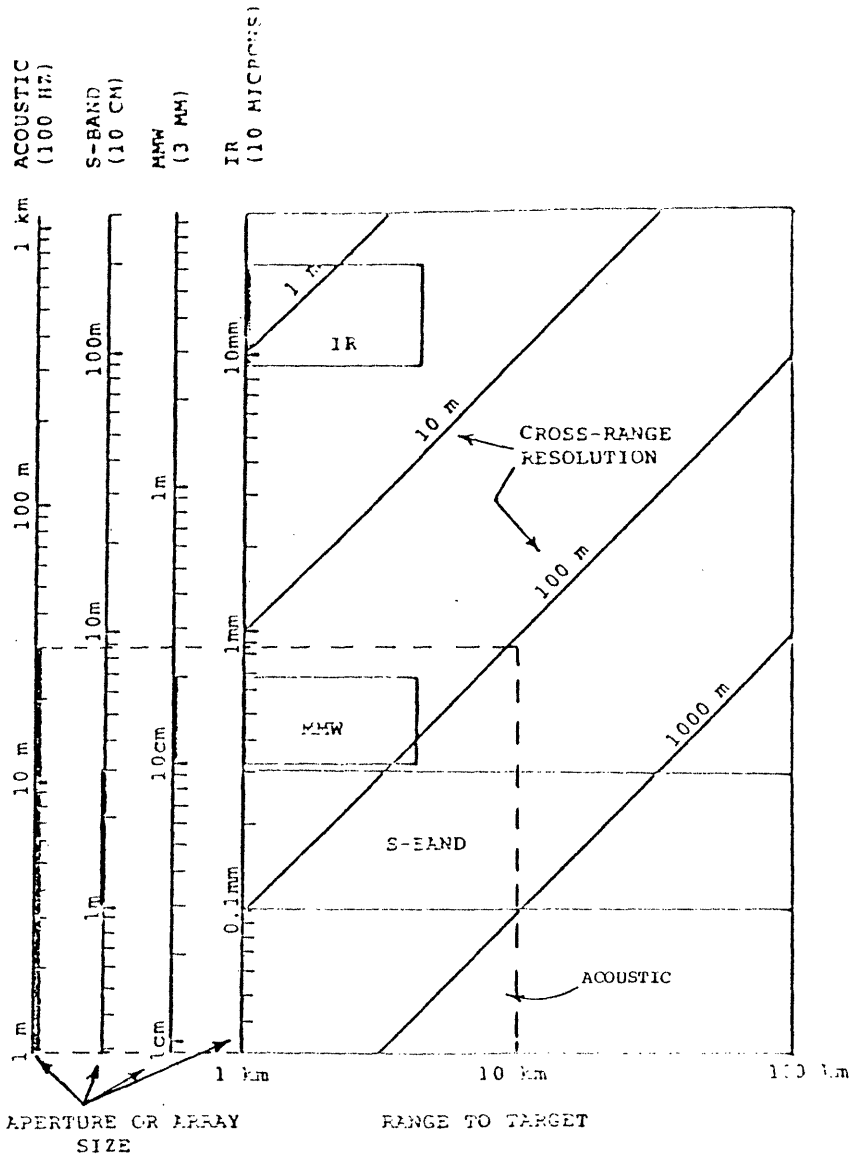

Figure 4. Resolution Versus Range and Aperture.

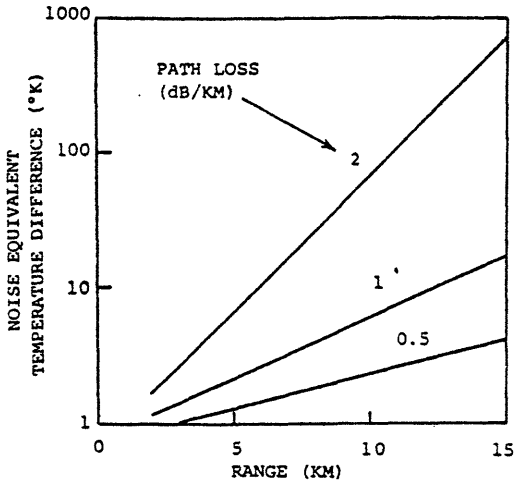

Figure 5. Passive IR.

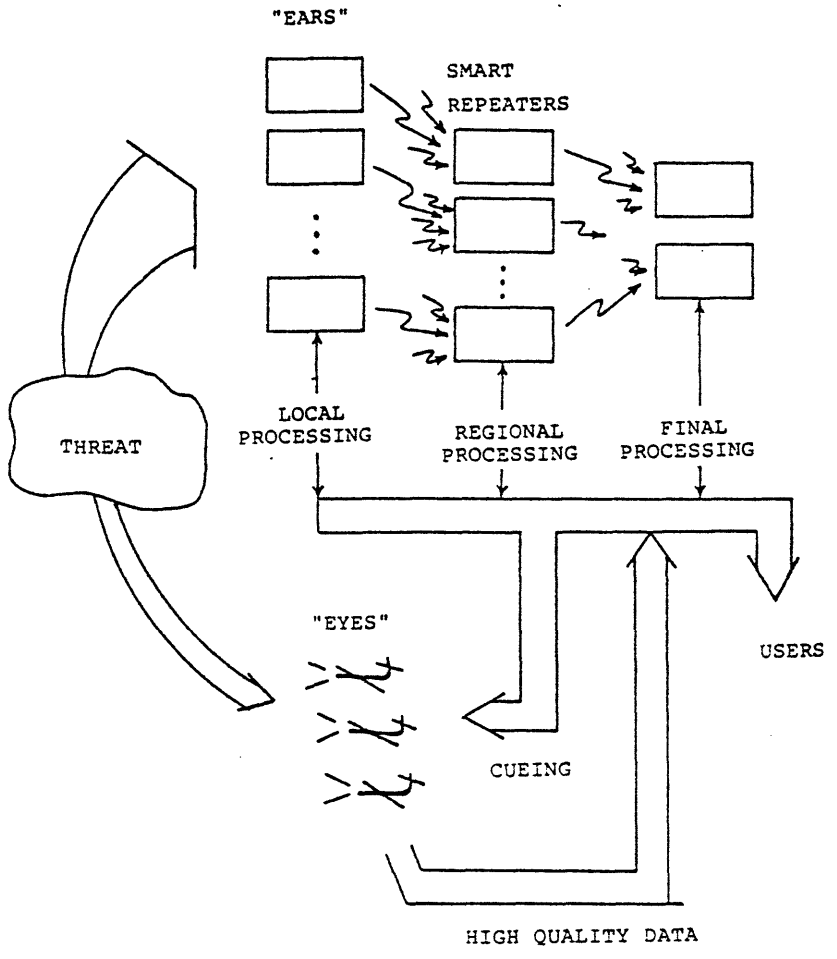

Figure 6. A System Architecture.

REFERENCES

1. Kramer, L.C. and N.R. Sandell, Jr., "Over-the-Horizon Detection Concepts," Technical Report TR-112, ALPHATECH, Inc., Burlington, MA., Dec. 15, 1980.

2. Skolnik, M.I., ed., Radar Handbook, McGraw-Hill, New York, 1980.

3. Sundaram, G.S., "REMBASS: The Army's New Battlefield Sensor System," International Defense Review, 4, 1980.

APPLICATION OF A. I. METHODOLOGIES TO OCEAN SURVEILLANCE PROBLEM

Leonard S. Gross
Michael S. Murphy
Charles L. Morefield

VERAC, INC.
10975 Torreyana Road
Suite 300
San Diego, CA 92121

APPLICATION OF A.I. METHODOLOGIES TO OCEAN SURVEILLANCE PROBLEM

Dr. Leonard S. Gross
Dr. Michael S. Murphy
Dr. Charles L. Morefield

VERAC, Incorporated

ABSTRACT

This paper will describe a data fusion system which combines artificial intelligence metnods with formal Bayesian techniques. Traditional approaches to the multisensor, multitarget ocean surveillance tracking problem have produced only limited success. Computational limitations, lack of flexibility and responsiveness, limited user understanding of program processing, and the inability of an analyst to guide the system are typical shortcomings of these systems. Previous applications of A.I. have approached some of these difficulties by use of "expert system" technology. In these cases, correlation is invariably based on simple mathematics or heuristics which generally do not take full advantage of the significant body of formal mathematical techniques available in the area of decision theory.

In principle, these mathematical techniques provide a firm basis for forming correlation decisions in a multisensor, multitarget situation. In practice, however, the ocean surveillance environment is such that important parameters required for the Bayesian methodology vary widely with sensor mix or surveillance scenario in a manner that is often poorly understood or even totally unknown. Thus, dependance on such techniques alone often results in an inflexible system which is unresponsive to the realities of an ocean surveillance problem.

For this reason, the approach we have taken in this work is to overlay an A.I.-based control structure on a set of Bayesian theoretic functional elements. In this way we hope to successfully tune the individual Bayesian techniques to the changing surveillance situation and to manage the ambiguities that necessarily arise when analytical decision procedures are applied to a real surveillance problem.

In particular, our research has identified several A.I. constructs which, when combined with Bayesian decision methods, can result in improved data fusion system capabilities. These constructs include the following:

1) A functional organization such as that found in A.I. systems like the Hearsay II speech understanding program can make the system both understandable to the analyst and highly flexible. This flexibility is most evident in the system's ability to incorporate diverse expert knowledge, encompassing

both quantitative and heuristic information, over a range of timelines, specific to an variety of sensors or scenarios, and responsive to a high degree to analyst review and editing requirements.

2) Production rule techniques are useful in dealing with the fuzzy control rules necessitated by the sensor mix and target scenarios inherent in the ocean surveillance environment. These techniques permit easy specification, review and modification of the rules that guide the Bayesian processing and tune it for operation over a spectrum of situations, ranging from the well-known and usual to the poorly understood and unexpected.

3) Search techniques developed in speech understanding and game theory are useful in guiding the generation, evaluation and selection criteria for investigating competing surveillance hypotheses. The diversity of search strategies embodied in these techniques permits flexible management of ambiguities in the various plausible surveillance pictures, and provides a mechanism for tuning the search tactics to those specific scenarios where they are most efficient.

The system we have developed to exploit these techniques is illustrated in the figure. We have termed the system the Intelligent Correlation Agent (INCA), and have derived its architecture from that of the HEARSAY II software system. In this design, development of a surveillance product is accomplished by a cooperating set of Knowledge Sources (KS) consisting of production rules and procedural code. These KS's communicate via a global data structure called a blackboard. There are essentially three tiers of knowledge sources. The lowest level "atomic" are concerned with detailed mathematical or symbolic correlation processes such as track scoring or filtering. The next level performs an observation/evaluation of the correlation modules to determine their success is propagating data up the blackboard data structure. Finally a control tier, using the conclusions of evaluation modules and the entire blackboard (if necessary), can make global decisions on system operation so that the user inputted goal state is most quickly achieved. Goal satisfaction occurs in either a forward or backward chaining mode.

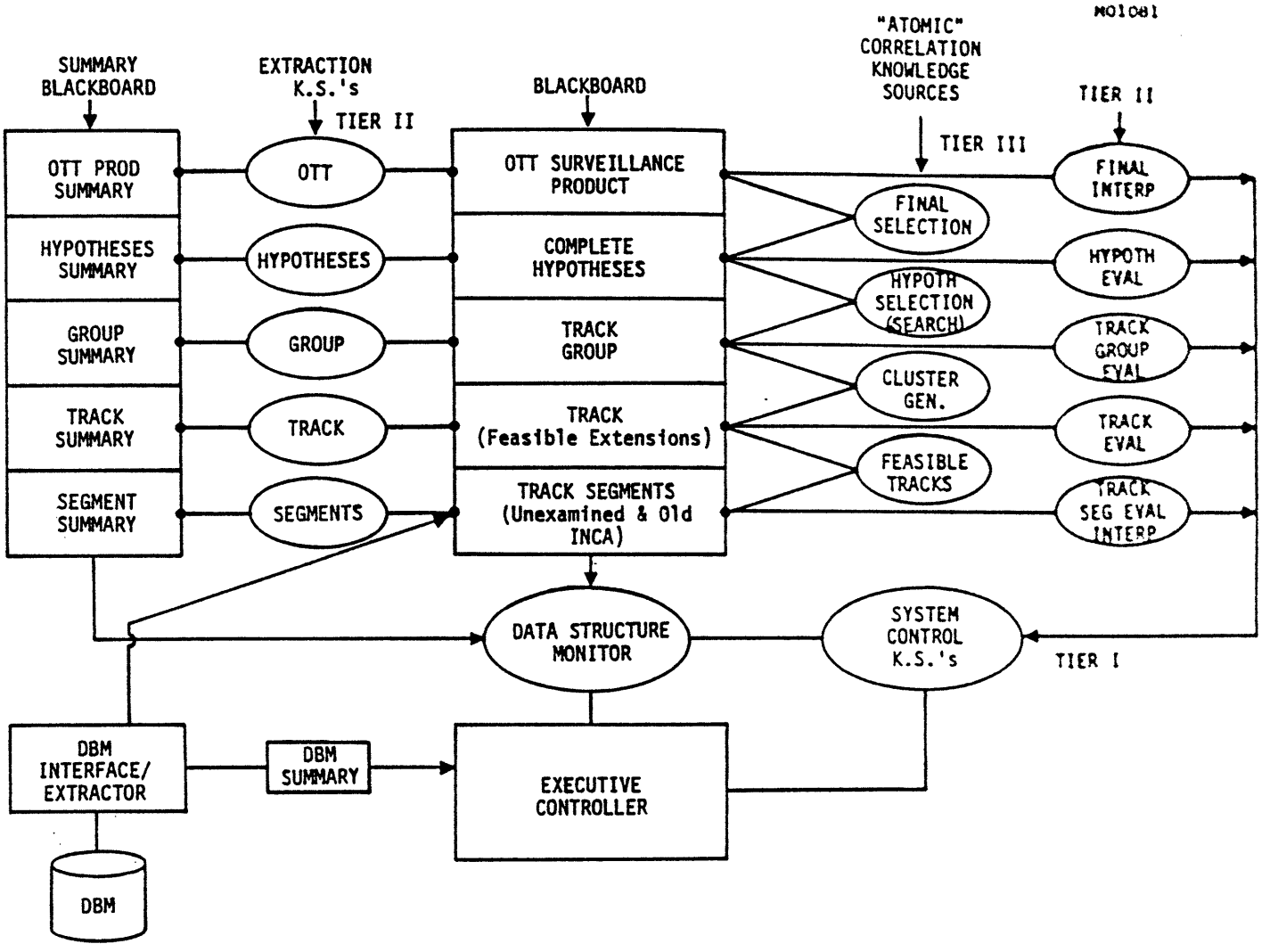

INCA System Structure

REFERENCES

(1) Pattern Directed Inference Systems, Waterman and Hayes-Roth, ed., Academic Press, 1978.

(2) Organization of the Hearsay II Speech Understanding System, Lesser, et.a., IEEE Transactions on Acoustics, Speech and Signal Processing, Vol. ASSP-23, Number 1, February 1975.

(3) Increasing Tree Search Efficiency for Constant Satisfaction Problems, Haralic and Elliot, Artificial Intelligence 14, (1980), pp. 263-313.

(4) A Parallel Tree Search Method, Nakagawa and Saka, IJCAI 1979, pp. 628.

(5) Application of A.I. Methods to Surveillance Data Fusion (U), Final Report(S), VERAC document control number 81:S-0037, Gross, Morefield, and Murphy.

A PLATFORM-TRACK ASSOCIATION PRODUCTION SUBSYSTEM

Robin Dillard
NAVAL OCEAN SYSTEMS CENTER
San Diego, California

A PLATFORM-TRACK ASSOCIATION PRODUCTION SUBSYSTEM

Robin A Dillard
Naval Ocean Systems Center

INTRODUCTION

This paper describes a method of extending the capability of a production system applied to Tactical Situation Assessment (TSA) by adding a "package" of system-logic rules. (A "production" is an if-then-rule implemented in a "production system," a system also having a data base and a number of control mechanisms.) The implementation of these rules within such a production system was termed a Platform-Track Association Production Subsystem (PTAPS) [1]. The function of PTAPS is to perform much of the logical reasoning such as process-of-elimination reasoning, needed to match tracks to specific platforms.

Proof-of-concept experiments with PTAPS rules were conducted in a modified version of STAMMER, a System for Tactical Assessment of Multisource Messages, Even Radar [2], [3]. STAMMER was developed to serve as a demonstration of the applicability of rule-based inference techniques to the TSA problem. A small, fast skeleton version of STAMMER was created for PTAPS experiments by stripping the original of its confidence mechanisms, explanation functions, and graphics interface. The experiments involed two basic scenarios: one concerned with the identification of submarines, and the other with the identification of members of a Soviet task group with the help of satellite reconnaissance data. The submarine scenario was later successfully run in STAMMER2 [4] and in Rosie-1, the first version of Rosie (A Rule-Oriented System for Implementing Expertise) implemented by The Rand Corporation [5]. It was concluded from these experiments with different production system structures that PTAPS rules should work in any system in which conventional TSA rules will work [6]. Since then, many of the rules were implemented in the second version of Rosie, under development by the Rand Corporation.

This effort has been just one phase of a larger research effort to develop automated data-fusion techniques using artificial intelligence tools. The work has been performed at NOSC under the Command Control & Communications Systems Theory project, sponsored by NAVELEX Code 613.

PTAPS OVERVIEW

Many of the PTAPS rules have the sole function of building into the data base an "intermediate framework" of membership files which permit, via other rules, chains of reasoning not otherwise possible. This framework includes many kinds of "track files" and "platform files." To become a member of some track file or platform file, a track or platform must satisfy the conditions of a certain membership rule, and a member is removed by another rule when the original conditions are no longer all satisified. (The term "member" has a special meaning in Rosie, so the concept of listing an element in a file was substituted for membership.) Of particular importance are "OR-files." The members of the OR-file of a platform are those tracks which have not been ruled out as the track of that platform. A platform is a member of a track's OR-file if that track has not been ruled out as a track of that platform. The platform-OR-file of an emission has, as members, platforms which have not been ruled out as the emitting platform.

It is assumed that no active track entered into the PTAPS data base is a false track, eg the result of a radar's false alarm. Also, no two active tracks can be the track of a single platform. The amount of time after contact is lost that must elapse before an active track is made an inactive track should depend on the situation and be specified by rules.

A track file is "complete" if the system holds an active track for every platform in that region (of that category, type, or class, if a subset file), even if none is identified. As a result of high-altitude surveillance, for example, the surface track file of a region may temporarily be complete. A platform file is complete if every platform in that region (of that category, type, or class, if a subset file) is a member of the file. Note that members of a complete platform file need not actually be in the region. Most platform files will be complete if the region is enclosed (eg the Persian Gulf, Red Sea, Mediterranean Sea) and the entrance/exit areas are continually monitored.

Another concept used in combination with file completeness is that of correspondence between platform files and track files. For example, the track file containing tracks of surface platforms has as its corresponding file the platform file of surface platforms thought to be in the region. A typical rule involving these concepts is: The OR-file of a track is complete if the track is a member of a track-file whose corresponding platform-file is complete. The OR-file of a surface track is complete, for example, if the file of surface platforms possibly in the region is complete. Examples of other rules are given below.

- If the OR-file of track t is complete and its only member is platform p, then t is the track of p.
- If t is the track of p, and track t' is not t, then t' is an impossible-track of p.
- If t' is an impossible-track of p, then remove p from the OR-file of t' and remove t' from the OR-file of p.

These rules are written in widely different forms for the different production systems in which they have been implemented. The last rule above is implemented in STAMMER2 as follows.

```
ORFILEREDUC
(CONDITIONS
 ((MEMBER RPF  *P)
  (ORFILE   *P *ORF)
  (MEMBER  *ORF *TR)
  (IMPOSTRACK *P *TR)
  (ORFILE *TR  *FRO))

ACTIONS
((MEMBER  *ORF  *TR)
 (MEMBER *FRO  *P))
```

CONF -1.0 PRINFORM
"A track and a platform are removed from each others' OR-files if the track is found to be an impossible-track of that platform.")

The same rule is implemented in Rosie in this English-like form:

For each platform,
for each track such that the OR-file of that platform does list that track,
if that track is an impossible-track of that platform,
deny the OR-file of that platform does list that track and the OR-file
of that track does list that platform
and send (return,
that track, "and", that platform, "have been deleted from each other's",
"OR-files because", that track, "was found to be an impossible-track", "of", that platform, ".",
return).

Examples of rules involving emissions are the following.

- For each platform p possibly in the region of an emission, if platforms of p's class or type carry the emitter type, then p is a member of the platform-OR-file of that emission
- [completeness rule and various removal rules]
- If the platform-OR-file of an emission is complete and has only one member, then that platform is the emitting-platform of that emission.
- If platform p is the emitting-platform of an emission and track t is inconsistent in bearing with that emission, then t is an impossible-track of p.

Some of the rules needed to support the chains of logical reasoning in PTAPS are also individually useful in an unextended system, and some of these require routine but extensive geometry calculations. Most of the latter were omitted from the experiments, and the data were obtained by other means. The geometry functions involved could be implemented without difficulty, but would increase execution time while not serving a purpose relative to the intent of the investigations.

SCENARIOS

The experiments involved two basic scenarios, one concerned with the identification of submarines and the other the identification of members of a Soviet task group with the help of satellite reconnaissance data. The two scenarios used in the recent experiments with Rosie are summarized below.

Two-Sub Scenario: Only two submarines could be in the region – a Delta and an Echo II; and two subsurface tracks are reported. The acoustic signature of one track shows that it cannot be a Delta; therefore, it must be the Echo II, and the other track must be the Delta.

UNREP Scenario: Recent positions on all major surface tracks are obtained from a satellite radar map, for a region corresponding to a segment of a radar swath. The positions of ownforce ships are known, leaving four unidentified tracks. From earlier surveillance, it is known that only four other ships could be in that region, an oiler, a destroyer, and a

cruiser, the latter three comprising a Soviet underway replenishment group. A signal which only the cruiser could emit is consistent in bearing with two tracks; and a visual sighting of the merchant eliminates one. It is then known which tracks correspond to the unrep group, so the lead-track of the group is eliminated as a track of the oiler. Every platform is then associated with its track.

CONCLUSIONS

Reference 1 discusses the additional kinds of rules and capabilities that must be included in an operational PTAPS and the problems involved in integrating PTAPS rules into an actual tactical situation assessment (TSA) system, and none of these conclusions has changed. The most difficult problem with compatibility with TSA rules may be the handling of confidence values. PTAPS does not use confidence values and must be constrained from operating on assertions that have less than a near-certainty confidence value. In discussions regarding confidence values, reference 1 describes how conclusions which would logically follow from different assumptions about particular tracks or platforms could be determined by PTAPS and assigned confidence values based on the confidence values of the initial data. Implementing this would not be an easy task.

The logical reasoning that can be implemented with PTAPS rules is essential to the function of associating tracks with platforms. If the other reasoning functions of tactical situation assessment are to be performed in a production system, then probably the PTAPS function also should be performed within that system, so that the functions can be easily coordinated and can share the data base. A possible alternative would be to create a specialized problem-solving technique for platform-track association and interface it with the production system, but coordination and data base sharing would be more difficult.

The next desirable step in continuing PTAPS investigations is to integrate experimentally PTAPS rules with TSA rules in a production system.

REFERENCES

1. Dillard RA. "Higher Order Logic for Platform Identification in a Production System," Technical Document 288, Naval Ocean Systems Center, October 17, 1979.

2. Bechtel RJ and Morris PH. "STAMMER: System for tactical assessment of multisource messages, even radar," Technical Document 252, Naval Ocean Systems Center, May, 1979.

3. McCall DC. "Tactical Situation Assessment Using a Rule-Based Inference System." In Proceedings of the Second MIT/ONR Workshop on Distributed Information and Decision Systems Motivated by Naval Command-Control-Communications (C3) Problems. Held at the Naval Postgraduate School, July, 1979.

4. McCall DC, Morris PH, Kibler DF, and Bechtel RJ. "STAMMER2: A Production System for Tactical Situation Assessment," Technical Document 298, Volumes 1 and 2, Naval Ocean Systems Center, October, 1979.

5. Waterman, DA, Anderson, RH, Hayes-Roth, F, Klahr, P, Martins, G, Rosenschein, SJ. "Design of a Rule-Oriented System for Implementing Expertise," N-1158-1-ARPA, The Rand Corporation, Santa Monica, CA, May, 1979.

6. Dillard RA. "Experimental Tests of PTAPS Performance in Three Types of Production System Structures," Technical Document 385, Naval Ocean Systems Center, September 17, 1980.

APPENDIX

FOURTH MIT/ONR WORKSHOP ON

DISTRIBUTED INFORMATION AND DECISION SYSTEMS

MOTIVATED BY COMMAND-CONTROL-COMMUNICATIONS (C^3) PROBLEMS

June 15, 1981 through June 26, 1981

San Diego, California

List of Attendees

Table of Contents Volumes I-IV

MIT/ONR WORKSHOP OF DISTRIBUTED INFORMATION AND DECISION SYSTEMS

MOTIVATED BY COMMAND-CONTROL-COMMUNICATIONS (C^3) PROBLEMS

JUNE 15, 1981 - JUNE 26, 1981

ATTENDEES

David S. Alberts
Special Asst. to Vice President
& General Manager
The MITRE Corporation
1820 Dolley Madison Blvd.
McLean, VA 22102
Tel: (703) 827-6528

Glen Allgaier
Electronics Engineer
Naval Ocean Systems Center
Code 8242
San Diego, CA 92152
Tel: (714) 225-7777

Ami Arbel
Senior Research Engineer
Advanced Information & Decision Systems
201 San Antonio Circle #201
Mountain View, CA 94040
Tel: (415) 941-3912

Michael Athans
Professor of Electrical Engineering
& Computer Science
Laboratory for Information and
Decision Systems
Massachusetts Institute of Technology
Room 35-406
Cambridge, MA 02139
Tel: (617) 253-6173

Daniel A. Atkinson
Executive Analyst
CTEC, Inc.
7777 Leesburg Pike
Falls Church, VA 22043
Tel: (703) 827-2769

Vidyadhana Raj Avilla
Electronics Engineer
Naval Ocean Systems Center
Code 8241
San Diego, CA 92152
Tel: (714) 225-6258

Dennis J. Baker
Research Staff
Naval Research Laboratory
Code 7558
Washington DC 20375
Tel: (202) 767-2586

Alan R. Barnum
Technical Director
Information Sciences Division
Rome Air Development Center
Griffiss AFB, NY 13441
Tel: (315) 330-2204

Jay K. Beam
Senior Engineer
Johns Hopkins University
Applied Physics Laboratory
Johns Hopkins Road
Laurel, MD 20810
Tel: (301) 953-7100 x3265

Robert Bechtel
Scientist
Naval Ocean Systems Center
Code 8242
San Diego, CA 92152
Tel: (714) 225-7778

Vitalius Benokraitis
Mathematician
US ARMY Material Systems Analysis
ATTN: DRXSY - AAG
Aberdeen Proving Ground, MD 21005
Tel: (301) 278-3476

Patricia A. Billingsley
Research Psychologist
Navy Personnel R&D Center
Code 17
San Diego, CA 92152
Tel: (714) 225-2081

William B. Bohan
Operations Research Analyst
Naval Ocean Systems Center
Code 722
San Diego, CA 92152
Tel: (714) 225-7778

James Bond
Senior Scientist
Naval Ocean Systems Center
Code 721
San Diego, CA 92152
Tel: (714) 225-2384

Paul L. Bongiovanni
Research Engineer
Naval Underwater Systems Center
Code 3521 Bldg. 1171-2
Newport, RI 02840
Tel: (401) 841-4872

Christopher Bowman
Member, Technical Staff
VERAC, Inc.
10975 Torreyana Road
Suite 300
San Diego, CA 92121
Tel: (714) 457-5550

Alfred Brandstein
Systems Analysis Branch
CDSA MCDEC USMC
Quantico, VA 22134
Tel: (703) 640-3236

James V. Bronson
Lieutenant Colonel USMC
Naval Ocean Systems Center
MCLNO Code 033
San Diego, CA 92152
Tel: (714) 225-2383

Rudolph C. Brown, Sr.
Westinghouse Electric Corporation
P. O. 746
MS - 434
Baltimore, MD 21203
Tel:

Thomas G. Bugenhagen
Group Supervisor
Applied Physics Laboratory
Johns Hopkins University
Johns Hopkins Road
Laurel, MD 20810
Tel: (301) 953-7100

James R. Callan
Research Psychologist
Navy Personnel R&D Center
Code 302
San Diego, CA 92152
Tel: (714) 225-2081

David Castanon
Research Associate
Laboratory for Information and
Decision Systems
Massachusetts Institute of
Technology
Room 35-331
Cambridge, MA 02139
Tel: (617) 253-2125

S. I. Chou
Engineer
Naval Ocean Systems Center
Code 713B
San Diego, CA 92152
Tel: (714) 225-2391

Gerald A. Clapp
Physicist
Naval Ocean Systems Center
Code 8105
San Diego, CA 92152
Tel: (714) 225-2044

Douglas Cochran
Scientist
Bolt Beranek & Newman Inc.
50 Moulton Street
Cambridge, MA 02138
Tel: (415) 968-9061

A. Brinton Cooper, III
Chief, C^3 Analysis
US ARMY Material Systems Analysis
ATTN: DRXSY-CC
Aberdeen Proving Ground, MD 21005
Tel: (301) 278-5478

David E. Corman
Engineer
Jonhs Hopkins University
Applied Physics Laboratory
Johns Hopkins Road
Laurel, MD 20810
Tel: (301) 953-7100 x521

Wilbur B. Davenport, Jr.
Professor of Communications Sciences & Engineering
Laboratory for Information and Decision Systems
Massachusetts Institute of Technology
Room 35-214
Cambridge, MA 02139
Tel: (617) 253-2150

Robin Dillard
Mathematician
Naval Ocean Systems Center
Code 824
San Diego, CA 92152
Tel: (714) 225-7778

Elizabeth R. Ducot
Research Staff
Laboratory for Information and Decision Systems
Massachusetts Institute of Technology
Room 35-410
Cambridge, MA 02139
Tel: (617) 253-7277

Donald R. Edmonds
Group Leader
MITRE Corporation
1820 Dolley Madison Blvd.
McLean, VA 22102
Tel: (702) 827-6808

Martin Einhorn
Scientist
Systems Development Corporation
4025 Hancock Street
San Diego, CA 92110
Tel: (714) 225-1980

Leon Ekchian
Graduate Student
Laboratory for Information and Decision Systems
Massachusetts Institute of Technology
Room 35-409
Cambrdige, MA 02139
Tel: (617) 253-5992

Thomas Fortmann
Senior Scientist
Bolt, Beranek & Newman, Inc.
50 Moulton Street
Cambridge, MA 02138
Tel: (617) 497-3521

Clarence J. Funk
Scientist
Naval Ocean Systems Center
Code 7211, Bldg. 146
San Diego, CA 92152
Tel: (714) 225-2386

Mario Gerla
Professor of Electrical Engineering
& Computer Science
University of California
Los Angeles
Boelter Hall 3732H
Los Angeles, CA 90024
Tel: (213) 825-4367

Donald T. Giles, Jr.
Technical Group
The MITRE Corproation
1820 Dolley Madison Bldv.
McLean, VA 22102
Tel: (703) 827-6311

Irwin R. Goodman
Scientist
Naval Ocean Systems Center
Code 7232
Bayside Bldg. 128 Room 122
San Diego, CA 92152
Tel: (714) 225-2718

Frank Greitzer
Research Psychologist
Navy Personnel R&D Center
San Diego, CA 92152
Tel: (714) 225-2081

Leonard S. Gross
Member of Technical Staff
VERAC, Inc.
10975 Torreyana Road
Suite 300
San Diego, CA 92121
Tel: (714) 457-5550

Peter P. Groumpos
Professor of Electrical Eng.
Cleveland State University
Cleveland, OH 44115
Tel: (216) 687-2592

George D. Halushynsky
Member of Senior Staff
Johns Hopkins University
Applied Physics Laboratory
Johns Hopkins Road
Laurel, MD 20810
Tel: (301) 953-7100 x2714

Scott Harmon
Electronics Engineer
Naval Ocean Systems Center
Code 8321
San Diego, CA 92152
Tel: (714) 225-2083

David Haut
Research Staff
Naval Ocean Systems Center
Code 722
San Diego, CA 92152
Tel: (714) 225-2014

C. W. Helstrom
Professor of Electrical Eng.
& Computer Science
University of California,
San Diego
La Jolla, CA 92093
Tel: (714) 452-3816

Ray L. Hershman
Research Psychologist
Navy Personnel R&D Center
Code P305
San Diego, CA 92152
Tel: (714) 225-2081

Sam R. Hollingsworth
Senior Research Scientist
Honeywell Systems & Research Center
2600 Ridgway Parkway
Minneapolis, MN 55413
Tel: (612) 378-4125

Kuan-Tsae Huang
Graduate Student
Laboratory for Information and
Decision Systems
Massachusetts Institute of Technology
Room 35-329
Cambridge, MA 02139
Tel: (617) 253-

James R. Hughes
Major, USMC
Concepts, Doctrine, and Studies
Development Center
Marine Corps Development & Education
Quantico, VA 22134
Tel: (703) 640-3235

Kent S. Hull
Commander, USN
Deputy Director,
Mathematical & Information Sciences
Office of Naval Research
Code 430B
800 N. Quincy
Arlington, VA 22217
Tel: (202) 696-4319

Carolyn Hutchinson
Systems Engineer
Comptek Research Inc.
10731 Treena Street
Suite 200
San Diego, CA 92131
Tel: (714) 566-3831

Carroll K. Johnson
Visiting Scientist
Naval Research Laboratory
Code 7510
Washington DC 20375
Tel: (202) 767-2110

Jesse Kasler
Electronics Engineer
Naval Ocean Systems Center
Code 9258, Bldg. 33
San Diego, CA 92152
Tel: (714) 225-2752

Richard T. Kelley
Research Psychologist
Navy Personnel R&D Center
Code 17 (Command Systems)
San Diego, CA 92152
Tel: (714) 225-2081

David Kleinman
Professor of Electrical Eng.
& Computer Science
University of Connecticut
Box U-157
Storrs, CT 06268
Tel: (203) 486-3066

Robert C. Kolb
Head Tactical Command
& Control Division
Naval Ocean Systems Center
Code 824
San Diego, CA 92152
Tel: (714) 225-2753

Michael Kovacich
Systems Engineer
Comptek Research Inc.
Mare Island Department
P.O. Box 2194
Vallejo, CA 94592
Tel: (707) 552-3538

Timothy Kraft
Systems Engineer
Comptek Research, Inc.
10731 Treena Street
Suite 200
San Diego, CA 92131
Tel: (714) 566-3831

Manfred Kraft
Diplom-Informatiker
Hochschule der Bundeswehr
Fachbereich Informatik
Werner-Heissenbergweg 39
8014 Neubiberg, West Germany
Tel: (0049) 6004-3351

Leslie Kramer
Senior Engineer
ALPHATECH, Inc.
3 New England Executive Park
Burlington, MA 01803
Tel: (617) 273-3388

Ronald W. Larsen
Division Head
Naval Ocean Systems Center
Code 721
San Diego, CA 92152
Tel: (714) 225-2384

Joel S. Lawson, Jr.
Chief Scientist C31
Naval Electronic Systems Command
Washington DC 20360
Tel: (202) 692-6410

Dan Leonard
Electronics Engineer
Naval Ocean Systems Center
Code 8105
San Diego, CA 92152
Tel: (714) 225-7093

Alexander H. Levis
Senior Research Scientist
Laboratory for Information and Decision Systems
Massachusetts Institute of Technology
Room 35-410
Cambridge, MA 02139
Tel: (617) 253-7262

Victor O.-K. Li
Professor of Electrical Eng. & Systems
PHE
University of Southern California
Los Angeles, CA 90007
Tel: (213) 743-5543

Glenn R. Linsenmayer
Westinghouse Electric Corporation
P. O. Box 746 - M.S. 434
Baltimore, MD 21203
Tel: (301) 765-2243

Pan-Tai Liu
Professor of Mathematics
University of Rhode Island
Kingston, RI 02881
Tel: (401) 792-1000

Robin Magonet-Neray
Graduate Student
Laboratory for Information and Decision Systems
Massachusetts Institute of Technology
Room 35-403
Cambridge, MA 02139
Tel: 617) 253-2163

Kevin Malloy
SCICON Consultancy
Sanderson House
49, Berners Street
London W1P 4AQ, United Kingdom
Tel: (01) 580-5599

Dennis C. McCall
Mathematician
Naval Ocean Systems Center
Code 8242
San Diego, CA 92152
Tel: (714) 225-7778

Marvin Medina
Scientist
Naval Ocean Systems Center
San Diego, CA 92152
Tel: (714) 225-2772

Michael Melich
Head, Command Information
Systems Laboratory
Naval Research Laboratory
Code 7577
Washington DC 20375
Tel: (202) 767-3959

John Melville
Naval Ocean Systems Center
Code 6322
San Diego, CA 92152
Tel: (714) 225-7459

Glenn E. Mitzel
Engineer
Johns Hopkins University
Applied Physics Laboratory
Johns Hopkins Road
Laurel, MD 20810
Tel: (301) 953-7100 x2638

Michael H. Moore
Senior Control System Engineer
Systems Development Corporation
4025 Hancock Street
San Diego, CA 92037
Tel: (714) 225-1980

Charles L. Morefield
Board Chairman
VERAC, Inc.
10975 Torreyana Road
Suite 300
San Diego, CA 92121
Tel: (714) 457-5550

Peter Morgan
SCICON Consultancy
49-57, Berners Street
London W1P 4AQ, United Kingdom
Tel: (01) 580-5599

John S. Morrison
Captain, USAF
TAFIG/IICJ
Langeley AFB, VA 23665
Tel: (804) 764-4975

Michael S. Murphy
Member of Technical Staff
VERAC, Inc.
10975 Torreyana Road
Suite 300
San Diego, CA 92121
Tel: (714) 357-5550

Jim Pack
Naval Ocean Systems Center
Code 6322
San Diego, CA 92152
Tel: (714) 225-7459

Bruce Patyk
Naval Ocean Systems Center
Code 9258, Bldg. 33
San Diego, CA 92152
Tel: (714) 225-2752

Roland Payne
Vice President
Advanced Information & Decision Systems
201 San Antonio Circle #286
Mountain View, CA 94040
Tel: (415) 941-3912

Anastassios Perakis
Graduate Student
Ocean Engineering
Massachusetts Institute of Technology
Room 5-426
Cambridge, MA 02139
Tel: (617) 253-6762

Lloyd S. Peters
Associate Director
Center for Defense Analysis
SRI International
EJ352
333 Ravenswood Avenue
Menlo Park, CA 94025
Tel: (415) 859-3650

Harilaos N. Psaraftis
Professor of Marine Systems
Massachusetts Institute of Technology
Room 5-213
Cambridge, MA 02139
Tel: (617) 253-7639

Paul M. Reeves
Electronics Engineer
Naval Ocean Systems Center
Code 632
San Diego, CA 92152
Tel: (714) 225-2365

Barry L. Reichard
Field Artillery Coordinator
US Army Ballistic Research
Laboratory
ATTN: DRDAR-BLB
Aberdeen Proving Ground, MD 21014
Tel: (301) 278-3467

David Rennels
Professor of Computer Science
University of California, LA
3732 Boelter Hall
Los Angeles, CA 90024
Tel: (213) 825-2660

Thomas P. Rona
Staff Scientist
Boeing Aerosapce Company
MS 84-56
P. O. Box 3999
Seattle, WA 98124
Tel: (206) 773-2435

Nils R. Sandell, Jr.
President & Treasurer
ALPHATECH, Inc.
3 New England Executive Park
Burlington, MA 01803
Tel: (617) 273-3388

Daniel Schutzer
Technical Director
Naval Intelligence
Chief of Naval Operations
NOP 009T
Washington DC 20350
Tel: (202) 697-3299

Adrian Segall
Professor of Electrical Engineering
Technion IIT
Haifa, Israel
Tel: (617) 253-2533

Prodip Sen
Polysystems Analysis Corporation
P. O. Box 846
Huntington, NY 11743
Tel: (516) 427-9888

Harlan Sexton
Naval Ocean Systems Center
Code 6322
San Diego, CA 92152
Tel: (714) 225-2502

Mark J. Shensa
Naval Ocean Systems Center
Code 6322
San Diego, CA 92152
Tel: (714) 225-2349 or 2501

J. R. Simpson
Office of Naval Research
800 N. Quincy
Arlington, VA 22217
Tel: (202) 696-4321

Stuart H. Starr
Director Systems Evaluation
The Pentagon
DUSD (C31), OSD
Room 3E182
Washington DC 20301
Tel: (202) 695-9229

T. Tao
Professor
Naval Postgraduate School
Code 62 TV
Monterey, CA 93940
Tel: (408) 646-2393 or 2421

H. Gregory Tornatore
Johns Hokpins University
Applied Physics Laboratory
Johns Hopkins Road
Laurel, MD 20810
Tel: (301) 953-7100 x2978

Edison Tse
Professor of Engineering
Economic Systems
Stanford University
Stanford, CA 94305
Tel: (415) 497-2300

E. B. Turnstall
Head, Ocean Surveillance
Systems Department
Naval Ocean Systems Center
Code 72
San Diego, CA 92152
Tel: (714) 225-7900

Lena Valavani
Research Scientist
Laboratory for Information and
Decision Systems
Massachusetts Institute of
Technology
Room 35-437
Cambridge, MA 02139
Tel: (617) 253-2157

Maniel Vineberg
Electronics Engineer
Naval Ocean Systems Center
Code 9258
San Diego, CA 92152
Tel: 714) 225-2752

Joseph H. Wack
Advisory Staff
Westinghouse Electric Corporation
P. O. Box 746 MS-237
Baltimore, MD 21203
Tel: (301) 765-3098

Jan D. Wald
Senior Research Scientist
Honeywell Inc.
Systems & Research Center
MN 17-2307
P. O. Box 312
Minneapolis, MN 55440
Tel: (612) 378-5018

Bruce K. Walker
Professor of Systems Engineering
Case Western Reserve University
Cleveland, OH 44106
Tel: (216) 368-4053

David White
Advanced Technology, Inc.
2120 San Diego Avenue
Suite 105
San Diego, CA 92110
Tel: (714) 981-9883

Jeffrey E. Wieselthier
Naval Research Laboratory
Code 7521
Washington DC 20375
Tel: (202) 767-2586

Richard P. Wishner
President
Advanced Information & Decision Systems
201 San Anotnio Circle
Suite 286
Mountain View, CA 94040
Tel: (415) 941-3912

Joseph G. Wohl
V. P. Research & Development
ALPHATECH, Inc.
3 New England Executive Park
Burlington, MA 01803
Tel: (617) 273-3388

John M. Wosencraft
Head of C^3 Curriculum
Naval Postgraduate School
Code 74
Monterey, CA 93940
Tel: (408) 646-2535

Lofti A. Zadeh
Professor of Computer Science
University of California
Berkeley, CA 94720
Tel: (415) 526-2569

I

SURVEILLANCE AND TARGET TRACKING

II

SYSTEM ARCHITECTURE AND EVALUATION

III

COMMUNICATION, DATA BASES & DECISION SUPPORT

IV

C^3 THEORY